

CASE STUDY OF AIR DISTRIBUTION OF THE HOSPITAL
OPERATING ROOM IN MALAYSIA

DING LAI CHET

THESIS SUBMITTED IN FULFILMENT
OF THE REQUIREMENTS FOR
THE DEGREE OF MASTER OF ENGINEERING SCIENCE

FACULTY OF ENGINEERING
UNIVERSITY OF MALAYA
KUALA LUMPUR

2012

DECLARATION BY THE CANDIDATE

UNIVERSITI MALAYA ORIGINAL LITERARY WORK DECLARATION

Name of Candidate: DNG LAI CHET (I.C/Passport No:
Registration/Matric No: KGA100004
Name of Degree: MASTER OF ENGINEERING SCIENCE
Title of Project Paper/Research Report/Dissertation/Thesis ("this Work"):
Case study of air distribution of the hospital operating room in
Malaysia
Field of Study: HEATING, VENTILATING AND AIR CONDITIONING (HVAC)

I do solemnly and sincerely declare that:

- (1) I am the sole author/writer of this Work;
- (2) This Work is original;
- (3) Any use of any work in which copyright exists was done by way of fair dealing and for permitted purposes and any excerpt or extract from, or reference to or reproduction of any copyright work has been disclosed expressly and sufficiently and the title of the Work and its authorship have been acknowledged in this Work;
- (4) I do not have any actual knowledge nor do I ought reasonably to know that the making of this work constitutes an infringement of any copyright work;
- (5) I hereby assign all and every rights in the copyright to this Work to the University of Malaya ("UM"), who henceforth shall be owner of the copyright in this Work and that any reproduction or use in any form or by any means whatsoever is prohibited without the written consent of UM having been first had and obtained;
- (6) I am fully aware that if in the course of making this Work I have infringed any copyright whether intentionally or otherwise, I may be subject to legal action or any other action as may be determined by UM.

Candidate's Signature

Date:

Subscribed and solemnly declared before,

Witness's Signature

Date:

Name:

Designation:

This work dedicated to

beloved family and friends

Abstract

In a hot and humid country, Malaysia shows the highest percentage of surgical site infection in comparison with other healthcare associated infections. The design of operating rooms is significantly different from on-site surveys on numbers of operating rooms (ORs) in Malaysia. To date, investigation on air distribution in OR is limited in developing country. Computer Fluid Dynamics (CFD) was used in this research for further study in purpose to analyze the air flow features in ORs. In current study, two ORs, namely Sarawak General Hospital Heart Centre OT-5 and University of Malaya Medical Centre OT-11 with different design features were studied. In the first case study, there were fieldwork measurement and simulation study at Sarawak General Hospital Heart Centre, which includes the study of comparison of the potential of reducing air flow rate. Then, the case study was continued with fieldwork measurement and simulation study at University of Malaya Medical Centre (UMMC). OT-11 of UMMC designed with up to 14 air inlets and 3 air outlets. The airflow features for such design will be analyzed. Since an OR needs to fulfill the requirement of a Class 7 clean room according to ISO 14644-1, hence the design of the array of inlets were studied through a comparison of 1 x 4 and 2 x 2 inlet array. It was found that, 1 x 4 inlet array performs better than 2 x 2 inlet array. In the last part of this work, the study on the effect of maldistribution of air velocities was also included by using a 2-D CFD simulation.

Abstrak

Dalam keadaan iklim yang panas dan lembap, jumlah kes jangkitan yang berpunca dari dewan bedah telah menunjukkan peratusan yang paling tinggi di antara kes-kes jangkitan yang berlaku dalam pusat pemulihan kesihatan di Malaysia. Hasil daripada kajian lapangan, didapati terdapat perbezaan yang ketara dalam reka bentuk dewan bedah dari tempat ke tempat di Malaysia. Sehingga kini, siasatan ke atas pengagihan udara di dalam dewan bedah adalah terhad dalam negara yang membangun seperti Malaysia. Dalam kajian ini, dinamik bendalir berkomputer (CFD) telah digunakan bagi memudahkan analisis terhadap ciri- ciri pengaliran udara dalam dewan bedah. Dalam kajian ini, dua buah dewan bedah, yakni Dewan Bedah Kelima dari Pusat Jantung Hospital Umum Sarawak serta Dewan Bedah Kesebelas dari Pusat Perubatan Universiti Malaya (PPUM). Dalam kes kajian yang pertama, pengukuran dan kerja lapangan telah dijalankan sebelum simulasi ke atas aliran udara dalam Dewan Bedah Kelima dilakukan. Menerusi simulasi yang dilakukan, potensi untuk mengurangkan kadar aliran udara telah dikaji. Seterusnya, kajian ini disambung dengan analisa pengaliran udara terhadap Dewan Bedah Kesebelas PPUM yang mempunyai 14 salur masuk udara dan 3 salur keluar udara. Hasil kajian menunjukkan bahawa Dewan Bedah Kesebelas tidak dapat berfungsi dengan baik disebabkan reka bentuk kedudukan salur udara. Memandangkan dewan bedah harus memenuhi keperluannya dalam Kelas 7 menurut ISO 14464-1, maka ia perlu direka untuk memenuhi kriteria tahap kebersihan yang tinggi. Dua jenis pemakaian salir masuk udara telah dibandingkan ke atas keberkesanannya dalam ertian pengaliran udara dalam sebuah bilik bersih Kelas 7. Pada masa yang sama, kesan daripada pembahagian halaju udara masuk yang tidak sekata pada salur masuk udara juga dibincangkan dalam penghujung kajian ini dengan bantuan simulasi dinamik bendalir berkomputer secara 2-Dimensi.

Acknowledgement

Firstly, i would like to thank and praise Lord Jesus Christ for his grace, wisdom and inspiration that He has imparted in me, which lead me to the completion of this study.

I would like to deliver my deepest appreciation to my supervisor, Associate Professor Ir. Dr. Yau Yat Huang for his guidance. Besides, i am grateful to University of Malaya for offering me a tutorship throughout the candidature.

Nevertheless, i would like to appreciate Miss Chew Bee Teng, Mr. Phuah Kok Sun, Mr. Lian Yee Cheng and Mr. Tommy Chang Chee Pang, for their help and suggestions throughout the candidature.

Here, we gained precious insight and knowledge.

Ding Lai Chet

August 2012

TABLE OF CONTENTS

DECLARATION BY THE CANDIDATE.....	ii
Abstract	iv
Abstrak	v
Acknowledgement.....	vi
TABLE OF CONTENTS	vii
LIST OF FIGURES	x
LIST OF TABLES	xv
LIST OF APPENDICES	xvi
LIST OF SYMBOLS AND ABBREVIATIONS	xvii
1.0 Introduction	1
1.1 Background	1
1.2 Scope of work.....	3
1.3 Objectives of the study	3
1.4 Significance of the study	4
1.5 Limitations of the study	4
2.0 Literature Review	6
2.1 Design of the operating room	6
2.1.1 Standard governing the air cleanliness	6
2.1.2 Operating room design consideration.....	8
2.1.3 Temperature.....	10
2.1.4 Humidity	12
2.1.5 Air velocity and air change rate.....	13
2.1.6 Pressure.....	16
2.2 HVAC systems & air distribution and ventilation systems	17
2.2.1 Air distribution and ventilation systems.....	17
2.2.2 Laminar airflow (LAF)	21
2.2.3 Upward displacement ventilation	28
2.3 Supply air and return air diffuser.....	29
2.4 Filters	31
2.5 ORs in Malaysia	33
2.6 Concluding summary for literature survey	34
3.0 Methodology	36
3.1 Overview	36
3.2.1 Governing equations and general form of governing equations	37

3.2.2 Boundary conditions.....	41
3.2.3 Fieldwork measurement	42
3.2.4 Equipment used in fieldwork measurement	44
3.3 CFD modeling	46
3.3.1 Modeling approaches.....	46
3.3.2 Verification.....	47
3.3.3 Accuracy.....	48
3.3.4 Considerations in modeling.....	52
3.3.5 Modeling of human	54
3.3.6 Modeling of humidity.....	55
3.3.7 Modeling of gaseous contaminant.....	55
3.3.8 Modeling of particle tracking	55
3.4 Simulations overview	56
3.5 Concluding summary	56
4.0 Case study on SGHHC OT-5	57
4.1 Assumptions	59
4.2 Measurement at SGHHC.....	61
4.3 Physical on-site measurement at SGHHC OT-5	62
4.4 Simulation for SGHHC OT-5.....	64
4.5 Mesh independence study for SGHHC OT-5 simulation.....	67
4.5 Fieldwork measurement and simulation – A comparison	71
4.6 CFD simulations of SGHHC OT-5	73
4.6.1. SGHHC OT-5: Uneven air velocities (current condition) versus even air velocities at inlets	74
4.6.2. SGHHC OT-5: Air velocity reduction	82
4.7. Concluding summary	86
5.0 Case study on UMMC OT-11	87
5.1 Assumptions	89
5.2 Measurement at UMMC.....	89
5.3 Physical on-site measurement at OT-11, UMMC	90
5.4 Mesh independence study for OT-11 UMMC simulation.....	92
5.5 Fieldwork measurement and simulation – A comparison	93
5.6 Simulation for UMMC OT-11	96
5.7 UMMC OT-11: Current condition	97
5.8 Concluding summary	107

6.0 The study on design variation in a Class 7 clean room.....	108
6.1 Study on the inlet design to ventilation performance – A 3-D simulation study	109
6.1.1 Background and problem formulation	109
6.1.2 Numerical model	112
6.1.3 Results and discussion.....	114
6.1.4 Concluding summary	142
6.2 Study on the effect of inlet air velocity variations and heat source location in a clean room – A 2-D simulation study.....	143
6.2.1 Background and problem formulation	143
6.2.2 Model for simulation	143
6.2.3 Numerical method and simulation overview.....	145
6.2.3.1 Grid independency	145
6.2.3.1 Boundary condition and settings.....	146
6.2.3.1 CFD Simulations overview	148
6.2.4 Results and discussion.....	149
6.2.5 Concluding summary	154
7.0 Conclusion and Recommendations	155
7.1 Conclusion.....	155
7.2 Recommendations	157
References	158
Appendices.....	168

LIST OF FIGURES

	Page
Figure 2.1: Typical ultraclean ventilation (UCV) arrangement in operating room.	26
Figure 2.2: Different inlet design of ORs.	33
Figure 2.3: Exhaust blockage-common problem found during surgical process.	34
Figure 3.1: Finite volume method with unstructured mesh.	49
Figure 4.1: View for OT 5 (Left: the condition during HEPA leaking test while picture in the Right: the condition during the measurement).	57
Figure 4.2: Drawing layout for OT-5 (without supply and return air duct).	57
Figure 4.3: Drawing layout for OT-5 (with supply and return air ducts).	58
Figure 4.4: Modeling for unoccupied SGHHC OT-5 in CAD.	58
Figure 4.5: Velocity matrix available in Alnor EBT721 balometer.	59
Figure 4.6: Typical condition during operation (taken in University Malaya Medical Centre).	60
Figure 4.7: The SGHHC OT-5 actual dimension measurement.	61
Figure 4.8: Nomenclature for HEPA inlets and exhausts SGHHC OT-5.	64
Figure 4.9: Air velocity difference (bottom half of the figure) for different mesh elements at mid-plane (Plane 1) of OT-5.	69
Figure 4.10: Average air temperature at Plane 1 versus number of mesh elements.	69
Figure 4.11: Air swirl behind the medical gas supply pendant.	70
Figure 4.12: Air flow pattern comparison of standard k-e model and RNG k-e model.	71
Figure 4.13: Comparison of result- measurement and simulation.	72
Figure 4.14: Location of Plane 1, Plane 2 and Plane 3.	74
Figure 4.15: The airflow in SGHHC OT-5 with uneven inlet air velocities at Plane 1.	75
Figure 4.16: Airflow above the patient in OT-5 with uneven (left) and even (right) inlets air velocities at Plane 1.	76

Figure 4.17: The airflow in SGHHC OT-5 with even inlet air velocities at Plane 2.	77
Figure 4.18: Airflow around the medical lamp.	78
Figure 4.19: The airflow in SGHHC OT-5 with uneven inlet air velocities at Plane 2.	79
Figure 4.20: Temperature distribution in OT-5 with uneven (left) and even (right) inlet air velocities.	80
Figure 4.21: Temperature distribution in OT-5 with uneven (left) and even (right) inlet air velocities at Plane 3.	80
Figure 4.22: RH distribution of in OT-5 with uneven (left) and even (right) inlet air velocities at Plane 3.	81
Figure 4.23: Particle tracking for particle with 12 μ m diameter release from machine.	82
Figure 4.24: Air temperature distribution for inlet $V=0.345$ m/s and $V=0.3$ m/s at 1.2 m & 1.7 m above the floor.	84
Figure 4.25: Particle tracking for particle with 12 μ m diameter release from machine for inlet air velocity reduction.	85
Figure 4.26: Gaseous contaminant, CO ₂ concentration 1.2 m above floor level.	85
Figure 5.1: OT-11 of UMMC (left) and OT-12 of UMMC (right).	87
Figure 5.2: Modeling of UMMC OT-11.	88
Figure 5.3: Generated computational mesh for UMMC OT-11.	88
Figure 5.4: Nomenclature for HEPA inlets and exhausts UMMC OT-11.	88
Figure 5.5: Measurement inside the UMMC OT-11.	93
Figure 5.6: Location of measurement points inside the UMMC OT-11.	94
Figure 5.7: Comparison of prediction and measurement result.	95
Figure 5.8: Velocity vector for $V_{in} = 0.2$ m/s at operating zone, x-z plane.	98
Figure 5.9: Velocity vector for $V_{in} = 0.2$ m/s at operating zone, y-z plane.	98
Figure 5.10: Velocity vector for $V_{in} = 0.2$ m/s at operating zone, x-y plane.	99

Figure 5.11: Velocity contour w-velocity component for $V_{in} = 0.2$ m/s at operating zone, x-y plane.	99
Figure 5.12: Temperature distribution for $V_{in} = 0.2$ m/s.	100
Figure 5.13: RH distribution for $V_{in} = 0.2$ m/s.	101
Figure 5.14: Gaseous contaminant concentration, 1.2 m above the floor, $V_{in} = 0.2$ m/s.	101
Figure 5.15: Temperature distribution across surgical site at height=1.7 m above the floor (Blue line, $V_{in} = 0.2$ m/s ; Red line, $V_{in} = 0.4$ m/s ; highlighted in red: surgical region).	102
Figure 5.16: Velocity vector for $V_{in} = 0.4$ m/s at operating zone, x-z plane.	103
Figure 5.17: Velocity vector for $V_{in} = 0.4$ m/s at operating zone, y-z plane.	103
Figure 5.18: Velocity vector for $V_{in} = 0.4$ m/s at operating zone, x-y plane.	104
Figure 5.19: Velocity contour w-velocity component for $V_{in} = 0.4$ m/s at operating zone, x-y plane.	104
Figure 5.20: Temperature distribution for $V_{in} = 0.4$ m/s.	105
Figure 5.21: RH distribution for $V_{in} = 0.4$ m/s.	105
Figure 5.22: Gaseous contaminant concentration, 1.2 m above the floor, $V_{in} = 0.4$ m/s.	106
Figure 5.23: Streamlines for air discharged from inlet 4 and inlet 8.	106
Figure 5.24: Particles releasing location.	107
Figure 6.1: Layout of room air inlets.	110
Figure 6.2: Tetrahedral mesh for current study.	112
Figure 6.3: Comparison of predicted and measured velocity decay.	114
Figure 6.4: Velocity decay for three-dimensional free jets (Rajaratnam, 1976).	116
Figure 6.5: Gaseous contaminant concentration for all cases.	117
Figure 6.6: Comparison of air velocity vector for case 1a (left) and case 2a (right) (1 x 4 array).	120

Figure 6.7: Comparison of air velocity vector for case 3a (left) and case 4a (right) (2 x 2 array).	121
Figure 6.8: Contour of v-velocity component 1.7 m above the floor, $V_{in}=0.2$ m/s for 1 x 4 array (left) and 2 x 2 array (right).	122
Figure 6.9: Contour of v-velocity component 1.7 m above the floor, $V_{in}=0.4$ m/s for 1 x 4 array (left) and 2 x 2 array (right).	123
Figure 6.10: Comparison of contaminant dispersion for case 1a (left) and case 2a (right) (1 x 4 array).	124
Figure 6.11: Comparison of contaminant dispersion for case 3a (left) and case 4a (right) (2 x 2 array).	125
Figure 6.12: Comparison of air temperature for case 1a (left) and case 2a (right) (1 x 4 array).	126
Figure 6.13: Comparison of air temperature for case 3a (left) and case 4a (right) (2 x 2 array).	127
Figure 6.14: Comparison of air velocity vector for case 1a (left) and case 3a (right) (Inlet velocity 0.2 m/s).	130
Figure 6.15a: Comparison of air velocity vector for case 2a (left) and case 4a (right) (Inlet velocity 0.4 m/s).	131
Figure 6.15b: Comparison of air velocity vector (y-z plane) for case 2a (left) and case 4a (right) (Inlet velocity 0.4 m/s).	132
Figure 6.16: Comparison of contaminant dispersion for case 1a (left) and case 3a (right) (Inlet velocity 0.2 m/s).	133
Figure 6.17: Comparison of contaminant dispersion for case 2a (left) and case 4a (right) (Inlet velocity 0.4 m/s).	134
Figure 6.18: Comparison of air temperature for case 1a (left) and case 3a (right) (Inlet velocity 0.2 m/s).	135
Figure 6.19: Comparison of air temperature for case 2a (left) and case 4a (right) (Inlet velocity 0.4 m/s).	136
Figure 6.20: Comparison of air velocity vector for case 1a (upper left) & case 1b (upper right); case 2a (bottom left) and 2b (bottom right).	138
Figure 6.21: Comparison of air velocity vector for case 3a (upper left) & case 3b (upper right); case 4a (bottom left) and 4b (bottom right).	139
Figure 6.22: Comparison of contaminant dispersion for case 1a (upper left) & case 1b (upper right); case 2a (bottom left) and 2b (bottom right).	140
Figure 6.23: Comparison of contaminant dispersion for case 3a (upper	141

left) & case 3b (upper right); case 4a (bottom left) and 4b (bottom right).

Figure 6.24: HEPA's air inlet array with two exhausts located at the bottom on same face of a sidewall.	141
Figure 6.25: Hypothetical 2-D model to study the effect of inlet air velocity variations and heat source location in a clean room.	143
Figure 6.26: Dimension for the hypothetical 2-D model (unit in meter).	144
Figure 6.27: Results for grid independency study (for uniform $V_{in} = 0.2$ m/s).	144
Figure 6.28: Recirculation zones in the 2-D room.	150
Figure 6.29: Comparison of inlet air velocity variations to the air distribution in the room.	153
Figure 6.30: Comparison of heat source (obstacle) variations to the air distribution in the room.	154

LIST OF TABLES

	Page
Table 2.1: ISO 12644-1:Air cleanliness classes and limits.	7
Table 2.2: OR design considerations.	9
Table 2.3: Recommended indoor conditions for operating room.	9
Table 2.4: Classified of OR by their effect on patients' temperature.	10
Table 2.5: Thermal comfort assessment for occupants in OR.	11
Table 2.6: Vertical airflow velocities and ACH versus cleanroom classes.	13
Table 2.7: The differences between turbulent ventilation and displacement ventilation.	19
Table 3.1: Dependent variables and the source term for general transport equation.	40
Table 3.2: List of equipment.	45
Table 3.3: Summary for Grid Convergence Index calculation.	51
Table 4.1: Measured air inlet conditions for OT-5.	62
Table 4.2: Particulate count in the non-operating SGHHC OT-5.	63
Table 4.3: Boundary condition settings for CFD simulation SGHHC OT-5.	65
Table 4.4: Settings for CFD simulation SGHHC OT-5.	65
Table 4.5: Heat dissipations of OR devices in simulated OR SGHHC OT-5.	66
Table 4.6: Identification for simulations SGHHC OT-5.	67
Table 4.7: Grid convergence index for simulation I, II and III SGHHC OT-5.	68
Table 4.8: Comparison of the concentration of gaseous contaminant, CO ₂ .	82
Table 4.9: Comparison on concentration of gaseous contaminant, CO ₂ for inlet air velocity reduction.	86
Table 5.1: Measured air condition at room air inlets.	90
Table 5.2: Particulate count in the non-operating UMMC OT-11.	92
Table 5.3: Identification for simulations UMMC OT-11.	92

Table 5.4: Boundary condition settings for CFD simulation UMMC OT-11.	96
Table 5.5: Heat dissipation of equipment in OR UMMC OT-11.	96
Table 6.1: Room's specification	111
Table 6.2: Summary of cases under current study.	111
Table 6.3: Result for grid independent test.	113
Table 6.4: Location of plane 1, 2, 3 and 4.	114
Table 6.5: Result summary.	116
Table 6.6: Details on the mesh size.	146
Table 6.7: Boundary condition and settings for CFD simulations.	146
Table 6.8: Specification of the inlet air velocity.	147
Table 6.9: Description for all cases.	148
Table 6.10: Definition for Line A-A', Line B-B' and Line C-C'.	149
Table 6.11: Local mean temperature index and particle residence time for all cases.	152

LIST OF APPENDICES

	Page
Appendix A: Permission letter for UMMC visit	168
Appendix B: The Star News on Sarawak General Hospital Heart Centre (Formerly known as Sarawak International Medical Centre, SIMC)	169
Appendix C: AHU design for OT-5	170
Appendix D: Room dimension (on-site measurement)	173
Appendix E: Equipment dimensions in OR modeling	174
Appendix F: Private communication	180
Appendix G: Requirement for the characteristic of velocity and temperature measurement	181
Appendix H: Temperature and velocity contour for UMMC OT-11 simulation	182
Appendix I: Grid independence study	187

LIST OF SYMBOLS AND ABBREVIATIONS

ACH	Air changes per hour
AHU	Air handling unit
ASH	Anesthetic scavenging hood
ASHRAE	American society of heating, refrigerating and air-conditioning engineers
CAD	Computer aided design
CFU	Colony forming units
CFD	Computational fluids dynamics
FPM	Feet per minute
GCI	Grid convergence index
HAI	Healthcare associated infections
HEPA	High efficiency particulate air
HTM	Health technical memorandum
HVAC	Heating, ventilation and air conditioning
IAQ	Indoor air quality
ISO	International organization of standardization
LAF	Laminar airflow
MERV	Minimum efficiency reporting values
OR	Operating room
PED	Percentage experiencing draft
RH	Relative humidity
SARS	Severe acute reparatory syndrome
SSI	Surgical site infection
UCV	Ultra clean ventilation
ULPA	Ultra low penetration
UV	Ultra violate
UVGI	Ultraviolet germicidal irradiation

Ar	Archimedes number
C	Concentration
D	Diameter
g	Gravity
Gr	Grashof number
H	Height
L	Length
\dot{Q}	Flow rate
Re	Reynolds number
t	Time
V	Velocity
W	Width
Δ	Difference (of)
ρ	Density
θ	Local mean temperature index

1.0 Introduction

1.1 Background

Hospitals are places which call for a particularly careful protection in HVAC systems, including hygiene, air route and airborne transmissions. Studies have shown that patients in a controlled environment recover faster than those in an uncontrolled environment. Patients with different illnesses require different indoor conditions (ASHRAE, 2003a). Modern antiseptic surgery was instituted in the 1860s, and since then surgical methods have improved enormously. Everyone involved, not just the surgeon and the surgical team but also the providers of equipment and facilities including HVAC engineers, have worked assiduously to improve surgical outcomes. Nevertheless, infections that occur during surgery have not been eliminated, and these so-called surgical site infections (SSI) still exact a huge human and economic cost. In ASEAN countries, studies on surgical site infections (SSI) are limited. Conflicting with the success of feedback systems to reduce SSIs in hospitals in the USA and Europe, a study done in Thailand showed no such reduction in SSIs. However, some limitations might be attributed to this study, as discussed by the author (Kasatpibal et al., 2006). According to the WHO Mission Report, SSIs were the highest Healthcare Associated Infections (HAIs) in Malaysian hospitals in 2007. In this survey, the majority of 108 cases of 432 total HAI cases resulted from SSIs, adding up to 25% of the total HAIs in Malaysia (McLaws, 2007).

Airborne pathogens are those pathogens produced in the respiratory system and released with the exhaled air as a method of propagation (Bolashikov, 2009). Wells (1934) explained in his research that droplets sized $5\mu\text{m}$ or less can remain airborne indefinitely. One point worth noting is that the spreading of the influenza virus is

negatively proportional to the surrounding temperature. The dispersal is more effective at 5°C, compared to 20°C or 30°C. In cool and temperate climates, airborne is the predominant route of influenza infection, while in a tropical and warm environment, the direct contact route is significant (Lowen et al., 2007). In 1970, Scoot (1970) pointed out; there are two main route of infection, direct contact with a contaminated source and airborne microorganisms. Meanwhile, personnel exposure to harmful gases should be avoided in the operating room (OR). As studied by Piziali et al. (1976), the main chemical substances found in the indoor air of ORs are anesthetics gases (nitrous protoxide and halogenated agents), as well as disinfection and sterilizing substances. It is clearly seen that a proper and correct air distribution is essential since it subsequently dictates the functionality of ventilation in OR.

In 2003, ASHRAE contributed a significant advance in OR air distribution design by publishing HVAC Design Manual for Hospitals and Clinics. This manual includes the results of extensive CFD analysis of alternative OR air distribution designs conducted by Memarzadeh and Manning (2003). These researchers definitely and reasonably conclude that vertically downward laminar flow at 30-35 FPM with low returns or a combination of low and high returns is the best OR air distribution design. This CFD analysis is clearly state of the art, and the results and conclusions are reasonable. The confidence in the results is restricted by lack of direct experimental verification and by its necessary dependence on several simulation parameters that lack experimental confirmation. Though vertically downward laminar flow with combination of low and high return is recommended, however, it still could lead to different air distribution outcomes since the design and layout of inlets and outlets are different from place to place.

1.2 Scope of work

In this study, the OR air distribution in two government hospitals in Malaysia will be investigated. Current work includes the on-site measurement of OR air inlet boundary conditions as well as air velocity inside the ORs. Both ORs under study are designed to have vertically downward laminar flow. The ORs were modeled and the airflow inside OR is predicted by using commercial CFD software, ANSYS Fluent. The results from the numerical prediction were further analyzed in terms of temperature air velocity distribution, airflow profile, and contaminants transport.

1.3 Objectives of the study

The overall objective of this study is to confirm and if necessary enhance the modeling of hospital OR air distribution that supports the recommendations in the ASHRAE Design Manual and the upcoming ASHRAE standard. The objectives are:

- ❖ To perform fieldwork measurement of airflow at Sarawak General Hospital Heart Centre and University of Malaya Medical Centre.
- ❖ To carry out CFD investigation of airflow at the hospital.
- ❖ To carry out parametric investigations (e.g. various inlet velocity and condition) based on CFD.

This overall objective will be achieved by accomplishing the following itemized technical objectives.

- i) Field measurements to establish the boundary conditions and transport parameters needed for realistic experiments and CFD modeling.
- ii) Quantitative assessment and verification of the CFD simulations by comparison with the experimental results, possibly after enhancement of the CFD simulations.

1.4 Significance of the study

The project has three key scientific significances:

- i. It provides a case study based on the actual ORs design exists in Malaysia and provides insight of airflow inside OR, in a local scenario (especially in Malaysia conditions)
- ii. With the absence of a full scale OR mock-up, this work provides an alternative approach for studying the air distribution of an OR via on-site visit.
- iii. It recommends improvements that can be implemented for improving current condition in ORs under-studied, and suggestions for the OR design.

1.5 Limitations of the study

- i. The scope of the current study is focused for one type of ventilation in OR, which is laminar type. It does not investigate the possibility of other types of ventilation such as displacement ventilation, horizontal laminar ventilation, and turbulent ventilation.
- ii. The lack of a full scale laboratory with a mock-up OR have restricted the scope of comparison (verification) between predicted and actual air distribution for an OR.

- iii. There is a limitation in the validation in the modeling of contaminants due to the fact that there is no measurement data taken during the on-site measurement.

2.0 Literature Review

2.1 Design of the operating room

The history of the OR began after operations were initially being carried out on hospital wards, in patients' homes, and in doctors' consulting rooms. Formal rooms designated for surgical operations were built in the 18th century as there developed a need for teaching purposes (Essex-Lopresti, 1999). In 1961, Smylie and Dudley (1961) made an important change in the operating room design, which involved the separation of clean and dirty traffic flow in order to achieve asepsis rather than antiseptics. Later, Essex-Lopresti and Hubert examined the working economy and ability to prevent cross-infection in the conventional OR. They noted some deficiencies in the existing design and proposed a centralized sink room and sterilizing unit to serve all ORs (Essex-Lopresti and Hubert, 1962).

Balaras et al. (2007) pointed out some common problem in OR design being the limited space availability and the small dimensions of the room, improper functions in the room space, as well as availability of rooms for storing medical supplies, sterile equipment and instruments. Ventilation systems in ORs were aimed at diluting the bacteria generated inside the OR, preventing dirty air from entering the OR from adjacent areas, removing contaminants by a proper airflow and providing a comfortable environment for occupants (Rao, 2004).

2.1.1 Standard governing the air cleanliness

Any renovations carried out on existing ORs are time consuming and costly. Besides, renovations and construction in hospitals can increase the risk of nosocomial infections (Carter and Barr, 1997, Krasinki et al., 1985). The standard which had the most major

impact on the design and operation of cleanrooms, serving as the basis of the present International Organization of Standardization (ISO) standard, ISO14644-1:1999, was the Federal Standard (FS) 209 (Whyte, 2010). According to the ISO Classification Air Cleanliness (ISO, 1999), there are nine levels of airborne particulate cleanliness as represented in Table 2.1. These class levels are differentiated by specified maximum allowable number of particles per cubic meter of air. An OR should be at least ISO 14644-1 Class 7 or Class 8.

Table 2.1: ISO 12644-1:Air cleanliness classes and limits (ISO,1999).

Limits in measured particle size per m ³ (equal to, greater than, stated size)						
ISO Class	0.1µm	0.2µm	0.3µm	0.5µm	1.0µm	5.0µm
1	10	2	-	-	-	-
2	100	24	10	4	-	-
3	1000	237	102	35	8	-
4	10000	2370	1020	352	83	-
5	100000	23700	10200	3520	832	29
6	1000000	237000	102000	35200	8320	293
7	-	-	-	352000	83200	2930
8	-	-	-	3520000	832000	29300
9	-	--	-	35200000	8320000	293000

The classification above is based on the following equation (ISO, 1999):

$$C_N = 10^N \left[\frac{0.1}{D} \right]^{2.08} \quad (1)$$

where

C_N = maximum allowable particle concentration, in (particles/m³),

N = ISO classification number, from 1 to 9,

D = particle size in µm.

Dharan et al. recommended the measurement of the presence of air particles to be treated as a routine procedure with the aid of a cleanroom technology standard (Dharan and Pittet, 2002). However, it is difficult to follow the requirement standard since it is hard to control the airborne bacteria colonies around the surgical site, unless the actions to minimize the airborne particles' concentration in the OR are taken immediately by the medical communities. Therefore, temperature, humidity, air velocity, air change rate, pressure, HVAC system, filter and air distribution pattern are the most important factors that need to be addressed in order to design optimal operating rooms and to avoid SSI cases (that may occur during surgical procedures).

2.1.2 Operating room design consideration

There are several considerations to be taken into account when designing an operating room as described in Table 2.2. Of course, the operation room must be aseptic and have an excellent control of temperature and humidity to maintain the indoor air state. In turn, the air velocity in the room should be kept at a relatively low speed in order to prevent the recirculation of microbes (National Research Council, 1976). Table 2.3 contains recommendations for temperature, relative humidity, air change rate and ventilation system for a general OR.

Table 2.2: OR design considerations.

OR design considerations	General design		
	Indoor Conditions	Temperature	
		Humidity	
		Ventilation	Air velocity & air change rate
			Pressure
HVAC Systems & Air Distribution and Ventilation Systems			
<ul style="list-style-type: none"> • <i>Air distribution and ventilation systems</i> • <i>Supply air and return air diffusers</i> • <i>Filter</i> 			

Table 2.3: Recommended indoor conditions for operating room.

Temperature (° C)	Relative Humidity (%)	Air Change Rate (ACH)	Ventilation	Source/Reference
20-24	30-60	Minimum 20 ACH with minimum 4 ACH of outdoor air.	Positive pressurization (at least 2.5 Pa).	2008 ASHRAE (ASHRAE,2008)
20-23	30-60	Minimum 15 ACH, with at least 3 ACH of outdoor air.	Positive pressurization.	American Institute of Architects (AIA,2006)
18-21	50-60	15-25 ACH	Positive pressurization.	Ministry of Health, Malaysia (MOH,2010)

2.1.3 Temperature

The temperature control of the operating room should be in an acceptable condition in accordance to the standard referred. Despite the range of temperature control, there should be a uniform air temperature distribution in the operating room. However, subject to the type of operation, the setting temperature will vary. For cardiac surgery, for example, room temperature of 17 °C should be maintained (ASHRAE, 2003). Operating room temperature should be maintained between 21°C and 24°C to prevent intra-operative hypothermia. Patient and surgeon or staff will have different perceptions of the room air temperature in the OR, which will form two distinct groups with regard to the acceptability of the thermal condition.

For a patient, there are significant linear correlations between patient esophageal temperatures and OR temperatures at the gap between the first and until the third hour after anesthesia induction (Morris, 1971b). Apart from this, an OR's temperature can be classified by its effect on the patients' temperature, as shown in Table 2.4.

Table 2.4: Classified of OR by their effect on patients' temperature (Morris, 1971b).

Classification	Description	Room temperature
1	Patients become hypothermic	$T_{room} < 21^{\circ}\text{C}$
2	70% of the patients remained normothermic whilst 30% become hypothermic	21°C – 24°C
3	All patients remained normothermic	24°C – 26°C

For elderly patients, under typical ambient OR temperature (20 °C -23 °C), inadvertent hypothermia often occurs during general anesthesia. From a study involving both younger and elderly patients receiving general anesthesia for orthopedic surgery, an ambient OR temperature around 26 °C was found to prevent core hypothermia, regardless of the age of the patient (El Gamal et al., 2000). However, when simple

warming measures are applied, an OR temperature of 24°C has been determined as effective in maintaining normothermia during liver transplantation in pediatric patients (Huang et al., 2005). Often, a system that delivers heated air through an inflatable blanket is used in order to prevent hypothermia in the patient. The disadvantages of this system are that, besides the air emitted altering the flow field, it also increases the bacteria in the operating field (Tumia and Ashcroft, 2002). Since the room temperature will affect the patient's body temperature, it is vital for all patients experiencing surgery for more than half an hour to receive an accurate core temperature monitoring (Morley-Forster, 1986, Putzu et al., 2007). From the assessment of thermal comfort of personnel in the OR during surgical operations, the room air temperatures required for desired thermal comfort (assuming a uniform thermal environment) are described in Table 2.5.

Table 2.5: Thermal comfort assessment for occupants in OR (Mora et al., 2001).

Classification	Clothing and Activity level	Temperature range,
Nurses	Clothing level (clo) of 0.42-0.78 Activity level (met) of 1.4	23°C – 24°C
Anesthetists	Clothing level (clo) of 0.42 Activity level (met) of 1.4	23°C – 24°C
Surgeon	Clothing level (clo) of 0.86 Activity level (met) of 1.6	18°C – 19°C
Patient	Fully covered with clo 1.1, met 0.69	24.5°C – 25.5°C

Surgical light produces radiant asymmetry from 6°C – 7°C over the operating table and 10°C – 12°C at a height of 1.1m over the floor level (Mora et al., 2001). Thus, surgeons will feel thermal discomfort no matter what temperature is. For child, the setting temperature should keep at higher range. Higher indoor temperature will result in favourable growth of bacteria and enforce the bacteria mitigation to and from the patient.

2.1.4 Humidity

Controlling air humidity is important as it is directly related to thermal comfort. Low humidity can generate problems related to static electricity in medical equipment and on surfaces. Since volatile anesthetics are flammable, to avoid any hazard from electrostatic discharge, the RH in the OR should be kept above 35% (Harriman, 2001). Thus, in countries with four seasons, humidification is needed during winter to increase humidity levels to ensure there is no possibility for transferring bacteria to the OR. Meanwhile, for hospitals located in the tropics, this problem becomes unimportant, and instead, dehumidification of outdoor air is a major concern. High humidity levels will cause thermal discomfort (Fanger, 1970), and promote the growth and transfer of bacteria that can conveniently become airborne in water molecules. Another problem caused by high humidity in the OR is the condensation of air. The ability of a system to easily keep the RH below 60% depends on the system design. If the system is designed to control the temperature at between 21°C and 23°C, it will have problems keeping RH below 60% at 17°C (Harriman, 2001). In the tropics, as the air is hot and humid all year round, the humidity control of RH becomes difficult. If the supply air is cooled down much lower, there will be wastage since the chiller efficiency drops and reheat energy increases. The use of pre-cooling equipment is favorable since it provides efficient humidity control while conserving energy (Yau, 2008, Li et al., 2005).

In RH between 40-60%, at 22°C with 15 minutes of exposure, influenza A has a low ability to survive. This suggests that the virus will survive longer in higher or lower humidity (Brundrett, 1990). This was supported by a previous research carried out by Songer (1967) at 23°C for viruses. However, in 1943, Loosli et al. studied the influence of humidity on survival of the influenza A virus in air, in temperature ranges

of 27-29°C. They found that at high RH (80-90%), one hour after release of the virus, it becomes non-infective (Loosli, 1943). This suggests that different temperatures affect the viability of the virus besides RH. Viruses which possess higher lipids content tend to survive longer at lower relative humidity, while viruses with less or no lipid content are more viable in higher relative humidity (Assar and Block, 2001). Thus, different types of virus will have different survivability for a given range of RHs. However, airborne particles can survive in various humidity levels. For example, on-pathogenic bacteria have shown to be more lethal in a mid-range of humidity conditions (40-60%) (Hatch and Wolochow, 1969).

Particularly in hot and humid country, in order to meet the stipulated requirement for RH control in an OR, an economical method by incorporating heat recovery device such as heat pipe heat exchanger, desiccant wheel will be a feasible mean in treating the moist air in a hot and humid climate.

2.1.5 Air velocity and air change rate

Since an OR must be at least in the ISO 14644-1 Class 7 or Class 8, the average room velocity setting should be at least from 0.02 to 0.09 m/s, and the air change rates at different rooms with a height of 2.5 m, 3 m, 6 m and 9 m are listed in Table 2.6.

Table 2.6: Vertical airflow velocities and ACH versus cleanroom classes (ASHRAE, 2003b).

Class ISO 209	Average Room Velocity, m/s	ACH			
		2.5 m Ceiling	3 m Ceiling	6 m Ceiling	9 m Ceiling
2	0.43 - 0.51	638 - 750	510 – 500	255 – 300	170 - 200
3	0.36 - 0.43	525 - 838	420 – 510	210 - 244	140 - 170
4	0.30 - 0.36	450 – 525	360 – 420	180 – 210	120 – 140

5	0.23 - 0.28	338 - 413	270 - 330	135 - 165	90 - 110
6	0.13 - 0.18	166 - 263	150 - 210	75 - 105	50 - 70
7	0.04 - 0.09	60 - 120	50 - 100	24 - 48	15 - 30
8	0.02 - 0.04	30 - 45	25 - 35	12 - 16	8 - 12
9	0.010 - 0.015	15 - 23	12 - 18	6 - 9	4 - 6

The air change rate can be calculated from the equation below (ASHRAE, 2003b):

$$ACH = \frac{3600Q}{LWH} = \frac{3600v}{H} \quad (2)$$

where L, W, H are the length (m), width (m), and height (m) of the room, respectively.

And,

v = room air velocity, m/s

ACH = air changes per hour

ASHRAE (2003) recommends a minimum of 25 ACH with a minimum of 5 ACH of outdoor air per hour, while ASHRAE (2008) suggests a minimum of 20 ACH with a minimum of 4 ACH of outdoor air (Table 2.3). Higher values of air change per hour should be used to maintain temperature and humidity conditions based on the cooling load of the space (ASHRAE, 2003a).

The number of ACH and filter efficiency will both influence the time required for airborne contaminant removal, as described by the relation below (Sehulster and Chinn, 2003):

$$t = -\frac{\ln\left(\frac{C_2}{C_1}\right)}{ACH} \times 60 \quad (3)$$

where $\frac{C_2}{C_1} = 1 - \frac{\text{Removal efficiency}}{100}$

ACH= Air change per hour

t= time required to achieve removal efficiency in minutes

The time needed for removing particles is shorter if the air change per hour is higher. The time needed for removing particles is halved if the ACH is doubled. For example, by increasing the ACH from 10 to 20, the minimum time for particles removal is reduced from 28 to 14 minutes with 99% efficiency. A parametric study by Chen et al. (1992) showed that it is desirable to apply a higher flow rate, larger inlet area, and a uniform velocity of supply air to achieve better air quality and air comfort. However, this does not necessarily indicate that the percentage of particles that strikes the surface of concern decrease continually (Memarzadeh and Manning, 2003). From this study, the ACH becomes an important parameter as the ceiling height is reduced. It was found that as Archimedes number, Ar increases, the contamination level will be reduced at the operating table (Memarzadeh and Jiang, 2004).

This suggests that Ar should be taken into account in the designation process in the OR. Archimedes number addresses buoyancy and inertial force, $Ar = \frac{Gr}{Re^2} = \frac{Lg\beta\Delta T}{u^2}$, where L represent the room characteristic length, ΔT is difference of maximum temperature and mean room temperature and U denotes supply air velocity. Also, g and β are gravity and thermal expansion coefficient, respectively. Natural convection is considered dominating when $Ar > 10$.

At higher ACH (30ACH), the natural convection effect diminishes. It causes the indicator of natural convection, Ar to reduce considerably, hence resulting in higher percentage of particle hitting surgical site. As the ceiling height is reduced to the lower limit of 2.74 m (9 ft) – 3.66 m (12 ft) for typical OR height, the supply air inflow should be kept low at 20 ACH (Memarzadeh and Jiang, 2004).

2.1.6 Pressure

In the OR, air is only allowed to flow from highly sterile to less sterile places in order to fulfil the hygienic requirements. Any pressure differential across the room will cause infiltration through leakage areas. The OR should be maintained at positive pressure to prevent contaminated air entering, with a minimum pressurization of 2.5 Pa, provided the room is tightly sealed. Opening a door will immediately cause the pressurized effect to annul (ASHRAE, 2003a). Owing to the special emphasis on the pressure differential for the OR, specific pressure control can be achieved by introducing zone pressurization like flow tracking and differential space pressurization (Jensen et al., 2005). For a typical case of an OR, which has a leakage area of 0.046 m^2 , by supplying an excess air of $212 \text{ m}^3/\text{h}$ compared to exhaust air, positive pressurization of 2.5 Pa can be achieved (Streifel, 2000). A sliding entry door is preferable over a swing door. If a swing door is used, it should be opening into the OR. Regular maintenance of the filtration system is needed to ensure the pressure difference as designed. In line with this, Leung et al., in their review, identified effective Indoor Air Quality (IAQ) monitoring methods as well as mitigation measures suitable for a hospital environment (Leung and Chan, 2006). A study on contamination diffusion to the OR when the door was open was performed by Dong et al. Again, as suggested, opening a door will cause the loss of positive pressurization. The pressure difference is significant when the temperature difference is high. In order to improve the prevention of contaminant intrusion, it is useful to lower the corridor temperature by 5°C compared to the OR, or to keep a 1°C temperature difference incorporated with increasing positive pressure and airflow (Dung et al., 2009).

When Hong Kong was affected by the Severe Acute Respiratory Syndrome (SARS) crisis during 2003, it introduced the need to convert the OR and the ward to negative pressure in order to isolate the patient and prevent the spreading of viruses,

since SARS was confirmed as an airborne infection case. For changing the OR to a negative pressure design, much stronger low level exhaust systems had to be installed on the side walls. The exhaust air passed through a pre-filter and High Efficiency Particulate Air (HEPA) filter before being discharged by the exhaust fan. Besides this, all doors leading to these negative pressure rooms were made airtight and interlocking. Automatic sliding doors were also built at the opposite side of the anteroom. Chow et al. found that the physical environment and the dispersion pattern of bacteria in a negative pressure OR was as good as the original positive pressure design after the comparison of both ORs on temperature, concentration distribution of bacteria and velocity vector that have been simulated through the computational fluid dynamics tool (Chow et al., 2006).

While temperature and RH control serve as a comfort for the occupants in an OR, pressure differential serves a protection shield that protect the OR from the intrusion of infectious particles. ACH, pressure differential checking, and microbiology sampling are important for commissioning a hospital. The details on the commissioning of both conventionally-ventilated and ultraclean ventilated ORs were summarized and discussed by Hoffman et al. (1993) , as well as Jowitt and Morris (2004).

2.2 HVAC systems & air distribution and ventilation systems

2.2.1 Air distribution and ventilation systems

The ventilation system in the OR may help to reduce the risk of airborne cross infection or may increase the transmission of disease depending on the airflow pattern. Ventilation with clean air is one of the easiest and well-known approaches to eliminate pathogens and reduce the risk infection in the OR, where air flows from a demanding zone to a less demanding zone. Ventilation, air distribution and room pressurization are

the main features of the airflow system in the operating room. Dilution models are often being used as an indication for HVAC supply air distribution effectiveness, which leads to better dilution by higher ACH. A dilution effect is achieved by the use of ventilation, which enables the reduction of airborne contaminants. The air quality evaluation in OR is assessed by performing air sampling for counting microbiological contents in terms of colony forming units (CFU/m³) or particle counting. One point to note is, albeit bacteria are always assumed to be transported by particles exist in OR, however, the test for particle count could not take the place of microbiological sampling for a routine evaluation. It is supported by the finding of Landrin et al. (2005), since the methods for both tests do not correlate with each other.

The relative significance and optimum design characteristics of the OR air distribution might vary as medical treatment and other factors vary over time for particular types of surgery. If postoperative infections can be ignored, the conventional operating room HVAC distribution with proper design may satisfy the indoor conditions. However, if postoperative infection is a vital issue, then it requires both the medical and engineering personnel's efforts to determine the relative importance, cost effectiveness and benefits of the HVAC air distribution system (Lewis, 1993). Controlling the central region, where the operating lights and surgical staff contribute large heat sources, is the main focus in designing an OR ventilation system. Conventionally, controlling the number and the movements of the personnel in the room is important in limiting the quantity of contaminants released into the air (Scott, 1970, Ayliffe, 1991). Moreover, the existence of medical equipment and staff will strongly influence the contaminant distribution (Woloszyn et al., 2004). There are various types of air distribution systems aimed at reducing bacteria, viruses and dust concentrations to the threshold level satisfying health guidelines of patients and staff. It is hard to state which type of air

distribution system is most suitable for the OR, since every researcher has their own opinion. Although those airflow patterns are separated into different types in the next discussion, they are still connected with each other.

Since the 1960s, two different methods have been used to ventilate the air in the OR, namely turbulent ventilation and displacement ventilation (Lidwell and Blowers, 1962). The differences of both methods are listed in Table 2.7.

Table 2.7: The differences between turbulent ventilation and displacement ventilation (Lidwell and Blowers, 1962, Hambræus and Laurell, 1980).

	Turbulent Ventilation	Displacement Ventilation
Supply air	Also known as conventional wall supply. The air is supplied through a high level ceiling grille to produce a turbulence air throughout the room, with a velocity of 0.2 m/s at the centre of the room.	The air is supplied through several diffusers installed over the ceiling which is able to create a low-turbulence by displacing the air downward over whole room. Exhaust air was discharged by the exhaust via low-level ports located around room periphery. The turbulence velocity at centre of the room was around 0.05 m/s.
Advantages	Bacteria released near to the operating table were quickly scattered away. Vigorous air movement able to provide a good thermal comfort to occupants though at high temperature and humidity level.	Microbes were cleared more rapidly compared with turbulence ventilation, where it was able to sweep away the microbes liberated around floor and room periphery away from operating zone. The system able to maintain low room temperature.
Disadvantages	There was possibility of the microbes liberated around the floor or room periphery transport into operating zone.	Microbes released near the wound are slowly dispersed due to low air velocity at room center. Significant movement by surgical staff will tend to create turbulent air movement and destroy piston effect.

In an OR with turbulent airflow, the level of microbial contamination will vary greatly, depending on the type of surgery performed (Zamuer, 1986). The momentum of supply air for displacement ventilation is usually small. Buoyancy is the dominant force for creating the air movement. In a no plume region, displacement ventilation becomes inefficient. Upward displacement and downward displacement are two methods derived from displacement ventilation. The former is widely used, since it is able to produce better IAQ for the occupants. If the contaminant is widespread inside the OR, undoubtedly a downward displacement will be better than turbulence ventilation. However, if the contamination sources are localized, turbulence will be superior (Blowers and Crew, 1960). In 1970, Scott (1970) noted that both turbulent ventilation and displacement were not able to oppose the convective air movement created by the heat transfer from the human bodies and operating lamps (Scott, 1970). In a moderate low level stratified room, the maximum centreline velocity of the thermal plume is 0.2 m/s, which corresponds to the plume flow rate of 20-30 L/s. The plume flow rate will further increase to 70-80 L/s in a uniform environment (plume maximum centreline velocity of 0.3 m/s) (Craven and Settles, 2006). Later, laminar airflow systems were suggested. A comparative research on different combination of ventilation in OR was investigated by Memarzadeh and Manning (2002). Conventional turbulent ventilation, different layout of laminar ventilation system and upward displacement ventilation were evaluated by the effectiveness of particle removal via ventilation incorporated with thermal plume consideration. Conventional ventilation is found to have a poor effectiveness compare with other laminar configurations, due to the generation of large recirculation in the room. Generally, the rule of thumb is that the main airflow pattern should directly flow, without any obstruction to the operating zone, with low air velocity to avoid turbulent flow and provide thermal comfort for occupants.

2.2.2 Laminar airflow (LAF)

Laminar airflow (LAF) in operating rooms is best known as unidirectional airflow, since true laminar airflow does not exist for a variety of reasons. This is a method that prevails the ventilation method using turbulent flow (Pfost, 1981). A LAF system requires the transport of a uniform huge volume of clean air, discharged from entire ceiling. However, this design will be costly. For the purpose of cost saving, Babb et al. (2005) studied the possibility of the use of a large room containing several units ventilated by LAF and a scrub area by assessing the risk of airborne spread of infection among the rooms. Another alternative is reducing the area of laminar flow to a critical zone around the operating room table. This method, however, will produce entrainment inside the room. LAF destroys convection currents due to heat or movement and entrains the particles away from the operating zone. LAF is defined as airflow of parallel flow lines with minimum eddies by no obstruction, and usually achieved with an air velocity of 0.45 m/s, which can be either directed vertically from the ceiling or horizontally from the wall, with or without fixed or movable walls around the operating table. Whenever there is any obstacle in the flow field of laminar flow, the laminar flow pattern will distort in a small area around the obstacle. Again, though it is defined as such, in real life it is deemed non-existent, since the existence of obstructions interferes with the airflow. In a three dimensional space, LAF could be achieved by two means: vertical flow (from ceiling to floor) and horizontal flow (from wall to wall).

Vertical laminar flow

In general, outlets for supply air should be located on the ceiling with few exhaust outlets close to the floor at the room periphery. This arrangement will provide a downward laminar movement of clean air through the operating table to the contaminated floor area, before flowing into an exhaust. Convection currents due to heat

or movement will be eliminated, and the re-entrainment of particles to the operating area will be stopped (Chow and Yang, 2004). If the ventilation (dilution) effect is higher, it will reduce the concentration of airborne contaminants. Low velocity laminar flow tends to minimize the spread of bacteria, viruses and anaesthetic gases by providing a relatively uniform and large clean airflow. Contaminated air or particles are exhausted as soon as they are released without migration to other areas. Small particles are more readily removed than larger particles, since the buoyancy force dominates the gravitational force on smaller particles, hence lifting them easily. Whereas for large particles, the gravitational force dominates the buoyancy force, causing large particles to be suspended on the surface (Woods et al., 1986). During surgery, movements often take place. These movements will influence the flow field. Yet, in flow simulation studies, movements are always disregarded due to their complexity. For surgery which requires an ultra-clean environment (such as orthopedic), the transport of bone cement from outside of the LAF field to the clean zone will introduce a serious risk of contaminant transport (Brohus et al., 2006). Traditionally, in order to prevent the contaminated peripheral air to be deflected into the ultraclean zone, walls were built to enclose the ultraclean zone. These, however, will be an obstacle for the surgical team. Since walls or panels restrict the movement of staff, an exponential flow of clean air was introduced. This is an overhead canopy, where the air flows centrally downwards, then radially outwards, with return grilles mounted at a low level near to the floor. This method was claimed to achieve zero cfm/m^3 (Horworth, 1985). However, it was challenged by the elimination of side walls. The prevention of peripheral air entrainment is achieved by using a ceiling of higher airflow, and lower flow in the peripheral zone, without compromising bacteriological safety (Friberg et al., 1996). This configuration will create an air curtain surrounding the primary clean zone around the operating table. Since it is costly and disruptive to renovate existing ventilation

facilities, a mobile exponential LAF screen can be used to compliment and improve current existing conventional turbulent OR ventilation (Friberg, 2002).

In many cases, the area in a vertical LAF room is too small to store all the equipment for a major surgery. An additional table, such as a horizontal LAF instrument table, is placed side by side with the existing main LAF unit. The smoke test confirmed that this additional table is efficient and can be safely used as an extension for an existing unit (Nilson, 2010). Considerations on the numbers of operating lamps and the numbers of persons in the room are important during the laminar airflow system installation, as they influence the thermal plume and cooling load.

Horizontal laminar flow

Recent studies on horizontal laminar airflow patterns were carried out by Liu et al.. In the design, the supply air and return air were installed on the same lateral wall. The heat generated by the surgical lamp and the thermal plume had no significant effect on the airflow pattern and the air was kept in a unidirectional flow. The relative position of the particle source and the layout of the OR will influence the particles' concentration around the patient, for both types of LAF (Liu et al., 2009, Chow and Yang, 2003). An unfavourable position of the medical lamp might create a high airborne bacteria concentration region. Some precautions have to be taken when using a horizontal LAF system. The position and movement of the surgical staff, which depends on the type of surgery, will affect the rate of infection (Lidwell and Towers, 1969, Salvati et al., 1982). A study on the effect of walking on wake and contaminant transport found that two different wake regions are formed behind the body, one being the unsteady bluff body wake behind the torso via recirculation and the other the unsteady vortex behind the leg by the air jet formed between the legs. This will produce a downwash behind the body,

and the contamination is found to be highly dependent on the source location (Edge and Paterson, 2005).

For a horizontal LAF, the air right after the discharge into the room is the cleanest. When it flows across the room, it becomes contaminated in a horizontal plane. If the wound is located downstream of the contaminant source, most probably infection will occur. Hence, a horizontal LAF may either result in a beneficial or damaging effect. A comparative study between horizontal airflow and the use of ultra violet (UV) light was carried out over a period of nineteen years. Ritter et al. found that the use of UV lighting (without horizontal LAF) is better than using a horizontal LAF (without UV lighting), since the infection rate of the latter was 3.1 times that of the former. They suggest the use of UV light as an effective means, compared with horizontal LAF (Ritter et al., 2007).

However, vertical laminar airflow systems are superior to the horizontal airflow systems because clean air is directed over the operating table. Horizontal airflow is 11 times more efficient, and vertical airflow is 35-90 times more efficient compared to a plenum ventilated OR (Whyte et al., 1973). A study on flow and temperature fields around the human body examined both horizontal and vertical flow (Murakami et al., 1997), determining that in horizontal airflow, the introduced air moves downward to the area below chest level. In a vertical airflow, the flow separation occurs at the head and shoulders, where reverse flow was observed.

The major problem for LAF is the cost benefits (Lipsett, 2008). The use of LAF should be considered on a case by case basis, depending on the type of surgery performed. Although there are many studies supporting the advantages of the use of

LAF, one should bear in mind that during the data collection, exclusion of patient-specific antibiotic prophylaxis, deviations on specific room conditions as well as the performance of ventilation equipment will certainly bias the outcome of the analysis. Usually, measurements of the numbers of bacteria-carrying particles in an OR environment are being used to study the infection rate, by assuming a correlation between contamination levels near the wound and the rate of postoperative infections. As commented by Dharan and Pittet (2002), during the examination of epidemics or the validation of changes in an OR only, environmental bacteria sampling should be performed.

Ultraclean ventilation

As a variation from LAF system, ultraclean ventilation is designed for high risk operations such as orthopaedic implant surgery, where a high level of clean air is necessary. According to the UK Health Technical Memorandum (HTM), HTM 2025, the down flow of a LAF system should cover an area of at least $2.8 \times 2.8 \text{ m}^2$, thus providing an excellent shelter, though there are complex interruptions and amended requirements for different surgeries. The ultraclean ventilation air (UCV), combined with HEPA filter is illustrated in the Figure 2.1.

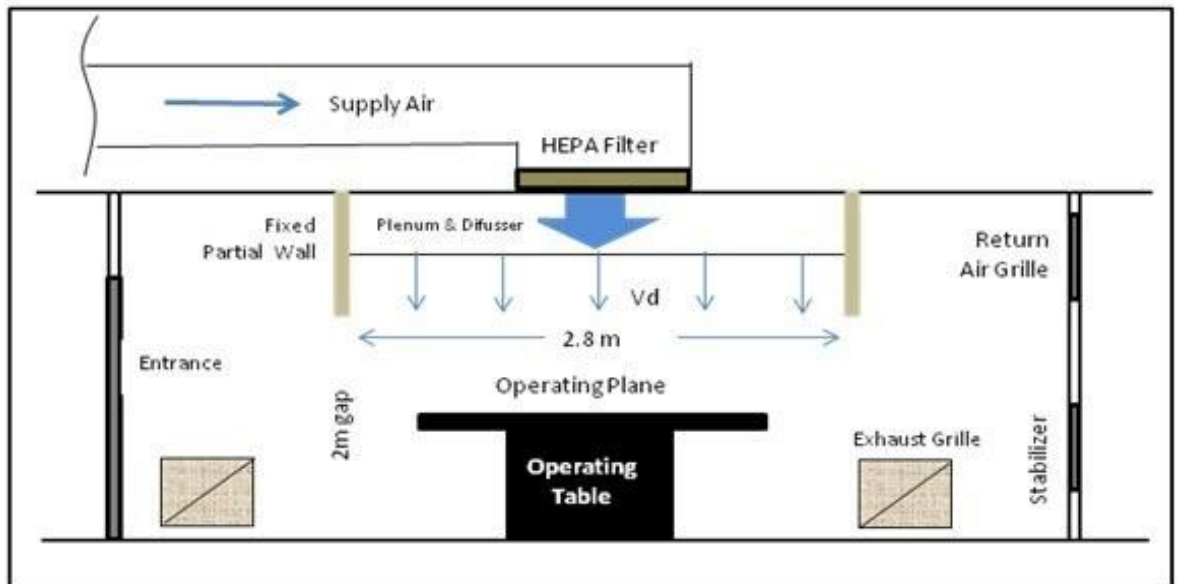


Figure 2.1: Typical ultraclean ventilation (UCV) arrangement in operating room (National Health Services Estate, 1994).

Whenever a partial wall is used, a minimum air velocity is 0.38 m/s at 2m from the floor (National Health Services Estate, 1994). The flow outside the UCV zone is fundamentally turbulent, which depends on the layout of exhaust vents, cabinets, medical equipments or heat source. Whyte et al. made the following suggestions on bacteriological standards in UCV operating rooms (Whyte et al., 1983):

- i. Concentration of bacteria in supply air transmitted from the final filters should not exceed 0.5 cfu/m^3 ;
- ii. Within 0.3 m of the wound they should not be greater than 10 cfu/m^3 on average; and
- iii. In the whole working area at the table height should not exceed 20 cfu/m^3 .

From the numerical study, at high air velocity (0.38 m/s) at the supply diffuser, the buoyant forces caused by the heat source (e.g. medical lamps and medical equipment) are not obvious. When the air velocity is lowered, the thermal plume of these pieces of equipment becomes observable. At high air velocity, the heat source and outlet location have a negligible influence on the distribution of the particle concentration in the room, hence the bacterial concentration in the vicinity of the wound is kept minimal (Chow

and Yang, 2005, Chen et al., 1992). The purpose of the curtain is to enhance the laminar flow. However, a lengthy curtain (e.g. 1 meter) will promote the thermal plume, and limit the entrainment of warm air. The researcher found, there is no interpretation could be made on the curtain will either reduce the pollution due to knotty relation between heat source and skirt length (Al-Waked, 2010, Memarzadeh, 2010, Al-Waked, 2010). The use of a forced-convection heater is common during the surgical procedure nowadays to prevent hypothermia of patient. Additional heat source beneath the curtain will certainly evoke the concern on the possibility of the heater become a contaminants' source in the OR. The use of the convection heater will create a small increment on the number of CFU in the UCV, but the increment of the CFU has low possibility giving a clinical impact (Tumia and Ashcroft, 2002). On the other hand, in a transient study on the benefit of the curtain, even at low supply air velocity (0.2 m/s), the existence of the curtain will foster the contaminant decay on surgical site (Fu et al., 2011). It is clearly seen that, there exists pro and con on the installation of curtain. As long as the curtain length is properly catered on heat source and OR design, the installation of the curtain will benefit on reducing contamination.

From the literature survey, the investigations on the airflow in an OR in recent years (particularly year 2000 onwards) have focused on the laminar type of OR design. Hence, LAF design has become a commonly accepted OR design nowadays. However, their overall design might vary from place to place. Since thermal plume is a phenomenon appears in OR that will harm the LAF, thus most of the study has included the consideration on the existence of thermal plume and some method to reduce its effect in OR. Meanwhile, the cost for treating the fresh air is higher compare with other ventilation design. When the operating cost becomes a main consideration in the design

of an OR, which particularly happens in developing country (Kelkar et al., 2004), a conventional type of OR ventilation can be an alternative option.

2.2.3 Upward displacement ventilation

Upward displacement ventilation (convection ventilation) provides cool clean air at the floor level. It blows the contaminated air to the ceiling by means of convection heat transfer. The advantage of upward displacement ventilation is the provision of thermal comfort to personnel. From the aspect of thermal comfort, the air temperature in the vicinity of the floor and the vertical temperature gradient in the occupied zone are significant and should be taken into account at the design stage. The vertical air temperature gradient should be less than 2 °C/m (Yuan et al., 1998). The air distribution for displacement ventilation is dependent on the flow rate of the thermal plume, wall layers due to buoyancy, and supply air. For example, a standing person in a 15.4 m³ displacement ventilation room with supply air at 22°C, air velocity of 0.12 m/s and 3.7 ACH will produce a thermal plume with maximum rising stream of 0.23 m/s over the head (Murakami, 2000). Hence, the airflow distribution is dependent on the flow rate of the thermal plume, supply air and buoyancy of the wall layer. The contaminant concentration in the occupied zone becomes low when the plume is able to reach the upper zone (Murakami, 2000). However, upward displacement ventilation relinquishes the function of reducing the number of bacteria-carrying particles in the OR. In order to prevent the recirculation of contaminated air into the occupied zone, the total rate of supply air near the floor must be equal to the sum of the flow rates, due to the convective currents from the vertical surface, the plumes and the outdoor air requirement of the occupants (Awbi, 2003). For an OR, the recommended outdoor air requirement is 15 L/s per person (ANSI/ASHRAE, 2003).

In comparison to standard positive pressure ventilation systems (supply air from the ceiling and evacuated at the floor), the airflow pattern of upward displacement ventilation is insufficient to transport larger particles up to the ceiling for evacuation. Upward displacement ventilation is more efficient in removing small dust particles sized 0.16 to $<10\mu\text{m}$. Normally, the size range of bacteria-carrying particles is between 4 - 28 μm , with a mean of 12 μm (Dharan and Pittet, 2002). Moreover, upward displacement ventilation is not recommended for normal surgery, since clean air discharged by the diffusers near the floor level is not able to be delivered to the wound area, as it is hindered by the table and surgical team. However, it is possible to be used in open laser surgery (Friberg et al., 1996). The dependency of upwards displacement on the existence of thermal plume, and limitations on transporting larger particles constrained the use of upward displacement ventilation in OR design.

2.3 Supply air and return air diffuser

Outdoor air intakes must be located away from the system's exhaust air and other building's emission outlets, by taking into account the prevailing winds, building geometry, adjacent buildings or other obstructions (ASHRAE, 2003a). In a general OR, the supply air outlet should be placed on the ceiling, while the few exhaust outlets must be placed at least two locations near the floor to provide proper downward flow of clean air through the critical zone, and eventually to the contaminated floor area for exhaustion. The ideal layout of the air exhaust outlets is one at every corner of the OR, one near the floor and one near the ceiling to contribute uniform air circulation inside the OR. A combination of exhaust locations level will perform better than merely on low or high level locations. It is pertinent to recap the point mentioned by Memarzadeh and Jiang (2004), when sizing the laminar flow array, designer has to ensure the array is

being sized to cover main heat dissipating object such as surgical team and operating lights as well as the operating table.

A laminar flow diffuser has been chosen in the OR to provide unidirectional or laminar discharge perpendicular to the mounting surface, so it can develop a uniform velocity profile over the full space. High induction ceiling or sidewall diffuser should be avoided. With at least two air-exhaust outlets near the floor, the first position of exhaust must be at least 75mm above the floor (ASHRAE, 2003a) to remove the anaesthetic gases, because these gases are heavier than the air. Anaesthetic gases must be cleared because they can cause health problems, discomfort to the medical staff and also create a fire hazard in the OR. The second air flow should be positioned near the ceiling in order to efficiently eliminate bacteria and other microorganisms and chemical substance that may become airborne during surgery. An air diffuser must have a good performance over a wide range of discharge velocities, since air distribution patterns are as important as the ACH. An ACH of 20-30 is recommended for a ceiling height from 9-12 ft (2.74-3.66 m). Non-aspirating diffusers with a face velocity of 0.13-0.18 m³/s per m² are recommended for maintaining the laminar flow and reducing strong drafts in the OR (Memarzadeh and Jiang, 2004). In a LAF system, particles are forced to the exhausts by the air flow. The diffuser array should cover the main heat dissipating objects (Memarzadeh and Manning, 2003).

For an OR with conventional ventilation, the best ventilation can be achieved by placing the supply grilles nearer to the vertical centreline of the wall, while the air is exhausted through low sidewall grilles on the opposite wall. The location of the exhaust grilles is negligible in affecting the overall ventilation performance (Ho et al., 2009).

2.4 Filters

In an OR, all central ventilation or air conditioning systems should be equipped with at least 2 filter beds. For ORs serving as orthopedic, bone marrow transplant or organ transplant surgeries, the filter efficiency should have a Minimum Efficiency Reporting Value (MERV) of 8 and 17, respectively. The first should be located prior to the air conditioning equipment, while the second should be placed downstream from the supply fan. For general procedures in the OR, filters with a MERV of 14 can be used downstream from the supply fan (ASHRAE, 2003a, Kowalski, 2006). If there is any recirculation of air, it will require greater demands on the filtration system. Proper maintenance of the filters is crucial to reducing the microbial growth in the indoor room air and in the AHU system. Sometimes, filters themselves can become a source of bacterial growth and thus contribute to the high level of pathogens in the occupied space, since during the periods of high humidity (>80% RH), a proliferation of bacteria on the air filter will be released into the filtered air later on. Therefore, controlling the relative humidity of the air filters to 80% is important to avoid microbial proliferation (Möritz et al., 2001). Filter efficacy should never be degraded by poor installation. Any gap existing post-installation will allow unfiltered air to bypass the filter. Consequently, sheet metal blank-off panels are required to be attached and sealed to the frame permanently (Ninomura et al., 2006). Besides, if the pathogens are generated inside the room, filters are not efficient in protecting the occupants. The main filter group includes filters for removing solid and liquid particles, filters for removing gases and vapors and, lastly, filters for removing bacteria (e.g. ultraviolet or germicidal lamps).

HEPA or ultra-low particulate air (ULPA) filters provide the greatest efficiency. A HEPA filter is more than 99.97% efficient in removing particles of 0.3 μ m size, while a ULPA filter is at least 99.999% efficient in removing particles of 0.12 μ m size. HEPA filters are only necessary to be used in the OR, while other rooms, such as the

washroom and anesthesia preparation room, do not require being treated with HEPA (Sherrer, 2003).

Ultraviolet Germicidal Irradiation (UVGI) is emitted at a wavelength of 253.7 nm by low pressure mercury vapour arc lamps, which damage DNA/RNA of pathogens and suppress the reproduction of pathogens (Bolashikov, 2009). Room ventilation rates, UV irradiance levels, airflow patterns, bacteria sepsis, RH, as well as photoreactivation will all influence the efficacy of the UVGI. Increasing the ventilation rate will also increase the overall removal of airborne contaminants, but it will reduce the relative effectiveness of the UVGI system, because the average time that the bacteria are exposed to the UV radiation is reduced (Xu et al. 2003). Photoreactivation will annul the effectiveness of UVGI, since once the microorganisms are exposed to visible light they have a chance to recover from the UV inactivation (Peccia and Hernandez, 2001). On the other hand, the effect of RH on the efficacy of UVGI is unclear, since different researchers reported different results on this subject (Riley and Kaufman, 1972, Peccia et al., 2001, Rentschler and Nagy, 1942).

2.5 ORs in Malaysia

Malaysia, which situated in vicinity with equator possess a tropical rainforest climate. In author's survey in different ORs located in Malaysia, the ORs adopted LAF design. However, the actual configuration for the inlets and exhausts may vary (Figure 2.2). The inlet could be an array centered above operating table, inlet array surrounds the operating table, or monofilament precision woven polyesters that cover the operating zone. From the measurements, most of the ORs are sized within 20-40 ACH.

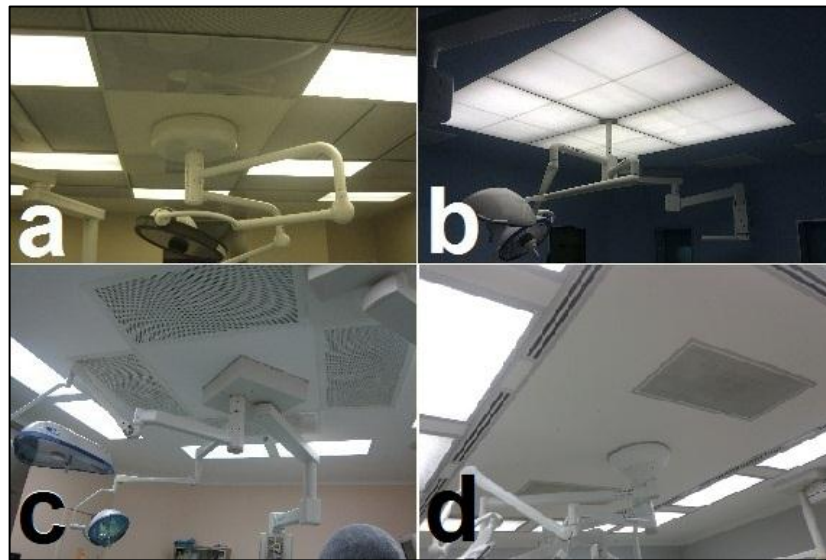


Figure 2.2: Different inlet design of ORs.

There is a common problem found during the surgery, due to massive equipment in OR, the exhausts are often blocked due to insufficient floor area. As shown in the Figure 2.3, surgical staff tends to move the trash or massive equipment to the corner of the OR which is also vicinity to exhaust during the surgery. This scenario is commonly happens in OR. The blockage of the exhaust will definitely obstruct the flow. It appears that, human factor contributed to improper airflow in OR. Hence, it is pertinent for surgical staff to be aware of the consequences on putting any major items that will obstruct the outflow.

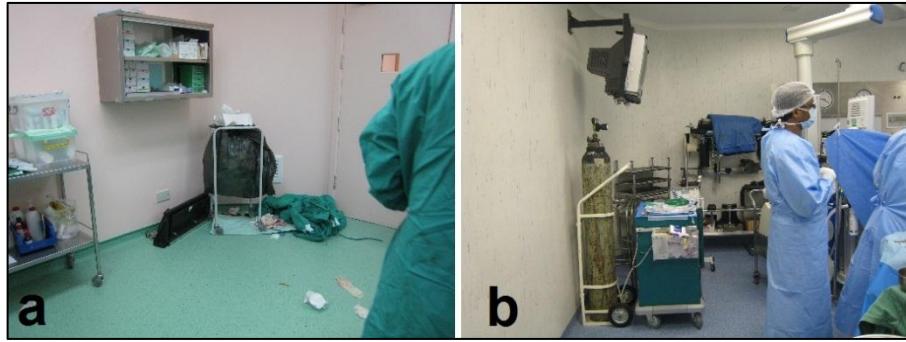


Figure 2.3: Exhaust blockage-common problem found during surgical process.

2.6 Concluding summary for literature survey

In the beginning of this chapter, main design considerations (temperature, humidity, air velocity, ACH and pressure) had been discussed. The development of OR ventilation design had undergone a shift of trend from turbulence, displacement ventilation to laminar airflow system, which is higher in operating cost. However, it does not reflect conventional designs of OR are obsolete since conventional design still has its advantage in terms of cost benefit. Treating the highly humid fresh air will certainly demands for high energy consumption. In order to meet the stipulated requirement for RH control in an OR, an economical method by incorporating heat recovery device for reducing energy consumption and better RH control is recommended.

There are numbers of aspect that influence the air path inside OR, starting from the inlet to until the air being discharged at exhaust and hence numerous studies have been conducted on the design parameters of OR. From the on-site survey in numbers of ORs located at Malaysia, most of the ORs designs are not fully comply with the recommended design criteria. As example, some of ORs were designed such the way that there were only two exhausts located at the same plane of sidewall, which void the symmetry of the exhaust design.

In designing an OR, there are number of issues need to be considered, such as type of surgeries performed, normal duration of surgeries which determine both comfort and patient's need. The system designed should able to control humidity level in both high and low indoor temperature setting. Usually, after years of operation, the layout inside OR will change. Conformity on the performance of air distribution, checking of ACH and pressure differential as well as microbiology sampling should be carried out, to ensure the sustainability of OR.

Computational fluid dynamics aids researchers to study the optimization of OR's design along with experimental investigation. At the same time, it is advisable to take into account the Archimedes number when designing OR. By using the same approach, during the design stage, the designer should evaluate different design schemes which the design of air inlet, air outlet, air flow rate and OR's layout are varied. The use of computational method should be performed in the scenario as close as actual situation where the OR will operate after commissioning.

Last but not least, from the literature survey, the investigation on ventilation and distribution of air in OR is limited in developing countries (that often operate with a non-standard OR). Therefore, it is favorable for a researcher to conduct a case study, in order provide a sufficient overview on the OR worldwide through case study.

3.0 Methodology

3.1 Overview

Workflow of the study is summarized in sequence as follows:

i. Permission to gain into access to hospital operating room

Permission is required in order to conduct on-site clinical observations and measurement in hospital operation room (as attached in Appendix A).

ii. Field measurement in hospital operation room

Measurements have been carried out at various location and on-site clinical activities have been recorded.

iii. Conduct CFD modeling via suitable solver to examine the room airflow pattern

iv. Quantitative assessment and verification of the CFD simulations

Assess and verify CFD simulations by comparison with the measurement result, possibly after enhancement of the CFD simulations.

v. Analysis on the current design and comparison with design with modifications

3.2.1 Governing equations and general form of governing equations

In CFD analysis of room airflow, transport equations are developed based on the conservation of mass, momentum, thermal energy, and sometimes along with concentration of species within the enclosure. It requires a balance among all the factors which are influencing these variables.

Conservation of mass

$$\frac{\partial \rho}{\partial t} + \frac{\partial}{\partial x}(\rho U) + \frac{\partial}{\partial y}(\rho V) + \frac{\partial}{\partial z}(\rho W) = 0 \quad (4)$$

In turbulence flow, fluctuation of air velocity occurs. Hence, summation of time-average component and fluctuating component are used in lieu the velocity of each component, which are described in equations (4.1)-(4.3).

$$U = u + u' \quad (4.1)$$

$$V = v + v' \quad (4.2)$$

$$W = w + w' \quad (4.3)$$

Substituting (4.1-4.3) into (4), yields

$$\frac{\partial \rho}{\partial t} + \frac{\partial}{\partial x}(\rho u) + \frac{\partial}{\partial y}(\rho v) + \frac{\partial}{\partial z}(\rho w) = 0 \quad (5)$$

The direct implication of the mass conservation in CFD is the continuity of flow, which gives an idea the increase in velocity in any component, will cause the reduction in velocity in adjacent component, since the mass flow into any control volume must conserve.

Conservation of momentum (Batchelor, 1970)

For x direction (U-momentum),

$$\begin{aligned} \frac{\partial}{\partial t}(\rho U) + \frac{\partial}{\partial x}(\rho U U) + \frac{\partial}{\partial y}(\rho U V) + \frac{\partial}{\partial z}(\rho U W) &= -\frac{\partial P}{\partial x} + \frac{\partial}{\partial x}\left(\mu \frac{\partial U}{\partial x}\right) + \frac{\partial}{\partial y}\left(\mu \frac{\partial U}{\partial y}\right) + \\ \frac{\partial}{\partial z}\left(\mu \frac{\partial U}{\partial z}\right) + \frac{1}{3} \frac{\partial}{\partial x}\left[\mu\left(\frac{\partial U}{\partial x} + \frac{\partial V}{\partial y} + \frac{\partial W}{\partial z}\right)\right] &+ \rho g_x \end{aligned}$$

(6.1)

For y direction (V-momentum),

$$\begin{aligned} \frac{\partial}{\partial t}(\rho V) + \frac{\partial}{\partial x}(\rho U V) + \frac{\partial}{\partial y}(\rho V V) + \frac{\partial}{\partial z}(\rho V W) &= -\frac{\partial P}{\partial y} + \frac{\partial}{\partial x}\left(\mu \frac{\partial V}{\partial x}\right) + \frac{\partial}{\partial y}\left(\mu \frac{\partial V}{\partial y}\right) + \\ \frac{\partial}{\partial z}\left(\mu \frac{\partial V}{\partial z}\right) + \frac{1}{3} \frac{\partial}{\partial y}\left[\mu\left(\frac{\partial U}{\partial x} + \frac{\partial V}{\partial y} + \frac{\partial W}{\partial z}\right)\right] &+ \rho g_y \end{aligned}$$

(6.2)

For z direction (W-momentum),

$$\begin{aligned} \frac{\partial}{\partial t}(\rho W) + \frac{\partial}{\partial x}(\rho U W) + \frac{\partial}{\partial y}(\rho V W) + \frac{\partial}{\partial z}(\rho W W) &= -\frac{\partial P}{\partial z} + \frac{\partial}{\partial x}\left(\mu \frac{\partial W}{\partial x}\right) + \frac{\partial}{\partial y}\left(\mu \frac{\partial W}{\partial y}\right) + \\ \frac{\partial}{\partial z}\left(\mu \frac{\partial W}{\partial z}\right) + \frac{1}{3} \frac{\partial}{\partial z}\left[\mu\left(\frac{\partial U}{\partial x} + \frac{\partial V}{\partial y} + \frac{\partial W}{\partial z}\right)\right] &+ \rho g_z \end{aligned} \quad (6.3)$$

where for equation (6.1) to (6.3),

P =static pressure

μ =fluid dynamic viscosity

$\rho g_x, \rho g_y, \rho g_z$ =body forces in x, y, z direction, respectively.

Conservation of thermal energy

$$\frac{\partial}{\partial t}(\rho \tilde{T}) + \frac{\partial}{\partial x}(\rho U \tilde{T}) + \frac{\partial}{\partial y}(\rho V \tilde{T}) + \frac{\partial}{\partial z}(\rho W \tilde{T}) = \frac{\partial}{\partial x}\left(\frac{\mu}{\sigma} \frac{\partial \tilde{T}}{\partial x}\right) + \frac{\partial}{\partial y}\left(\frac{\mu}{\sigma} \frac{\partial \tilde{T}}{\partial y}\right) + \frac{\partial}{\partial z}\left(\frac{\mu}{\sigma} \frac{\partial \tilde{T}}{\partial z}\right) \quad (7)$$

Where $\frac{\mu}{\sigma} = \Gamma$ = diffusion coefficient (i.e. diffusivity)

And $\sigma = \mu C_p / \lambda$ is the Prandtl number or Schmidt for the fluid.

Similar with velocity fluctuation, by taking into account the thermal fluctuation, $\tilde{T} = T + T'$, which take into account time-averaged component and fluctuating component, the equation becomes:

$$\begin{aligned} \frac{\partial}{\partial t}(\rho T) + \frac{\partial}{\partial x}(\rho u T) + \frac{\partial}{\partial y}(\rho v T) + \frac{\partial}{\partial z}(\rho w T) &= \frac{\partial}{\partial x}\left(\Gamma \frac{\partial T}{\partial x}\right) + \frac{\partial}{\partial y}\left(\Gamma \frac{\partial T}{\partial y}\right) + \frac{\partial}{\partial z}\left(\Gamma \frac{\partial T}{\partial z}\right) + \\ \frac{\partial}{\partial x}(-\rho \overline{u' T'}) + \frac{\partial}{\partial y}(-\rho \overline{v' T'}) + \frac{\partial}{\partial z}(-\rho \overline{w' T'}) + S_T \end{aligned} \quad (8)$$

The equation (8) above has additional terms which consist turbulent heat fluxes, and S_T , being a source term which allocate the rate of thermal energy production.

Concentration of species equation

$$\begin{aligned} \frac{\partial}{\partial t}(\rho c) + \frac{\partial}{\partial x}(\rho u c) + \frac{\partial}{\partial y}(\rho v c) + \frac{\partial}{\partial z}(\rho w c) &= \frac{\partial}{\partial x}\left(\Gamma \frac{\partial c}{\partial x}\right) + \frac{\partial}{\partial y}\left(\Gamma \frac{\partial c}{\partial y}\right) + \frac{\partial}{\partial z}\left(\Gamma \frac{\partial c}{\partial z}\right) + \\ \frac{\partial}{\partial x}(-\rho \overline{u' c'}) + \frac{\partial}{\partial y}(-\rho \overline{v' c'}) + \frac{\partial}{\partial z}(-\rho \overline{w' c'}) + S_c \end{aligned} \quad (9)$$

Time-averaged concentration, c and the deviation from the averaged value c' are incorporated in the transport equation for species concentration. Equations (7), (8), (9) have a general form as follows.

The General Transport Equation

$$\underbrace{\frac{\partial}{\partial t}(\rho \phi)}_{\text{transient}} + \underbrace{\frac{\partial}{\partial x}(\rho u \phi) + \frac{\partial}{\partial y}(\rho v \phi) + \frac{\partial}{\partial z}(\rho w \phi)}_{\text{convection}} = \underbrace{\frac{\partial}{\partial x}\left(\Gamma \phi \frac{\partial \phi}{\partial x}\right) + \frac{\partial}{\partial y}\left(\Gamma \phi \frac{\partial \phi}{\partial y}\right) + \frac{\partial}{\partial z}\left(\Gamma \phi \frac{\partial \phi}{\partial z}\right)}_{\text{diffusion}} + \underbrace{S_\phi}_{\text{source}} \quad (10)$$

which ϕ describes the dependent variable and S_ϕ is the source term. Table 3.1 summarize the dependent variables and sources terms for equation (10).

Table 3.1: Dependent variables and the source term for general transport equation.

Equation	ϕ	Γ_ϕ	S_ϕ
continuity	1		0
u-momentum	u	μ_e	$-\frac{\partial p}{\partial x} + \frac{\partial}{\partial x} \left(\mu_e \frac{\partial u}{\partial x} \right) + \frac{\partial}{\partial y} \left(\mu_e \frac{\partial v}{\partial x} \right)$ $+ \frac{\partial}{\partial z} \left(\mu_e \frac{\partial w}{\partial x} \right)$
v-momentum	v	μ_e	$-\frac{\partial p}{\partial y} + \frac{\partial}{\partial x} \left(\mu_e \frac{\partial u}{\partial y} \right) + \frac{\partial}{\partial y} \left(\mu_e \frac{\partial v}{\partial y} \right)$ $+ \frac{\partial}{\partial z} \left(\mu_e \frac{\partial w}{\partial y} \right) - g(\rho - \rho_o)$
w-momentum	w	μ_e	$-\frac{\partial p}{\partial z} + \frac{\partial}{\partial x} \left(\mu_e \frac{\partial u}{\partial z} \right) + \frac{\partial}{\partial y} \left(\mu_e \frac{\partial v}{\partial z} \right)$ $+ \frac{\partial}{\partial z} \left(\mu_e \frac{\partial w}{\partial z} \right)$
temperature	T	Γ_k	$\frac{q}{C_p}$
concentration	c	Γ_k	ρC
kinetic energy	k	Γ_k	$G_s - \rho \varepsilon + G_B$
dissipation rate	ε	Γ_ε	$\frac{\varepsilon}{k} (C_1 G_s - C_3 G_B) - C_2 \rho \frac{\varepsilon^2}{k}$

3.2.2 Boundary conditions

Wall

From the on-site visit, the OR is surrounded by the corridors that the outer wall surfaces adjacent to OR are neither directly exposed to heat source such as sunlight nor experiencing heat gain or heat loss, and thus assumed to be adiabatic.

In treating the near wall condition, there are several approaches that could be adopted. They are, namely, wall function, low Reynolds turbulence model as well as two-layer zonal model. In dealing with natural convection, wall function deemed inappropriate due to its suitability for forced convection flow. On the other hand, the use of low Reynolds turbulence model in complicated geometry is unmatched, and it requires the need of fine grid discretization in the vicinity of the wall to solve viscous effect. Hence, the adoption of the last candidate, two-layer zonal model is considered. The zones in the domain are distinguished by the local Reynolds number. The region with $Re_y = \frac{y\sqrt{k}}{\nu} < 200$ (y, k, ν are distance to nearest wall, turbulent kinetic energy and kinematic viscosity) is treated as viscosity affected region based on Wolfstein's model (Wolfstein, 1969). At the region where $Re_y > 200$, the computational domain is treated as fully turbulent region. Further details for this method are available in Fluent user's guide (ANSYS, 2009a).

Room air inlets

Room air inlets are usually the dominant sources of momentum that attributed for air distribution. Velocity components (U, V, W), supply outlet temperature (T), kinetic energy (k) and dissipation rate (ϵ) are need to be specified. By knowing the velocity

components and the turbulence intensity of supply air, the turbulence kinetic energy can be calculated as,

$$k = \frac{1}{2}(\bar{u}'^2 + \bar{v}'^2 + \bar{w}'^2) = \frac{1}{2}(I_u^2 U_s^2 + I_v^2 V_s^2 + I_w^2 W_s^2) \dots (11)$$

where $I_y = \frac{\bar{y}'}{Y_s}$, y and Y denotes turbulence intensity of particular velocity component, subscript s denotes supply air. For isotropic case, $\bar{u}' = \bar{v}' = \bar{w}'$, equation above can further reduce. Dissipation rate of supply air could be calculated by $\epsilon = \frac{k^{1.5}}{\lambda H}$. H is the enclosure height and λ is a constant ≈ 0.005 . For most of the cases for airflow in a room, the turbulent intensity are usually less than 10%.

Exhaust outlets

The longitudinal exit velocity is calculated from mass balance equation, $U_e = U_o \frac{A_s \rho_s}{A_o \rho_o}$ with nonexistent of traverse velocity component. However, for the room with in/exfiltration, this equation is not exact. Subscript e represent exhaust whilst A and ρ represent the opening and air density of both supply and exhaust outlets.

3.2.3 Fieldwork measurement

The air conditioning system had been let operated for 48 hours prior to the visit. Such condition was assumed adequate for the OR to discharge remaining heat, and reached an isothermal condition during the measurement. Besides, there are minimum requirements for the equipment that will be used for the measurement of velocity and temperature, as tabulated in Appendix G. During the measurement, the dimension of OR and equipment were identified and recorded. According to ANSI/ASHRAE (2006a), method of testing the performance of air outlets and air inlets, a difference below 1 °C between tested air and average room temperature could be considered as an isothermal

case. Meanwhile, a temperature difference of more than 2.5°C is considered as non-isothermal air, thus for non-isothermal air, the data measured only valid for that particular temperature difference. Average room temperature in this context is the average of at least four measurements in the spatially distributed in the room to within 0.303 m (1 ft) of increment in a steady state condition.

Air Inlets

Before passing through HEPA, the HEPA casing is designed in such a way that it able to distribute the air evenly into each section of HEPA. During the measurement, air velocity at each inlet had been measured in at least two different of the inlet. The readings were averaged to represent the air velocity for particular inlet. Supply air velocity had been measured by a velocity matrix 2.5 cm (1 inch) below the grille. Main air velocity component in this case is oriented vertically downward.

Exhaust

The air flow at each exhaust had been measured by using a flow hood (Anor balometer) since the method of measuring the air velocity, by fixing the anemometer sensor perpendicular to flow direction cause inaccuracy since the exact flow direction near the exhaust is not known. The measurement at the exhausts had been performed in order to comprehend the proportion of air flow through each exhaust. By using a flow hood for air flow rate measurement will introduce flow resistance due to the existence of the hood. It could be corrected by knowing the pressure difference across the device in the absence and presence of the hood, $Q = Q_h \sqrt{(\Delta p / \Delta p_h)}$. Q denotes the actual flow rate, while subscript h denotes the presence of the hood. Backpressure compensated measurements provides the most accurate flow measurement results, by taking two consecutive flow measurements at a diffuser or grille, the first with the back pressure flap opened and continued with the flap closed.

Air space in room

Room condition had been measured at five different height from the floor (0.1 meter, 0.6 meter, 1.1 meter, 1.7 and 2.3 meter) and it will be used in the verification of the CFD model by the measurement profile (Fong et al. 2009). The velocity measurements had taken into the consideration on which velocity component is more dominant.

As the room air motion is determined by air velocity measurement (ANSI/ASHRAE, 2006b), the speed and direction of the air velocity at any point fluctuate with time. An omnidirectional anemometer should be used for measuring the air speed. However, due to availability of equipment for on-site measurement, a hot wire meter, which is directionally sensitive, had been used during the measurement. The use of this equipment demands for knowledge of primary flow direction. During the fieldwork measurement, the air velocity had been measured in three orthogonal directions. Then the maximum velocity recorded among three orthogonal directions shall be used as the representation of mean air speed. The measurement has to be conducted under steady state condition after the reference temperature is within 1°C of the design temperature. At each measurement point, the air speed and air temperature shall be recorded for minimum 3 minutes with the sampling interval of every 2-4 seconds, for determining the mean value.

3.2.4 Equipment used in fieldwork measurement

As noted by Sun and Zhang (2007), which summarized modern methods for airflow measurement, direct air distribution measurement can provide some quantitative information on local air velocity and flow field pattern. Table 3.2 illustrates the list of equipment used during the measurement.

Table 3.2: List of equipment.

Equipment	Description
<p data-bbox="300 255 603 327"><i>Airflow, differential pressure measurement</i></p>  <p data-bbox="300 730 576 757">Alnor EBT721 balometer</p>	<p data-bbox="676 255 1447 472">The detachable multi-purpose digital manometer is used to measure the air flow rate when it is being attached with measuring hood. When the hood is detached, it able to measure the average air velocity with 16 grids. The static pressure measurement can be done when the digital manometer is connected with static tube.</p> <p data-bbox="676 479 858 506"><u>Operating range</u></p> <p data-bbox="676 510 1206 595">Differential pressure: ± 3735 Pa Velocity: 0.125 to 12.5 m/s using velocity matrix Volume: 42 to 4250 m³/h using capture hood</p> <p data-bbox="676 600 783 627"><u>Accuracy</u></p> <p data-bbox="676 631 1406 716">Differential pressure: $\pm 2\%$ of reading for both static and differential Velocity: $\pm 3\%$ of reading ± 0.04 m/s > 0.25 m/s Volume: $\pm 3\%$ of reading ± 12 m³/h > 85 m³/h</p> <p data-bbox="676 721 794 748"><u>Resolution</u></p> <p data-bbox="676 752 1313 837">Differential pressure: 0.001 Pa (both static and differential) Velocity: 0.01 m/s Volume: 1 m³/h</p> <p data-bbox="676 842 1007 869"><u>Calibration</u> Yearly calibration</p>
<p data-bbox="300 904 571 976"><i>Indoor air condition measurement</i></p>  <p data-bbox="300 1301 660 1364">(i) TSI VelociCalc air velocity meter</p>	<p data-bbox="676 904 1447 1021">Hot wire anemometer is an instrument for turbulent fluid flow. However, main disadvantage of this instrument is its' sensitivity to flow accounted to cosine law which only sense the normal to wire axis.</p> <p data-bbox="676 1048 868 1075"><u>Operating range</u></p> <p data-bbox="676 1079 975 1142">Temperature: -17.8-93.3°C Velocity: 0-30 m/s</p> <p data-bbox="676 1146 794 1173"><u>Accuracy</u></p> <p data-bbox="676 1178 1358 1240">Temperature: $\pm 0.3^\circ\text{C}$ Velocity: $\pm 3\%$ of reading or ± 0.015 m/s, whichever is greater</p> <p data-bbox="676 1245 804 1272"><u>Resolution</u></p> <p data-bbox="676 1290 1018 1317"><u>Calibration</u> Yearly calibration</p>
 <p data-bbox="300 1778 660 1841">(ii) Alnor thermo anemometer model 440-A</p>	<p data-bbox="676 1397 1447 1460">It measures the temperature, humidity as well as the air velocity,</p> <p data-bbox="676 1487 868 1514"><u>Operating range</u></p> <p data-bbox="676 1518 954 1617">Temperature: -10 to 60°C RH: 0 to 90% Velocity: 0 to 30 m/s</p> <p data-bbox="676 1621 794 1648"><u>Accuracy</u></p> <p data-bbox="676 1653 1358 1738">Temperature: $\pm 0.3^\circ\text{C}$ RH: $\pm 3\%$ RH Velocity: $\pm 3\%$ of reading or ± 0.015 m/s, whichever is greater</p> <p data-bbox="676 1742 804 1769"><u>Resolution</u></p> <p data-bbox="676 1774 900 1859">Temperature: 0.1°C RH: 0.1 % RH Velocity: 0.01 m/s</p> <p data-bbox="676 1863 1018 1890"><u>Calibration</u> Yearly calibration</p>

Particulate count measurement



TSI handheld particle counter 8220

Operating range

Temperature: 5 to 35 °C
Sampling flow rate: 2.8 l/s with 5% accuracy

Calibration

Yearly calibration
Calibrated at 0.3µm, 0.5µm, 1µm, 3µm, 5µm and 10µm
Comply with JIS

3.3 CFD modeling

3.3.1 Modeling approaches

i. Planning Stage

The aim for current study is to capture an insight on the air distribution inside the OR. Consequently, the flow pattern and the overall picture of possible air flow have to be estimated. The simulations done will illustrate a steady state conditions where OR is operate long enough and reaching equilibrium.

ii. Dimensional and structural representation of OR in CAD

Grid and computational cost will certainly increase when the architectural aspect in OR is represented with detail. Throughout this study, the doors will be represented as walls, and the cabinets in the OR are represented as square boxes, which the surfaces deemed as walls. Since OR is positively pressurized, definitely exfiltration will occur. Hence, it is a good practice to check the flow volume of supply and exhaust air, in order to have an insight on to what extent the exfiltration is. The apparatus in OR had been modeled in the simplest dimension. Human model had been represented in simplest form (details of dimensions is available in Appendix E).

iii. Simulation

It is advisable to commence the simulation by using basic CFD code. From the literature, most of the problems for room airflow study can be solved well by using Reynolds-

averaged Navier-Stokes (RANS) $k - \epsilon$ two equations models. Both standard $k - \epsilon$ model and renormalization group (RNG) $k - \epsilon$ model could be used in predicting the airflows characteristics in OR (Zhang et al., 2007). It is always a wise choice to use standard $k - \epsilon$ as the first solver to be used before using any other possible solver scheme being used. In current study, commercial software, ANSYS Fluent 12.0 is being used to perform the simulation and details on user's guide are available in ANSYS (2009a).

3.3.2 Verification

There is no excellent agreement between measured data and computed result. From the measurement data, since most of the indoor air velocity measurement is done by using hot-wire or hot-sphere anemometer, heat generated and convected by the probes could generate a false velocity. Over and above, many turbulence models were developed from some basic flows of high Reynolds number. Hence, the airflow characteristic in a room with relatively lower Reynolds number could not be solved perfectly (Chen, 1997). Confirmation on the predicted result should be carried out to ensure the discretization method, grid resolution is correct on performing the task.

There is a difference exists between verification and validation (AIAA, 1998). Verification is a process to ensure the physical or mathematical model could represents the conceptual description and the solutions of the model accurately. Whilst validation determine to what extent the CFD model represents the real scenario accurately. However, in indoor environmental modeling (ASHRAE, 2009), the validation shall refine to the representation of physical realities, consist of one or a few flow and heat transfer features of whole system.

The comparison between the simulation and on-site measurement should start by comparing the airflow pattern qualitatively. Upon the qualitative comparison, it should follow by assessment of first order parameter such as air velocity, temperature and species concentrations. However, comparison for species concentration is not available in current study. The comparison of second order parameter such as turbulence kinetic energy, Reynolds stresses are unnecessary since they are incorporated with larger uncertainties (ASHRAE, 2009). Despite of describing the results from comparison qualitatively (such as excellent, poor, fairly, etc.), it should come along with quantitative comparison, and provide the judgment by referring to other literatures available. Moreover, if the result obtained from the simulation have a lesser accuracy, it could be considered acceptable as long as the predicted trends are consistent (Chen & Srebric, 2002).

3.3.3 Accuracy

The accuracy of the CFD results which employed iterative solution depends on various factors. Thus, concern has to be taken particularly in:

- i. Discretization scheme

In current 3-dimensional ORs airflow modeling, the computational domain is discretized by finite volume method using unstructured mesh that is suitable for complicated domains. On the other hand, it provides convenience to perform refinement with minimal difficulty.

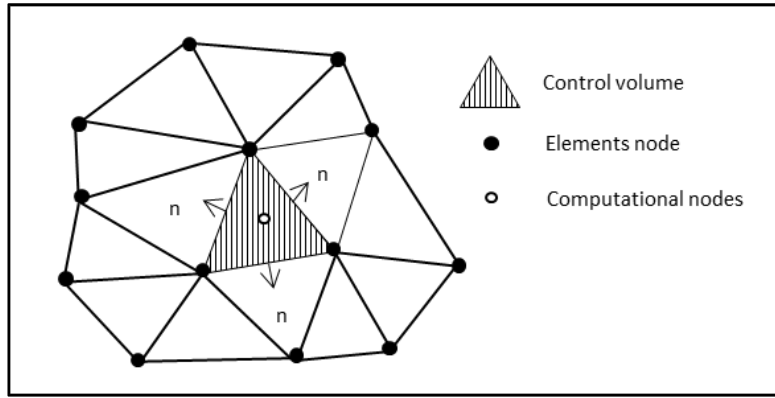


Figure 3.1: Finite volume method with unstructured mesh.

ii. Computational grid

Ideally, CFD solution is supposed to be independent of the computational grid. Errors resulted from interpolation could be minimized by increasing number of grid points. For non-uniform grid, the dimension ratio of two adjacent cells (expansion ratio) should be limited to 1.5 (Awbi, 2003). Nonetheless, sensitivity analysis on the grid refinement should be performed in order to have a optimization on the grid size and simulation result. In order to achieve grid convergence, the solution obtained should asymptotically approach the exact solution as in transport equation. As propose by Wilcox (1993), doubling the grid number is the common way to check the difference in CFD results. Since the exact solution is unknown, Grid Convergence Index (GCI) is being used to estimate the error between solution and unknown exact solution (Roache, 1994). The calculation of grid convergence index, GCI is explained as follows (Roache, 1998):

In order to perform this calculation, the CFD solution on three distinct number of mesh generated on the same model is needed. It starts with the estimation of mesh size, h

$$h = \left[\frac{1}{N} \sum_{i=1}^N (\Delta V) \right]^{\frac{1}{3}} = \left[\frac{V}{N} \right]^{\frac{1}{3}} \quad (12)$$

whereby N , ΔV , V number of cells, volume of each cell and volume of computational domain, respectively. Hence, if 1, 2, 3 denoted as the model with fine, medium and coarser mesh, respectively. It implies $h_1 < h_2 < h_3$. Then

$$h_1 = \left(\frac{V_1}{N_1}\right)^{\frac{1}{3}}, h_2 = \left(\frac{V_2}{N_2}\right)^{\frac{1}{3}}, h_3 = \left(\frac{V_3}{N_3}\right)^{\frac{1}{3}}$$

For a fix case study with same meshing domain, we have $V_1 = V_2 = V_3$

Next, the grid refinement, r is the ratio of mesh size, denoted by

$$r_{21} = \frac{h_2}{h_1} \text{ and } r_{32} = \frac{h_3}{h_2}. \text{ It will further simplify to } r_{21} = \left(\frac{N_1}{N_2}\right)^{\frac{1}{3}} > 1.1 \text{ and}$$

$$r_{32} = \left(\frac{N_2}{N_3}\right)^{\frac{1}{3}} > 1.1$$

The error, $\varepsilon_{32} = f_3 - f_2$ and $\varepsilon_{21} = f_2 - f_1$ are used to estimate approximate relative error, where, $e_a^{21} = \left|\frac{f_1 - f_2}{f_1}\right|$ and $e_a^{32} = \left|\frac{f_2 - f_3}{f_2}\right|$. The symbol f represent a solution function (e.g. temperature at certain location). Apparent

order, p , it has to be calculated by $p = \frac{\ln\left|\frac{\varepsilon_{32}}{\varepsilon_{21}}\right| + \ln\left[\frac{r_{21}^{p-s}}{r_{32}^{p-s}}\right]}{\ln(r_{21})}$ where $s = 1$

$\cdot \text{sgn}\left(\frac{\varepsilon_{32}}{\varepsilon_{21}}\right)$. The value of s is obtained based on signum function, which

equal to -1 if $\frac{\varepsilon_{32}}{\varepsilon_{21}} < 0$ and equal to $+1$ if $\frac{\varepsilon_{32}}{\varepsilon_{21}} > 0$. For non-consistent value of

r , the value of p needs to be calculated via iteration. Eventually, GCI of each refinement ratio is calculated by,

$$GCI_{\text{fine}}^{21} = \frac{1.25e_a^{21}}{r_{21}^{p-1}} \quad (13a)$$

$$\text{and } GCI_{\text{fine}}^{32} = \frac{1.25e_a^{32}}{r_{32}^{p-1}} \quad (13b)$$

Overall procedure for GCI calculation is summarized in Table 3.3.

Table 3.3: Summary for Grid Convergence Index calculation.

Case	1	2	3
Calculation process	N_1	N_2	N_3
For determining			
Grid convergence index	f_1	f_2	f_3
↓	$h_1 = \left(\frac{V_1}{N_1}\right)^{\frac{1}{3}}$	$h_2 = \left(\frac{V_2}{N_2}\right)^{\frac{1}{3}}$	$h_3 = \left(\frac{V_3}{N_3}\right)^{\frac{1}{3}}$
Refinement ratio, r	$r_{21} = \frac{h_2}{h_1} = \left(\frac{N_1}{N_2}\right)^{\frac{1}{3}}$	$r_{32} = \frac{h_3}{h_2} = \left(\frac{N_2}{N_3}\right)^{\frac{1}{3}}$	
Error, ϵ	$\epsilon_{21} = f_2 - f_1$	$\epsilon_{32} = f_3 - f_2$	
Approximate relative error, e_a	$e_a^{21} = \left \frac{f_1 - f_2}{f_1}\right $	$e_a^{32} = \left \frac{f_2 - f_3}{f_2}\right $	
s	$s = \begin{cases} -1, & \frac{\epsilon_{32}}{\epsilon_{21}} < 0 \\ +1, & \frac{\epsilon_{32}}{\epsilon_{21}} \geq 0 \end{cases}$		
Apparent factor, p	$p = \frac{\ln\left \frac{\epsilon_{32}}{\epsilon_{21}}\right + \ln\left[\frac{r_{21}^{p-s}}{r_{32}^{p-s}}\right]}{\ln(r_{21})}$, via iteration if $r_{21} \neq r_{32}$		
Grid convergence index, GCI_{fine}	$GCI_{\text{fine}}^{21} = \frac{1.25e_a^{21}}{r_{21}^p - 1}$	$GCI_{\text{fine}}^{32} = \frac{1.25e_a^{32}}{r_{32}^p - 1}$	

iii. Near-wall boundary conditions

iv. Convergence criteria

The recommended approach to examine the convergence is by examining the residuals. The solutions are considered converged when residual of each equation solved decreased to at least three orders of magnitude (10^{-3}) and six orders of magnitude (10^{-6}) for energy (Chen & Srebric, 2002).

3.3.4 Considerations in modeling

When the mesh spacing larger than zero, there will be truncation error due to the discretization of governing equation. Truncation error will account for the consistency of the solution. During computation, round-off error (due to single/double precision selection) will certainly occur since storage of significant number is limited in computer. Hence, as long as this error does not enlarged in the interval of solving process, the solution method is deemed as stable.

Mesh size

In order to compare the differences of CFD solutions, a large difference on grid size (which is commonly halving the grid size) should be compared to keep the discretization error minimal. Initially, course mesh is tested prior to fine mesh since it allows more tests run in order to examine the convergence behavior of the calculations. The mesh element at inlet/outlet openings and heat sources are smaller. The change of cell size should keep below 120% and maximum skewness of the mess should be carefully monitored by keeping it below 0.95.

Precision selection

In order to avoid overloading on the computational power, single precision is adopted in the calculation.

Solution method

- *Pressure-Velocity coupling*

For incompressible flow, density remains constant. Density and pressure become separate entity that results in difficulty on solving Navier-Stokes equations. The lack of explicit equation for pressure hence demand for derivation of equation from momentum and continuity equation. SIMPLE (Semi-Implicit Method for Pressure-Linked

Equations) and SIMPLEC (SIMPLE-Consistent) are both adoptable P-V coupling method. Both solve each of the velocity component and pressure separately, then pressure and velocity correction are performed to couple both pressure-velocity. In current study, SIMPLE had been used for P-V coupling.

- *Spatial discretization for gradient, momentum, energy, turbulent kinetic energy, and turbulent dissipation rate*

Least square cell based had been chosen for gradient since its accuracy is comparable to Green-Gauss node based and having less expensive computational cost. More accurate result could be achieved in a higher order scheme but the computation process will take a longer time and less stable. However, for tetrahedral meshes, second order discretization is desired for more accurate result since the flow is not aligned with the mesh.

- *Relaxation factor*

Setting relaxation factor lesser than unity will reduce the speed of convergence. However, it will decrease the possibility of divergence and increase the stability of the calculation. Although over-relaxation will speed up convergence, but it will sacrifice the stability of solution. Hence, throughout the calculation process, the relaxation factors were manipulated as to speed up the convergence.

Model Selection

For surgical operating room, Kameel et al. (2003) suggested the use of standard $k - \varepsilon$ model and RNG $k - \varepsilon$ model are superior in the prediction of flow characteristics in near wall and steep gradient zones. For steady incompressible flow without body forces, both standard $k - \varepsilon$ and RNG $k - \varepsilon$ model are written as:

Standard $k - \varepsilon$ model

$$\text{Turbulent kinetic energy, } \underbrace{\rho U_i \frac{\partial k}{\partial x_i}}_{\text{convection}} = \underbrace{\mu_t \left(\frac{\partial U_j}{\partial x_i} + \frac{\partial U_i}{\partial x_j} \right) \frac{\partial U_j}{\partial x_i}}_{\text{generation}} + \underbrace{\frac{\partial}{\partial x_i} \left[\frac{\mu_t}{\sigma_k} \frac{\partial k}{\partial x_i} \right]}_{\text{diffusion}} - \underbrace{\rho \varepsilon}_{\text{dissipation}} \quad (14)$$

$$\text{Dissipation rate, } \underbrace{\rho U_i \frac{\partial \varepsilon}{\partial x_i}}_{\text{convection}} = \underbrace{C_{1\varepsilon} \left(\frac{\varepsilon}{k} \right) \mu_t \left(\frac{\partial U_j}{\partial x_i} + \frac{\partial U_i}{\partial x_j} \right) \frac{\partial U_j}{\partial x_i}}_{\text{generation}} + \underbrace{\frac{\partial}{\partial x_i} \left[\frac{\mu_t}{\sigma_\varepsilon} \frac{\partial \varepsilon}{\partial x_i} \right]}_{\text{diffusion}} - \underbrace{C_{2\varepsilon} \rho \left(\frac{\varepsilon}{k} \right)}_{\text{destruction}} \quad (15)$$

RNG $k - \varepsilon$ model

$$\text{Turbulent kinetic energy, } \underbrace{\rho U_i \frac{\partial k}{\partial x_i}}_{\text{convection}} = \underbrace{\mu_t S^2}_{\text{generation}} + \underbrace{\frac{\partial}{\partial x_i} \left[\alpha_k \mu_{\text{eff}} \frac{\partial k}{\partial x_i} \right]}_{\text{diffusion}} - \underbrace{\rho \varepsilon}_{\text{dissipation}} \quad (16)$$

$$\text{and } S \equiv \sqrt{2S_{ij}S_{ij}}$$

Dissipation rate,

$$\underbrace{\rho U_i \frac{\partial \varepsilon}{\partial x_i}}_{\text{convection}} = \underbrace{C_{1\varepsilon} \left(\frac{\varepsilon}{k} \right) \mu_t S^2}_{\text{generation}} + \underbrace{\frac{\partial}{\partial x_i} \left[\alpha_\varepsilon \mu_{\text{eff}} \frac{\partial \varepsilon}{\partial x_i} \right]}_{\text{diffusion}} - \underbrace{C_{2\varepsilon} \rho \left(\frac{\varepsilon}{k} \right)}_{\text{destruction}} - \underbrace{R}_{\text{mean strain and turbulence quantities}} \quad (17)$$

3.3.5 Modeling of human

In the CAD modeling, the human model had been modeled in a simplified block- shape (as available in Appendix E). When a simplified model is compared with standard or realistic model, simplified model tends to underestimate the convection heat transfer by human body (Zhang et al., 2009). In the range of air velocity lower than 0.4m/s, the underestimation is around 20% based on Zhang et al. (2009). A complicated geometry and computational cost compromised each other. Furthermore, the airflow in macro-environment is the main interest in this study, thus a simplified human model had been modeled to represent human subject.

3.3.6 Modeling of humidity

The air had been modeled as a mixture of dry air and vapor without chemical reaction among the species and behaved as an ideal gas. The substance's properties are determined as follows:

- iv. Density: incompressible ideal gas
- v. C_p : mixing law
- vi. Thermal conductivity and viscosity: ideal gas mixing law
- vii. Mass diffusivity: $2.5 \times 10^{-5} \text{ m}^2/\text{s}$ at 25°C, 1atm.

In the boundary condition setting, the species (H_2O) had been specified in terms of mass fraction, which is equivalent to humidity ratio in psychrometric chart. The mass fraction was determined by knowing the dry bulb temperature and RH of the air. Besides, the wall boundary generates zero diffusive flux for moisture. For this particular species, the convergence criteria is set to 1×10^{-5} .

3.3.7 Modeling of gaseous contaminant

The gaseous contaminant had been assumed to be CO_2 . The contaminant was released from the top surface of the source at a mass fraction of 2×10^{-4} (200 ppm). The mass diffusion coefficient, $D_{c,a}$ for air and the gaseous contaminant is $16 \text{ mm}^2/\text{s}$, since the room air temperature in the OR is at vicinity of 20°C. For other gas properties of CO_2 , the gas properties at normal temperature and pressure (20°C, 1 atm) were used.

3.3.8 Modeling of particle tracking

Particle tracking had been performed using the discrete phase model, which the particle is not interaction with the continuous phase. The particles were modeled in the diameter of $12 \mu\text{m}$ to represent the mean particle size. These inert particles were assumed to obey

with spherical drag law as mentioned by Morsi and Alexander (1972). When the particle hits a wall, it will reflect with a unity restitution coefficient.

3.4 Simulations overview

For both SGHHC OT-5& UMMC OT-11, current conditions will be simulated in CFD to serve as the baseline for comparison purpose. Hence, following chapters for results and discussion will be arranged in the following manner:

Chapter 4: Case study on Sarawak General Hospital Heart Centre (SGHHC) OT-5

Chapter 5: Case study on University of Malaya Medical Centre (UMMC) OT-11

Chapter 6: The study on design variation in a Class 7 clean room

3.5 Concluding summary

In previous chapter (Chapter 2), one can observe the CFD has served as an important tool for researchers to conduct the prediction on the airflow in an OR. Hence, current chapter has discussed the governing equations, boundary conditions, on-site measurement and a proper CFD modeling approaches that need to be taken into consideration in order to achieve the objective in current study, which the results of the air distribution in the will be discussed in following chapters, as mentioned in Section 3.4.

4.0 Case study on SGHHC OT-5

Sarawak General Hospital Heart Centre (SGHHC) was formerly named as Sarawak International Medical Centre. The hospital was officiated on January 2011. There are total of 6 ORs in SGHHC, with OT-5 designed to serve for cardiovascular surgery. The views and layout plan for OT-5 are pictured as follows (Figures 4.1 to 4.3). Figure 4.4 displays the layout of OT-5 in CAD. Besides, the news for SGHHC, AHU design for OT-5 and the measured room dimension are attached in Appendix B, C and D.



Figure 4.1: View for OT 5 (Left: the condition during HEPA leaking test while picture in the Right: the condition during the measurement).

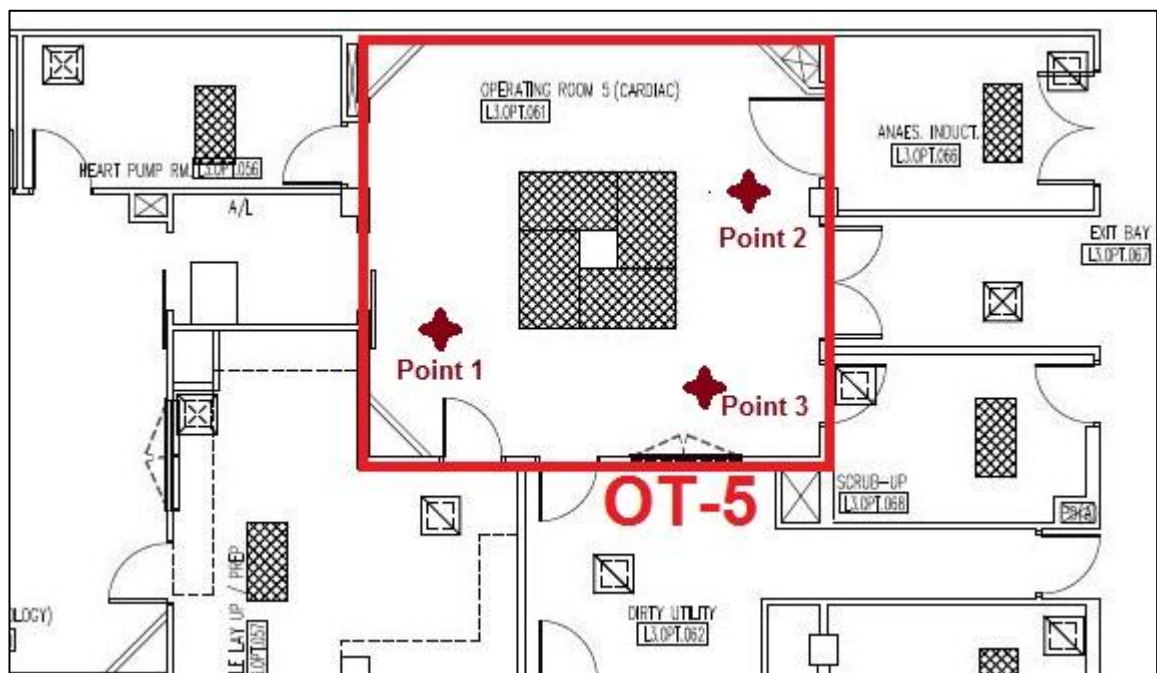


Figure 4.2: Drawing layout for OT-5 (without supply and return air ducts).

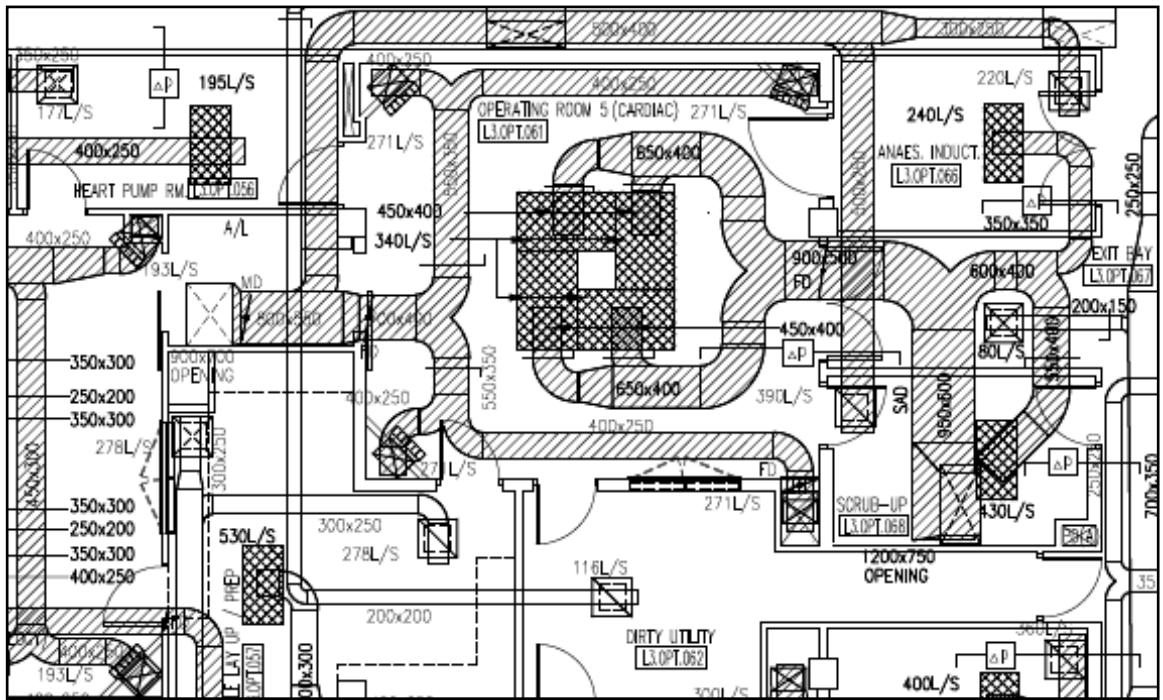


Figure 4.3: Drawing layout for OT-5 (with supply and return air duct).

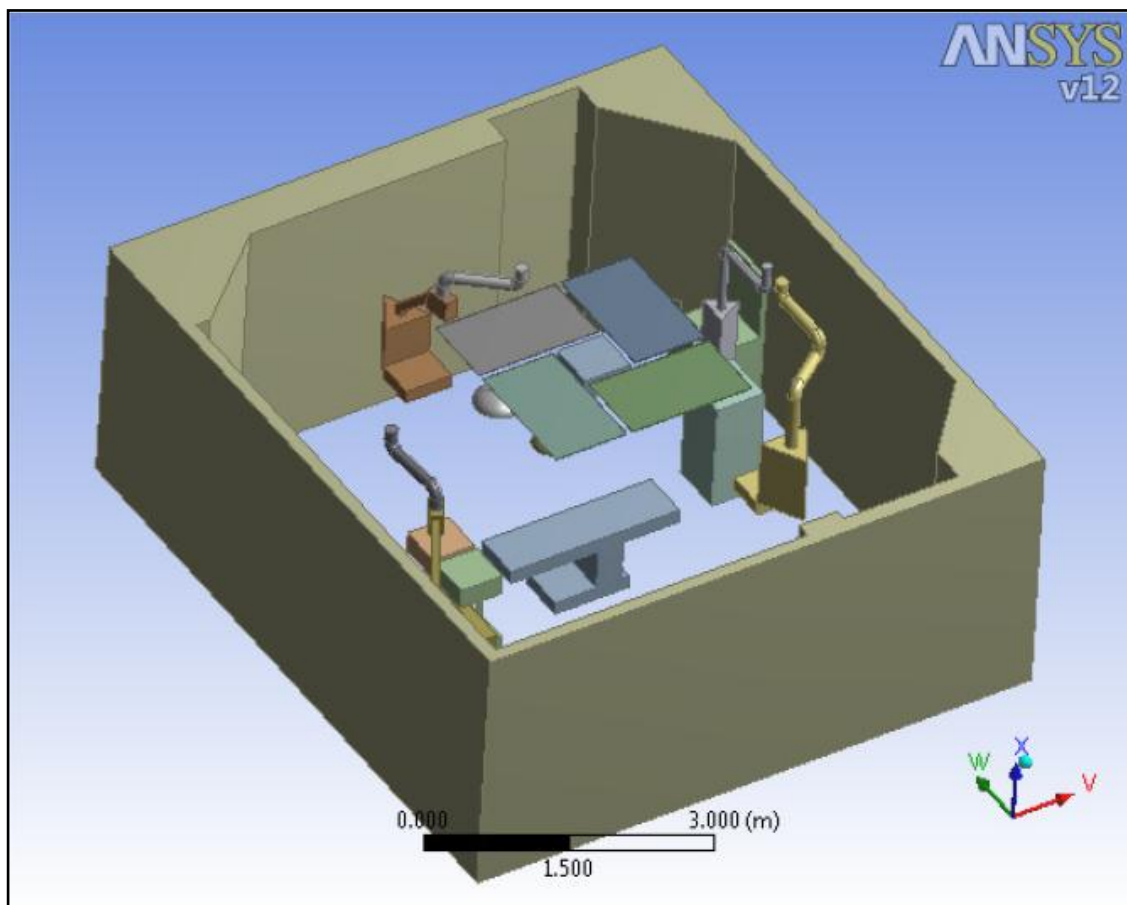


Figure 4.4: Modeling for unoccupied SGHHC OT-5 in CAD.

4.1 Assumptions

There were several assumptions need to be made prior to the indoor airflow measurement.

- i. The room had reached steady state condition since the air-conditioning system had been operated for a continuous 48 hours prior to the measurement.
- ii. The air condition in the OR was considered as isothermal case since the difference of the supply air and average room temperature was $0.7^{\circ}\text{C} < 1^{\circ}\text{C}$.
- iii. After averaging done by velocity matrix for 2×16 points (Figure 4.5) for a single room air inlet, the air volume flow rate could be calculated based on the air velocity and area of the room air inlet.



Figure 4.5: Velocity matrix available in Alnor EBT721 balometer.

- iv. The layout of OR during measurement was approximated to the layout during the actual operation process, by referring to the information provided after consulting the hospital matron.

There were several assumptions had been made in indoor airflow simulation.

- i. The airflow prediction in the simulation had a steady state condition.
- ii. For human body modeling, human body was assumed to have a skin temperature of 34 °C (body core temperature of 36.8 °C) which is approximated to skin temperature (33.7 °C) reported by Prek (2005).
- iii. The contaminant was assumed carried by inert particle with a diameter of 12 µm.

The trajectory of the particle is affected by the drag force exerted by the air resistance and the relative velocity will determine the motion of particle. In order to estimate the drag coefficient of a spherical smooth particle, spherical drag law was assumed and the following equation (18) is used,

$$C_D = \frac{k_1}{Re} + \frac{k_2}{Re^2} + k_3 \quad (18)$$

The value of the coefficient and constant k_1 , k_2 , k_3 are dependent on the range of Reynolds number, and they were given in the appendix section of Morsi and Alexander (1972).

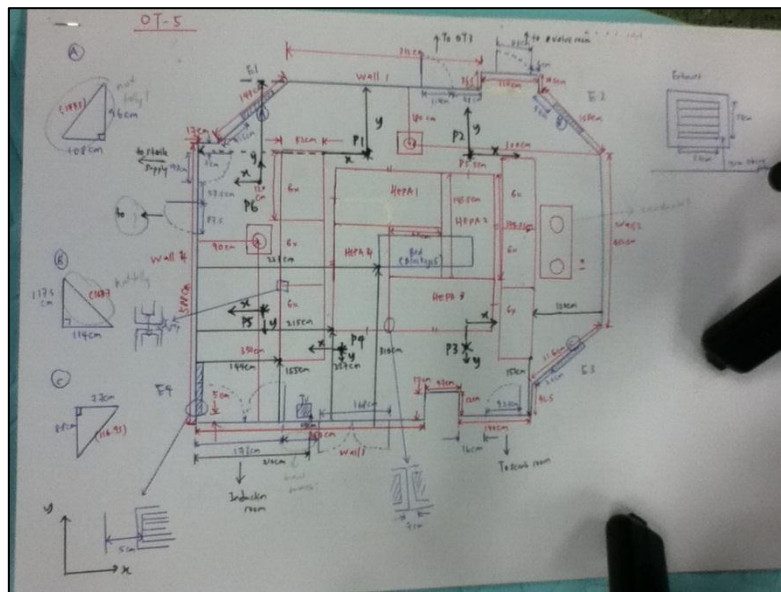
- iv. Normally, there are 5 staffs surrounding the operating table during the operation process, as indicated in Figure 4.6.



Figure 4.6: Typical condition during operation (taken in University of Malaya Medical Centre).

4.2 Measurement at SGHHC

The on-site measurement in OT-5 was conducted on 22 January 2011. The physical layout and dimensions of the OR as well as the dimension of the equipment were recorded, which will be used in the modeling process. At the same time, the inlet boundary condition was measured, and some measurement points were chosen for the purpose of comparison with the simulation outcome at the later stage.



4.3 Physical on-site measurement at SGHHC OT-5

The measured inlet air condition for the OR are tabulated in Table 4.1

Table 4.1: Measured air d inlet condition.

HEPA No.	Measurement	DBT, °C	RH, %	Average velocity, (m/s)	Dimension	Supply air flow rate, (m ³ /h)
1	I	17.2	70.2	0.32	1.455m x 0.855m (each)	1477.90
	II	17.2	70.1	0.39		
	III	17.2	70.4	0.28		
	IV	17.3	69.9	0.34		
	Average	17.2	70.2	0.33		
2	I	17.2	68.0	0.28		1253.98
	II	17.3	69.1	0.31		
	III	17.3	68.2	0.21		
	IV	17.1	69.9	0.30		
	Average	17.2	68.8	0.28		
3	I	17.1	69.4	0.32		1657.04
	II	17.1	68.6	0.35		
	III	17.0	68.8	0.41		
	IV	17.1	69.6	0.41		
	Average	17.1	69.1	0.37		
4	I	17.0	69.3	0.38		1791.40
	II	17.1	69.5	0.41		
	III	17.1	69.0	0.32		
	IV	16.9	69.5	0.50		
	Average	17.0	69.3	0.40		
Average air condition at inlet		17.1	69.4	0.345	Total supply air flow rate	6180.32

From the on-site measurement, OT-5 had an air change per hour, ACH around 42.5, corresponding to the built area of 48.5 m² or volume of 48.5 m² x 3 m = 145.5 m³. The ACH is not considering the actual air volume. Consequently, in the actual case, it results in slightly higher ACH than the calculated value. Note that the ACH of the current design is 70% higher than required 25 ACH. The nominal time constant for the rooms is equal to, $\tau_n = \frac{3600}{ACH} = 84.7$ seconds . Average velocity discharged from the inlet is 0.345 m/s. Considering the minimum requirement of $u > 0.1\sqrt{\Delta T}$ to minimize influence of thermal buoyancy from occupant, the air velocity of 0.41 m/s is needed. However, theoretically, the inlet should provide airflow with minimal variation of air velocity. Since the air duct for each inlet is branched prior to the entrance (refer to Figure 4.3), and hence, maldistribution of equal fraction of air into each branch will certainly occur resulted from different downstream pressure as the duct bent. Maldistribution of the equal fraction of air prior to the entrance to HEPA caused the inlet air velocity variation among inlets, which is inevitable for such design. The average inlet air temperature was lower than the recommendation made by MOH (2010). The RH measured was 69.4 %, which was higher than recommended 60% RH, which indeed was a flaw in the system design. After the HEPA filter leaking test, the particulate counts were conducted and from the measurement (Table 4.2), the OR satisfied the requirement for Class 7 clean room.

Table 4.2: Particulate count in the non-operating SGHHC OT-5.

Particle size, μm	Reading 1	Reading 2	Average count	Particulate count requirement for Class 7 clean room
> 0.3	423612	425520	424566	-
> 0.5	18234	18352	18293	<352000
> 1.0	5783	5745	5764	<83200
> 3.0	2502	2538	2520	-
> 5.0	692	668	680	<2930
> 10.0	136	120	128	-

4.4 Simulation for SGHHC OT-5

The simulation was performed by using ANSYS Workbench 12.0. It equips with design modeler, meshing, Fluent, and CFD Post, which allow users to perform the simulation in a single interface. Details of the software are available at ANSYS (2009b). After building the physical model with SolidWork CAD, the model is imported into ANSYS Design modeler, which the air space from the physical model is frozen, and the airspace is filled as fluid domain. Then, the physical model is cut/subtracted from the entire domain, leaving the fluid domain alone. Subsequently, the fluid domain is meshed and ready for the setting of CFD simulation in Fluent.

Boundary Conditions

The nomenclature for inlet and outlet as well as boundary conditions in the simulations as follows (Figure 4.8 and Table 4.3):

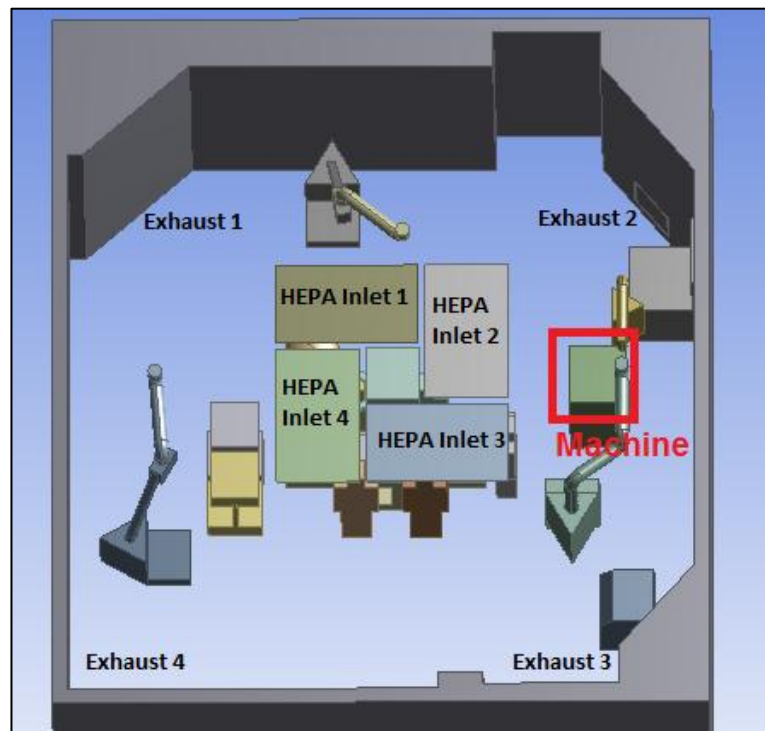


Figure 4.8: Nomenclature for HEPA inlets and exhausts SGHHC OT-5.

Table 4.3: Boundary condition settings for CFD simulation SGHHC OT-5.

Item	Details
<i>Air inlet</i>	It is set as velocity inlet which is intended for incompressible flow. The air inlets are modeled as a rectangle which discharges air vertically downward to the operating table with turbulent intensity of 5%.
<i>Details</i>	
Inlet 1	1447.90 m ³ /h , velocity: 0.33 m/s, Area:1.244 m ³ , Air temperature: 17.1 °C
Inlet 2	1253.98 m ³ /h , velocity: 0.28 m/s, Area:1.244 m ³ , Air temperature: 17.1 °C
Inlet 3	1654.07 m ³ /h , velocity: 0.37 m/s, Area:1.244 m ³ , Air temperature: 17.1 °C
Inlet 4	1791.40 m ³ /h , velocity: 0.40 m/s, Area:1.244 m ³ , Air temperature: 17.1 °C
<i>Air outlet</i>	The air outlets are modeled as a square which the air is being discharged through the surface. Pressure outlet was set to zero gauge pressure.
Exhaust 1,2,3,4	
<i>Walls</i>	No slip condition on the surface, adiabatic walls. Surface of the equipment exist in OR are treated as wall.

The settings for simulation and heat dissipation of devices

The settings for the simulations are listed in Table 4.4, while Table 4.5 lists the heat generation of devices in the OR.

Table 4.4: Settings for CFD simulation SGHHC OT-5.

Mesh	Approximately 3×10^6 mesh elements
Solver	Pressure based coupled solver and steady state
Model	$k - \varepsilon$ model, $\sigma_k = 1.0$, $\sigma_\varepsilon = 1.3$, $C_{1\varepsilon} = 1.44$ $C_{2\varepsilon} = 1.92$, $C_\mu = 0.09$, Full buoyancy effects is on to include buoyancy effects on ε .
Boundary condition	As described in Table 4.3. The geometry of the items available in appendices.
Heat sources	Included in Table 4.5
Solution method	Scheme: SIMPLE Gradient: Least –square cell based Pressure: Standard

	Momentum: 2 nd order upwind
	Turbulent kinetic energy: 2 nd order upwind
	Turbulent dissipation rate: 2 nd order upwind
	Energy: 2 nd order upwind
Solution control	<i>Under relaxation factor</i> ¹ Pressure: 0.3 Density: 1 Body forces: 1 Momentum: 0.7 Turbulent kinetic energy: 0.8 Turbulent dissipation rate: 0.8 Turbulent viscosity: 0.5 Energy: 1
Convergence criterion (absolute)	Continuity, x, y, z-velocity, k, epsilon: 1×10^{-3} Energy: 1×10^{-6}

¹ Represent initial setting for the numerical calculation.

Table 4.5: Heat dissipations of OR devices in simulated OR SGHHC OT-5.

Item ¹	Quantity	Heat dissipation ²
Operating table	1	Nil., represent wall
Surgical lights	2	Heat dissipation Big light : 200W(Lamp face) 5W(Lamp back) Small light : 150W (Lamp face) 3W (Lamp back)
Medical gas supply pendant	4	Nil, represent obstacle.
Machine	1	Heat dissipation: 250 W
Personnel	5	Heat dissipation: 100 W each ³
Patient	1	Heat dissipation: 70 W
Suction machine	1	Heat dissipation: 250W
Drawer	1	Nil, represent obstacle.
Diathermy	2	Nil, represent obstacle.

¹ Please refer to Appendix E for the dimension of the items above.

²Total cooling load of approximately 1428 W.

³The convection heat transfer for human referred on Kurazami *et al.* (2008).

There are two distinct treatments for particle transport modeling. Lagrangian approach treating the particles as a single constituent while the fluid phase act as a

continuum. Different with Lagrangian approach, the Eulerian approach treating solid particles as a continuum. Former approach solves particle trajectory by solving force acting on the particle while the later solve both fluid phase and solid particle using transport equation. On the comparison and details on these methods, Chang and Chen (2007) discussed the difference of both methods for predicting particle transport in enclosed spaces. In current study, the particles were modeled as a urea with 12 μ m in size that obeys spherical drag law using Lagrangian approach.

4.5 Mesh independence study for SGHHC OT-5 simulation

For grid independent study, 5 different numbers of meshing element were examined, which are 0.95×10^6 , 1.27×10^6 , 1.69×10^6 , 2.70×10^6 , 3.96×10^6 of elements in tetrahedral meshing. For simplicity, the simulations are denoted as follows:

Table 4.6: Identification for simulations SGHHC OT-5.

<i>Mesh number</i>	<i>ID</i>
3.96×10^6	I
2.70×10^6	II
1.69×10^6	III
1.27×10^6	IV
0.95×10^6	V

The number of elements are corresponding to 100, 80, 50, 30, 10 relevance in fine relevance center at Workbench meshing setting for simulation I, II, III, IV, V, respectively. When examined visually at the temperature contour at the middle plane of the OT-5 (Plane 1), it shows that simulations I and II provide similar pattern. On the other hand, the results from different mesh elements are extended to the examination of velocity profile (Figure 4.9). Similar velocity patterns are found in simulations I and II.

Overall, the average temperature at Plane 1 resulted from different mesh elements are plotted in graphs (as indicated in Figure 4.10) to show the mesh independency. The solution approaches a constant value as the number of mesh increases. By using Richardson extrapolation (h^2 extrapolation), the exact solution can be estimated. This is given by $f_{exact} \cong f_1 + \frac{f_1 - f_2}{r^2 - 1}$, where f_1 and f_2 are the solution for finer mesh and coarser mesh, respectively. It yields an extrapolated average temperature of 18.01°C at Plane 1. Hence, it is clearly seen that, 2.70×10^6 mesh elements (i.e. 80 relevance) was adequate for the current case study. The result for GCI on simulations I, II and III are tabulated in Table 4.7.

Table 4.7: Grid convergence index for simulation I, II and III SGHHC OT-5.

Simulation	I	II	III
Domain volume, (m^3)	123.877	123.877	123.877
Number of cells	3964602	2702408	1690853
Solution function, f	17.98	17.97	17.90
Representative mesh size, h (m)	0.0315	0.0358	0.0418
Refinement ratio, r	1.136		1.169
Error, ϵ	-0.01		-0.07
Approximate relative error, e_a	-0.000556		-0.003895
s	1		
Apparent factor, p	11.9561		
Grid convergence index, GCI_{fine} (%)	-0.019 %		-0.089 %

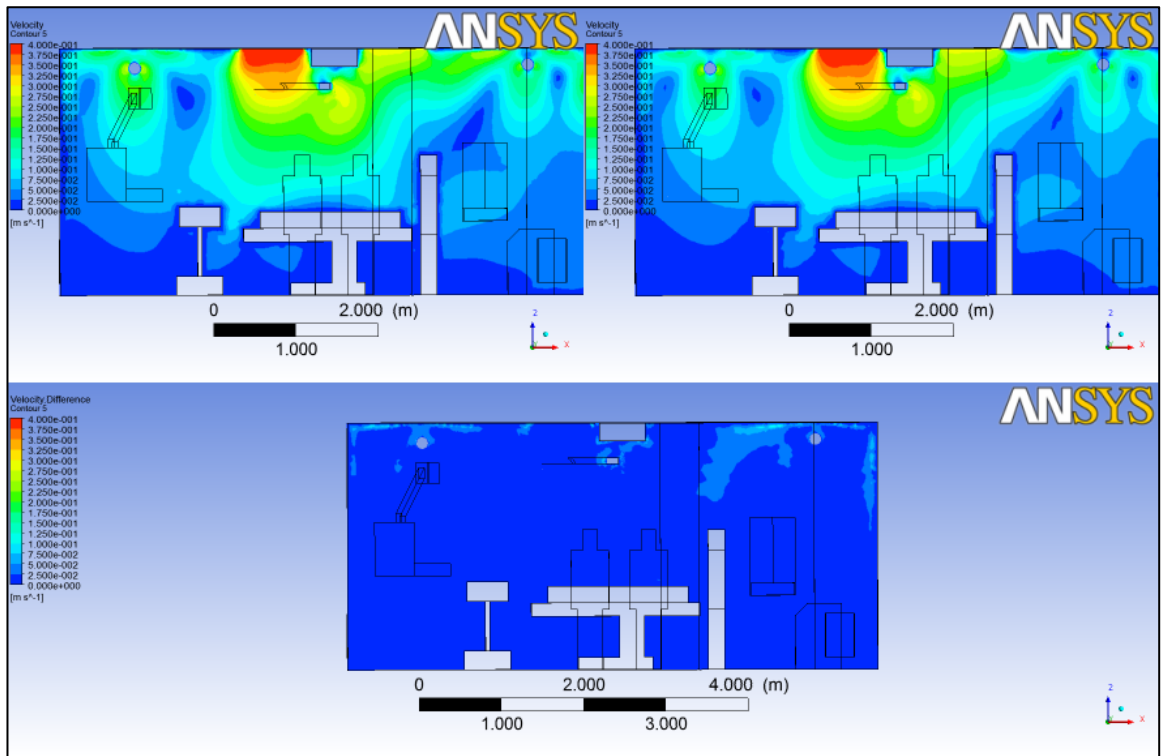


Figure 4.9: Air velocity difference (bottom half of the figure) for different mesh elements at mid-plane (Plane 1) of OT-5.

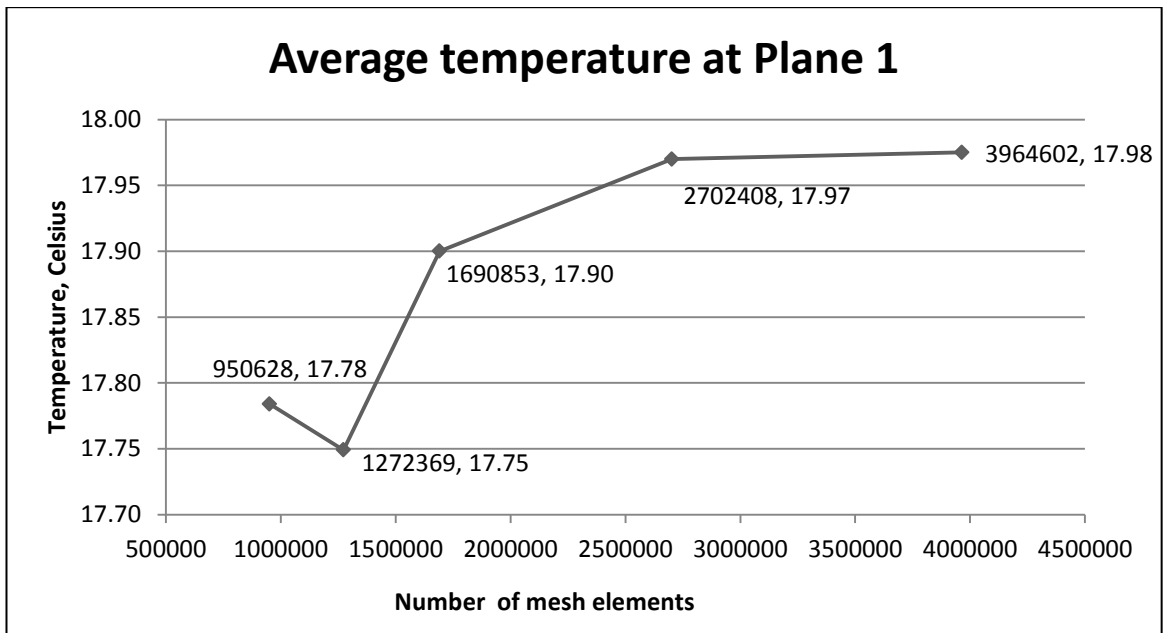


Figure 4.10: Average air temperature at Plane 1 versus number of mesh elements.

From the simulation using standard $k - \varepsilon$ model, swirl was identified behind the medical gas supply pendant, which is discharged from inlet 2, as shown in Figure 4.11.

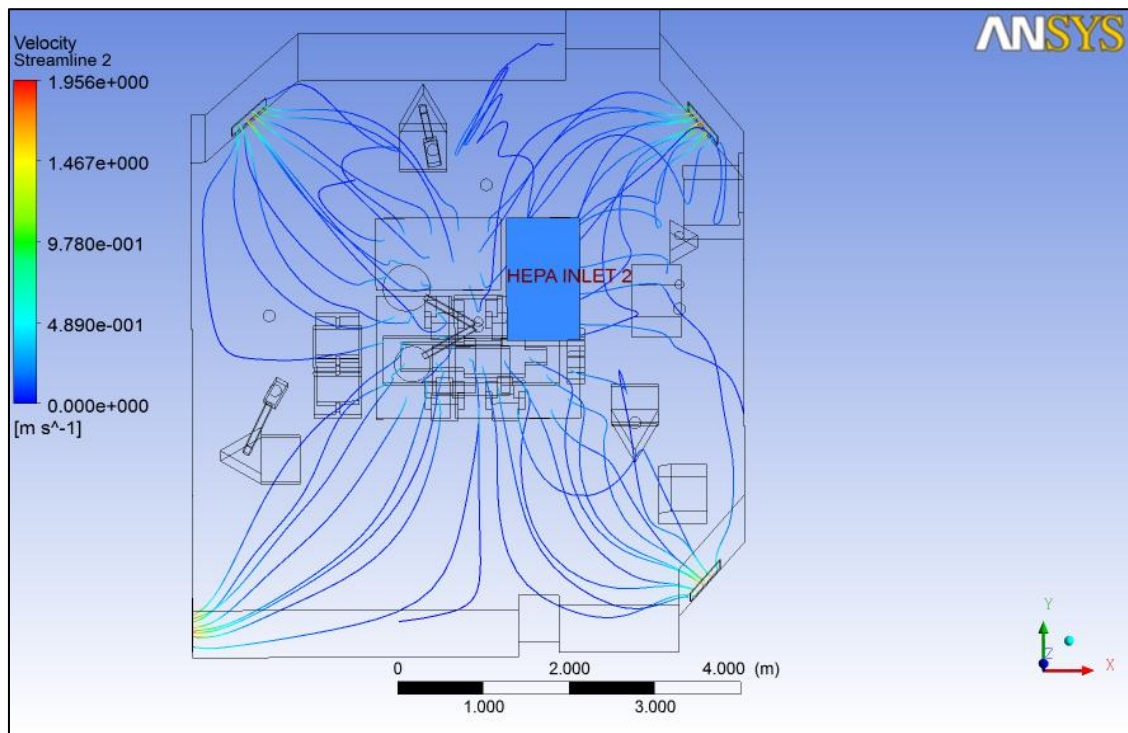


Figure 4.11: Air swirl behind the medical gas supply pendant.

It should be noted that, the standard $k - \varepsilon$ has been identified having limited performance in flow with a high streamline curvature and air swirl. Hence, the RNG $k - \varepsilon$ model, have better performance than the standard $k - \varepsilon$ in coping and aiding the prediction for the case with the air swirl was considered for checking and comparing whether the influence of air swirl to the simulation result is significant. However, both standard $k - \varepsilon$ and RNG $k - \varepsilon$ models predicted the similar air flow pattern regardless of model used (Figure 4.12). Hence, the standard $k - \varepsilon$ is suitable for flow prediction in the current case study.

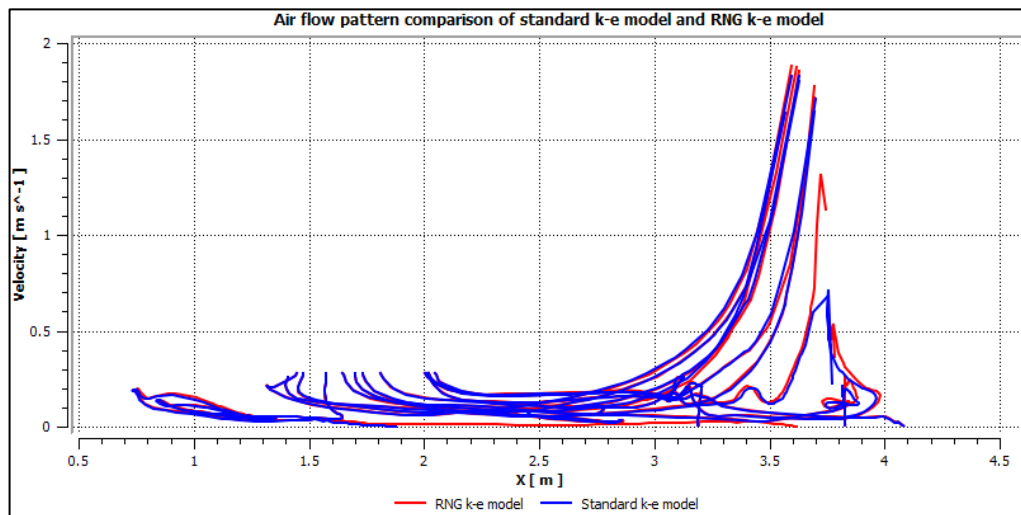


Figure 4.12: Air flow pattern comparison of standard k-e model and RNG k-e model.

4.5 Fieldwork measurement and simulation – A comparison

During the on-site measurement, the OR was in a non-operating condition. During the measurement, the difference of the supply air and average room temperature is 0.7°C , which is less than 1°C . Thus, the assumption of isothermal condition in the room could be made safely. In order to compare the on-site measurement result with the simulation result, an isothermal case is modeled, without the existence of personnel and heat source. The heat generated by fluorescent light was disregarded since the lights were embedded in the ceiling, and the heat source contribution was insignificant. Note that careful attention should be given on the selection of measurement point in on-site measurement for comparison purpose. The point selected should be free from disturbance of equipment. Three points were chosen for comparison purpose (as shown in Figure 4.2).

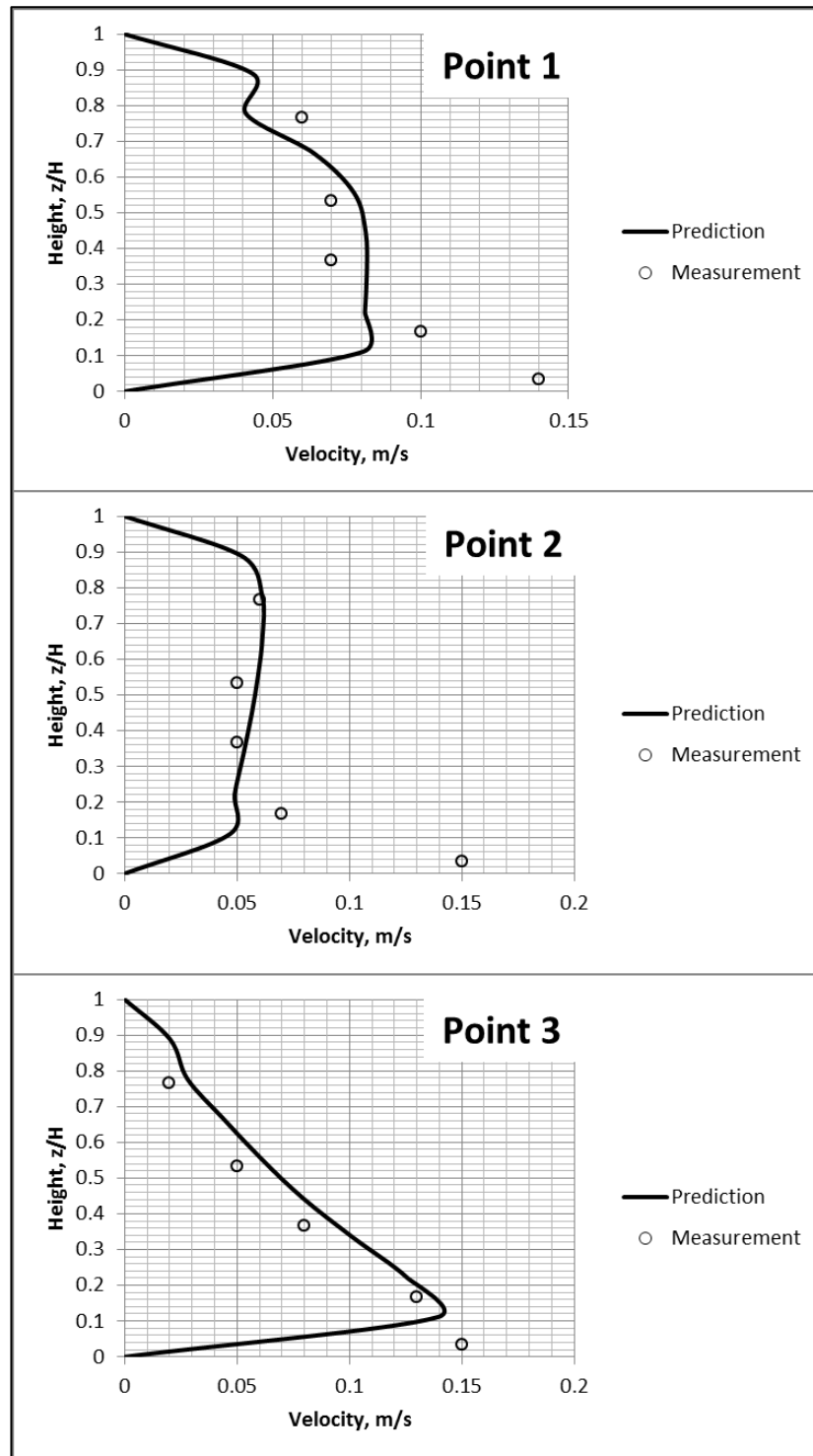


Figure 4.13: Comparison of result- measurement and simulation.

In the evaluation on whether the simulation result is acceptable compared to the field measurement, the error reported by Memarzadeh and Jiang (2004) was taken as reference. Hence, error between 15-20% can be considered as in good agreement.

From the comparison, there was a deviation between the measured air velocities with simulation result. The deviations were very high (80-90%) at 0.1 m above the floor for all of the points measured. Possible reason for this error was, in simulation, no air leakage was assumed. In actual, for a positively pressured OR, there will be small amount of air will infiltrate into the adjacent room. Hence, the gap under the door was a possible way for the air to infiltrate, which will cause the air to accelerate (with high velocity) at the region near to the surface of the floor. Setting the exhaust to be a zero gauge pressure boundary condition may underestimate the fluid acceleration near the floor, since the exhaust with non-zero pressure differential will provide extra pulling on extracting the air in OR. Besides, hot wire anemometer measures air velocity by heating the hot wire since the air flow through the wire produces convection cooling effect. It is good to mention that 'accurate measurement of a low air velocity is difficult' (Melikov et al., 2007). In the measurement of air velocity, especially when measuring low air velocity using the hot wire anemometer, the measured value was located at the lower measurement threshold of the device, has most probably caused the false value. Generally, when examining the overall pattern of the graph, it shows a consistent pattern. Thus, simulation result was accepted.

4.6 CFD simulations of SGHHC OT-5

A good OR design should possess certain characteristic, which includes:

- i. As the most crucial part, the ability to provide good air distribution, meaning that with a uniform air flow velocity, acceptable temperature distribution and low turbulence.
- ii. Ability to meet stipulated standards' requirement.
- iii. Without major modification, it can adapt to facility utilisation such as the layout changes for equipment rearrangement.

- iv. A low capital investment during process modification.
- v. Adaptability to energy savings for lowering maintenance costs.

In the current study, interest was paid on the characteristics (i) and (v), which will be discussed in Sections 4.6.1 and 4.6.2. In the discussion, there three planes had been defined in order to ensure a lucidness on the comparisons made. As shown in Figure 4.14, Plane 1 (x -z plane) and Plane 2 (y-z plane) cut the middle of the surgical site, while Plane 3 represents x-y plane located 1.2 m from the floor.

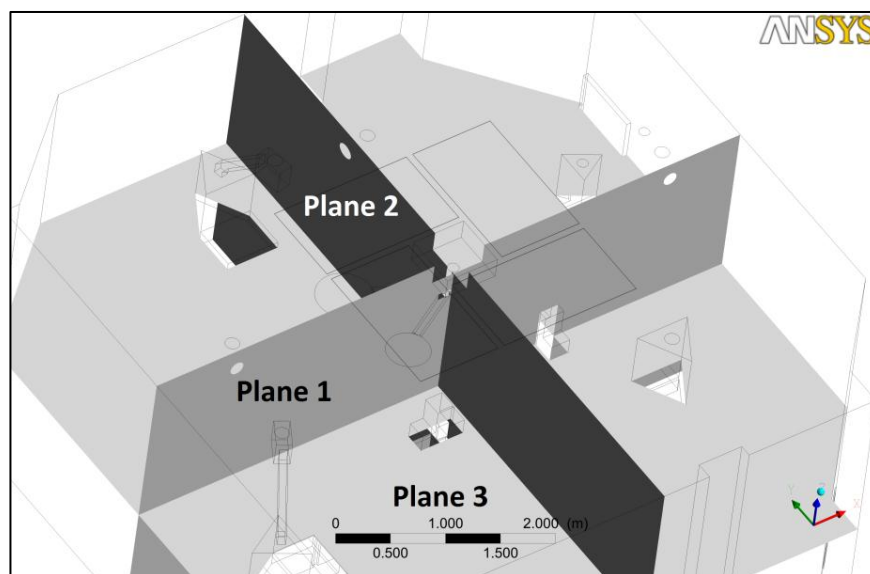


Figure 4.14: Location of Plane 1, Plane 2 and Plane 3.

4.6.1. SGHHC OT-5: Uneven air velocities (current condition) versus even air velocities at inlets

Through an experiment and simulations conducted, Lee et al. (2002) demonstrated the air velocities distribution at the air inlet is able to affect the airflow throughout the room. They further concluded the assumption of applying uniform inlet velocities leading to a larger error. In Figure 4.15, the surgical staff (red box in Figure 4.15) experiences different direction of airflow on his body, since there is a downward airflow in front of the staff, and an upward airflow at the back of the staff. Nonetheless, it is evident that the airflow is turbulent below the operating table.

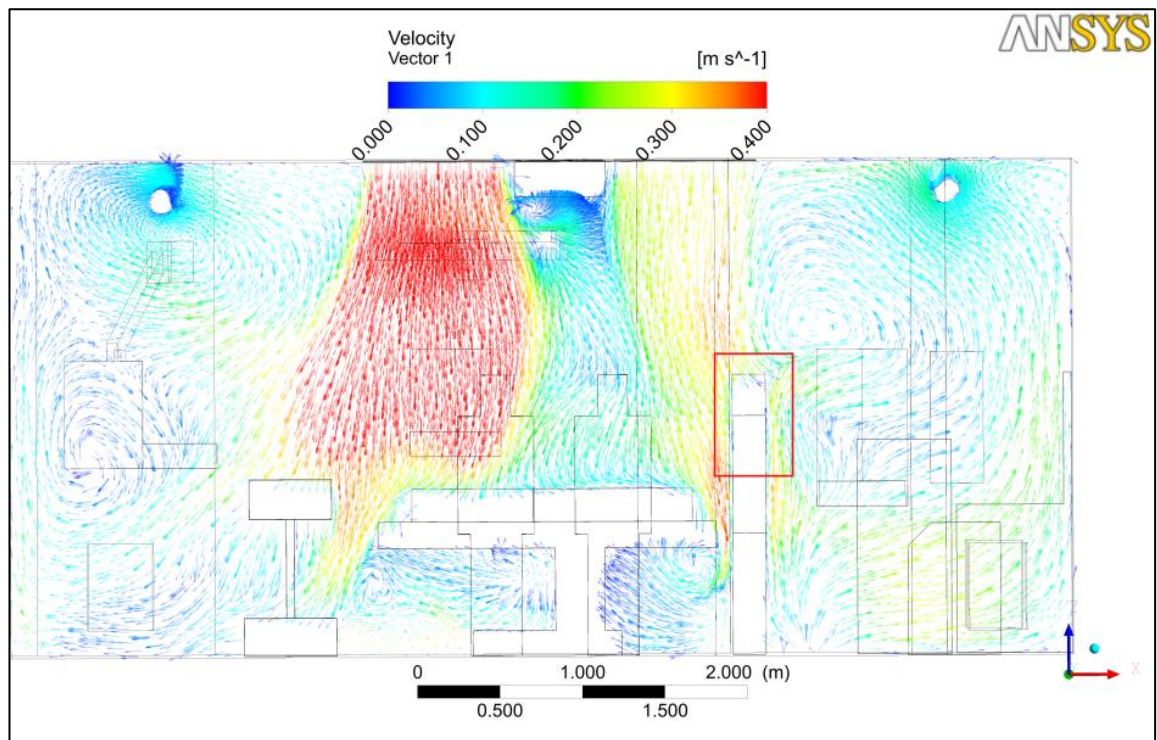


Figure 4.15: The airflow in SGHHC OT-5 with uneven inlet air velocities at Plane 1.

Figure 4.16 compares the airflow above the patient in an OR with uneven and even inlets air velocities. By referring to Figure 4.8, the centre among the room air inlets is an area without the supply of the air, since the area is used for mounting the surgical lights at the ceiling. In the other words, the motion of air in the region right below this area is relying on the pressure difference with the adjacent region (with a faster air jet discharged from the inlets), as related to the Bernoulli's principle. There is a noticeable different between both conditions, as shown in Figures 4.16, 4.17 and 4.19. Similar magnitude of air velocities surrounds the centre region with relatively lower air velocity (< 0.1 m/s) will create a small recirculation at the region with a lower air velocity.

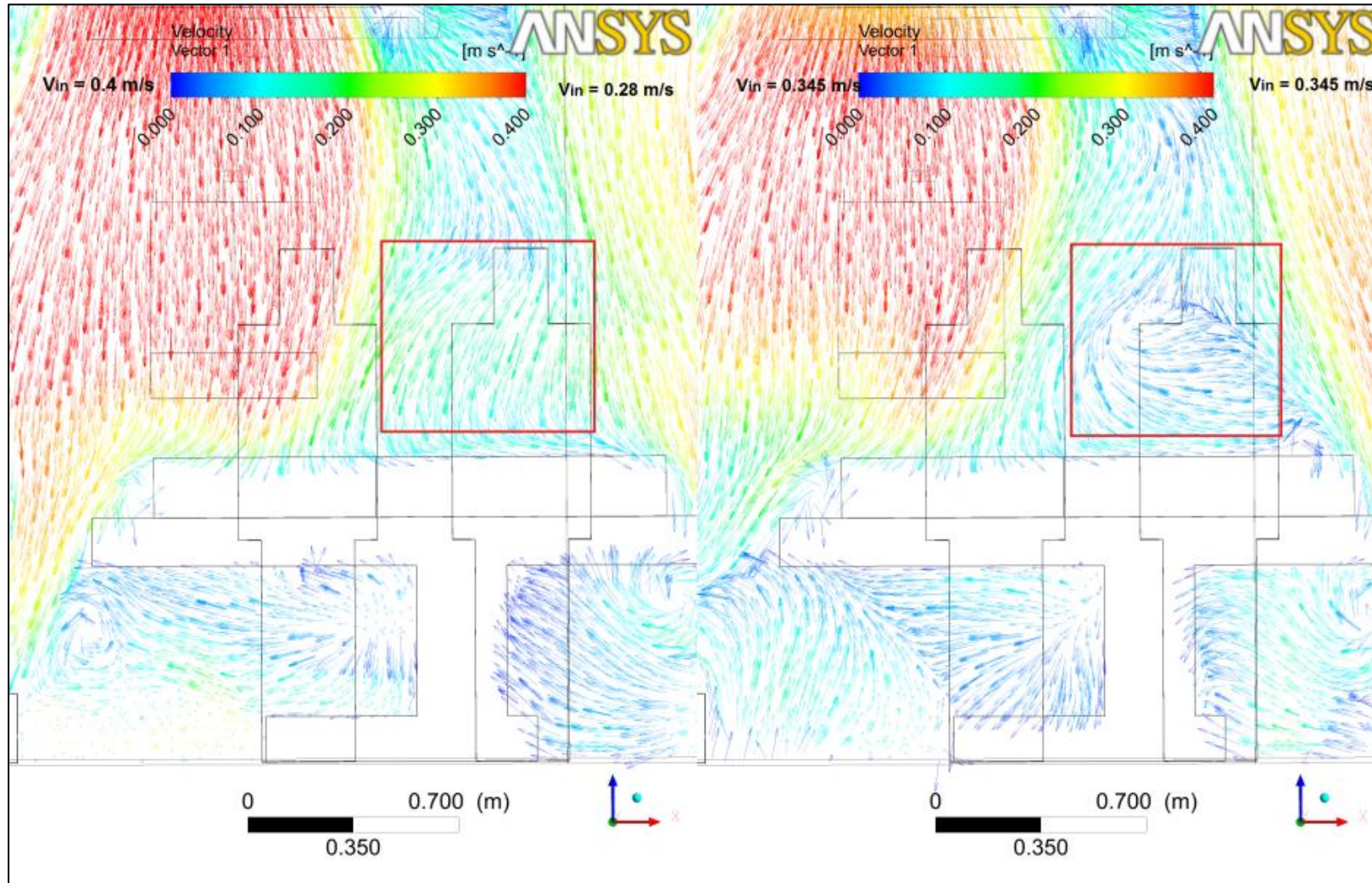


Figure 4.16: Airflow above the patient in OT-5 with uneven (left) and even (right) inlets air velocities at Plane 1.

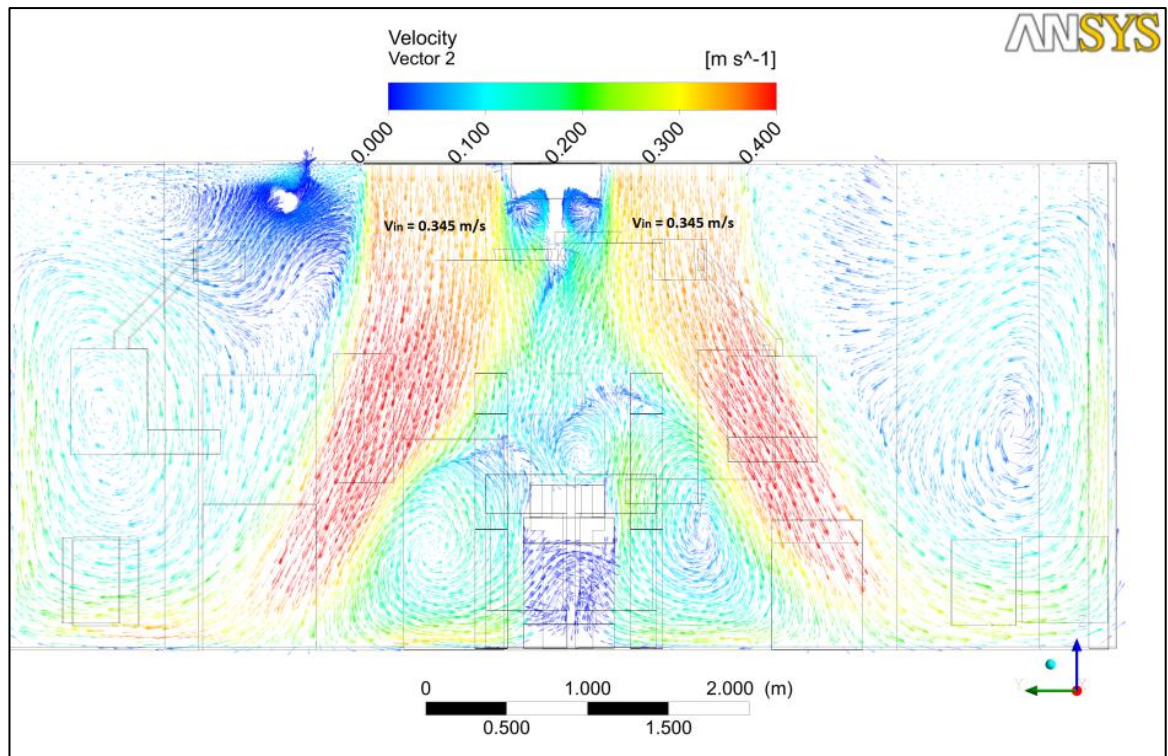


Figure 4.17: The airflow in SGHHC OT-5 with even inlet air velocities at Plane 2.

From the study conducted by Chow and Yang (2005) on ultra-clean ventilation in OR, he concluded that the inlet air velocity is the most important factor that dictates the cleanliness in an OR. Besides, the existence of medical lamp will bring two impacts on the airflow. Firstly, it obstructs the airflow, and secondly, the effect of heat dissipation. In the current study, obviously the air accelerates as it passes through the gap between both medical lamps (red- squared in Figure 4.18). Since the medical lamps dissipate heat, and hence it provokes the air recirculation below the lamp via natural convection. The temperature gradient created due to the heat dissipation gives rise to natural convection, with an aided entrainment. It was observed that downward airflow with higher air velocity surrounds the medical lamps cause the air below the medical lamp entrain improperly, since a higher air velocity surrounds the medical lamps serve as an air curtain in such condition. From the current observation, it can be deduced that the position and location of the surgical lights at the surgical site will affect the airflow

profile at the region right below the surgical lights, diminishing the washing effect of a downward unidirectional airflow. This was slightly different from the conclusion made by Chow and Yang (2005), stating that *'the obstruction effect of the medical lamp carries more weight than its heat dissipation effect'*, since in the current observation, the obstruction effect has created an 'air barrier' and the heat dissipation from the surgical lights aids the air recirculation underneath the surgical light via convection. Again, since there is an obstruction effect created by the medical lights, it is prudent that the geometry of the medical light must be modelled closely to the existing geometry.

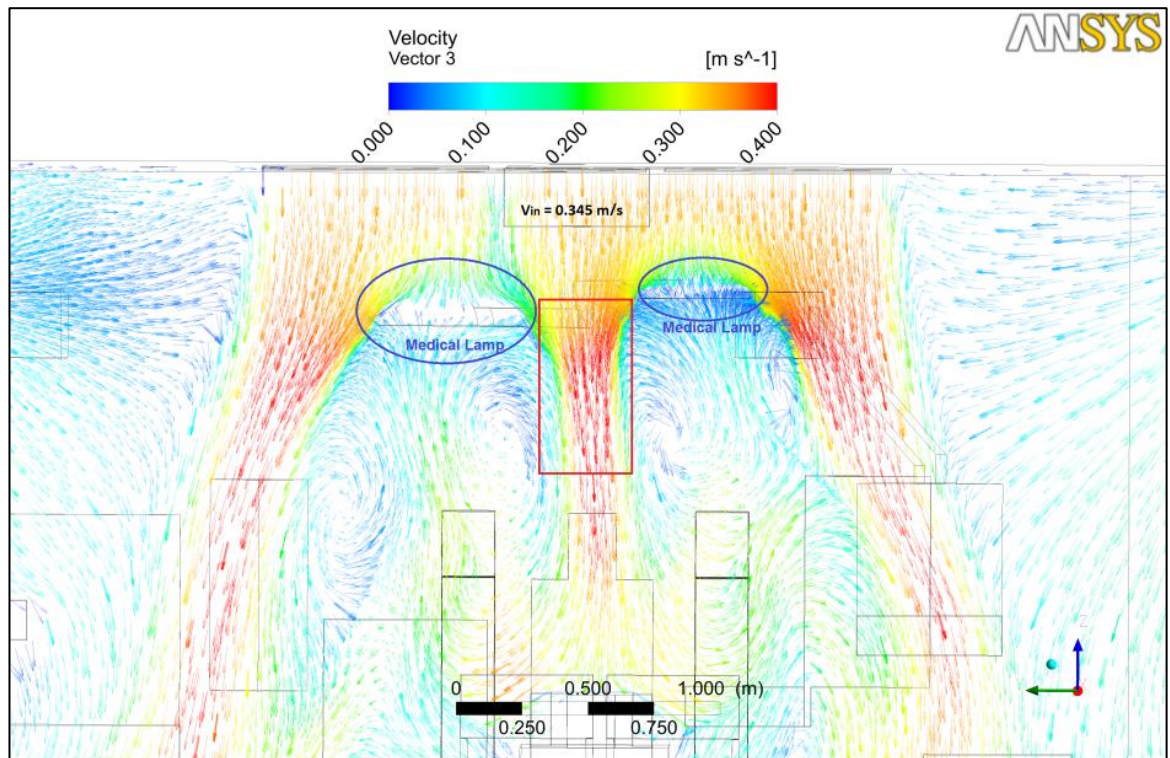


Figure 4.18: Airflow around the medical lamp.

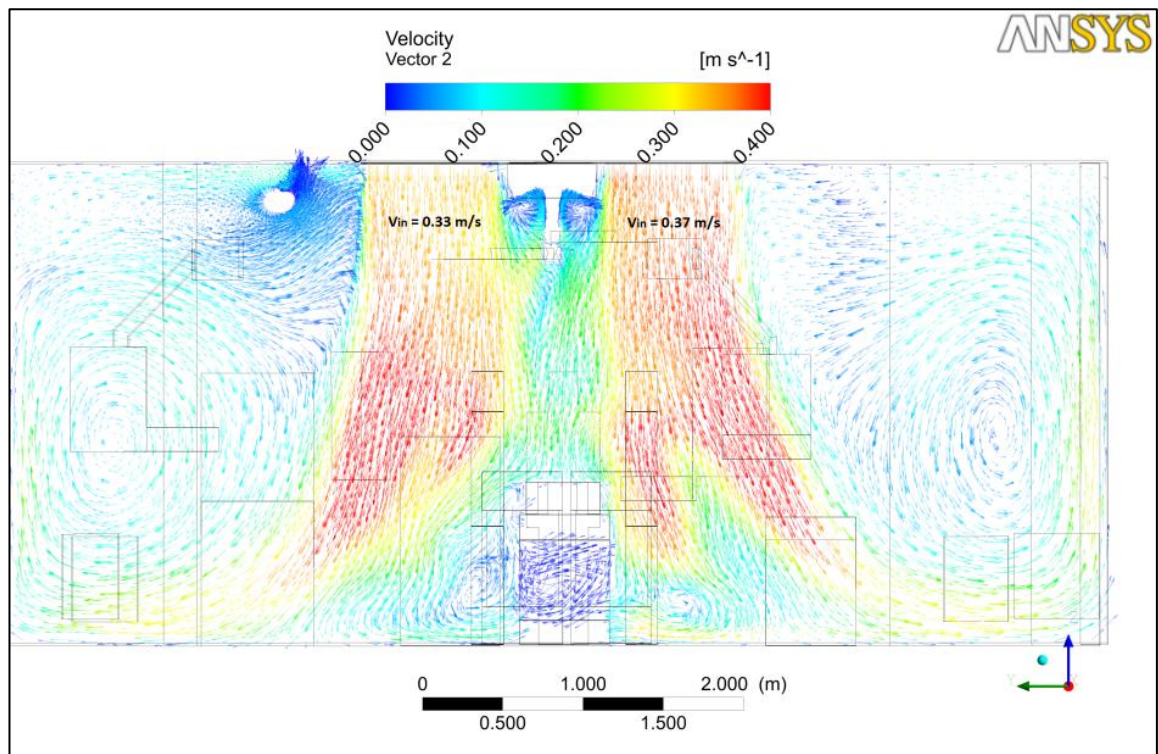


Figure 4.19: The airflow in SGHHC OT-5 with uneven inlet air velocities at Plane 2.

In terms of temperature distribution, the comparisons of temperature distribution are shown in Figures 4.20 and 4.21. Generally, temperature distribution is better when there is an even velocities distribution of inlet air. Uneven inlet air velocities distribution causes different staff experiences different surrounding temperature. Nonetheless, surgical staffs will experience lower RH (50-55 % RH) in an OR with even inlet air velocities as shown in Figure 4.22.

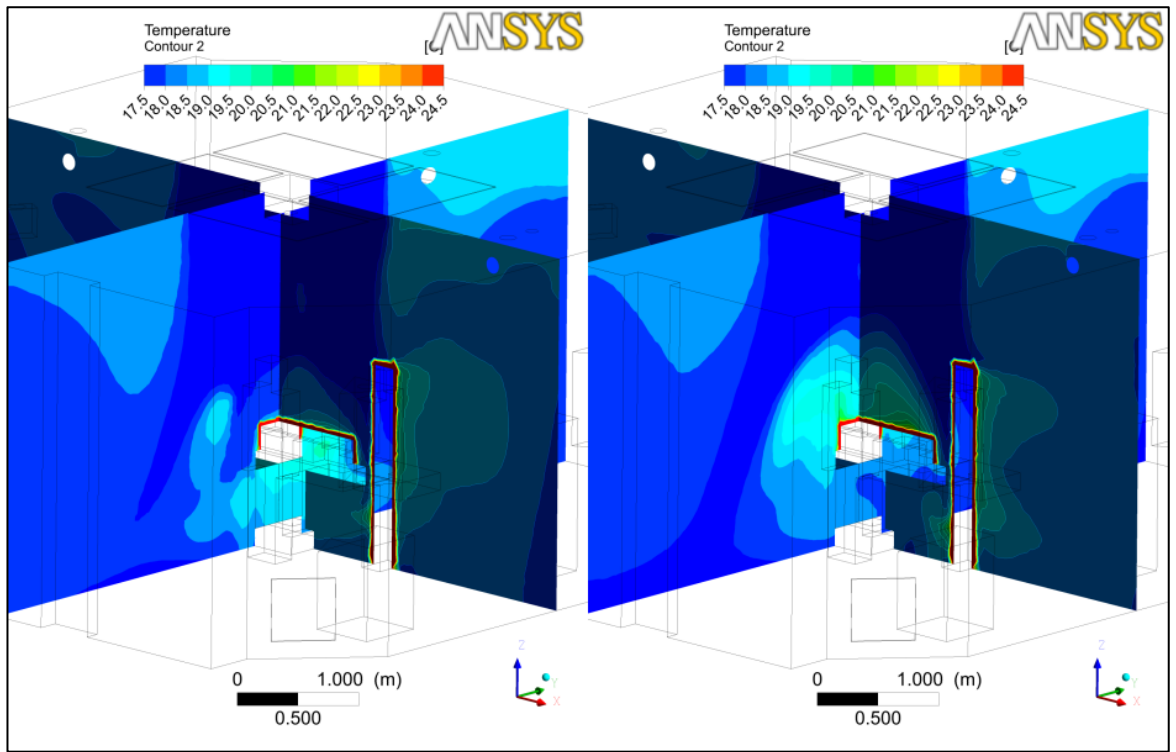


Figure 4.20: Temperature distribution in OT-5 with uneven (left) and even (right) inlet air velocities.

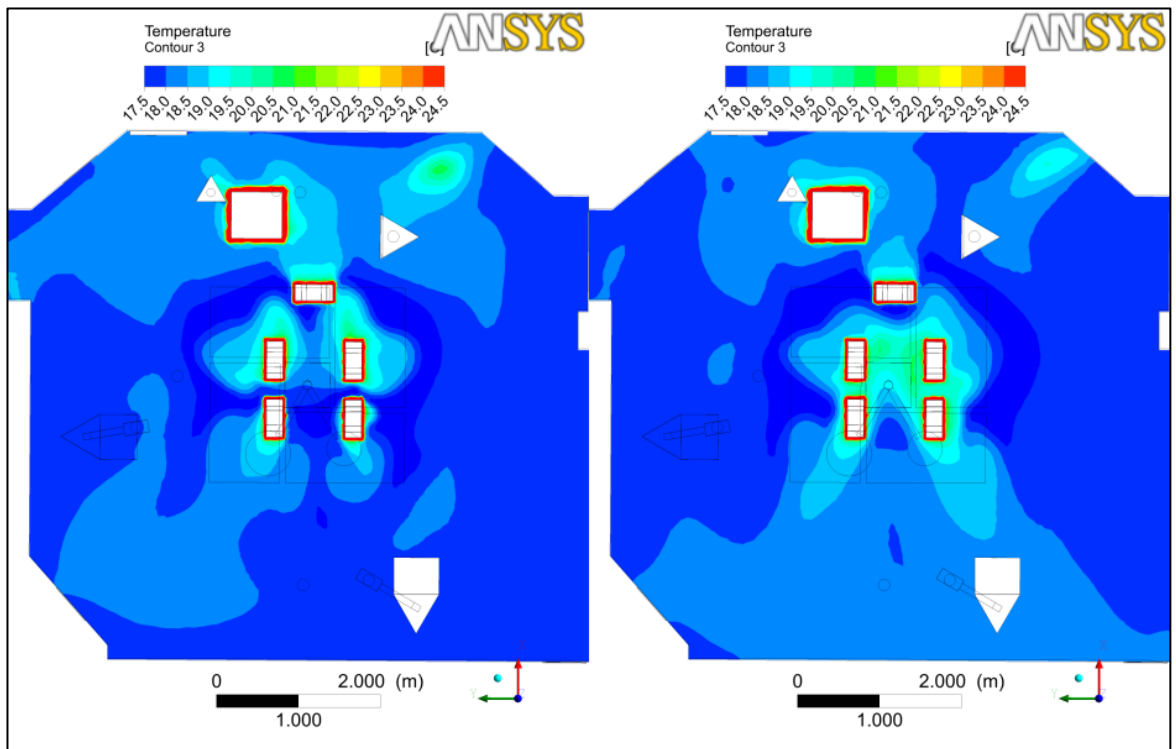


Figure 4.21: Temperature distribution in OT-5 with uneven (left) and even (right) inlet air velocities at Plane 3.

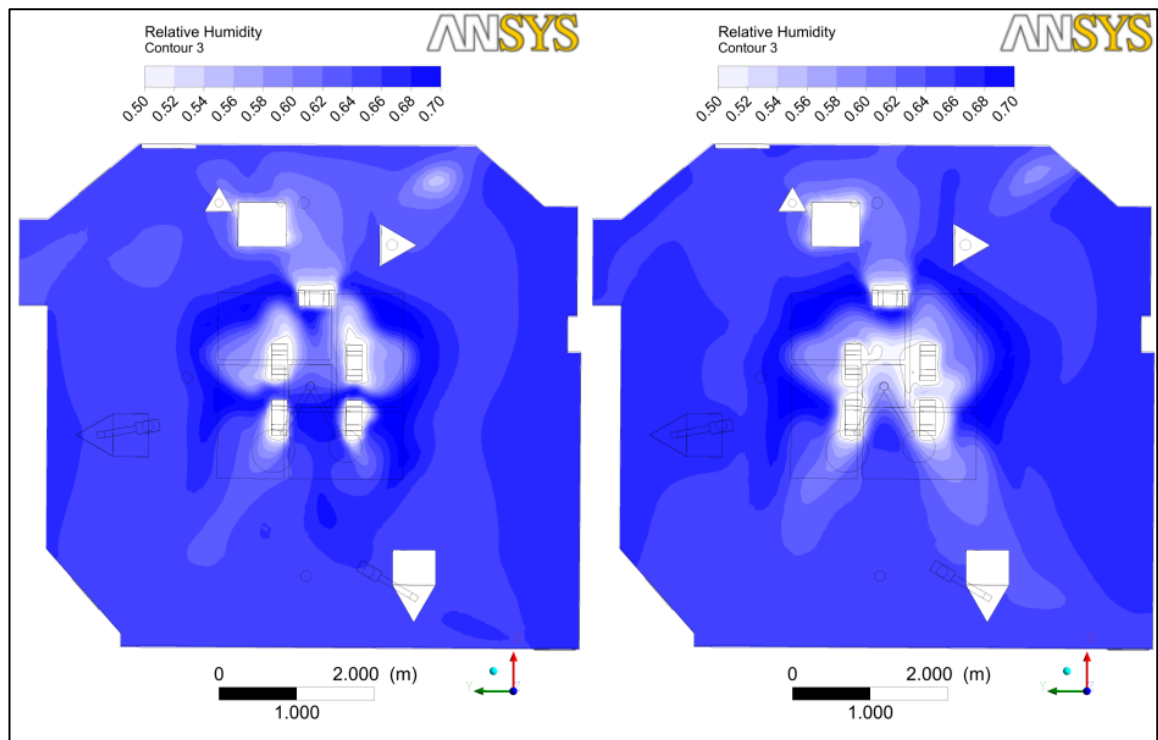


Figure 4.22: RH distribution of in OT-5 with uneven (left) and even (right) inlet air velocities at Plane 3.

In this study, particles with $12\mu\text{m}$ in diameter release from the machine (as in Figure 4.8) were modelled. There were equal numbers of 76 particles in both cases for comparison purpose. Surprisingly, OT-5 with uneven inlet velocities performed better in entraining the particles. From 76 particles released, there are 75 particles discharged from the OR, compared to 64 particles for even inlet velocities (Figure 4.23). For the modelling of gaseous contaminant, the contaminant was assumed to be released from the surface of the patient. The result in Table 4.8 shown that the OR with uneven inlet velocities performs better than even inlet air velocities. It can be seen that the OR with uneven inlet velocities has a lower average concentration and lower maximum concentration at the surgical site (both 1.2 m and 1.7 m above the floor).

OR with uneven inlet velocities.									
Fate	Number	Elapsed Time (s)				Injection, Index			
		Min	Max	Avg	Std Dev	Min	Max	Min	Max
Incomplete	1	1.290e+005	1.290e+005	1.290e+005	0.000e+000	injection-0	34	injection-0	34
Escaped - Zone 7	21	2.853e+001	2.467e+002	1.123e+002	6.491e+001	injection-0	63	injection-0	7
Escaped - Zone 8	17	3.188e+001	1.298e+002	7.068e+001	3.545e+001	injection-0	43	injection-0	26
Escaped - Zone 9	37	8.573e+001	1.466e+002	1.118e+002	1.868e+001	injection-0	73	injection-0	68
OR with even inlet velocities.									
Fate	Number	Elapsed Time (s)				Injection, Index			
		Min	Max	Avg	Std Dev	Min	Max	Min	Max
Incomplete	12	7.396e+003	6.115e+005	1.345e+005	1.508e+005	injection-0	16	injection-0	26
Escaped - Zone 6	14	5.196e+001	2.207e+002	1.388e+002	3.809e+001	injection-0	65	injection-0	43
Escaped - Zone 7	40	2.794e+001	5.401e+002	9.942e+001	1.065e+002	injection-0	50	injection-0	53
Escaped - Zone 8	5	3.507e+001	1.904e+002	8.866e+001	6.548e+001	injection-0	70	injection-0	72
Escaped - Zone 9	5	2.423e+002	9.082e+002	4.373e+002	2.454e+002	injection-0	40	injection-0	69
Note: Zone 6 represents Exhaust 1 Zone 7 represents Exhaust 2 Zone 8 represents Exhaust 3 Zone 9 represents Exhaust 4									

Figure 4.23: Particle tracking for particle with 12µm diameter release from machine.

Table 4.8: Comparison of the concentration of gaseous contaminant, CO₂.

Height from the floor, m	Concentration ($\times 10^{-6}$), ppm			
	uneven inlet velocities		even inlet velocities	
	Average	Maximum	Average	Maximum
1.7	0.16	0.5	0.17	3.2
1.2	0.25	4.8	0.34	8.0

4.6.2. SGHHC OT-5: Air velocity reduction

In this subsection, the potential of reducing inlet air flow rate by 15% was studied. In other words, it means that there is a reduction of air velocity by 15% (and thus 15% reduction of original ACH). In this section, the inlet air velocities of 0.345 m/s and 0.3 m/s (even air velocities) were compared. The air inlet velocity was not reduced significantly (e.g. to 0.2 m/s), since it will significantly increase the overall Archimedes number of the OR by 5.4 times, and reducing the efficiency of the blower in the AHU.

Generally, the reduction of inlet velocity has resulted in an increase of air temperature at the surgical region. From Figure 4.24, the reduction of air velocity will rise the maximum temperature at Plane 1 (1.2 m above the floor) from 19.9°C to

20.3 °C. Overall, the air temperature is still maintained well below 20°C with the reduction of the inlet velocity.

The ability of removing particles does not diminished by the reduction of inlet velocity (Figure 4.25). Although the result in Figure 4.25 has shown an improvement in the particulate removal ability from the reduction of the inlet velocity, it does not guarantee the improvement is directly attributed to the changes made on the inlet velocity, since in the actual condition, the generation of particulate contaminants are arbitrary in the OR. Meanwhile, the reduction of the inlet velocity will cause the average concentration of gaseous contaminant increase by 12% and 41 %, 1.2 m and 1.7 m above the floor, respectively (Figure 4.26 and Table 4.9).

From the comparison, a slight reduction of inlet velocity to 0.3 m/s is possible, if the increment of the air temperature at the surgical area can be tolerated.

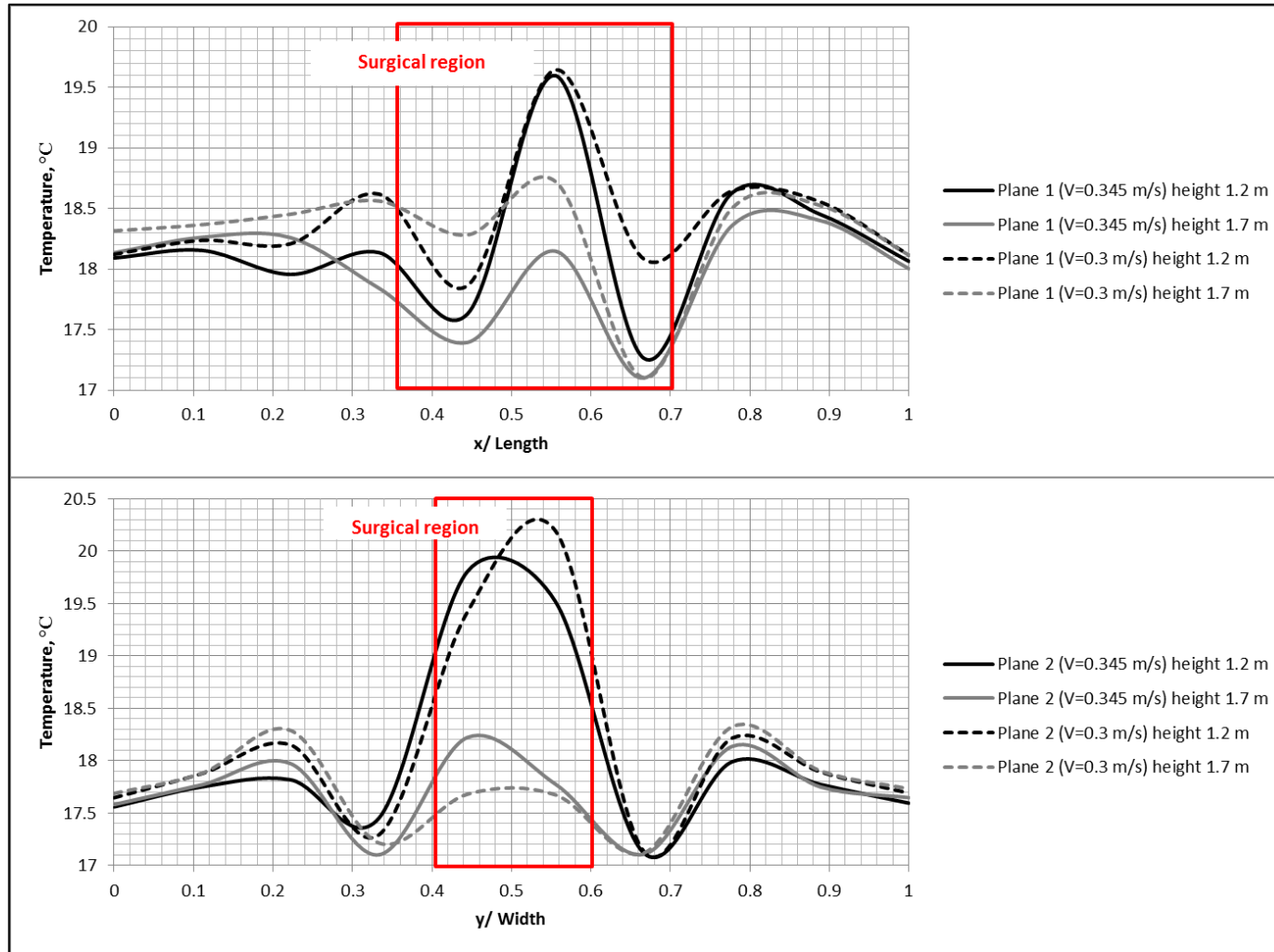


Figure 4.24: Air temperature distribution for inlet $V=0.345$ m/s and $V=0.3$ m/s at 1.2 m & 1.7 m above the floor.

OR with even inlet velocities (0.345 m/s)									
Fate	Number	Elapsed Time (s)				Injection, Index		Min	Max
		Min	Max	Avg	Std Dev	Min	Max		
Incomplete	12	7.396e+003	6.115e+005	1.345e+005	1.508e+005	injection-0	16	injection-0	26
Escaped - Zone 6	14	5.196e+001	2.207e+002	1.388e+002	3.809e+001	injection-0	65	injection-0	43
Escaped - Zone 7	40	2.794e+001	5.401e+002	9.942e+001	1.065e+002	injection-0	50	injection-0	53
Escaped - Zone 8	5	3.507e+001	1.904e+002	8.866e+001	6.548e+001	injection-0	70	injection-0	72
Escaped - Zone 9	5	2.423e+002	9.082e+002	4.373e+002	2.454e+002	injection-0	40	injection-0	69

OR with even inlet velocities.(0.3 m/s)									
Fate	Number	Elapsed Time (s)				Injection, Index		Min	Max
		Min	Max	Avg	Std Dev	Min	Max		
Incomplete	6	2.370e+004	1.472e+005	1.014e+005	4.207e+004	injection-0	72	injection-0	61
Escaped - Zone 6	1	3.353e+002	3.353e+002	3.353e+002	0.000e+000	injection-0	69	injection-0	69
Escaped - Zone 7	46	2.627e+001	6.969e+002	1.021e+002	1.153e+002	injection-0	63	injection-0	27
Escaped - Zone 8	12	3.694e+001	1.335e+002	9.897e+001	3.819e+001	injection-0	49	injection-0	37
Escaped - Zone 9	11	1.679e+002	3.754e+002	2.408e+002	5.946e+001	injection-0	20	injection-0	12

Note:
Zone 6 represents Exhaust 1
Zone 7 represents Exhaust 2
Zone 8 represents Exhaust 3
Zone 9 represents Exhaust 4

Figure 4.25: Particle tracking for particle with 12µm diameter release from machine for inlet air velocity reduction.

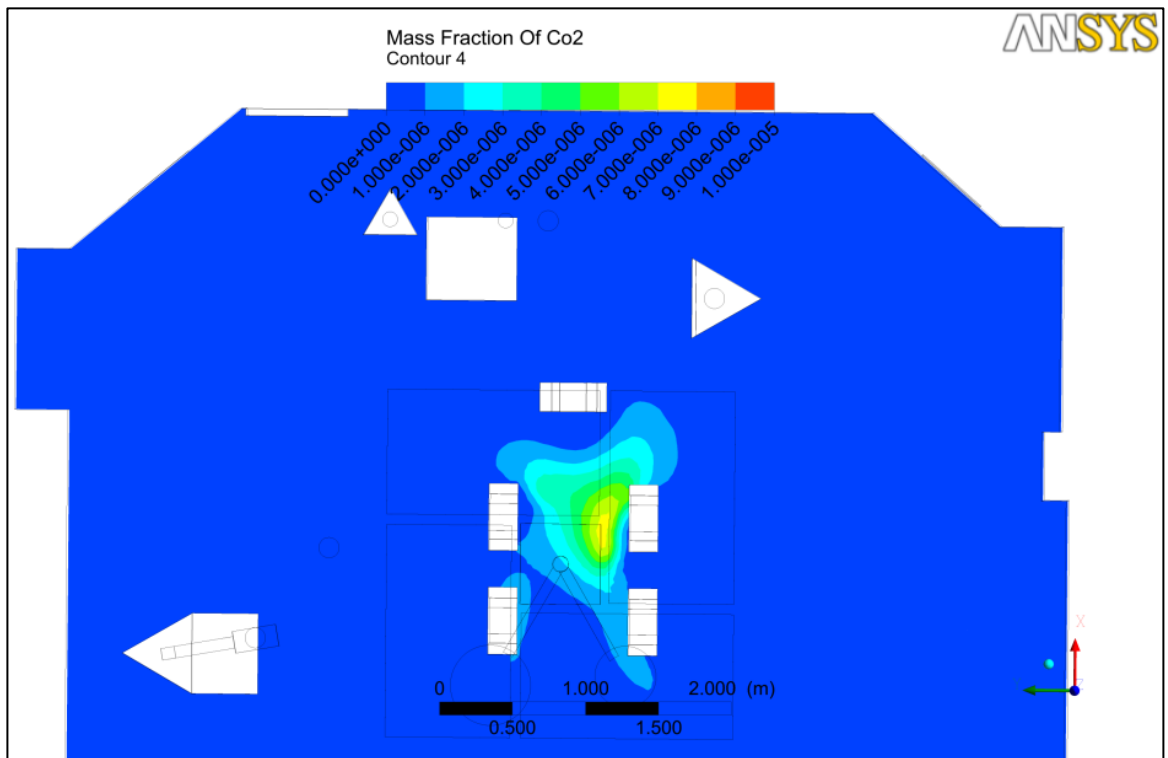


Figure 4.26: Gaseous contaminant, CO₂ concentration 1.2 m above floor level.

Table 4.9: Comparison on concentration of gaseous contaminant, CO₂ for inlet air velocity reduction.

Height from the floor, m	Concentration ($\times 10^{-6}$), ppm			
	Inlet velocity 0.345 m/s		Inlet velocity 0.3 m/s	
	Average	Maximum	Average	Maximum
1.7	0.17	3.2	0.24	2.7
1.2	0.34	8.0	0.38	8.3

4.7. Concluding summary

This chapter has demonstrated the air distribution in SGHHC OT-5, an OR with 42 ACH (average inlet air velocity of 0.345 m/s).

There are few points that need to be highlighted worthily.

- i. The obstruction and heat dissipation effects from the surgical light cannot be neglected. The combination of both effects will result in a heat trap at the region below the surgical light.
- ii. From this study, under the same total flow volume for OT-5, the OT-5 with the uneven inlet velocities performs better than OT-5 with the even velocities distribution at the inlets.
- iii. The reduction of air flow rate by 15% (to average inlet air velocity of 0.3 m/s) is possible in OT-5.
- iv. The outcome for the case study suggests, the room air inlet should locate above the surgical site, rather than periphery of the surgical site, since current design will result in inefficiency in ventilation.

5.0 Case study on UMMC OT-11

University of Malaya Medical Centre is a government hospital in South-West of Kuala Lumpur that provides an affordable health care to public, founded by the late Tan Sri Datuk Professor Dr. Thumboo John Danaraj. It is located adjacent to Federal Highway Kuala Lumpur and University of Malaya, serving the residents in Klang Valley, Malaysia since 1968. There are a total of 20 ORs in UMMC. However, the geometry and design of ORs are different from OR to OR, means that it was built without a standardized layout, with a significant variation on room air inlets layout. As an example, the differences between OT-11 and OT-12 are as shown in Figure 5.1. In this chapter, air distribution in UMMC OT-11 will be investigated. Figures 5.2-5.4 provides the information on the general layout and overview of mesh generation for this OR.



Figure 5.1: OT-11 of UMMC (left) and OT-12 of UMMC (right).

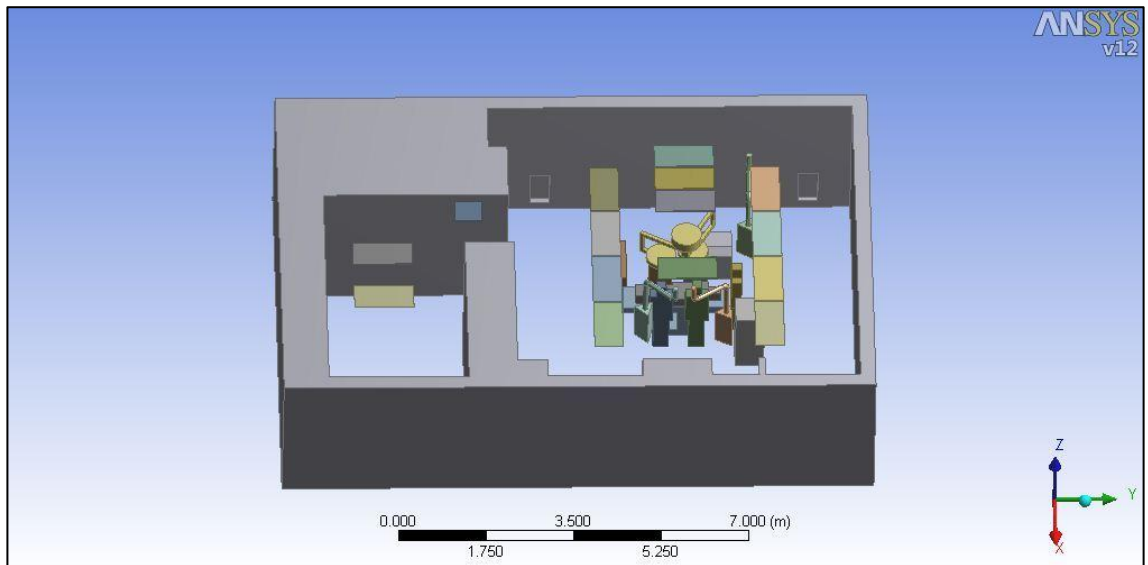


Figure 5.2: Modeling of UMMC OT-11.

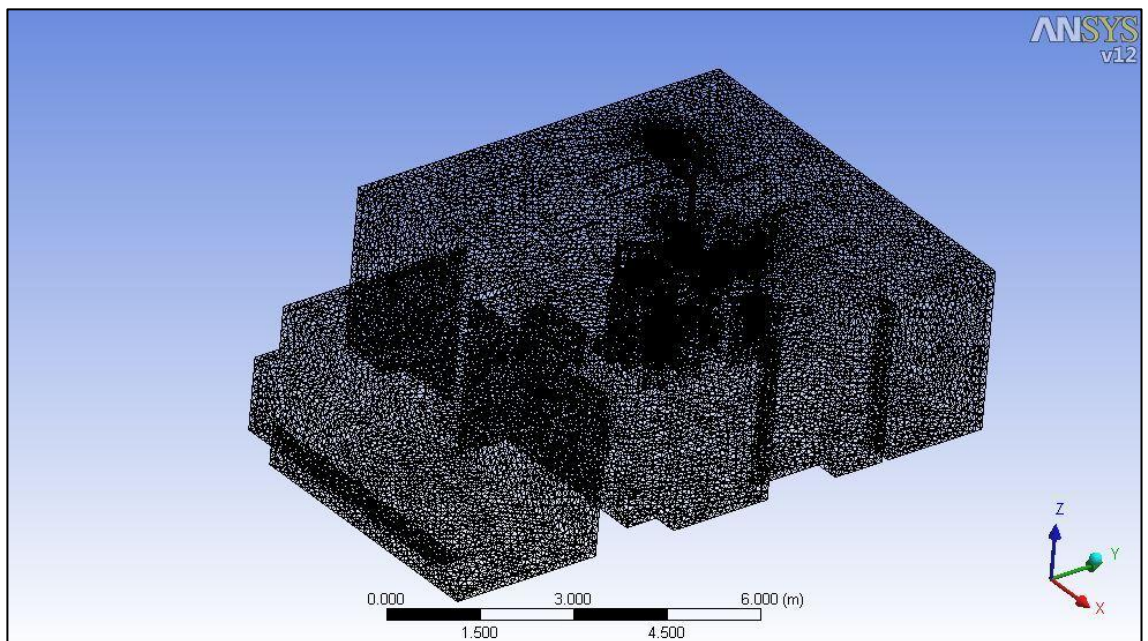


Figure 5.3: Generated computational mesh for UMMC OT-11.

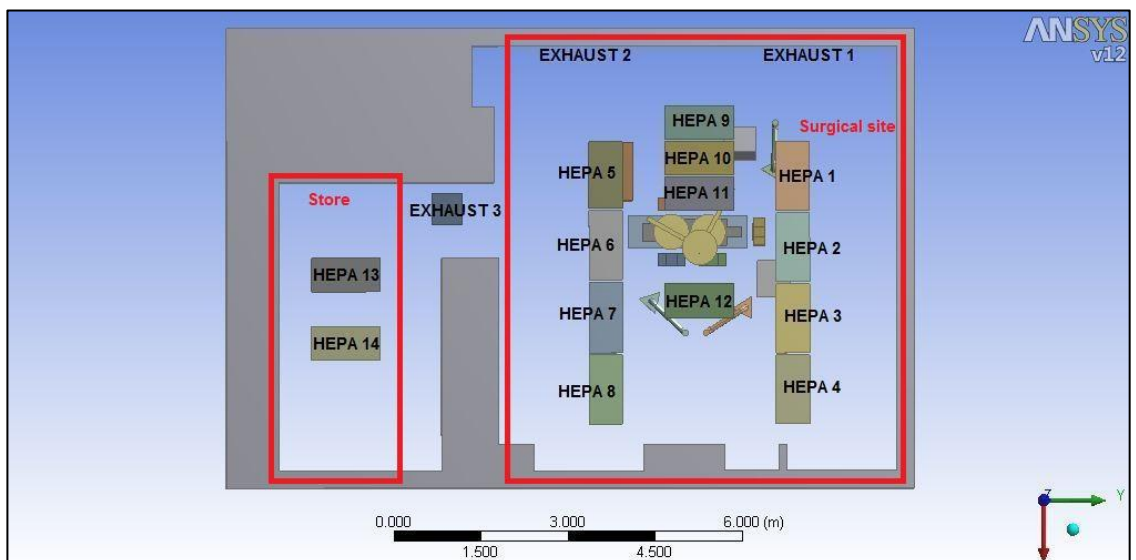


Figure 5.4: Nomenclature for HEPA inlets and exhausts UMMC OT-11.

5.1 Assumptions

There were several assumptions need to be made prior to the indoor airflow measurement.

- i. The room has reached steady state condition.
- ii. The air condition in the non-operating OR during measurement was considered as an isothermal case.
- iii. The layout of OR in the modeling was approximated to the layout during the actual operation process referring to the information provided by matron.

Besides, there were several assumptions made in the indoor airflow simulation.

- i. The room modeled in the simulation had a steady state condition.
- ii. The surgical site layout in the OR was an approximation based on the information provided by the nurses and facilities management during the discussion in the visit.
- iii. For the human body modeling, human body was assumed to have a skin temperature of 34 °C .

5.2 Measurement at UMMC

The visit was conducted on 2 August 2011. At the moment of the visit, the OR was emptied (major surgical equipment and operating table were removed from OR) since cleaning process were being conducted by the hospital's management. Prior to the visit, there was a short discussion with the nurses and facilities management on the details of ORs in UMMC.

5.3 Physical on-site measurement at OT-11, UMMC

Table 5.1: Measured air condition at room air inlets.

HEPA Inlet No.	Part	DBT, C	RH, %	Average velocity, (m/s)	Dimension	Supply air flow rate, (m ³ /h)
1	I	19.1	81.4	0.18	1.185m x 0.575m (4 ft x 2 ft)	453.80
	II	19.1	81.4	0.19		
	Average	19.1	81.4	0.19		
2	I	19.2	74.3	0.21		515.12
	II	19.2	74.5	0.21		
	Average	19.2	74.4	0.21		
3	I	18.5	78.4	0.24		551.91
	II	18.1	78.4	0.21		
	Average	18.3	78.4	0.23		
4	I	18.3	79.6	0.20		429.27
	II	18.6	79.8	0.15		
	Average	18.5	79.7	0.18		
5	I	18.9	80.6	0.22		564.18
	II	19.1	82.9	0.24		
	Average	19.0	81.8	0.23		
6	I	19.3	83.2	0.16	392.47	
	II	19.1	82.4	0.16		
	Average	19.2	82.8	0.16		
7	I	18	76.9	0.18	502.85	
	II	18.1	79.1	0.23		
	Average	18.1	78.0	0.21		
8	I	18.6	80.8	0.14	331.15	
	II	18.8	81.0	0.13		
	Average	18.7	80.9	0.14		
9	I	19.1	81.2	0.21	539.65	
	II	19.2	82.0	0.23		
	Average	19.2	81.6	0.22		
10	I	19.3	82.5	0.14	331.15	
	II	19.3	82.1	0.13		
	Average	19.3	82.3	0.14		
11	I	18.8	74.4	0.21	478.33	
	II	18.3	72.7	0.18		
	Average	18.6	73.6	0.20		
12	I	18.1	74.8	0.18	453.80	
	II	18.2	75.3	0.19		
	Average	18.2	75.1	0.19		
13	I	18.6	79.5	0.18	453.80	
	II	18.8	80.0	0.19		
	Average	18.7	79.8	0.19		
14	I	19.0	80.7	0.17	404.74	
	II	19.2	81.0	0.16		
	Average	19.1	80.9	0.17		
Average air condition at inlet		18.8	79.3	0.186	Total air flow rate	6402.200

There are total of 14 HEPAs (with dimension of 1.185 m x 0.575 m each) serving this OR. The air velocity for each inlet was measured by dividing each HEPA into two areas and the readings were averaged and the results were tabulated in Table 5.1.

From the measurement done, it revealed UMMC OT-11 was oversized in terms of ACH. In current design, the ACH for OT-11 is 33.5, with a built-up area of 64.7 m², height of 2.95 m. There are total of 14 HEPAs (with dimension of 1.185 m x 0.575 m each) serving this OR. The air velocity for each inlet was measured by dividing each HEPA air inlets into two areas and the readings were averaged. However, as shown in Table 5.3, the velocity distribution for each inlet was not equal. It deviates by a standard deviation of 0.030 m/s from an average air velocity of 0.186 m/s , implying 10 out of 14 inlets having a supply velocity between 0.156 m/s -0.216 m/s. Lowest inlet air velocity reported is 0.186 m/s, which are located at HEPA inlet 8 and HEPA inlet 10 (HEPA Inlet 10 located above the surgical area).

During the measurement, the OR was in non-operating condition, and there was minimum heat source in the OR (except fluorescent lamp lighting). From the measurement in 3 locations at 5 different heights (0.1, 0.6, 1.1, 1.7 m and 2.3 m from the floor), the difference between the average room temperature and inlet temperature is 1°C, hence the room condition could be safely being considered as an isothermal room.

It should be noted that, the measured relative humidity in the OR was very high, exceeded the limit set by any standards' recommendation. However, this was an OR in non-operating condition. By assuming a sensible heat load of 1500 W inside the OR (and ignoring moisture released by occupants), it will result in a RH of approximately 75%, still exceeds the recommendations. In such a case, the OR failed to meet the design requirement for RH.

In terms of particulate counting, OT-11 satisfied the requirement for a Class 7 clean room.

Table 5.2: Particulate count in the non-operating UMMC OT-11.

Particle size, μm	Reading 1	Reading 2	Average count	Particulate count requirement for Class 7 clean room
> 0.3	513209	524549	518879	-
> 0.5	16834	17150	16992	<352000
> 1.0	1414	1686	1550	<83200
> 3.0	317	240	278.5	-
> 5.0	98	80	89	<2930
> 10.0	19	20	19.5	-

5.4 Mesh independence study for OT-11 UMMC simulation

There were six simulations with different number of mesh elements (3766201, 2822150, 1987196, 1275198, 883431, and 741115) had been conducted. Table 5.3 lists a denotation given for these simulations for simplicity. The graphical simulation results are attached in the Appendix H.

Table 5.3: Identification for simulations UMMC OT-11.

<i>Mesh number</i>	<i>ID</i>
3766201	I
2822150	II
1987196	III
1275198	IV
883431	V
741115	VI

Plane 1 cut the cross section of surgical light. Since the heat from surgical light is defined in heat flux, it is favorable to examine the maximum temperature over the plane that by intuition will occur at the surface of the surgical lamp. Oscillatory convergence

was observed in simulation I, II and III with a convergence ratio of -0.67 (less than zero). Hence, the results could not be interpreted clearly (Coleman et al., 2001). From the comparison of different mesh number, mesh density as in simulation II was sufficient to perform the study on airflow in this OR.

5.5 Fieldwork measurement and simulation – A comparison

In this section, the air velocity of between measurement and simulation were compared. Note that the OR was emptied during the measurement. The air temperature was not compared, since the room was considered as isothermal case during the measurement as the difference between average room air temperature and supply air temperature was $0.8\text{ }^{\circ}\text{C}$ ($1 < ^{\circ}\text{C}$). The air velocity in were compared in 5 heights (0.1 m, 0.6 m, 1.1 m, 1.6 m, 2.3 m) , at 3 measurement points, as indicated in Figure 5.6. Generally, there was a large deviation of air velocity between prediction and measurement result at 0.1 m above the floor. Besides, the trend from the prediction satisfies the measurement result. Hence, current model was accepted.



Figure 5.5: Measurement inside the UMMC OT-11.

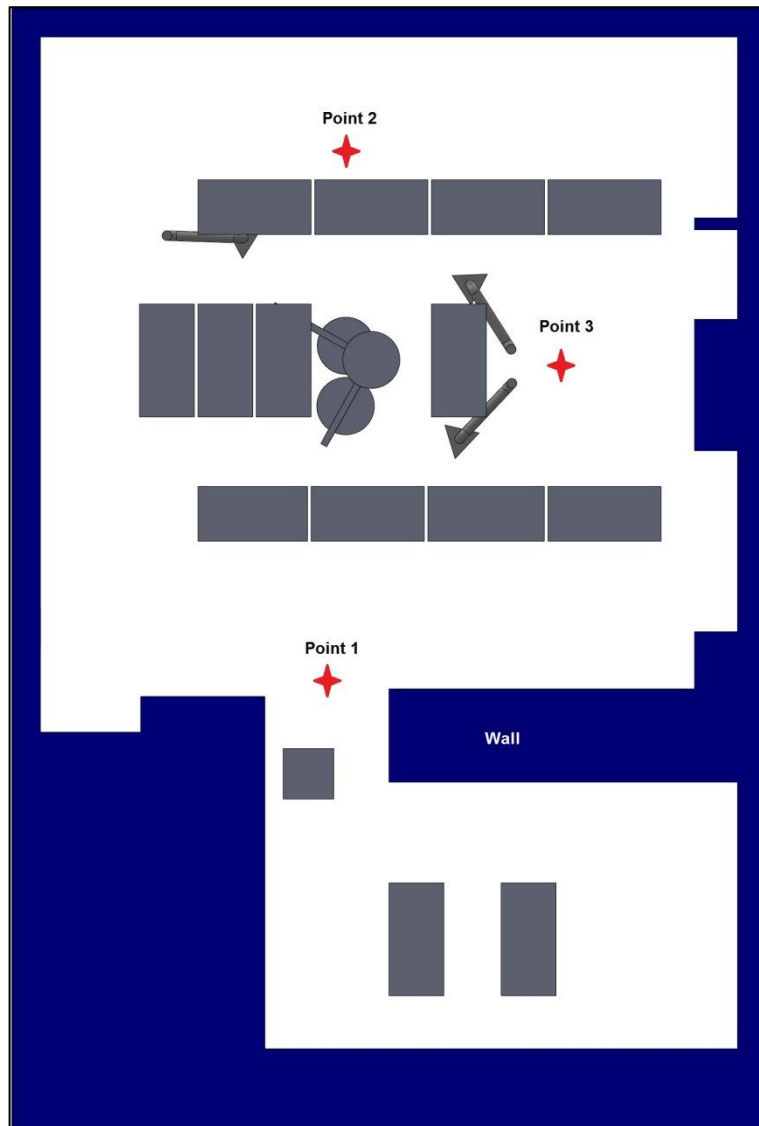


Figure 5.6: Location of measurement points inside the UMMC OT-11.

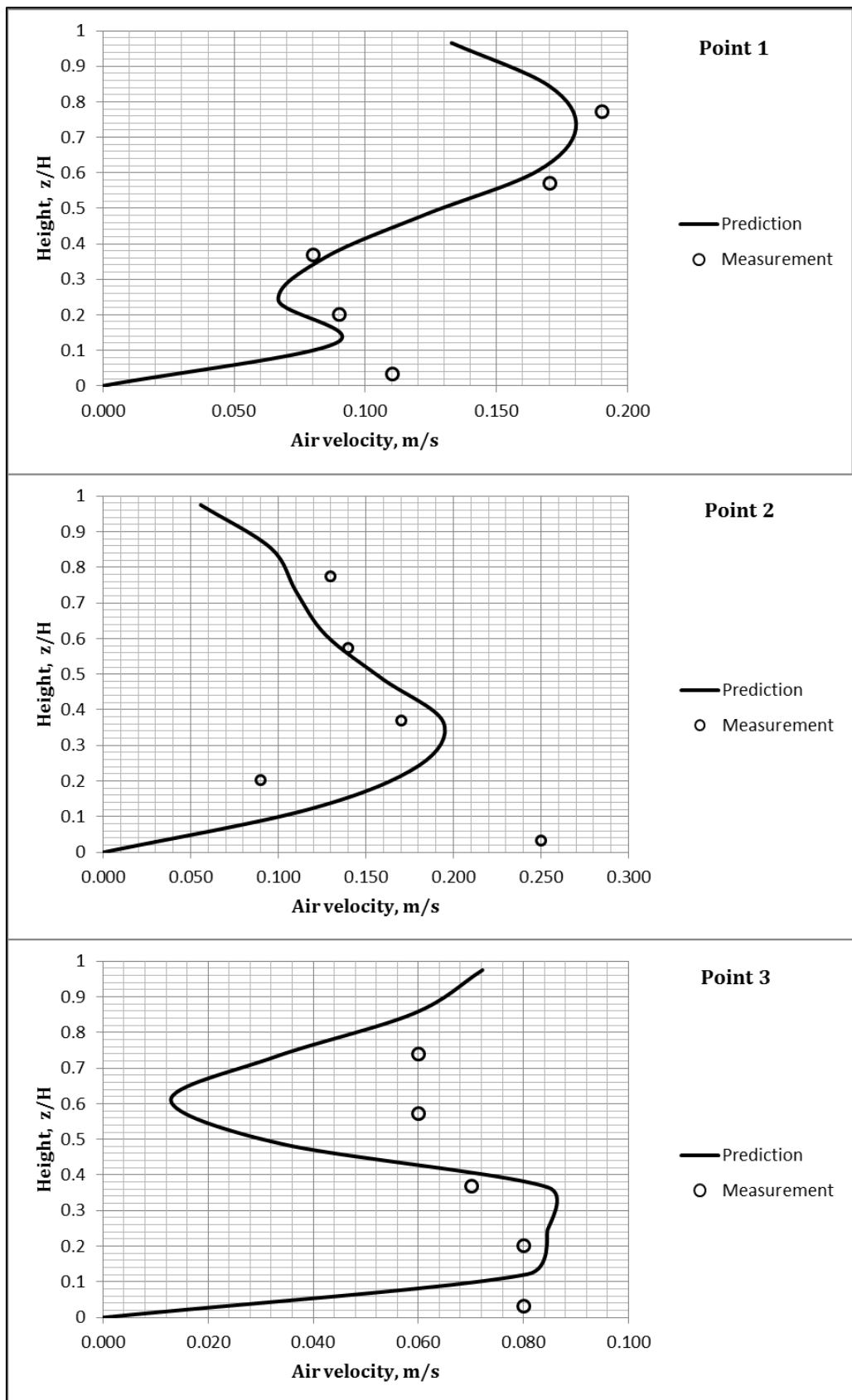


Figure 5.7: Comparison of prediction and measurement result.

5.6 Simulation for UMMC OT-11

In this subsection, the information on the setting and boundary condition are provided in Table 5.4 and Table 5.5.

Table 5.4: Boundary condition settings for CFD simulation UMMC OT-11.

Item	Details
<i>Air inlet</i>	It is set as velocity inlet which is intended for incompressible flow. The air inlets are modeled as a rectangle (1.185m x 0.575m) which discharges air vertically downward to the operating table. Air temperature is set at 18.8°C, with humidity ratio (mass fraction) of 0.0081. The air velocity for all inlets were set at $V_{in} = 0.2$ m/s, turbulent intensity of 5%.
<i>Air outlet</i>	There are 2 outlets (Exhaust 1 and Exhaust 2) located at the bottom part of a side wall, and an outlet Exhaust 3) located at the ceiling at the corridor connecting store and surgical site (Refer to Figure 5.2).
	Exhaust 1 Dimension: 0.39m x 0.79m, pressure outlet.
	Exhaust 2 Dimension: 0.39m x 0.79m , pressure outlet.
	Exhaust 3 Dimension: 0.53m x 0.53m, pressure outlet.
<i>Walls</i>	No slip condition on the surface, adiabatic walls. Surface of the equipment exist in OR are treated as wall.

Settings for simulation

The settings in the simulations were the same as setting for SGHHC OT-5, as given in Table 4.4. The heat source for current simulations was included in Table 5.5.

Table 5.5: Heat dissipation of equipment in OR UMMC OT-11.

Item ¹	Quantity	Heat dissipation ²
Operating table	1	Nil., represent wall
Surgical lights	2	Heat dissipation 200W(Lamp face) 5W (Lamp back), for each lamp.
Medical gas supply pendant	3	Nil, represent obstacle.
Machine	1	Heat dissipation: 250 W
Personnel	5	Heat dissipation: 100 W each

Patient	1	Heat dissipation: 70 W
Suction machine	1	Heat dissipation: 250W
Table	1	Nil, represent obstacle.

¹Please refer to Appendix E for the dimension of the items above.

²Total cooling load of approximately 1480 W.

5.7 UMMC OT-11: Current condition

As mentioned earlier, the ACH measured in current design condition was 33.5. By adjusting the inlet air velocity, V_{in} to 0.2 m/s for each inlet, it slightly increases the ACH to 36. By examining the vector field for air velocity, it is clearly seen that (Figures 5.8-5.10), the area right below the surgical light was not ventilated with a downward airflow. In Figure 5.11, colored contour showed the region where the air velocity has a negative w-velocity component (facing to the floor). As illustrated in Figure 5.11, the air velocity at the operating region flow was in an upward direction. In UMMC OT-11, there were two rows of HEPAs array for serving ventilating air which were HEPA 1-2-3-4 and HEPA 5-6-7-8. Such configuration will result in a confluent flow, which the air discharged from different HEPAs combines and coalesces, and then moves in a single flow, as indicated in Figure 5.8.

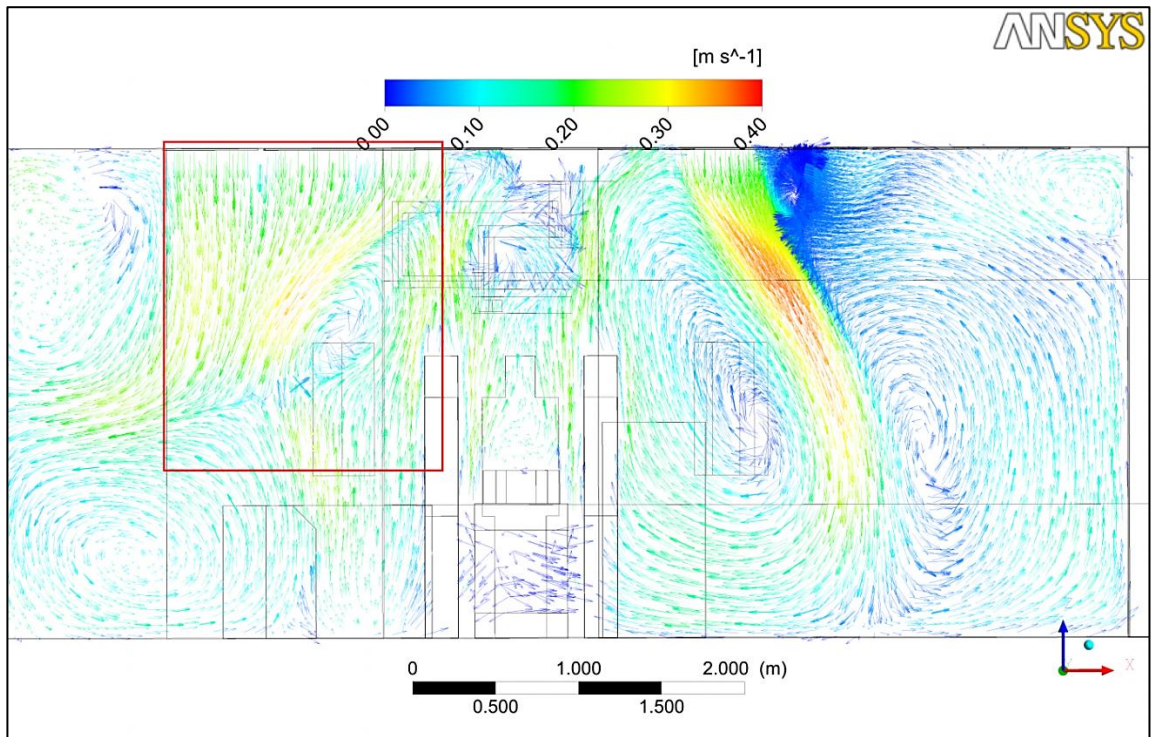


Figure 5.8: Velocity vector for $V_{in} = 0.2\text{m/s}$ at operating zone, x-z plane.

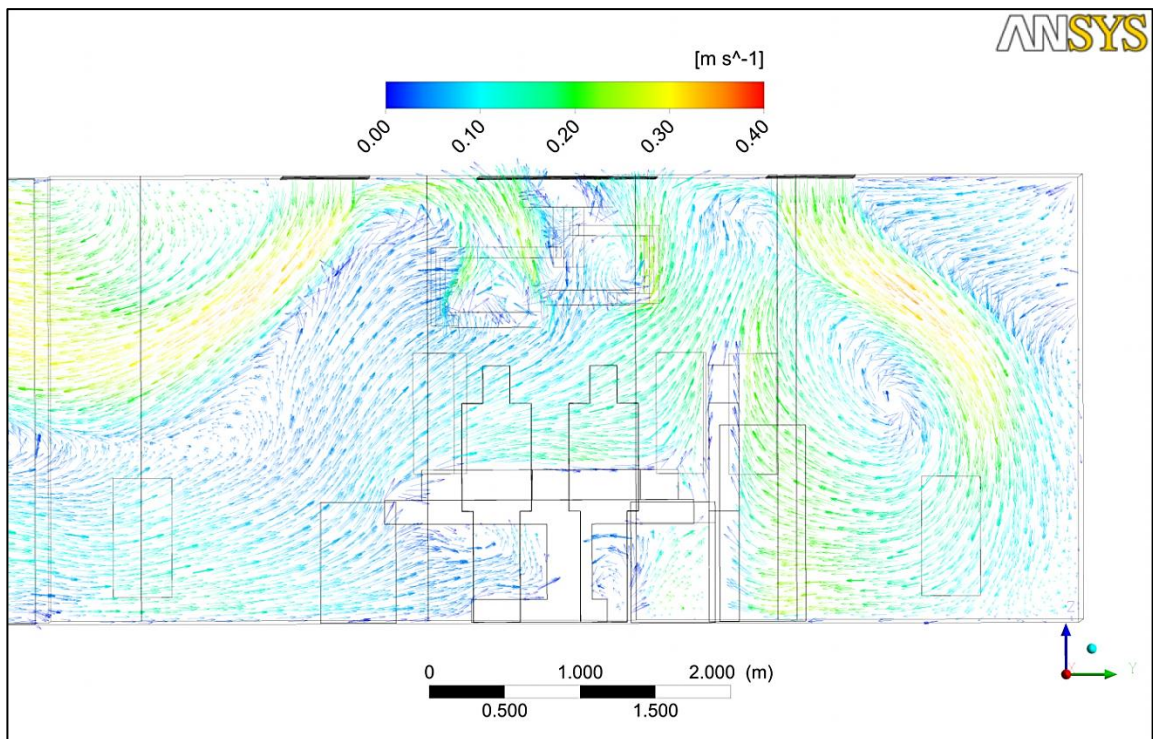


Figure 5.9: Velocity vector for $V_{in} = 0.2\text{ m/s}$ at operating zone, y-z plane.

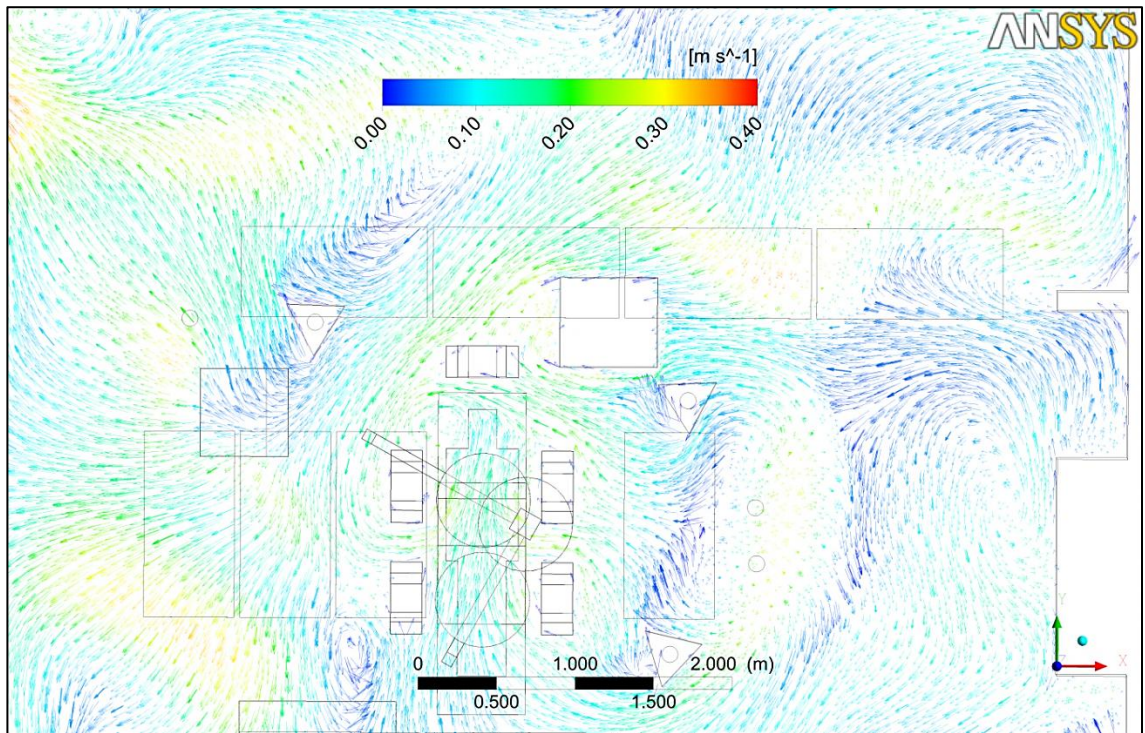


Figure 5.10: Velocity vector for $V_{in} = 0.2 \text{ m/s}$ at operating zone, x-y plane.

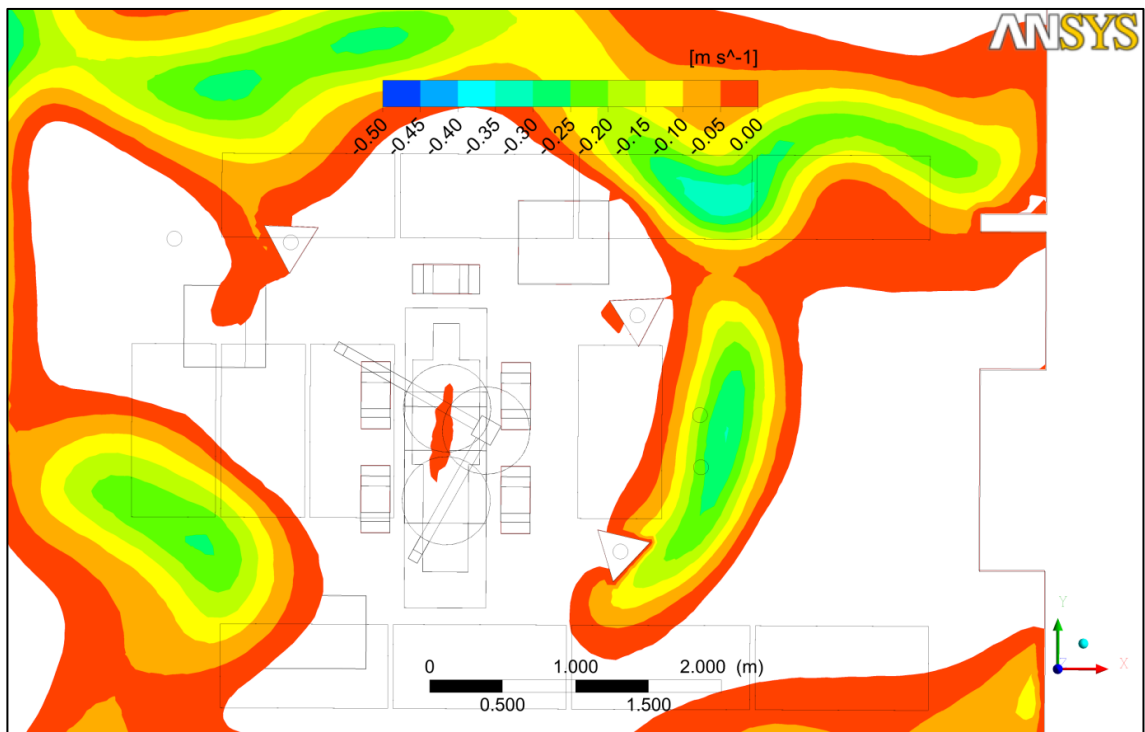


Figure 5.11: Velocity contour w-velocity component for $V_{in} = 0.2 \text{ m/s}$ at operating zone, x-y plane.

The flow in the surgical area was generated by the recirculating air. The major impact of this scenario is: the generated in the operating zone could not be entrained causing it traps in the operating zone (Figure 5.12), hence a higher temperature relative

to average ambient temperature (19.9 °C), that resulted by a temperature around 20-21 °C around the surgical area. Figure 5.15 shown it exists a high temperature gradient of operating zone with its adjacent region. In the operating zone, major heat flux comes from the surgical light. Inasmuch to the high heat flux by the surgical lamp, there should be an adequate airflow around the surgical lamp to aid the convection heat transfer, to reduce the surface temperature of the lamp. Poor heat convection causes relatively high surface temperature on the lamp, increasing the difference between the surface and occupants. Consequently, will have a significant impact on the radiation heat transfer (though radiation heat exchange was not included in this study), since radiation heat transfer is relates by , $\dot{Q}_{1-2} = \sigma AF_{1-2}(T_1^4 - T_2^4)$, causing discomfort to the personnel. In terms of RH, with an inlet air RH of 60%, it has resulted a variation of 45-60% RH in the operating region (Figure 5.13).

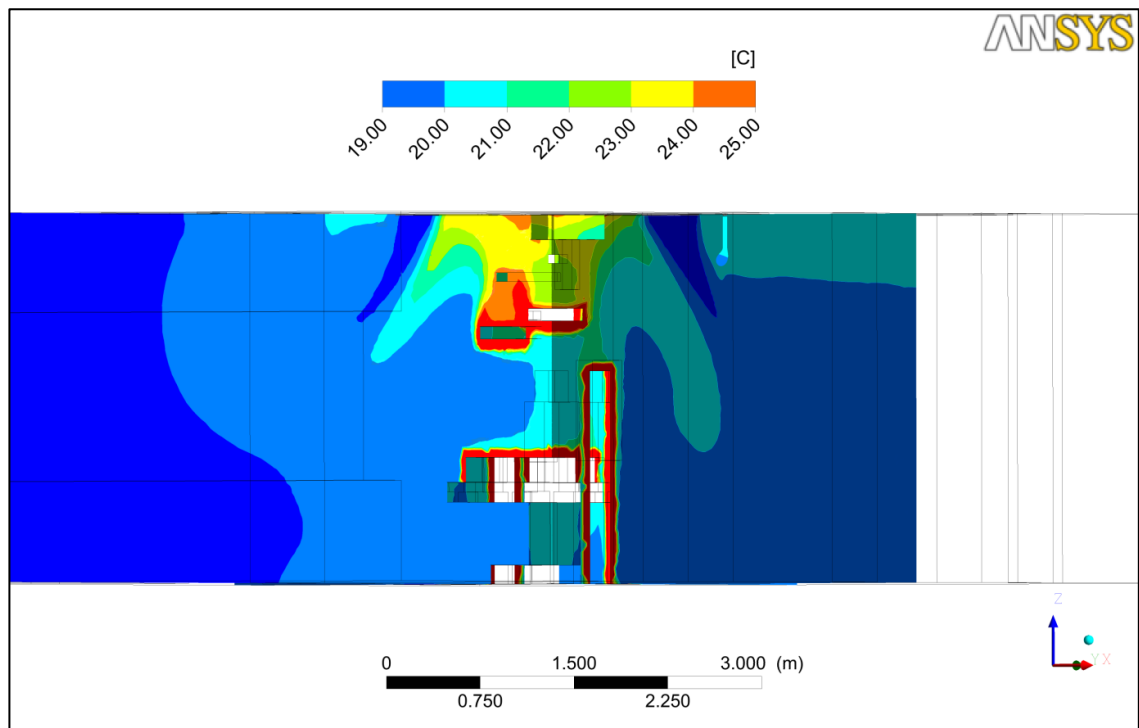


Figure 5.12: Temperature distribution for $V_{in} = 0.2$ m/s.

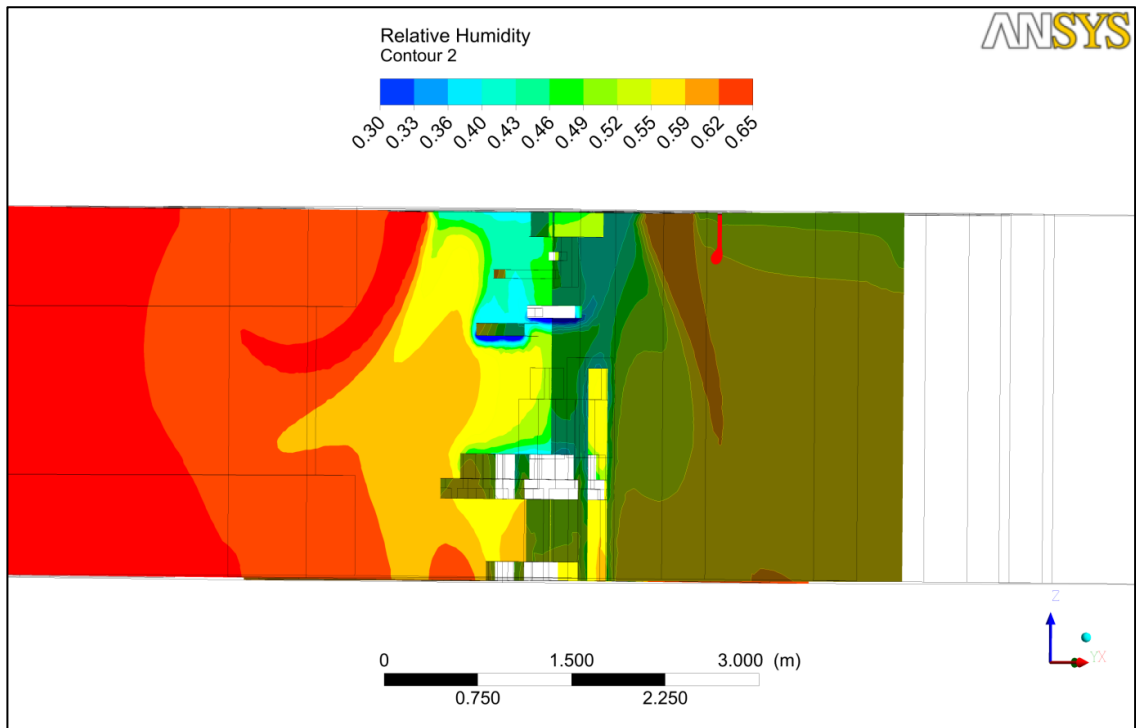


Figure 5.13: RH distribution for $V_{in} = 0.2$ m/s.

Assuming the surface of patient body as a boundary for a gaseous contaminant, CO_2 , with 200 ppm, at a distance 0.28 m the boundary (i.e. 1.2 m above floor level, Figure 5.14), maximum contaminant concentration is 10.6 ppm.

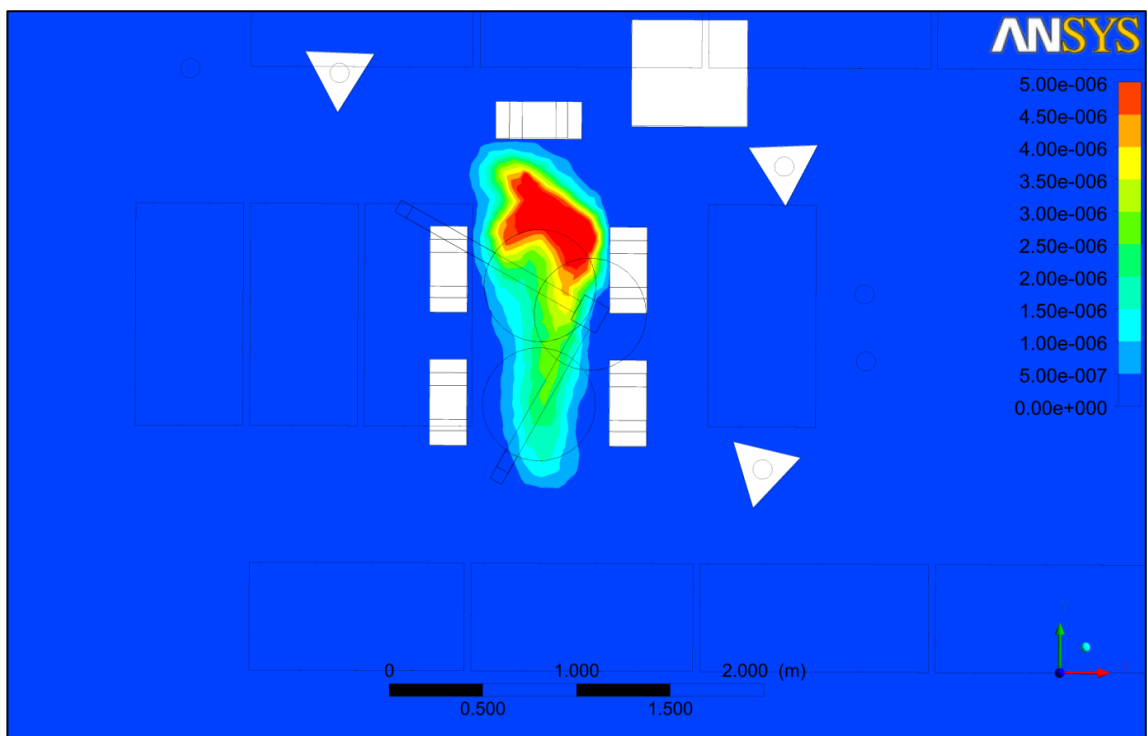


Figure 5.14: Gaseous contaminant concentration, 1.2 m above the floor, $V_{in} = 0.2$ m/s.

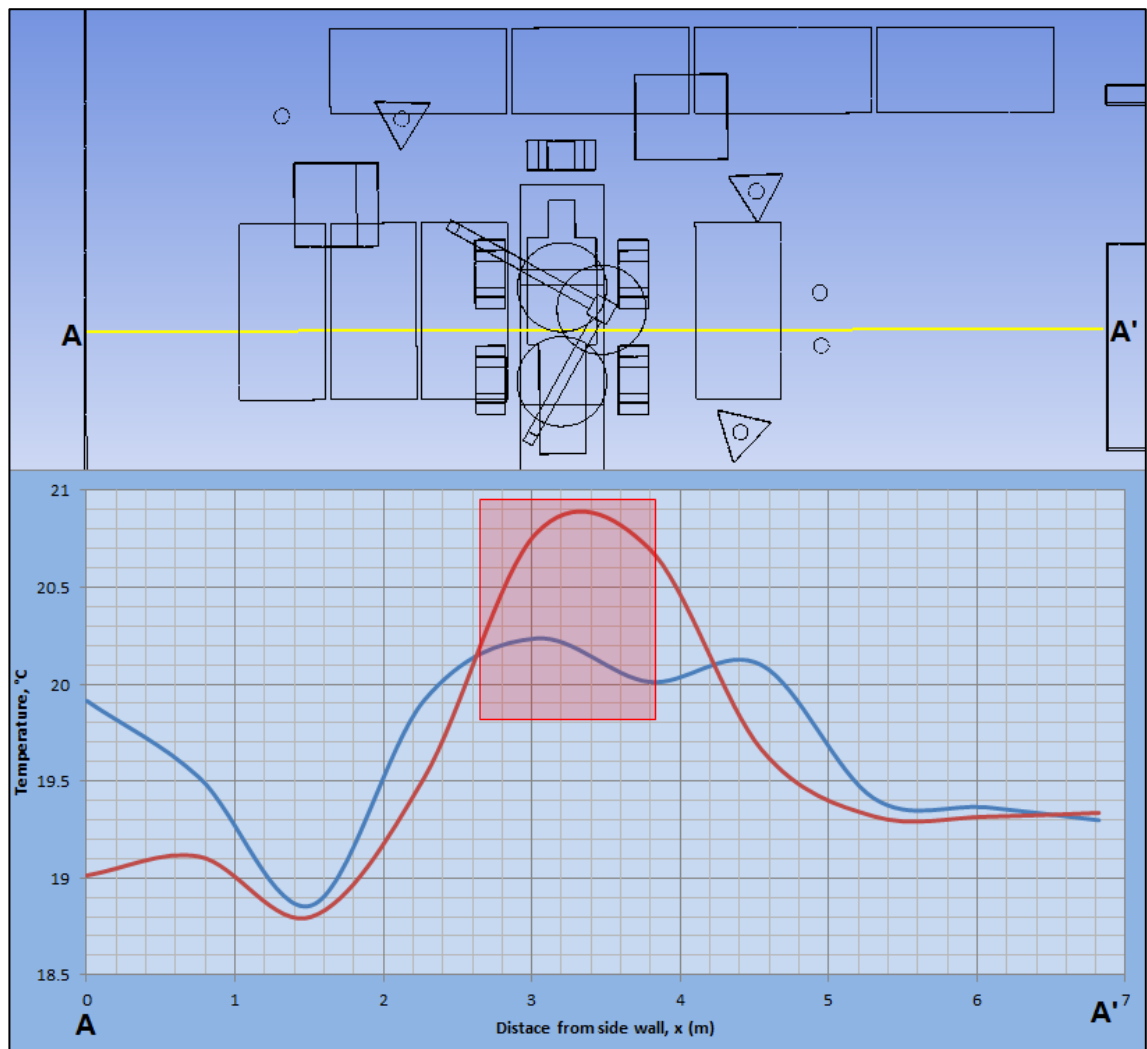


Figure 5.15: Temperature distribution across surgical site at height=1.7 m above the floor (Blue line, $V_{in} = 0.2\text{m/s}$; Red line, $V_{in} = 0.4\text{m/s}$; highlighted in red: surgical region).

With $V_{in} = 0.2\text{m/s}$, the overall Ar number for the room is 75, despite of large floor area and high ACH. A high value of Ar is undesirable in OR. In order to study whether the use higher inlet velocity $V_{in} = 0.4 \text{ m/s}$ (equivalent to 72 ACH and $Ar = 9.4$) will ease current scenario in OT-11, hence another simulation was conducted. From Figure 5.16-5.19 ($V_{in} = 0.4 \text{ m/s}$), the airflow inside the OR does not improve (compare with Figure 5.8-5.11), operating region still suffers from the domination of convective plume. Besides, higher inlet velocity does not improve the temperature and RH distribution in the operating region (Figure 5.20-5.21). However, the mean air temperature at breathing zone (1.2 m – 1.7 m above the floor) was reduced from 19.5 °C to 19.3 °C, by doubling the inlet volume flow rate. Besides, the gaseous contaminant

did not reduce, and there was a maximum concentration of 12.7 ppm, 1.2 m above the floor (Figure 5.22).

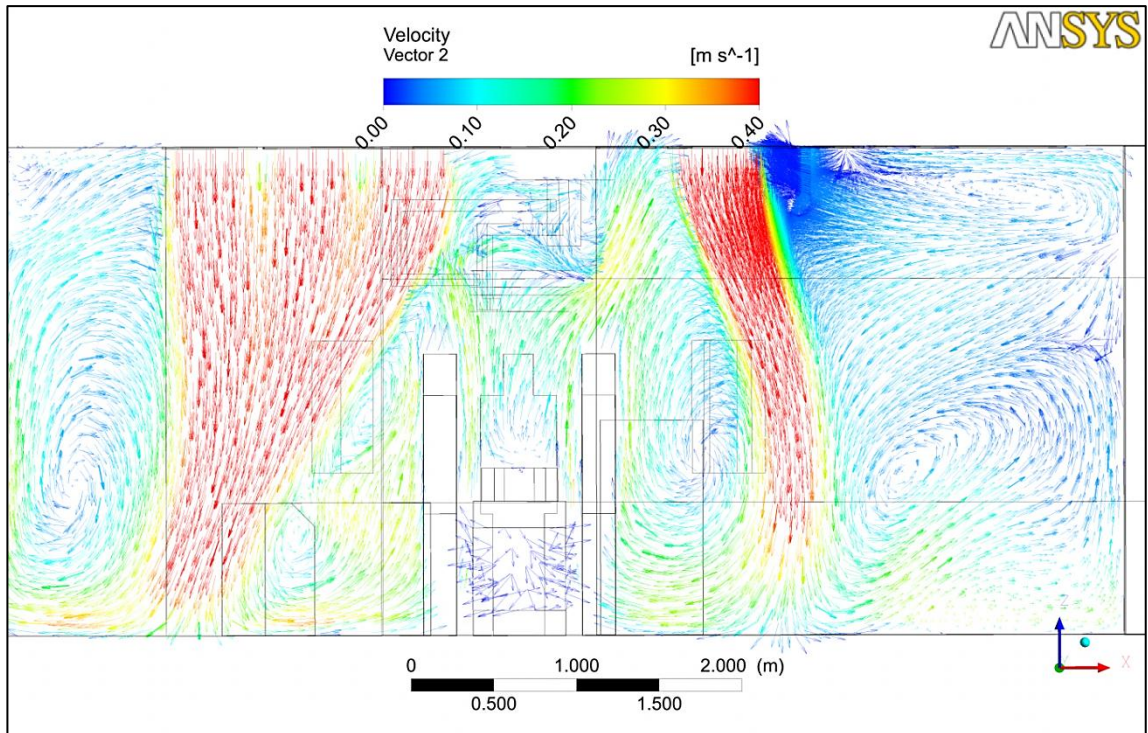


Figure 5.16: Velocity vector for $V_{in} = 0.4 \text{ m/s}$ at operating zone, x-z plane.

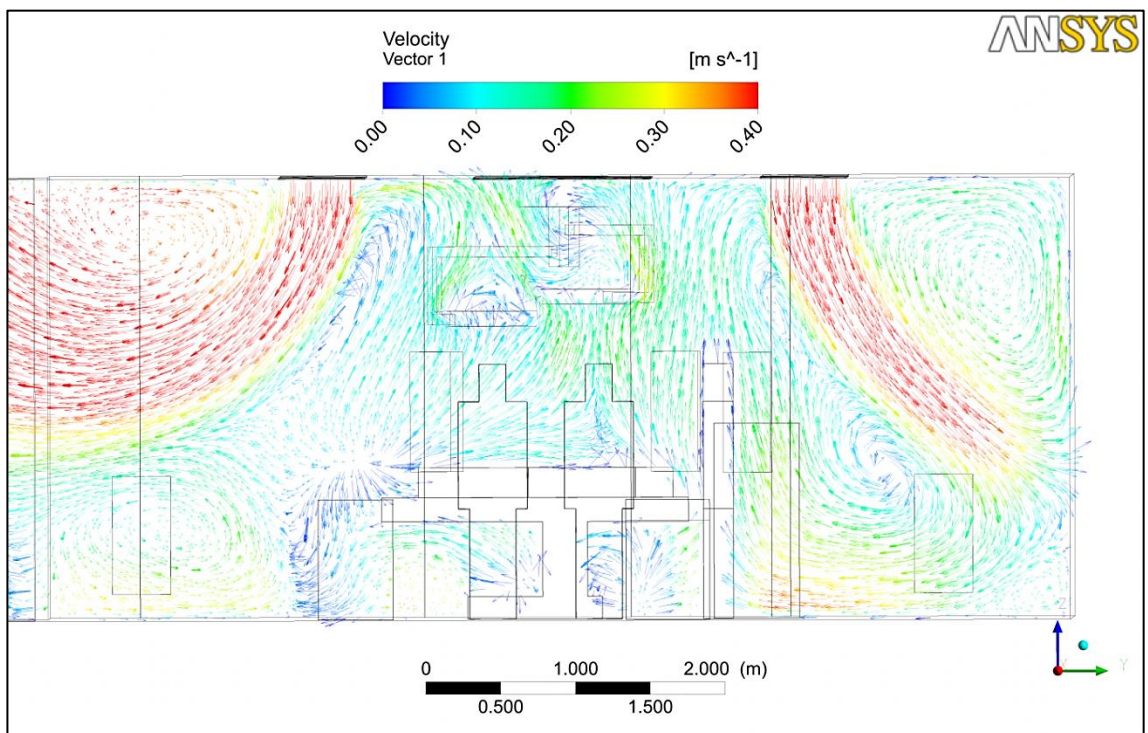


Figure 5.17: Velocity vector for $V_{in} = 0.4 \text{ m/s}$ at operating zone, y-z plane.

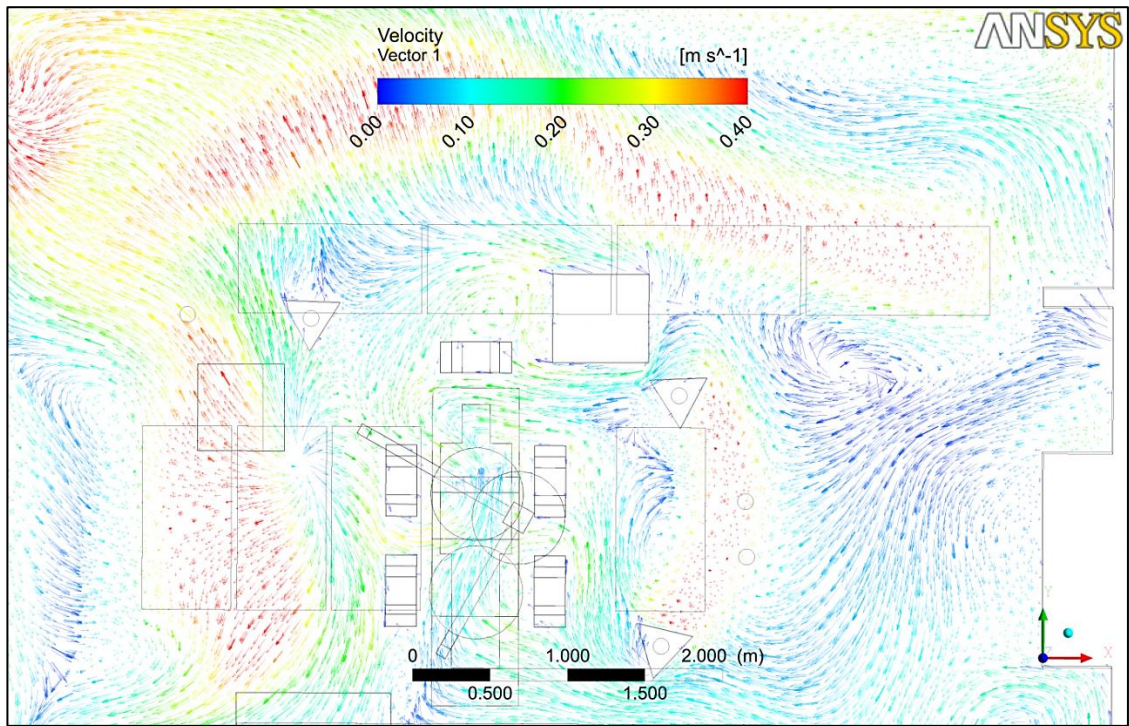


Figure 5.18: Velocity vector for $V_{in} = 0.4$ m/s at operating zone, x-y plane.

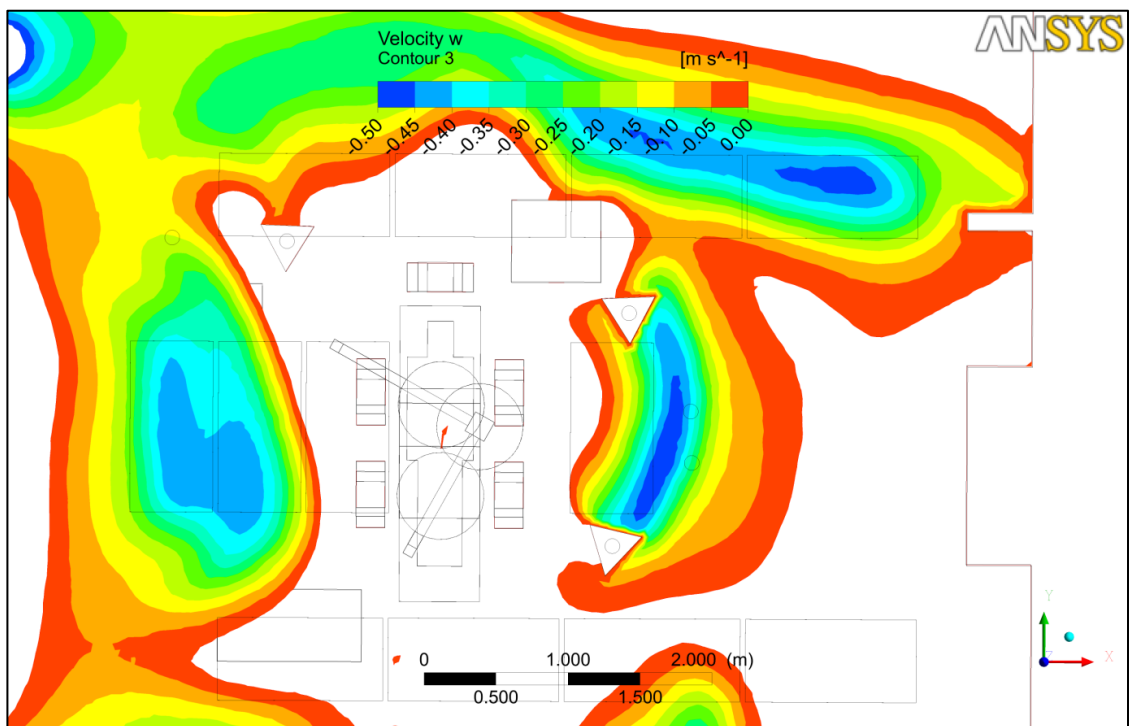


Figure 5.19: Velocity contour w-velocity component for $V_{in} = 0.4$ m/s at operating zone, x-y plane.

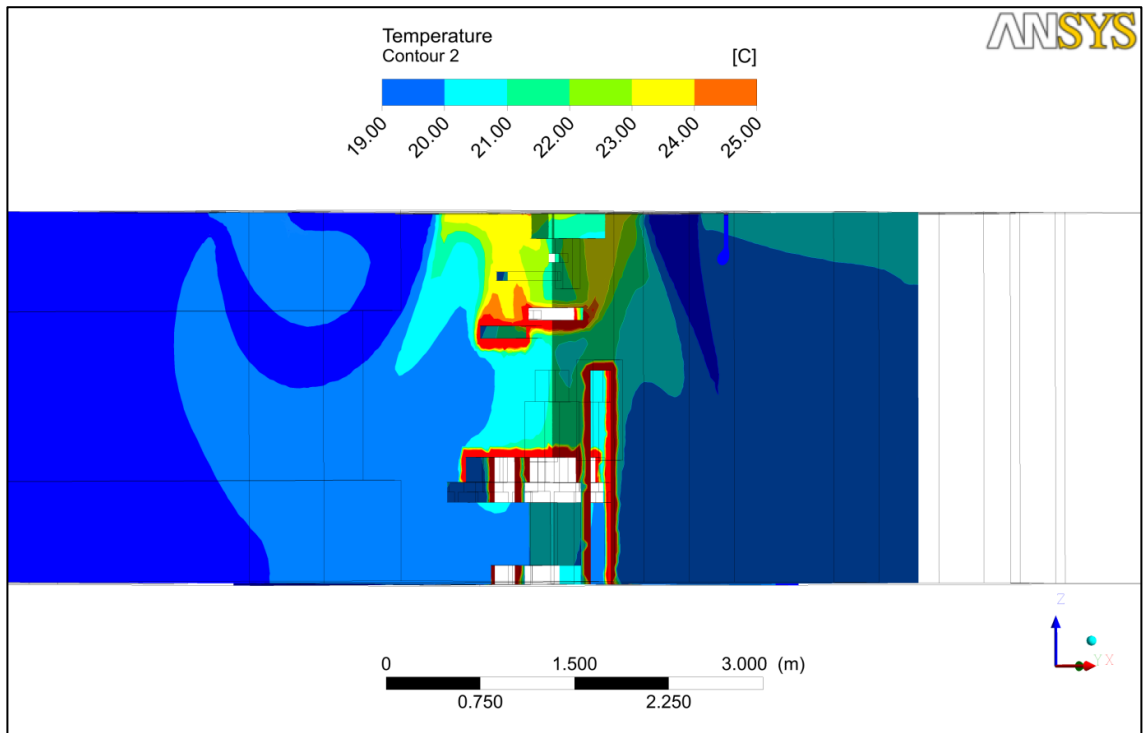


Figure 5.20: Temperature distribution for $V_{in} = 0.4$ m/s.

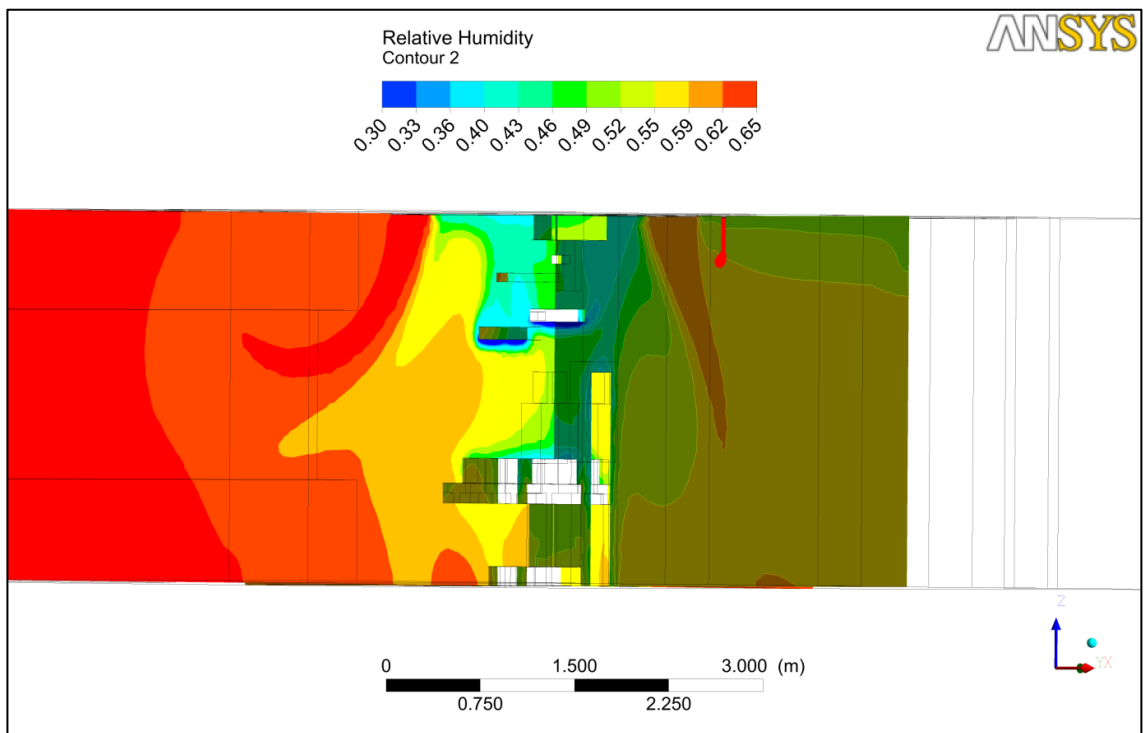


Figure 5.21: RH distribution for $V_{in} = 0.4$ m/s.

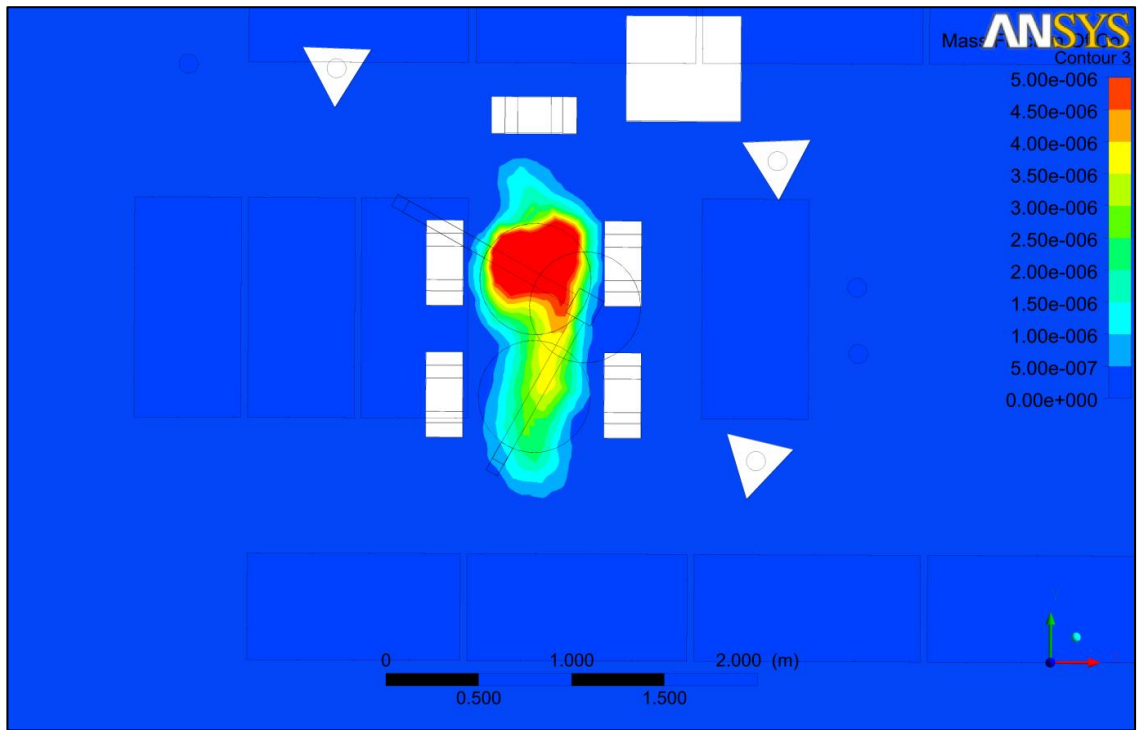


Figure 5.22: Gaseous contaminant concentration, 1.2 m above the floor, $V_{in} = 0.4$ m/s.

Moreover, a large amount of fresh supply air bypass the surgical site is a waste, since it was discharged straight away after entering the OR (Figure 5.23). From the simulation, the air discharged from inlets 4 and inlet 8 that located far away from the operating region is wasted, since it accounted for 14% (2/14) of wastage of incoming air.



Figure 5.23: Streamlines for air discharged from inlet 4 and inlet 8.

The particles were assumed released from the table (Figure 5.24), with a diameter of $12\mu\text{m}$. For each case, total of 120 particles with diameter of $12\mu\text{m}$ were release. The use of $V_{\text{in}} = 0.4 \text{ m/s}$ has improve the number of particles that discharged successfully from the OR from 96 particles to 108 particles.

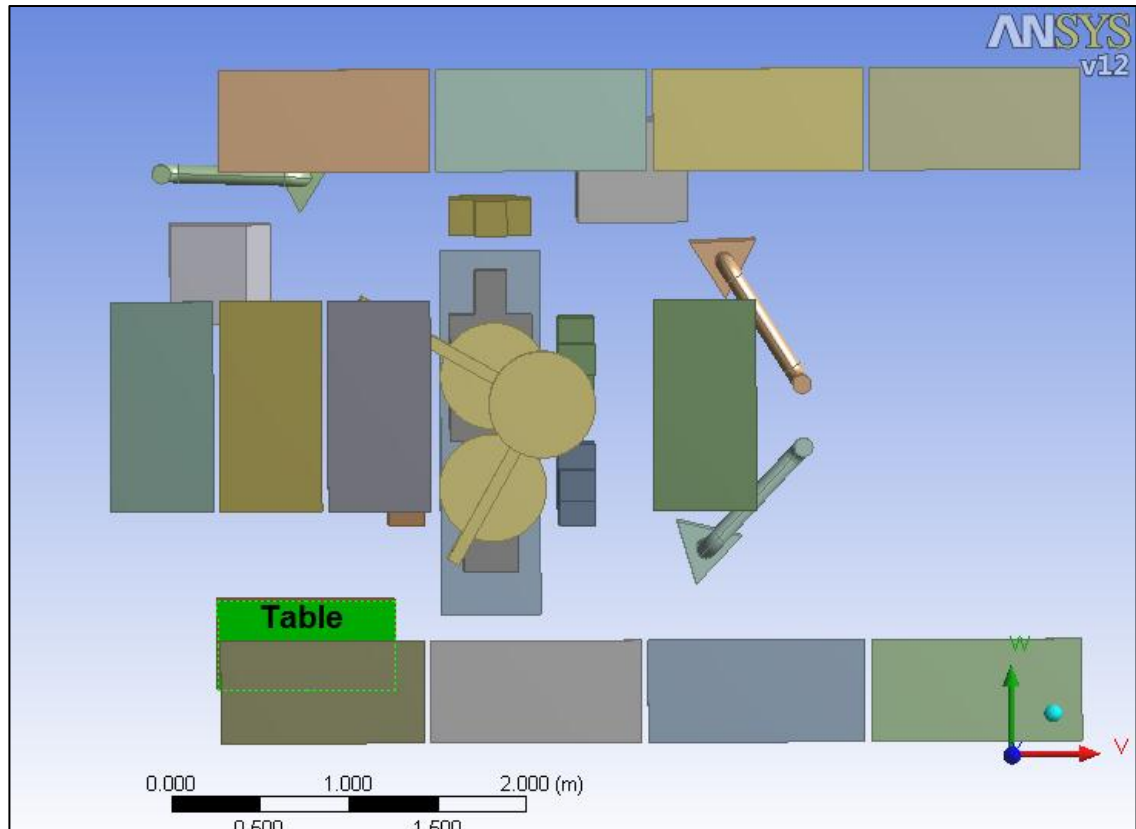


Figure 5.24: Particles releasing location.

5.8 Concluding summary

For UMMC OT-11, the current design with 14 inlets seems excessive, since the air discharge from inlets 4 and 8 bypass the operating region. The higher ACH does not improve the airflow inside the OR and does not reduce the maximum contaminant concentration at the operating zone. Present chapter had shown that the function of high ACH will badly curtailed in UMMC OT-11 due to the improper design of the OR.

6.0 The study on design variation in a Class 7 clean room

To date, immense of studies have been carried out for the airflow in a room. For a clean room, the requirement for the air flow pattern is straight forward: a downward unidirectional airflow. The requirement of downward unidirectional airflow throughout the domain does not applied in an operating room, which is not as stringent as required in electronic industries. For a clean room with class ≥ 7 , which is normally an OR or pharmaceutical cleanroom, it does not require the installation of perforated ceiling and normally, the air is supplied through individual room air inlet filtered by a HEPA filter. The location of exhaust may vary, in spite of there is standard suggesting the location and layout of exhaust. Such ventilation layout creates non unidirectional airflow throughout the room. However, since OR should satisfy at least class 7 or class 8 in ISO 14644-1, proper airflow should be provided in OR for both heat and contaminant removal.

Some studies had been carried out for the experimental measurement of airflow characteristics in a full scaled clean room (Hu et al., 1996) and sub-scaled model room (Posner et al., 2002). The effect for air inlet velocity on the dispersion of indoor contaminants was studies numerically by Lee et al. (2002). They proposed, the air velocity distribution have a significant impact on the airflow throughout the room. The use of measured inlet velocity distribution as the input for boundary condition yields a more reliable results. If there is an absence of the actual measurement data, a scrutiny assumption have to be made on the velocity profile.

In order to optimize the OR environment particularly in minimizing bacterial contamination, attention on several factors need to be paid: instrument and

patient setup, operative site preparation, the use of ultra violet light, surgical garments will aid the reduction of contaminants if there are proper sterilization and careful preparation on these items (Howard et al., 2007). However, a designer will take careful attention on the airflow studies in an OR since proper airflow serves as a ‘prerequisite’ for the reduction of contaminants.

6.1 Study on the inlet design to ventilation performance – A 3-D simulation study

6.1.1 Background and problem formulation

One of the requirements that govern the clean room is the ACH requirement. For similar ACH, different layout of room air inlets will result in different outcome of airflow inside the room. This section was aimed to compare the effect of room air inlets array to their ventilation performance. Two layouts were compared, by using similar number of inlets, which were differentiated by their layout at ceiling as depicted in Figure 6.1.

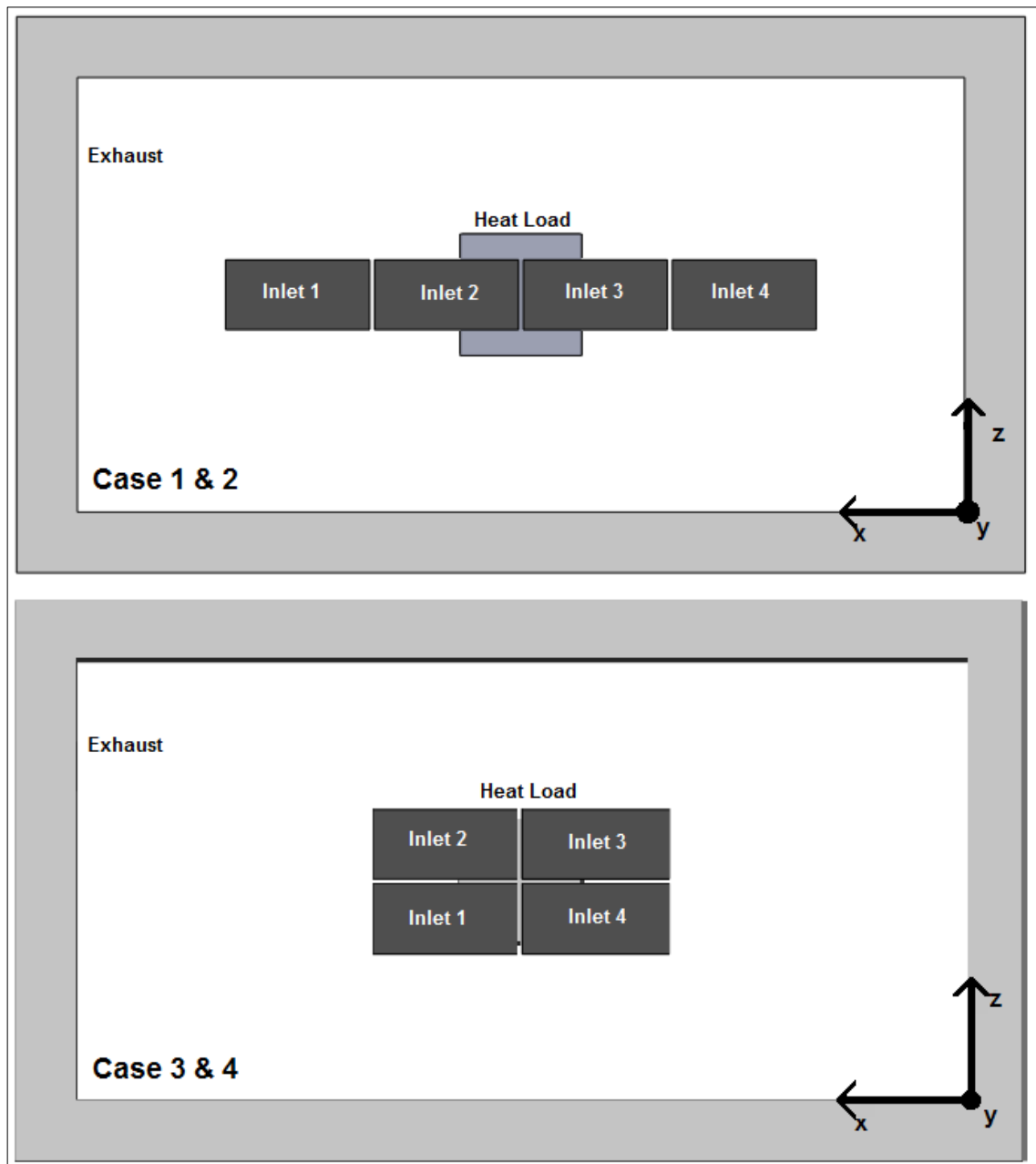


Figure 6.1: Layout of room air inlets.

A room with 7.3 m (L) x 3.575 (W) x 3 m (H) was modeled to represent a clean room of class ≥ 7 (As described in Table 6.1). The inlet arrangement was based on the design features at UMMC OT-11, rather than a hypothetical design. In this model, there were four inlets located at the ceiling and one exhaust located at the bottom corner of the side wall. Single exhaust system was analyzed, since base on an ISO Class 7 non-unidirectional cleanroom (ASHRAE, 2003b).

Table 6.1: Room's specification.

Item	Specifications
Room dimension	7.3 m (L) x 3.575 (W) x 3 m (H)
Heat load dimension / Heat dissipation	1 m (L) x 1 m (W) x 1 m (H) / 100W/m ²
Inlet	1.185 m (L) x 0.575 m (W) each (4 ft x 2 ft)
Exhaust	0.79 m (L) x 0.39 m (W)

Along with this study, two different inlet air velocity (0.2 m/s and 0.4 m/s), as well as the operating conditions with and without heat load were modeled, *ceteris paribus*. Hence, there were eight cases in the current study, as summarized in Table 6.2.

Table 6.2: Summary of cases under current study.

	Case 1a	Case 1b	Case 2a	Case 2b	Case 3a	Case 3b	Case 4a	Case 4b
Room volume, m ³	78							
Inlet array	1 x 4				2 x 2			
Supply air velocity (m/s) / ACH	0.2 / 25		0.4 / 50		0.2 / 25		0.4 / 50	
Archimedes number, Ar	200	0	200	0	25	0	25	0

For all cases, air discharged at 18.8 °C with uniform velocity. Air inlet velocity of 0.2 m/s is corresponding to 25 ACH and doubling the air velocity to 0.4 m/s implies a room with an air change rate of 50 ACH. A box with 1 m (L) x 1m (W) x 1 m (H) was located at the centre of the room, generating heat with a heat flux of 100W/m². The box was modeled to represent heat dissipating devices that heat and mass insulated at the bottom

surface. By definition, $Ar = \beta g H \Delta T_o / v_r^2$, where v_r is mean room air speed, calculated by dividing inlets air flow rate, \dot{V} ($m^3 s^{-1}$) with floor area, A . Meanwhile, ΔT_o can be estimate by using the relation $Q = \rho C_p \dot{V} \Delta T_o$. Hence, with the air inlet velocity of 0.2 m/s at four inlets, it produces a mean room air speed of 0.02 m/s, and ΔT_o of 0.8 °C. This resulted an Ar of 200. By doubling inlet the velocity will cause Ar reduction of 2^3 times, as a result of the reduction ΔT_o as well as an increase in v_r . It implies that increasing the inlet velocity to 0.4 m/s will yield an Ar of 25 for the current setup.

6.1.2 Numerical model

The model was solved by ANSYS Fluent 12.0, using standard $k - \epsilon$ model, with enhanced wall treatment. The governing equations for this model will not repeated herein, since it had been included in Chapter 3. The mesh in the computational domain was generated in tetrahedral (as shown in Figure 6.2), with 6 inflation layers for the wall including heat source. The mesh was further refined at the vicinity of exhaust, since large velocity gradient will occur due to the fact that there is only one exhaust in this system and thus the velocity at the vicinity of exhaust will rise 8.8 times than inlet velocity.

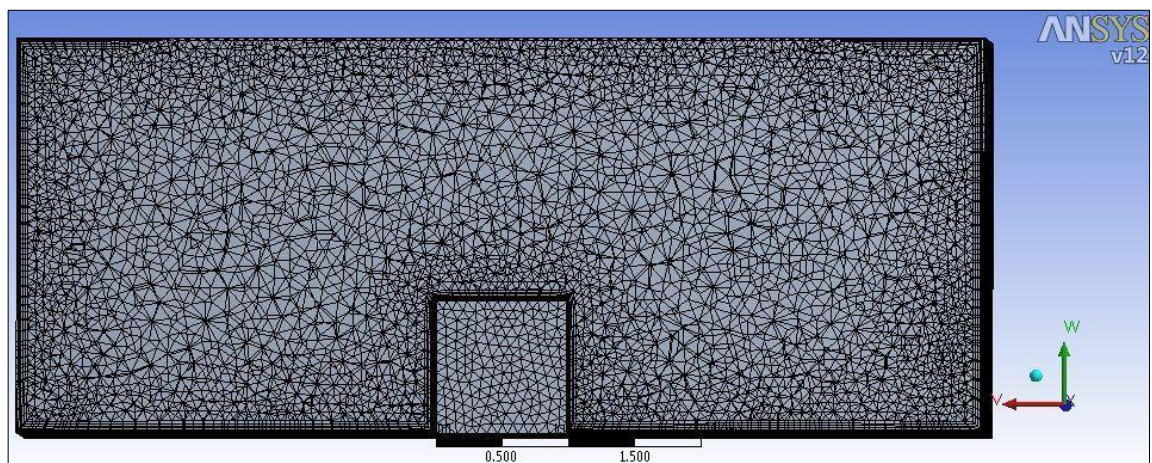


Figure 6.2: Tetrahedral mesh for current study.

In this study, species transport of a gaseous contaminant, CO₂ was included and the contaminant was released from the top surface of the box at a mass fraction of 2×10^{-4} . The mass diffusion coefficient, $D_{c,a}$ for air and the gaseous contaminant is 16 mm²/s. The convergence criteria for continuity, x, y, z-velocity, k, epsilon were 1×10^{-3} , as well as 1×10^{-5} and 1×10^{-6} for species and energy, respectively. The mass and energy imbalance were kept below 0.2% for all cases. There were three distinct numbers of meshes generated, in order to select a suitable mesh number for this study. From Table 6.3, mesh number of approximately 1.3 million was adequate for the current study.

Table 6.3: Result for grid independent test.

	Fine	Medium	Coarse
Cell number, N	2742622	1283279	808445
Representative mesh size, cm	3.0	4.0	4.5
Average room temperature, °C	19.6	19.6	19.5
Maximum temperature, °C	54.3	54.2	63.0
Average CO ₂ concentration at breathing zone (1.2 m above the floor), ppm	1.0	1.0	1.4
Average CO ₂ concentration breathing zone (1.7 m above the floor), ppm	1.1	1.2	1.6

In order to study the availability of current model in prediction of velocity decay, a simple test was carried out. The dimensions for both inlet and exhaust in this setup was 17cm x 17cm, an obstacle located right below the inlet was located in a chamber with W x L x H of 1.36m x 1.36m x 1.85m. It was shown from Figure 6.3, standard $k - \epsilon$ model with tetrahedral mesh able to predict the velocity decay well.

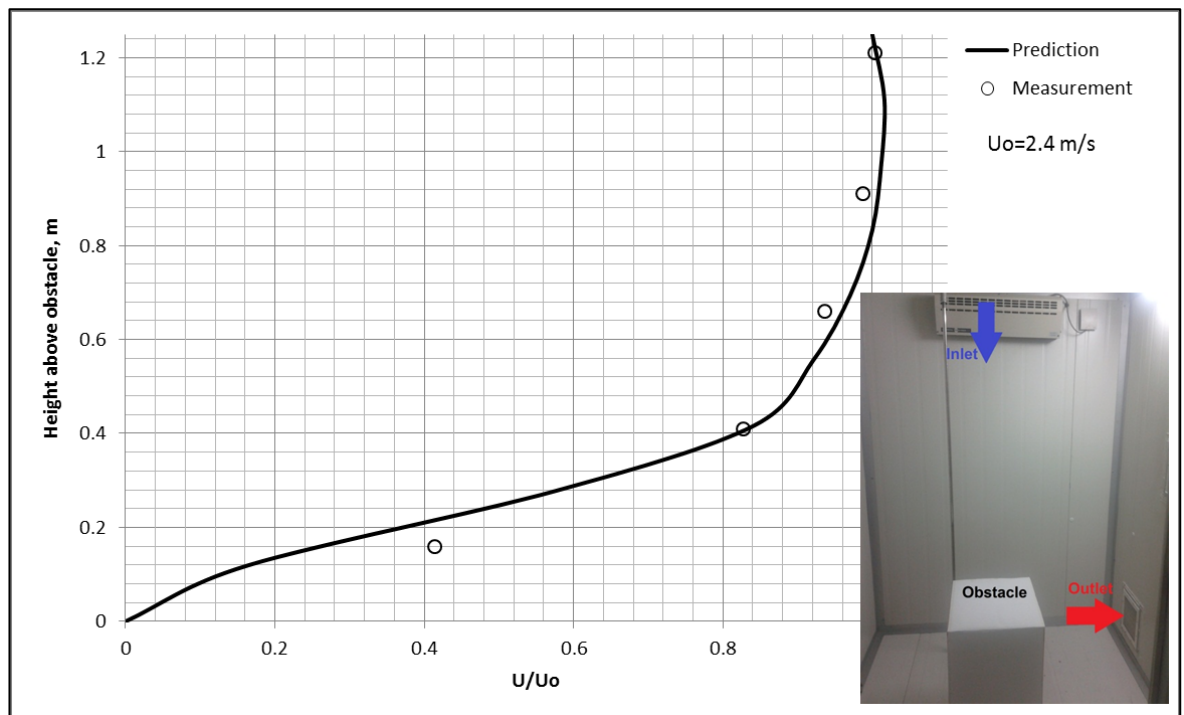


Figure 6.3: Comparison of predicted and measured velocity decay.

6.1.3 Results and discussion

Although air was discharged into the room by different inlet, however, the cluster of inlets can be deemed as a single discharge with aspect ratio of 8 and 2, for 1 x 4 and 2 x 2 array, respectively. For convenience, the clean room model was analyzed in four planes, which were as denoted in Table 6.4.

Table 6.4: Location of plane 1, 2, 3 and 4.

	$\left \frac{x}{L}\right $	$\left \frac{z}{W}\right $	$\left \frac{y}{H}\right $
Plane 1 (x-y plane)	-	0.5	-
Plane 2 (y-z plane)	0.5	-	-
Plane 3 (x-z plane)	-	-	0.40
Breathing zone 1.2 m from floor			
Plane 4 (x-z plane)	-	-	0.57
Breathing zone 1.7 m from floor			

Aspect ratio is a ratio to indicate “squareness” of a rectangular, Note that the aspect ratio closer to unity implies a square. Since there is a velocity discontinuity when air discharged from the inlets, the shear layer is developed. Hence, it will cause the decrease of centreline velocity of the air stream over distance. In an isothermal condition without obstacle, when the air hits the floor, it will sweep on the floor before the air is exhausted since Coandă effect tends to attract the moving fluid to its surface nearby. The rate of centreline velocity decay is depending on the free jet region (namely potential core, characteristic decay, axisymmetric decay and terminal region). The decay of the velocity often related as $\frac{U_m}{U_o} \propto \frac{1}{x^n}$, where the decay rate increase as the increase of distance with supply air opening. Study on the velocity decay for three dimensional free jets discharged from rectangular discharge had been carried out by Yevdjevich (1966). After discharging from inlets, the air hits the floor, which carries a characteristic of a perpendicular impinging jet. This phenomenon was studied by Beltaos and Rajaratnam (1973). The jet impingement was characterized into three regions, namely free jet region, impingement region and wall jet region. Within a distance of 75% from the discharge to the floor, the jet impingement remains unaffected (Gutmark et al., 1978). Hence, one can deduce, the will exhibit the behavior of three dimensional free jet up to 1.7 m above the floor. Hence, comparing with the result obtained by Yevdjevich (as shown in Figure 6.4), we could expect no or insignificant air velocity decay over this distance. Of course, this is the case with the presence of isothermal condition. For inlet with 2 x 2 array, the air jet is discharged and concentrated towards the heat and contaminant source. For the contaminants in a room with 1 x 4 array, the contaminants is mainly being diluted by the air entrainment from inlet 2 and inlet 3. Table 6.5 summarizes the result for concentration contaminant for all cases.

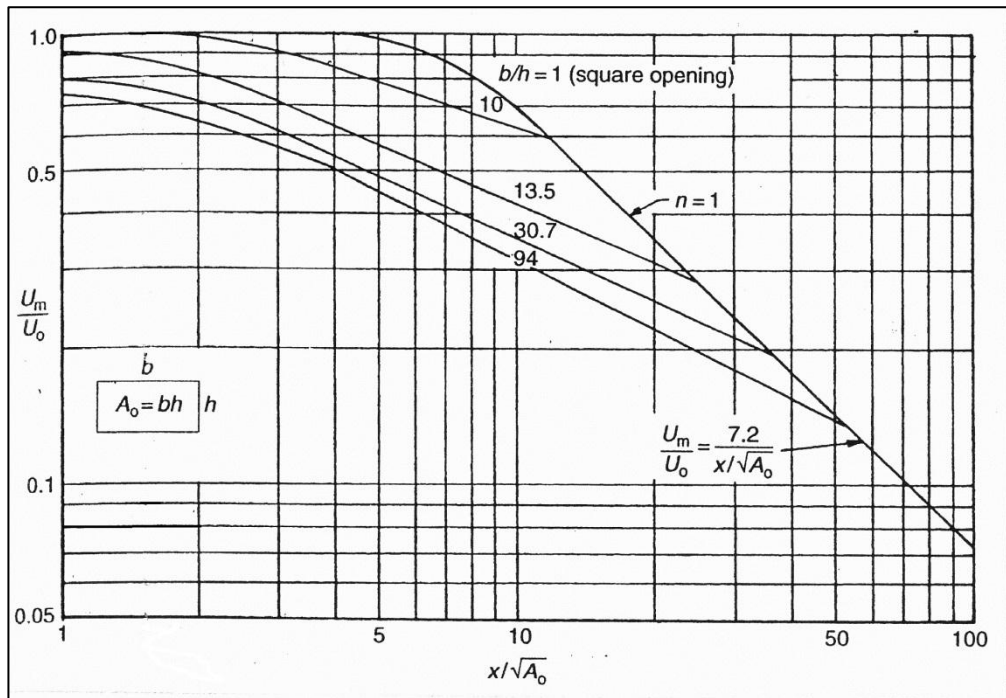


Figure 6.4: Velocity decay for three-dimensional free jets (Rajaratnam, 1976).

Table 6.5: Result summary.

Case	1a	2a	3a	4a	1b	2b	3b	4b
Max. CO ₂ concentration Breathing zone (1.2 m above the floor), ppm	24.6	7.2	37.4	18.2	3.3	3.2	1.4	1.1
Average CO ₂ concentration Breathing zone (1.2 m above the floor), ppm	1.4	0.4	1.4	0.8	0.6	0.5	0.5	0.3
Max. CO ₂ concentration Breathing zone (1.7 m above the floor), ppm	7.8	2.3	12.0	1.9	2.9	2.7	1.2	0.8
Average CO ₂ concentration Breathing zone (1.7 m above the floor), ppm	1.8	0.4	1.2	0.7	0.5	0.4	0.6	0.3

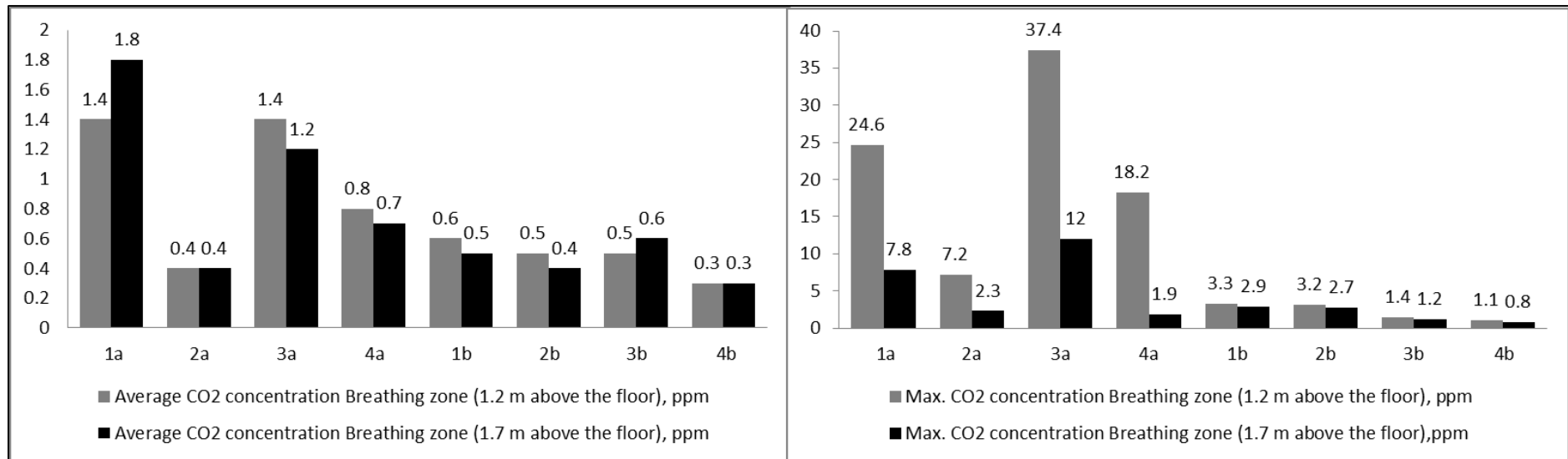


Figure 6.5: Gaseous contaminant concentration for all cases.

Effect of inlet air velocity on air velocity distribution

From Figures 6.6 and 6.7, the air inlet velocity has significant effect on the room airflow. With an Ar of 200, the room airflow with $V_{in} = 0.2$ m/s is significantly affected by the thermal plume from the heat load. For both 1 x 4 and 2 x 2 arrays, an inlet air velocity of 0.2 m/s is unable to oppose the buoyant force from the plume, resulted a distinct velocity vector towards the ceiling above the thermal load, even at a distance 1.7 m above the floor. Figure 6.8 presents the contour of v-velocity vector (in y-direction in current model). Colored area represent a negative velocity vector (facing to the floor) while an uncolored area illustrates the area with positive velocity (facing to the ceiling), at 1.7 m above the floor. With $V_{in} = 0.4$ m/s, Ar reduced by 8 folds to 25. In this case, the area in the vicinity of heat load 1.7 m above the floor does not affected by thermal plume. Albeit there is uncolored region at the area vicinity to the wall, however, it is inevitable since recirculation will certainly occur in such room design, especially in the stagnant region with low air velocity, as shown in Figure 6.7.

Effect of inlet air velocity on contaminant dispersion

With the aid of thermal plume, the gaseous contaminant becomes easily to disperse. As shown in Figure 6.5, the average and maximum concentration at breathing zone (1.2 m and 1.7 m above the floor) for $V_{in} = 0.2$ m/s are higher than with $V_{in} = 0.4$ m/s. Maximum concentration occurs at the region directly above the heat load. It should be noted that, this condition hold true for both 1 x 2 array (Figure 6.10) and 2 x 2 array (Figure 6.11), by comparing Case 1a vs Case 2a, and Case 3a vs Case 4a.

Effect of the inlet air velocity on temperature distribution

Besides causing wide spread of gaseous contaminant, the low inlet velocity causes large temperature difference in a room (Figure 6.12 and 6.13), due to poor heat entrainment.

Less temperature variation is found for the examined cases with $V_{in} = 0.4$ m/s (both 1 x 4 and 2 x 2 arrays), since force convection aid the entrainment of heat and distribute the heat effectively over the room.

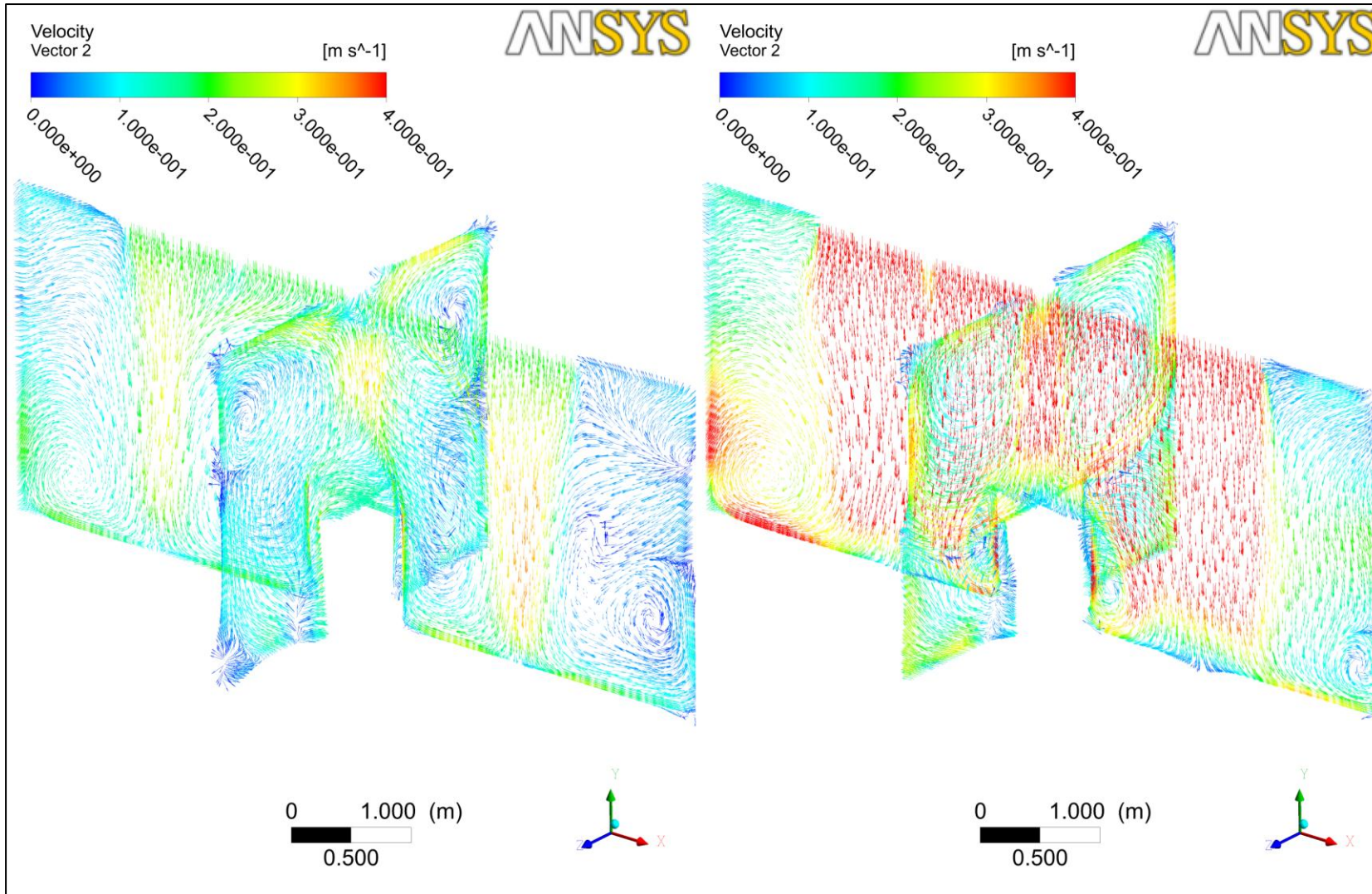


Figure 6.6: Comparison of air velocity vector for case 1a (left) and case 2a (right) (1 x 4 array).

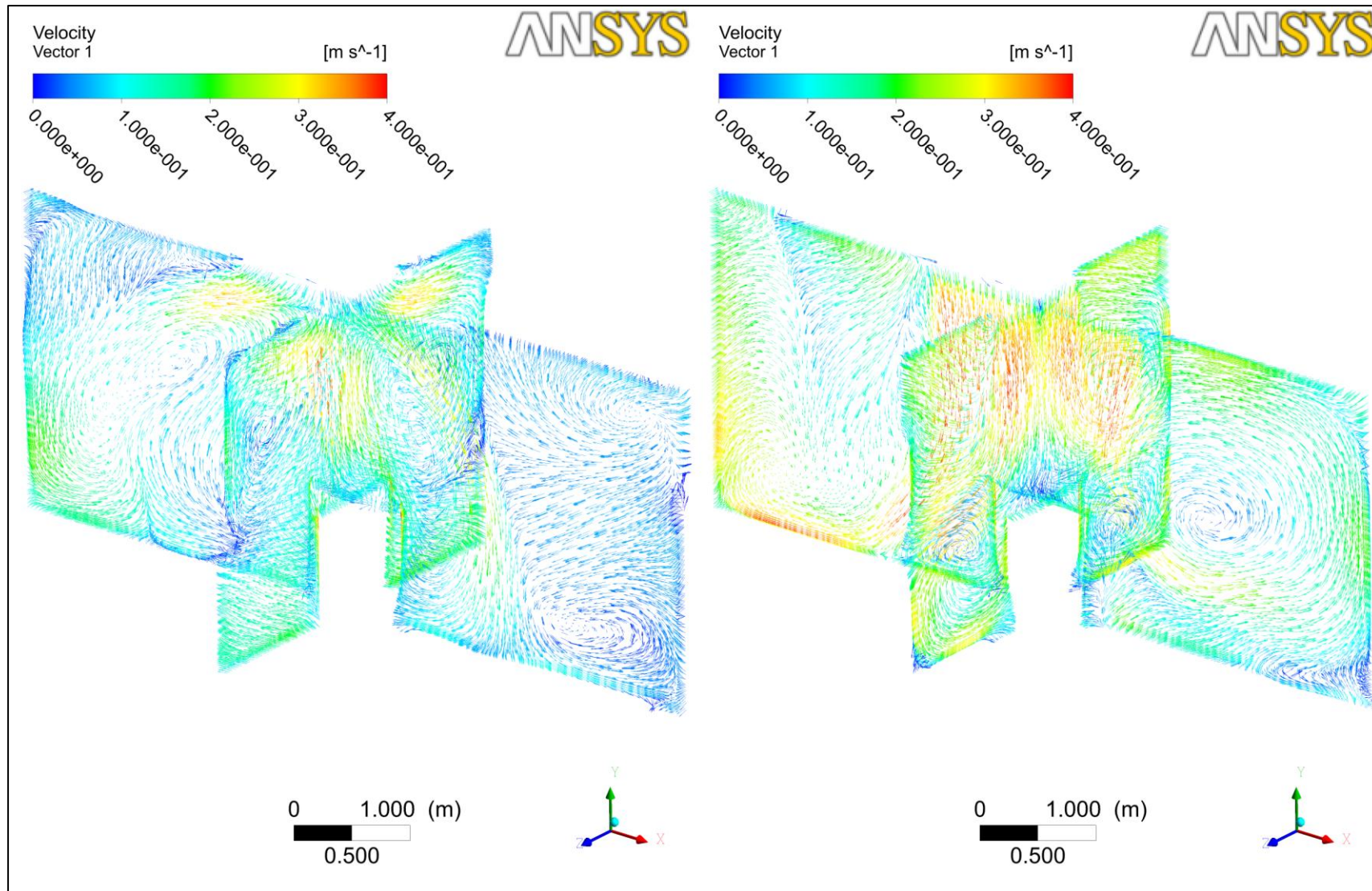


Figure 6.7: Comparison of air velocity vector for case 3a (left) and case 4a (right) (2 x 2 array).

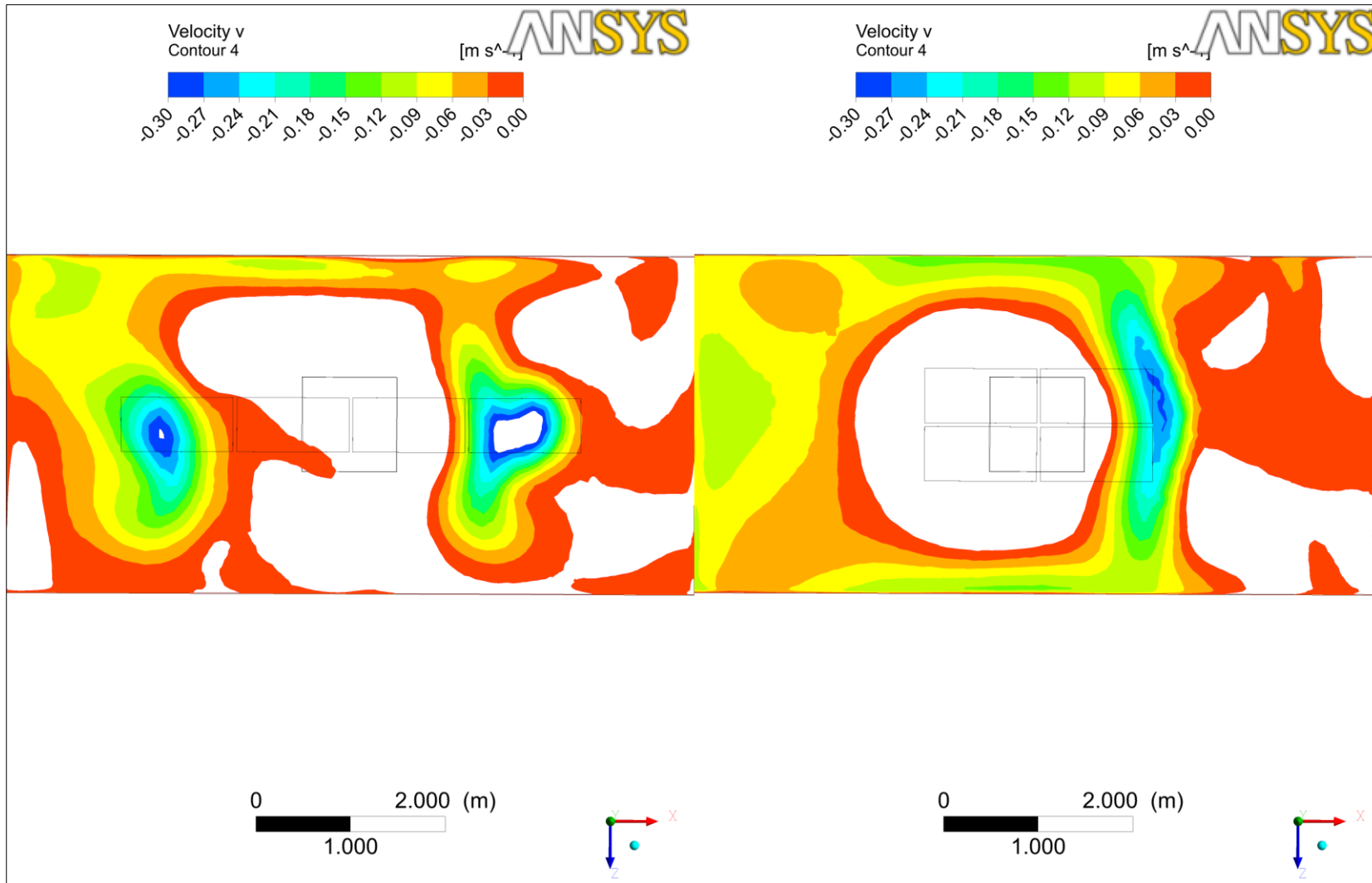


Figure 6.8: Contour of v-velocity component 1.7 m above the floor, $V_{in}=0.2$ m/s for 1 x 4 array (left) and 2 x 2 array (right).

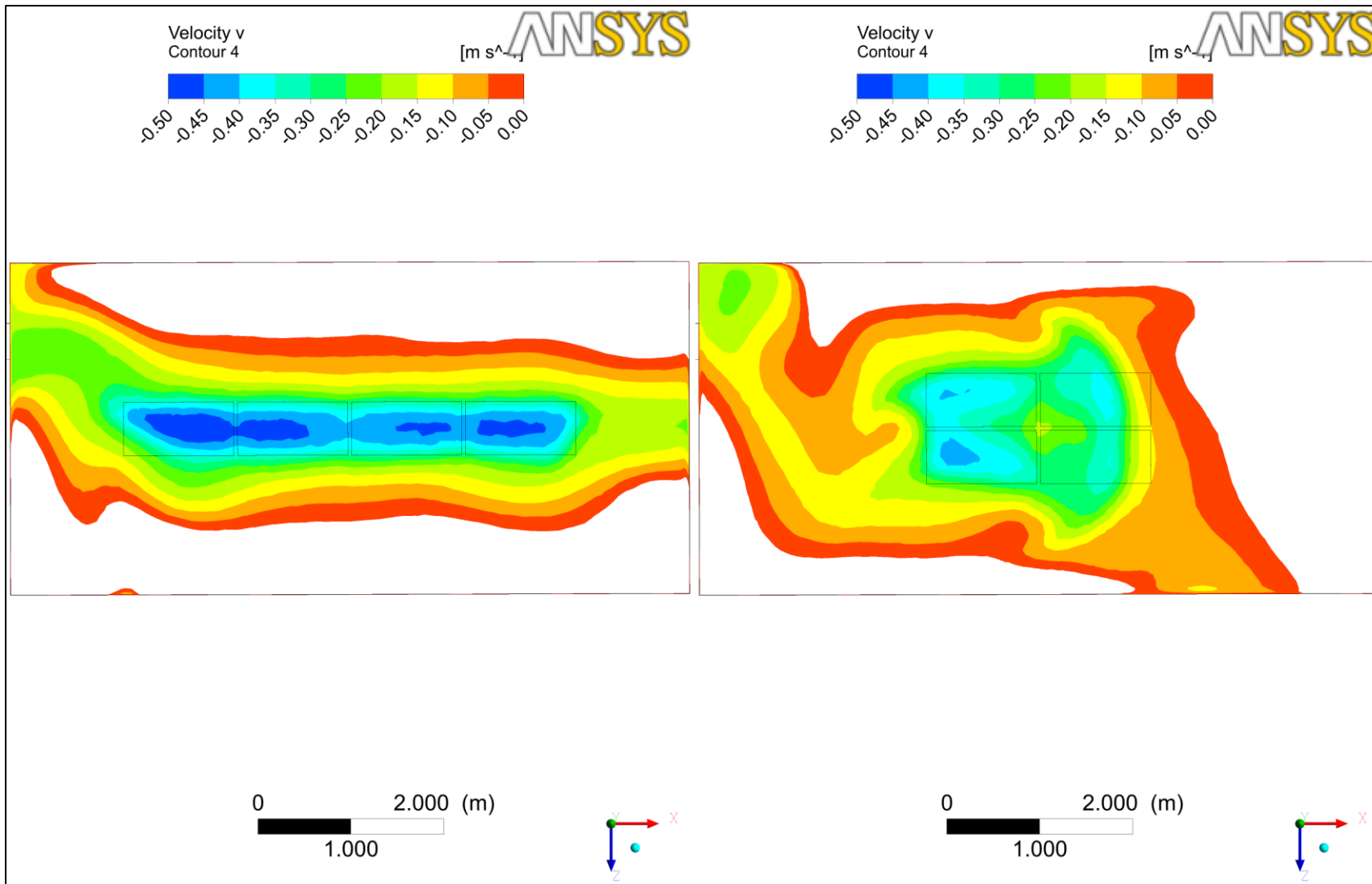


Figure 6.9: Contour of v-velocity component 1.7 m above the floor, $V_{in}=0.4$ m/s for 1 x 4 array (left) and 2 x 2 array (right).

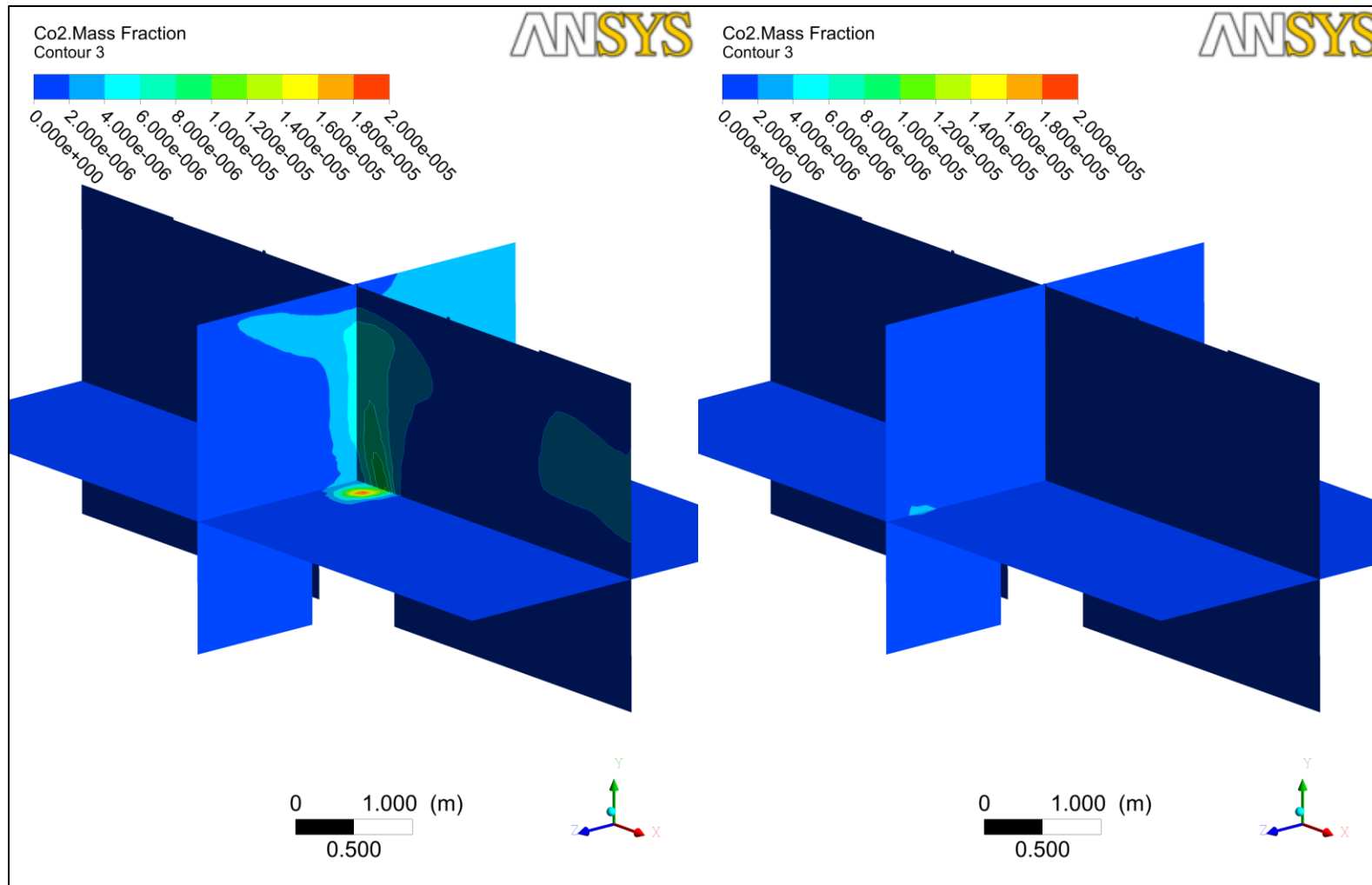


Figure 6.10: Comparison of contaminant dispersion for case 1a (left) and case 2a (right) (1 x 4 array).

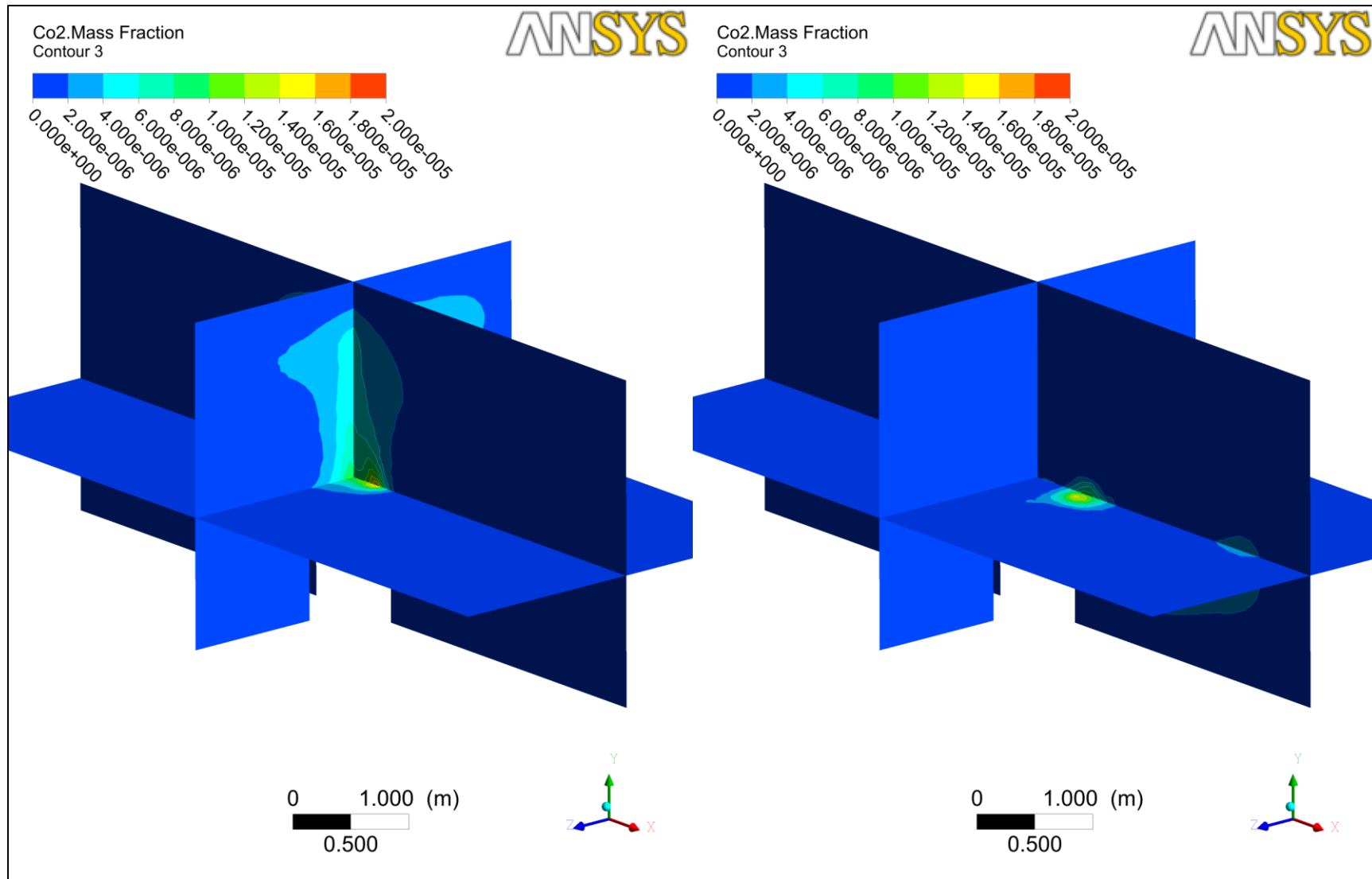


Figure 6.11: Comparison of contaminant dispersion for case 3a (left) and case 4a (right) (2 x 2 array).

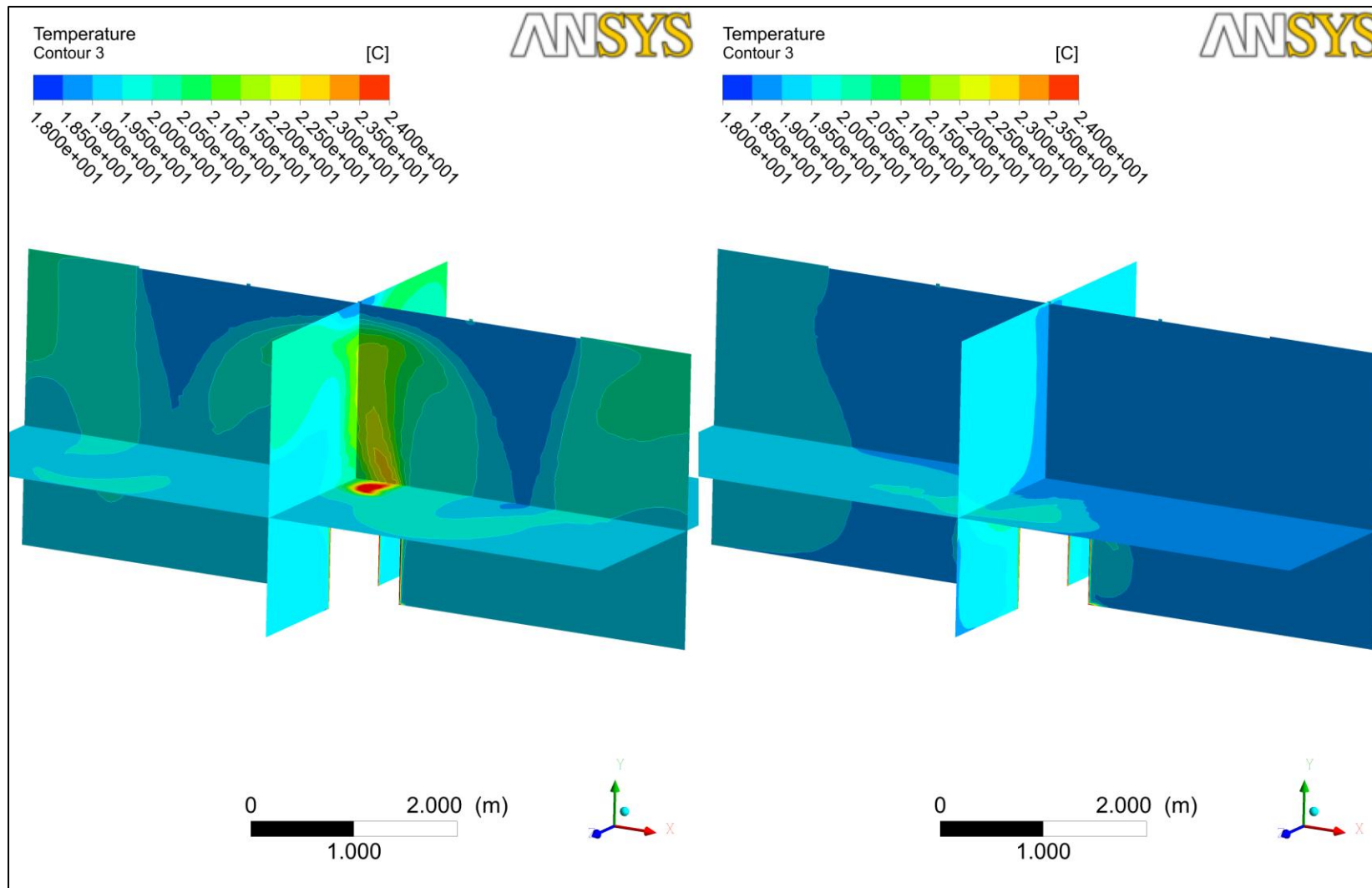


Figure 6.12: Comparison of air temperature for case 1a (left) and case 2a (right) (1 x 4 array).

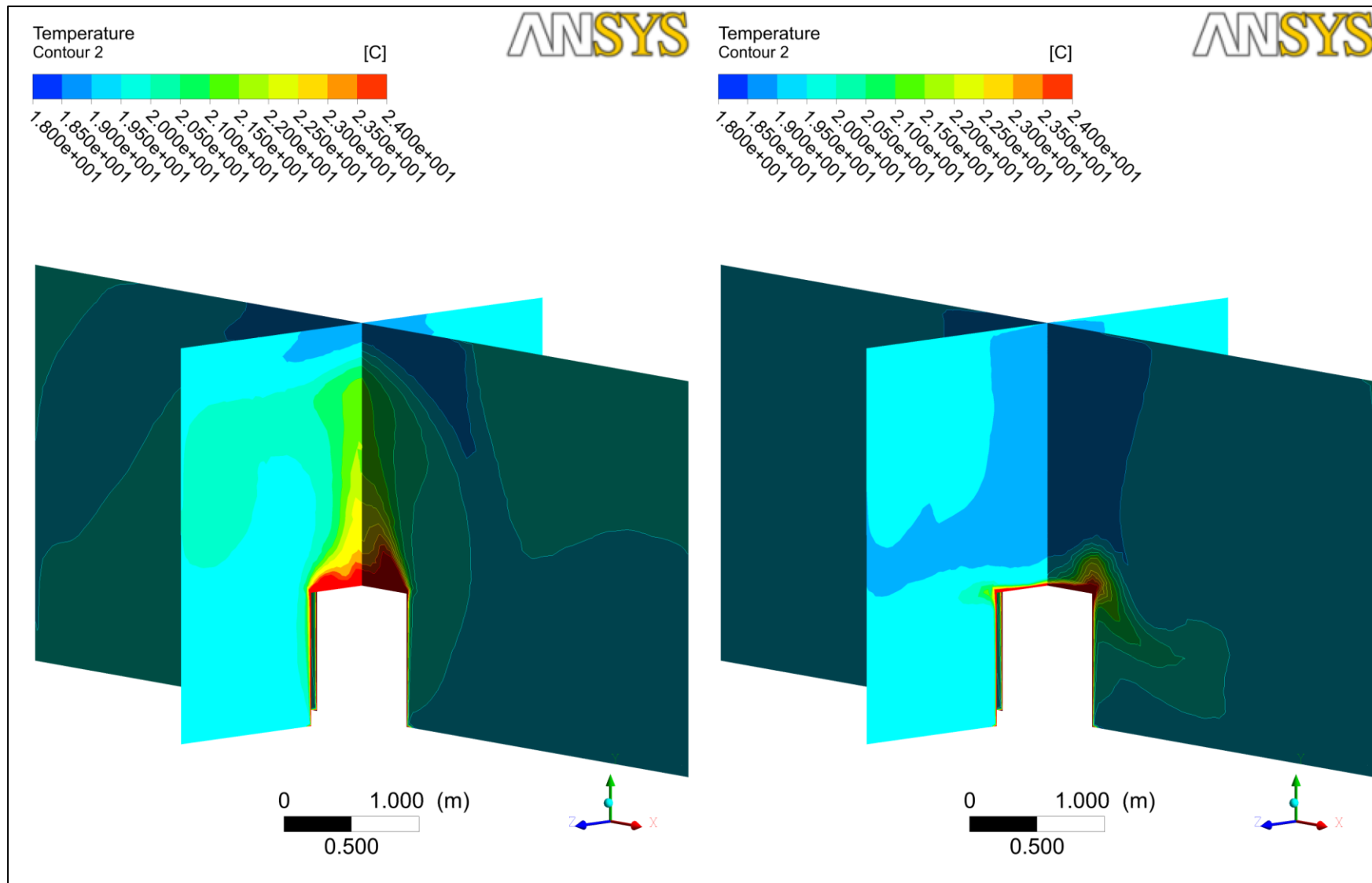


Figure 6.13: Comparison of air temperature for case 3a (left) and case 4a (right) (2 x 2 array).

Effect of inlets array on air velocity distribution

Since the momentum provided by the jet with $V_{in} = 0.2$ m/s per se is not sufficient to overcome the buoyant force, it results in domination of thermal buoyancy. It implies, for $V_{in} = 0.2$ m/s, the array of air inlets does not carry significant impact on air velocity distribution (Figure 6.8 and Figure 6.14). However, with $V_{in} = 0.4$ m/s, the design of inlet array affect the zone for air recirculation in the room (Figure 6.15a , Figure 6.15b). As shown in the earlier part of current study, the difference between 1 x 4 array and 2 x 2 array is, when they are projected from ceiling (x-z plane), 1 x 4 array partially covers the heat load (that analogy to activity area) while 2 x 2 array fully cover the working area. In current context, the benefit of 2 x 2 array becomes clearer, since it could serve as a barrier for the intrusion of recirculating air into the primary inlet jet. The 1 x 4 array is unable to prevent the circulation of recirculating air into the area above the heat load (refer to the red-rectangled region in Figure 6.15b).

When an air jet hits an obstacle (i.e. the heat load in this case), the jet will split and behave as a wall jet (blue-rectangled region in Figure 6.15b). This is a condition similar to as studied by Beltaos and Rajaratnam (1973). For 1x 4 array, it has a larger free jet region (hence smaller impingement region) than 2 x 2 array. With larger impingement region for 2 x 2 array, it creates a ‘void’ (stagnant area) with low magnitude of air velocity above the top surface of the heat load.

It is worth to mention, this study only accommodates single exhaust for the room that will subjected to high recirculation. Thus, in order to reduce the recirculation, one should consider adding more exhausts vicinity to stagnant zone if the room.

Effect of inlets array on contaminant dispersion

For $V_{in} = 0.2$ m/s, a 2 x 2 array yield higher maximum concentration for both area 1.2 m and 1.7 m above the floor (Figure 6.5 and Figure 6.16). Same condition happens for $V_{in} = 0.4$ m/s (Figure 6.5 and Figure 6.17). It suggests, when considering the layout of inlets array, the behavior of air jet impingement on the surface that emanating gaseous contaminant should take into account. A larger impingement region (expressed in blue box in Figure 6.15b) will give rise to the dispersion of gaseous contaminant.

Effect of inlets array on temperature distribution

The heat generated by the heat load is transferred via convection (forced and natural convection). Since convection heat transfer is dependent to the air speed, the evenness of temperature distribution is dependent on the efficacy of air mixing ability for particular ventilating system. From Figure 6.18 and Figure 6.19, inlets design with 1 x 4 arrays, $V_{in} = 0.4$ m/s provides a better evenness of temperatures, compared with other cases.

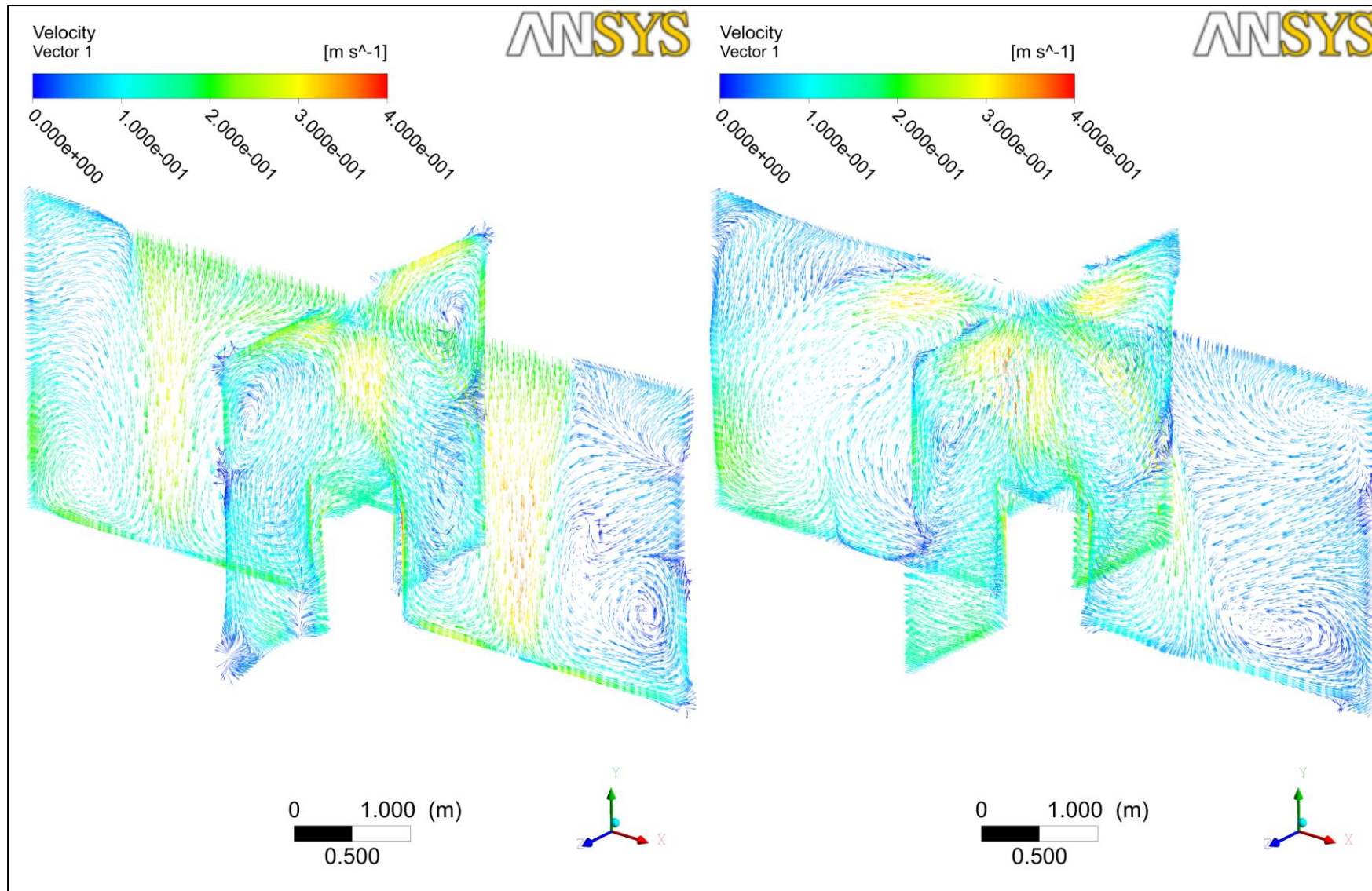


Figure 6.14: Comparison of air velocity vector for case 1a (left) and case 3a (right) (Inlet velocity 0.2 m/s).

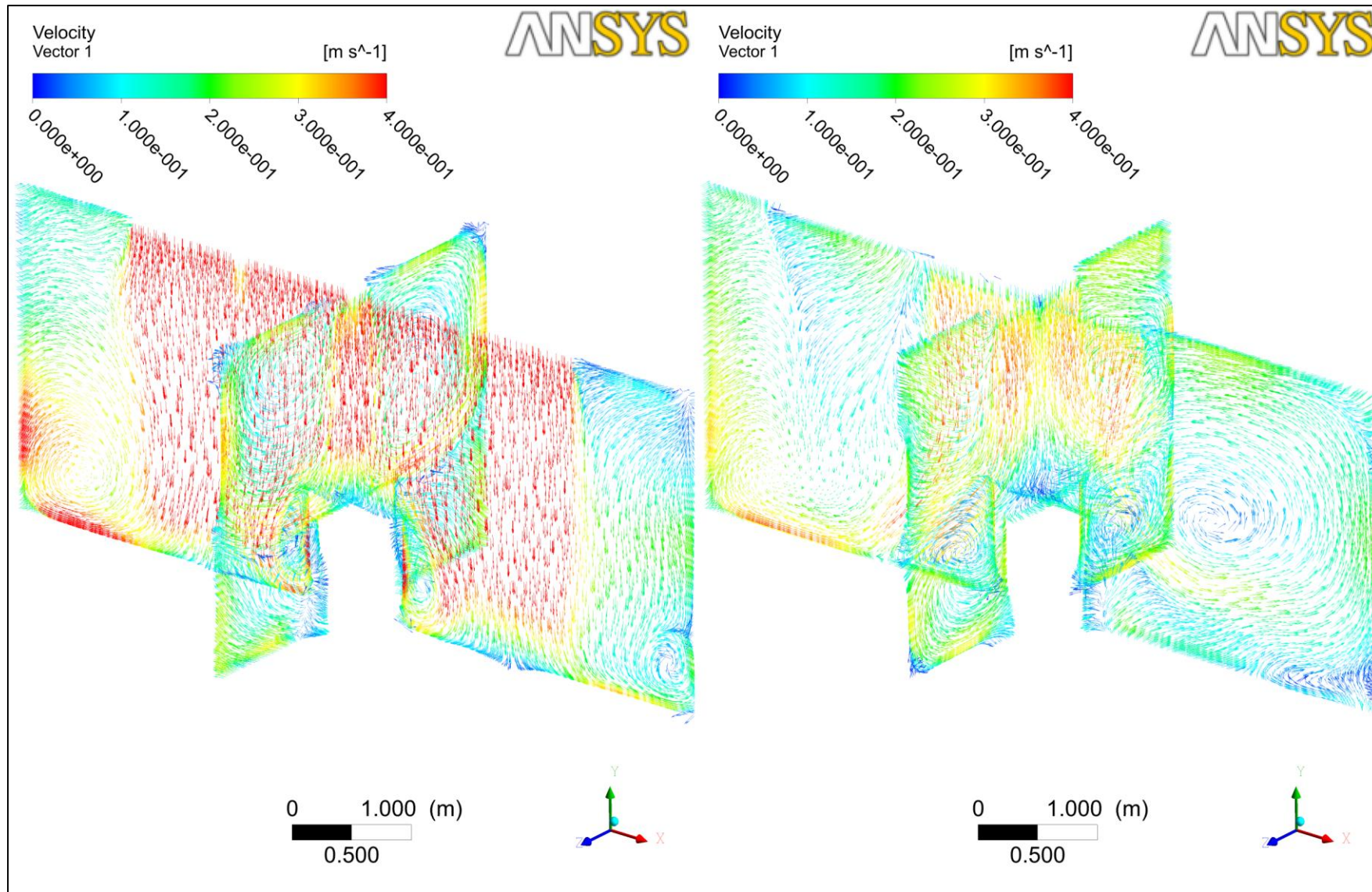


Figure 6.15a: Comparison of air velocity vector for case 2a (left) and case 4a (right) (Inlet velocity 0.4 m/s).

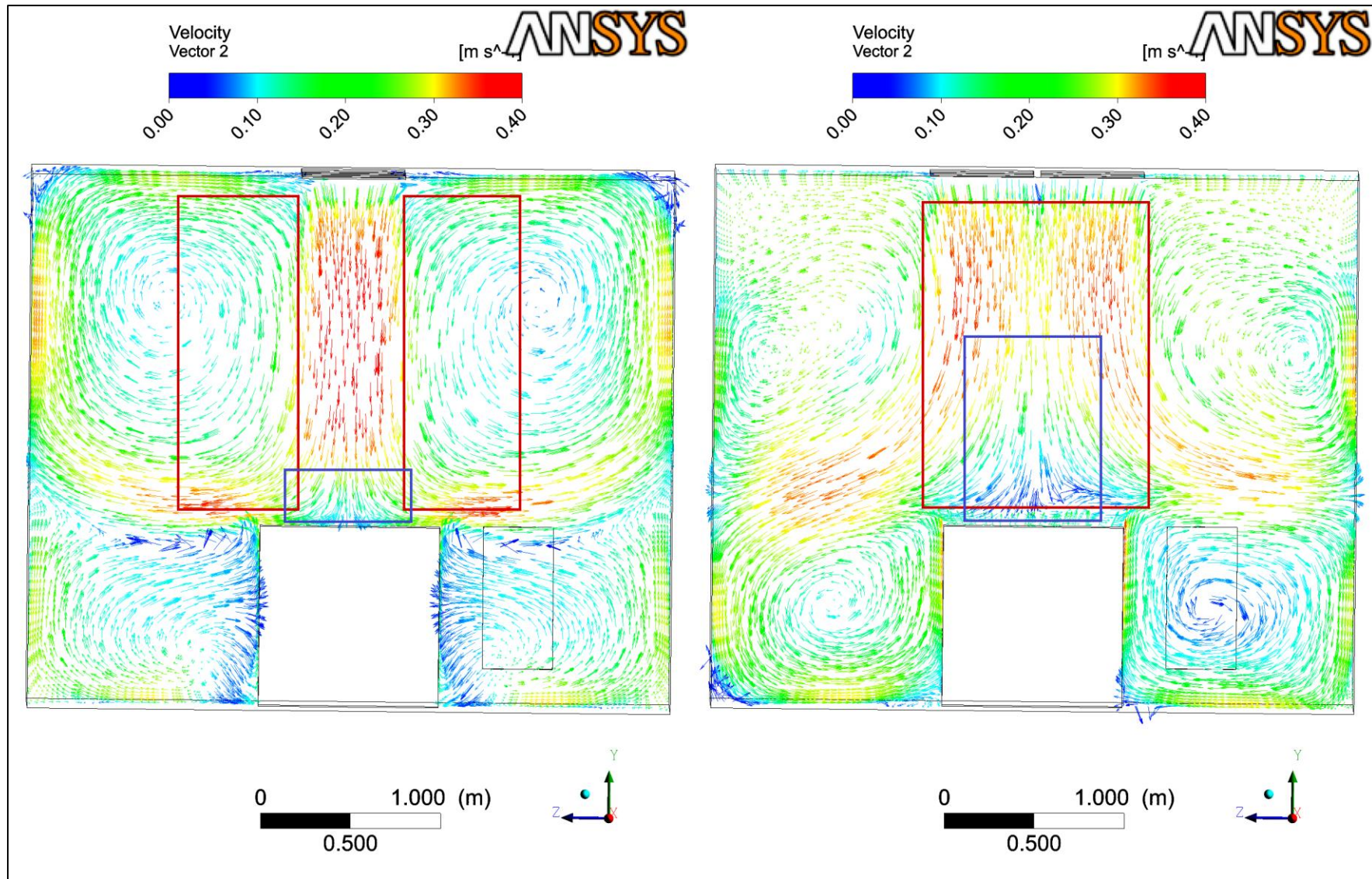


Figure 6.15b: Comparison of air velocity vector (y-z plane) for case 2a (left) and case 4a (right) (Inlet velocity 0.4 m/s).

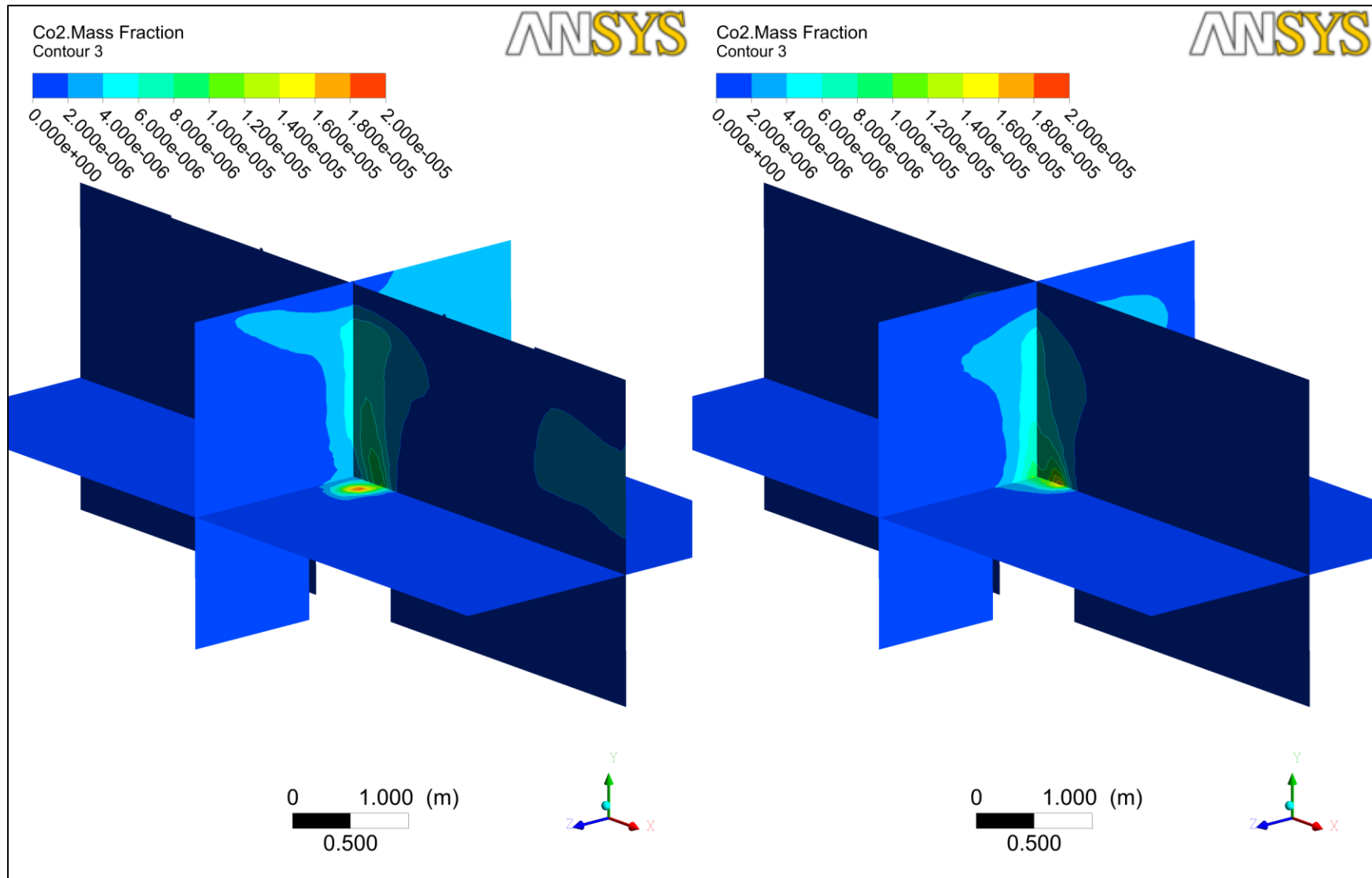


Figure 6.16: Comparison of contaminant dispersion for case 1a (left) and case 3a (right) (Inlet velocity 0.2 m/s).

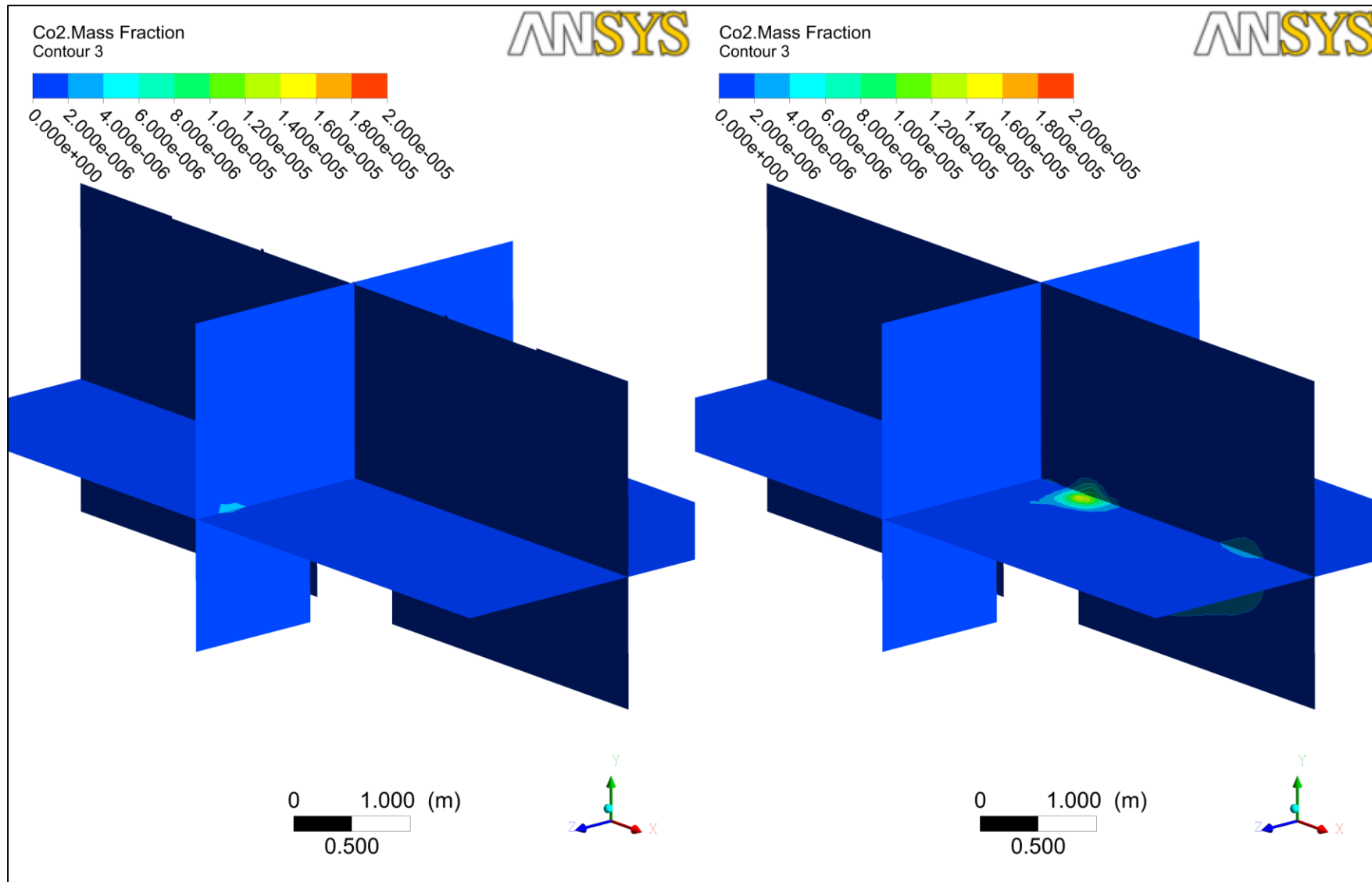


Figure 6.17: Comparison of contaminant dispersion for case 2a (left) and case 4a (right) (Inlet velocity 0.4 m/s).

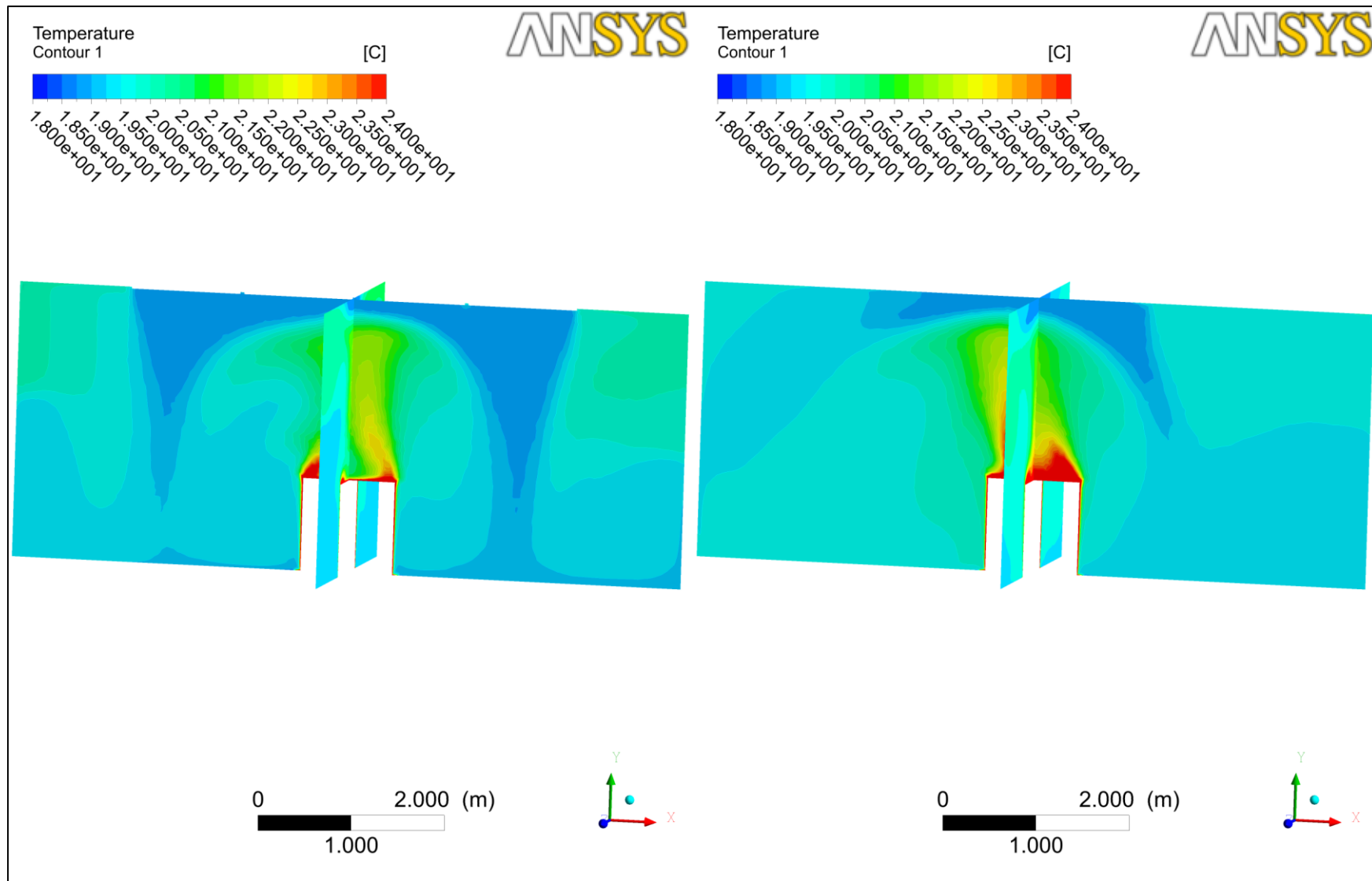


Figure 6.18: Comparison of air temperature for case 1a (left) and case 3a (right) (Inlet velocity 0.2 m/s).

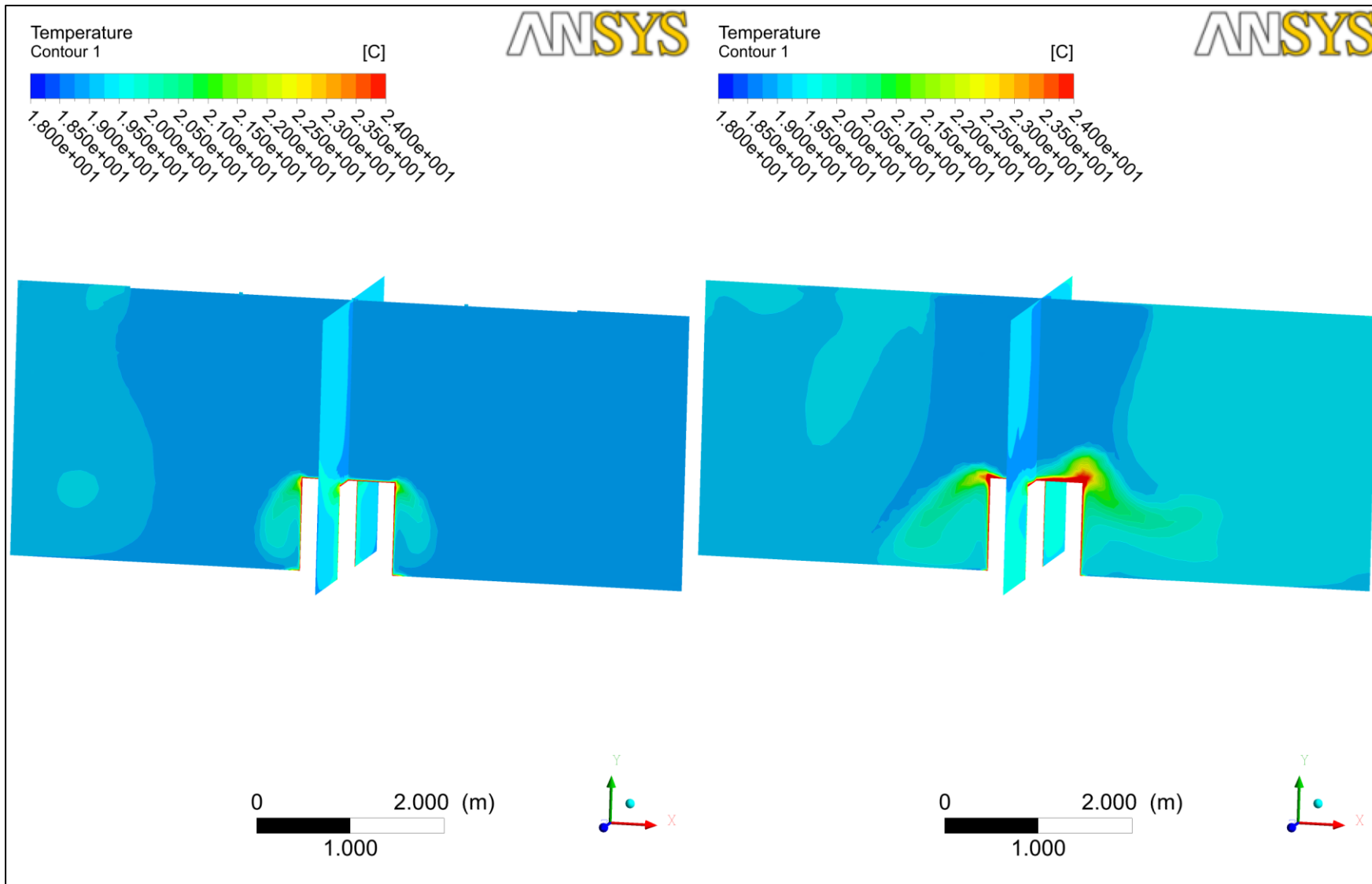


Figure 6.19: Comparison of air temperature for case 2a (left) and case 4a (right) (Inlet velocity 0.4 m/s).

Effect of the presence of heat load

In the absence of the heat load, by referring to Figure 6.21, the air jet collides with the surface of the obstacle, and then splits into two flows. The airflow pattern in current simulation is consistent with the study conducted by Akabayashi et al. (1986) on the visualization of airflow on a simple rectangular obstacle using a laser light sheet. Besides causing perturbation on the velocity field vicinity to heat load, in terms of contaminant dispersion, the presence of heat load encourages the spread of contaminant (by comparing Case 1a, 2a, 3a, 4a to Case 1b, 2b,3b,4b, respectively) (Figures 6.20-6.23). In actual conditions, the diffusion coefficient is never a constant in a non-isothermal condition, since mass diffusivity is proportionate to temperature in a power of $3/2$, according to Chapman-Enskog theory. The presence of heat load causes temperature gradient aiding the spread of contaminant.

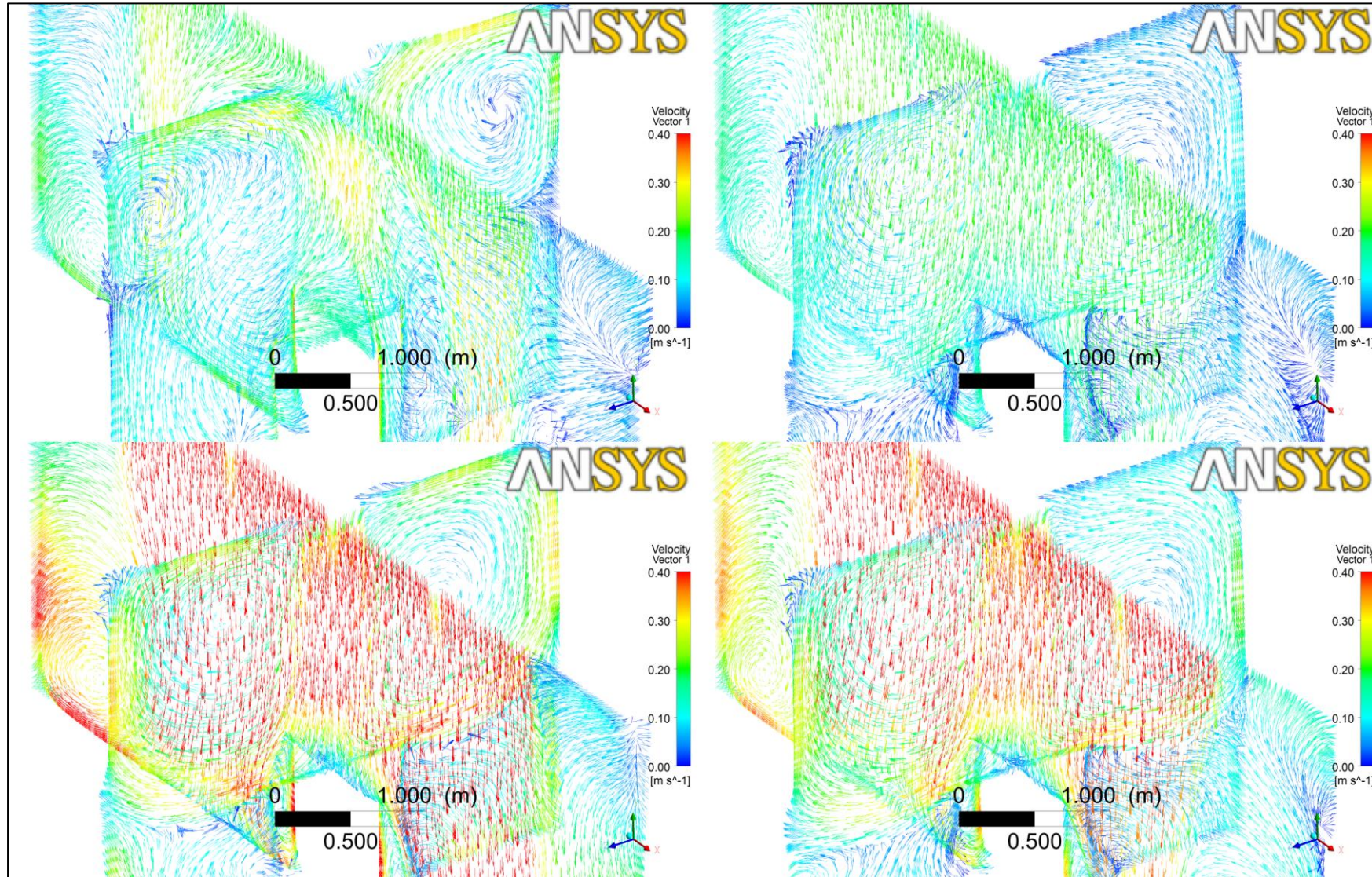


Figure 6.20: Comparison of air velocity vector for case 1a (upper left) & case 1b (upper right); case 2a (bottom left) and 2b (bottom right).

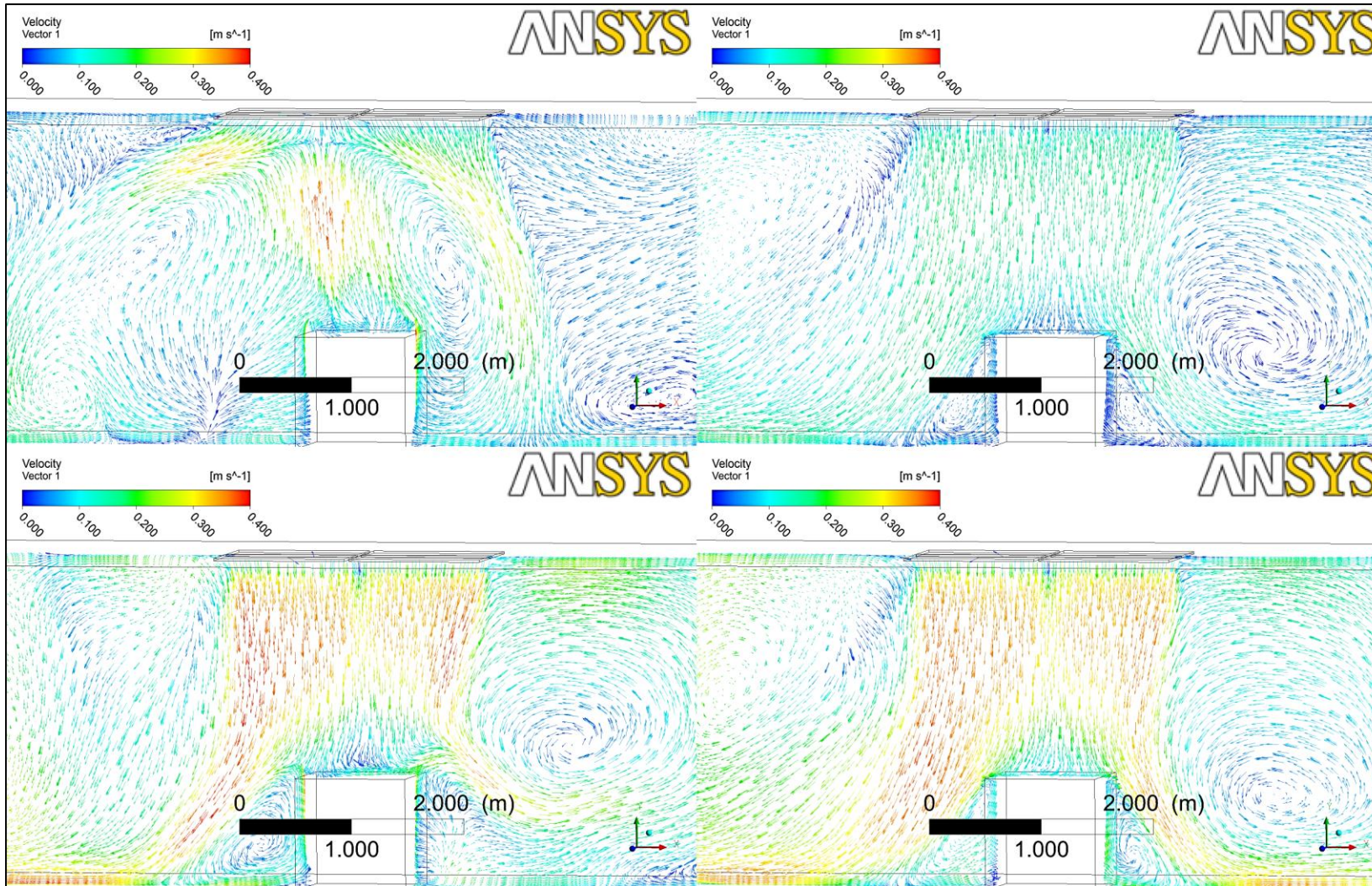


Figure 6.21: Comparison of air velocity vector for case 3a (upper left) & case 3b (upper right); case 4a (bottom left) and 4b (bottom right).

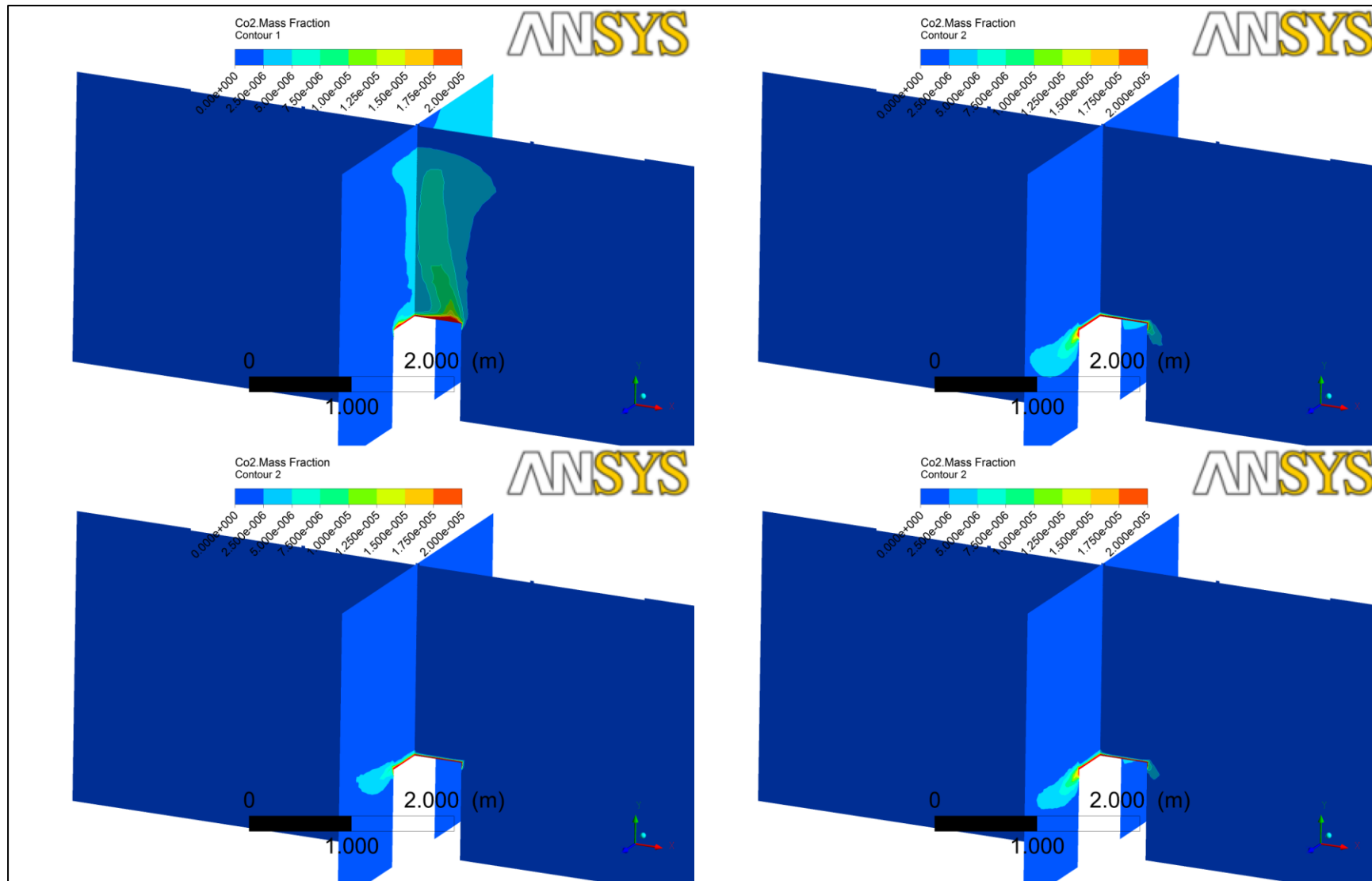


Figure 6.22: Comparison of contaminant dispersion for case 1a (upper left) & case 1b (upper right); case 2a (bottom left) and 2b (bottom right).

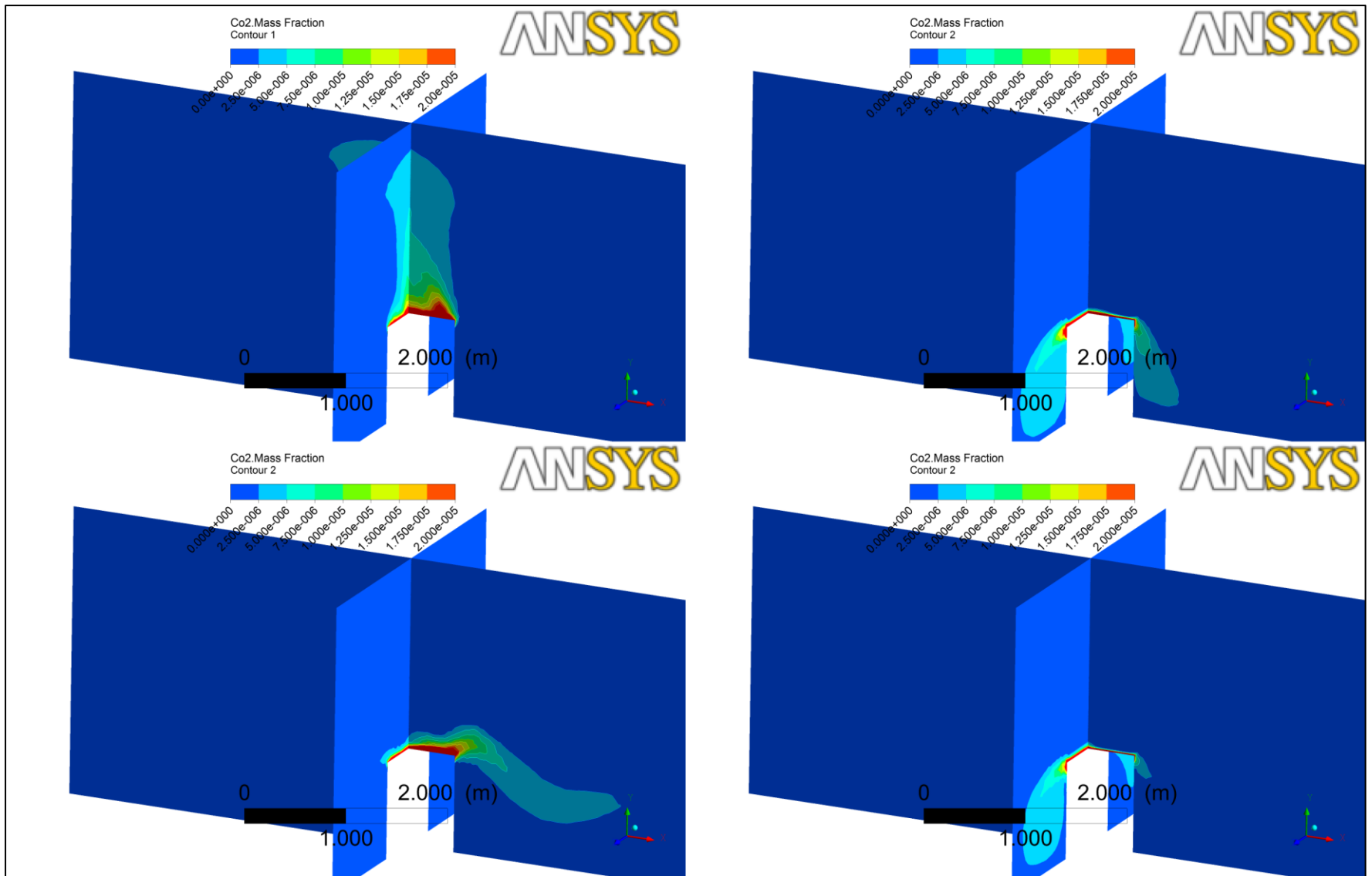


Figure 6.23: Comparison of contaminant dispersion for case 3a (upper left) & case 3b (upper right); case 4a (bottom left) and 4b (bottom right).

6.1.4 Concluding summary

From this study, inlet velocity of 0.2 m/s does not possess the ability to oppose the buoyant force from the heat source, even at a height of 1.7 m above the floor. With a velocity inlet of 0.4 m/s, the effect of thermal plume is diminished. The maximum concentration of the contaminant at inlet velocity of 0.2 m/s is higher than 0.4 m/s.

The array of air inlets does not carry significant influence on the airflow distribution for inlet velocity of 0.2 m/s since buoyant force dominating the airflow inside the room. For both inlet velocity of 0.2 m/s and 0.4 m/s, inlets with 1 x 4 array performs better than 2 x 2 array in terms of diluting the contaminant and better evenness of temperature distribution. Also, from this study, in determining the design of inlet array in a clean room, the behaviour of air jet impingement on the surface of the obstacle should be considered.

6.2 Study on the effect of inlet air velocity variations and heat source location in a clean room – A 2-D simulation study

6.2.1 Background and problem formulation

During the visit to UMMC OT-11, the OR's ventilation design and layout had drawn special attention. Two rows of HEPA's air inlet array with two exhausts located at the bottom on same face of a sidewall, and the operating zone vicinity to exhaust, as shown in Figure 6.24. Moreover, if there are multiple supply air outlets that branched from a main air duct, distributing an equal volume flow rate in each branch is hardly achievable since each branch exerts different downstream pressure. Current observation gives rise to the question on the effect of inlet air velocity variations and heat source location in a clean room.



Figure 6.24: HEPA's air inlet array with two exhausts located at the bottom on same face of a sidewall.

6.2.2 Model for simulation

From the on-site measurement, the air velocity of each HEPA varies. In current context, the airflow in the clean room could be affected by the mean inlet air velocity and temperature, their variations (deviations of air velocity among inlets), and the location of heat load. Aforementioned scenario was simplified and translated into a 2 dimensional problem, and the dimensional details were given in Figure 6.26. The problem was solved numerically using a commercially available CFD solver, Fluent.

The heat load is assumed as a machine that dissipating heat at 70 W/m^2 . Different cases were studied by the means of design of experiment.

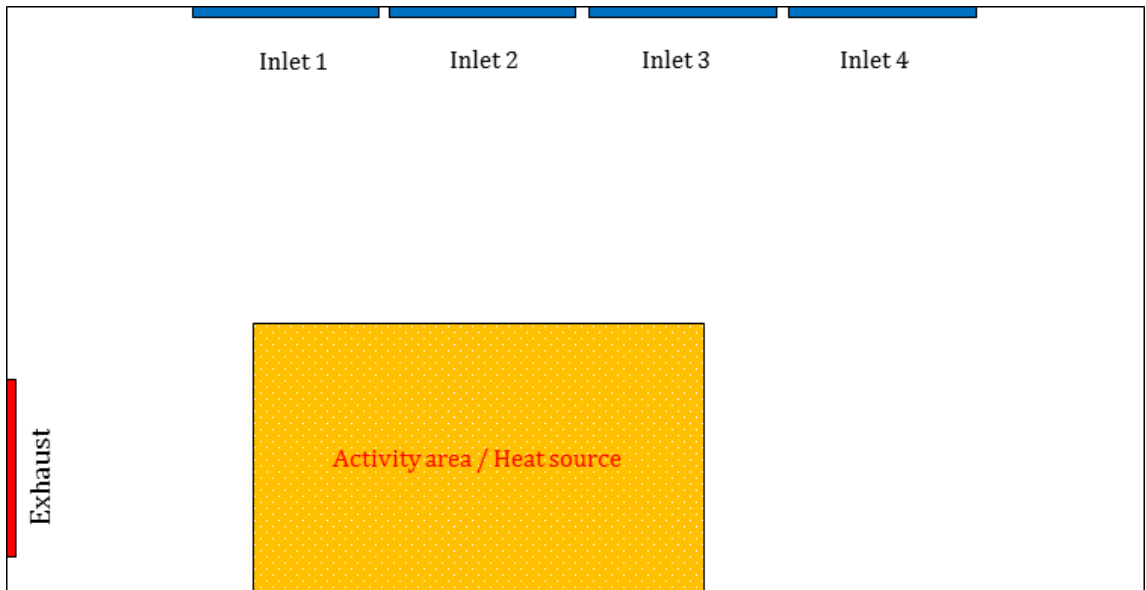


Figure 6.25: Hypothetical 2-D model to study the effect of inlet air velocity variations and heat source location in a clean room.

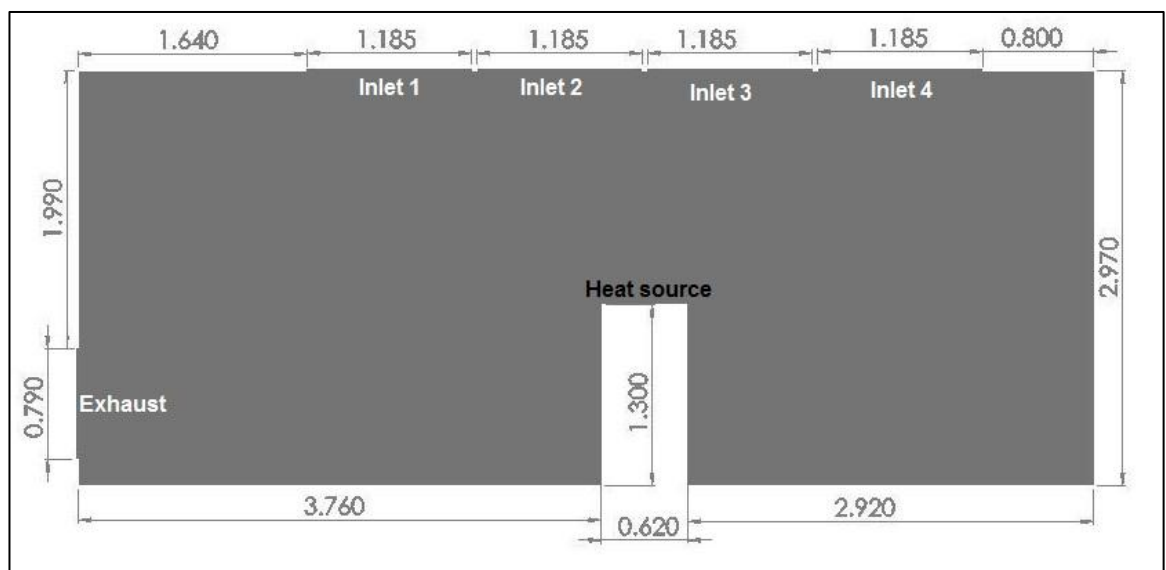


Figure 6.26: Dimension for the hypothetical 2-D model (unit in meter).

6.2.3 Numerical method and simulation overview

6.2.3.1 Grid independency

Prior to the simulations, grid independence test was carried out using quadrilateral mesh via ANSYS Workbench 12.0. Nine cases of mesh number were considered. The details of the test were given in Figure 6.27 and Table 6.6. Approximately 35000 mesh elements with nominal size of 2.4 cm were needed to achieve the grid independency. Further details on the grid independency test are included in Appendix I. For the generation of computational mesh, the mesh in the computational domain was generated by quadrilateral meshes with Q-morph. The wall was layered with ten inflation layers and the inflation vicinity the inlets were controlled using a sphere of influence.

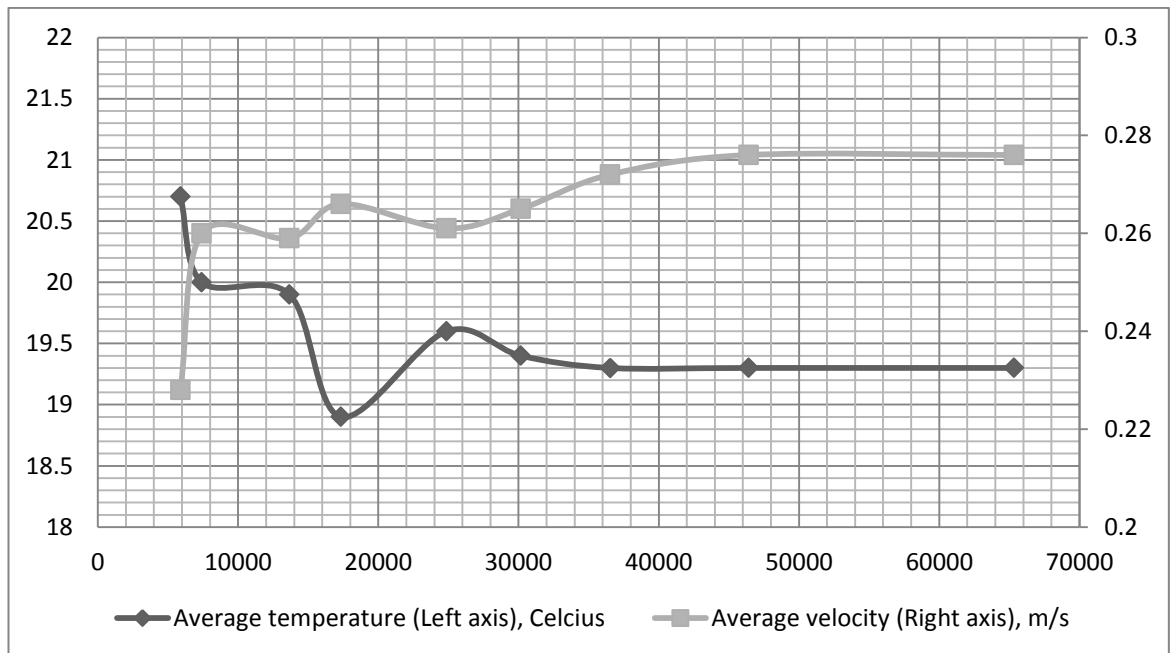


Figure 6.27: Results for grid independency study (for uniform $V_{in} = 0.2$ m/s).

Table 6.6: Details on the mesh size.

No.	Number of elements	Maximum skewness	Representative mesh size, h (m)	Ratio, $\frac{h_{n+1}}{h_n}$
1	65348	0.882	0.0179	-
2	46412	0.874	0.0213	1.187
3	36535	0.825	0.0239	1.127
4	30170	0.734	0.0263	1.100
5	24874	0.965	0.0290	1.101
6	17337	0.710	0.0348	1.198
7	13665	0.744	0.0391	1.126
8	7411	0.821	0.0531	1.358
9	5891	0.840	0.0596	1.122

6.2.3.1 Boundary condition and settings

The boundary conditions and settings for the current 2-D simulations are given in Tables 6.7 and 6.8.

Table 6.7: Boundary condition and settings for CFD simulations.

Item	Details
<i>Air inlet</i>	Velocity inlet is set as the inlet boundary. It is modeled as a line in 1.185m that discharges air vertically downward. Air temperature is set at 18.8°C, with turbulent intensity of 5%. The specification of air velocity for each inlet varies, as given in Table 6.8.
<i>Air outlet</i>	There is one outlet located at the bottom part of a side wall
<i>Walls</i>	No slip condition on the surface, adiabatic walls.
<i>Heat Load</i>	No slip condition on the surface, generate heat at 70 W/m^2
Mesh	Approximately 3×10^4 mesh elements
Solver	Pressure based coupled solver and steady state
Model	$k - \varepsilon$ model, $\sigma_k = 1.0$,

	$\sigma_\epsilon = 1.3$, $C_{1\epsilon} = 1.44$ $C_{2\epsilon} = 1.92$, $C_\mu = 0.09$, Full buoyancy effects is on to include buoyancy effects on ϵ . Enhanced wall treatment.
Solution method	Scheme: SIMPLE Gradient: Least –square cell based Pressure: Standard Momentum: 2 nd order upwind Turbulent kinetic energy: 2 nd order upwind Turbulent dissipation rate: 2 nd order upwind Energy: 2 nd order upwind
Solution control	<i>Under relaxation factor</i> ¹ Pressure: 0.3 Density: 1 Body forces: 1 Momentum: 0.7 Turbulent kinetic energy: 0.8 Turbulent dissipation rate: 0.8 Turbulent viscosity: 0.5 Energy: 1
Convergence criterion ² (absolute)	Continuity, x, y, z-velocity, k, epsilon: 5×10^{-4} Energy: 1×10^{-7}

1 Represent initial setting. Under relaxation factors are manipulated throughout the simulation to achieve convergence.

2 Smaller value of convergence criterion will be adopted if the mass and heat transfer imbalance were found larger than 0.2%.

Table 6.8: Specification of the inlet air velocity.

Simulation	Average inlets velocity, m/s	Velocity Difference, m/s	Inlet 1	Inlet 2	Inlet 3	Inlet 4
1	0.20	0.00	0.20	0.20	0.20	0.20
2	0.20	0.02	0.18	0.22	0.22	0.18
3	0.20	0.05	0.15	0.25	0.25	0.15
4	0.40	0.00	0.40	0.40	0.40	0.40
5	0.40	0.02	0.38	0.40	0.40	0.38
6	0.40	0.05	0.35	0.45	0.45	0.35
7	0.20	0.00	0.20	0.20	0.20	0.20
8	0.40	0.00	0.40	0.40	0.40	0.40

Besides iterating the residual of the solution to the setting value, in order to ensure the convergence criterion is adequate, the net heat transfer and mass transfer imbalance should be examined. A solution is only considered converged if the net imbalance of the mass and energy balance is less than 0.2%. From the simulations done, the net imbalances of energy and mass are less than 0.2%.

6.2.3.1 CFD Simulations overview

As shown in Figure 6.9, there are 8 simulations in this comparative study. For simulation 1-6, the air velocity distribution at each inlet was varied, and the heat source location was being fixed, located in the middle of the inlets. Simulation 7 and 8 was performed in order to study the effect of the position of the heat source (i.e. an obstacle) to the airflow, compare to simulation 1 and simulation 4. For Simulation 7 and 8, the heat source was shifted 1 meter to the left from its original middle position. The Ar number corresponded to each case was calculated, by using the same calculation procedure in section 6.1.

Table 6.9: Description for all cases.

Simulation	Average inlets velocity, m/s	Velocity Difference, m/s	Archimedes number, Ar	Heat source location
1	0.20	0.00	1.25	Middle
2	0.20	0.02	1.25	Middle
3	0.20	0.05	1.25	Middle
4	0.40	0.00	0.16	Middle
5	0.40	0.02	0.16	Middle
6	0.40	0.05	0.16	Middle
7	0.20	0.00	1.25	Left
8	0.40	0.00	0.16	Left

In current study, the particles were modeled as a urea with $12\mu\text{m}$ in size that obeys spherical drag law. It was generated from the surface of the heat source and (coordinate: 3.23 m, 1.3 m) and the particle trajectory was solved by Lagrangian approach. In order to facilitate the comparisons, three lines were specified, namely Line A-A', Line B-B' and Line C-C', as defined in Table 6.10.

Table 6.10: Definition for Line A-A', Line B-B' and Line C-C'.

Item	Description ¹	Coordinate (x, y)/m
Line A-A'	Horizontal line (1.7 m above the floor)	(-7.3, 1.7) to (0, 1.7)
Line B-B'	Vertical line (5.1 m from the right wall)	(-5.1,0) to (-5.1,3)
Line C-C'	Vertical line (1.4 m from the right wall)	(-1.4,0) to (-1.4,3)

¹ The lines are shown in Figure 6.28

6.2.4 Results and discussion

Generally, there are three main recirculation zones. The recirculation regions are formed as the flow attached to the wall due to Coandă effect. The confluence of individual jet is affected by the distance across each discharge as well as the number of the room air inlets in parallel direction. During the initial stage of the coalescence, faster velocity decay happens as there is an increment of the number of room air inlets in parallel direction in the same plane. General explanation for this phenomenon is understandable. As the flow rate remains constant, the coalescence of jets will extend the surface area normal to the fluid flow causing the reduction of flow momentum and thus reducing the overall velocity of the flow. In region 2, the reverse flow region, reattachment region and wall jet region are formed before the air being exhausted. As the inlet air velocity decrease from 0.4 m/s to 0.2 m/s, the length of reverse flow region increase 0.25 m. From the velocity vector, region 3 occurs upstream of heat source (or activity area). The

air in region 3 will be entrained into the main air stream, and flowing through activity area before being discharged from the room (Figure 6.28).

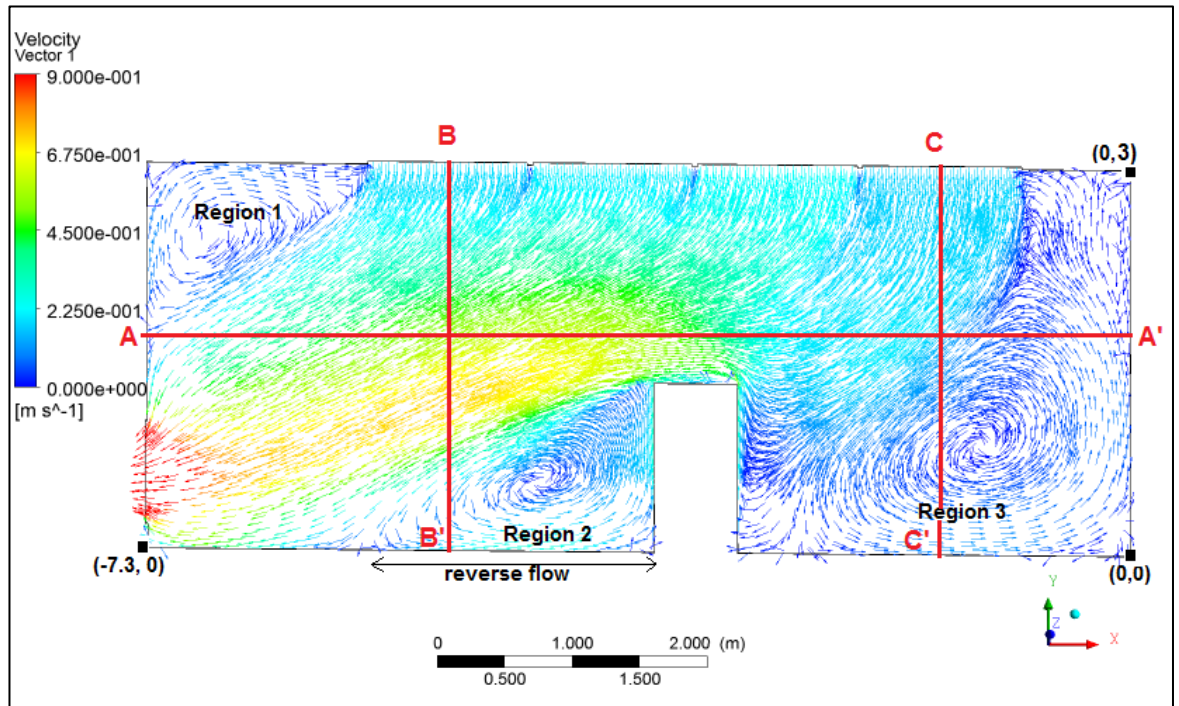


Figure 6.28: Recirculation zones in the 2-D room.

In terms of the variations of the inlet air velocity, the variation of inlet air velocity distribution for Line A-A', Line B-B' and Line C-C' is small (Figure 6.29). However, a distinguishable difference is found at the region where maximum local air velocity occurs. The velocity difference does not significantly affect the average room air velocity, for both $V_{in} = 0.2$ m/s and $V_{in} = 0.4$ m/s as reported in Table 6.11. For air temperature distribution, lower air velocity will cause higher vertical temperature gradient on the room (Charts d & f in Figure 6.29). Meanwhile, the recirculation region located upstream of the obstacle always resulted in lower local mean temperature index (by comparing all the local mean temperature index for Line C-C' with Line A-A' and Line B-B' in Table 6.11).

There is no general conclusion can be drawn on the effect of inlet air velocity variations on the particle residence time. However, lower inlet air velocity will resulted in higher particle residence time.

The shift of the heat source (to the left) closer to the exhaust which functioned as an obstacle will tends to accelerate the fluid downstream. Hence, it resulted in greater air velocity in the activity area as indicated by Figure 6.30 (chart a). At the location upstream of the activity area, the air velocity decreased. The recirculation region produces stagnant region that poor in entraining the surrounding air. It results in higher temperature in the stagnant region, which could cause a high temperature gradient. Overall, from the simulations performed, the air temperature remains unaffected (hence showing a vertical straight line in the graphs) from the inlet to a distance at least 1 m below the inlet.

Table 6.11: Local mean temperature index and particle residence time for all cases.

Simulation	Average room temperature, °C	Average room velocity, m/s	Local mean temperature index, $\theta = \frac{T_p - T_{in}}{T_{exhaust} - T_{in}}$						Particle residence time, seconds
			Line A-A'		Line B-B'		Line C-C'		
			Min	Max	Min	Max	Min	Max	
1	19.04	0.278	0	6.996	0	6.996	0	0.116	187.2
2	19.04	0.279	0	7.113	0	7.116	0	0.065	120.5
3	19.04	0.275	0	7.265	0	7.265	0	0.019	135.6
4	18.93	0.549	0	6.933	0	6.933	0	0.143	11.7
5	18.93	0.548	0	6.936	0	6.936	0	0.133	12.2
6	18.93	0.545	0	7.056	0	8.266	0	0.051	11.9
7	18.93	0.280	0	6.519	0	6.519	0	0.000	631.4
8	18.87	0.556	0	8.255	0	8.255	0	0.024	8.2

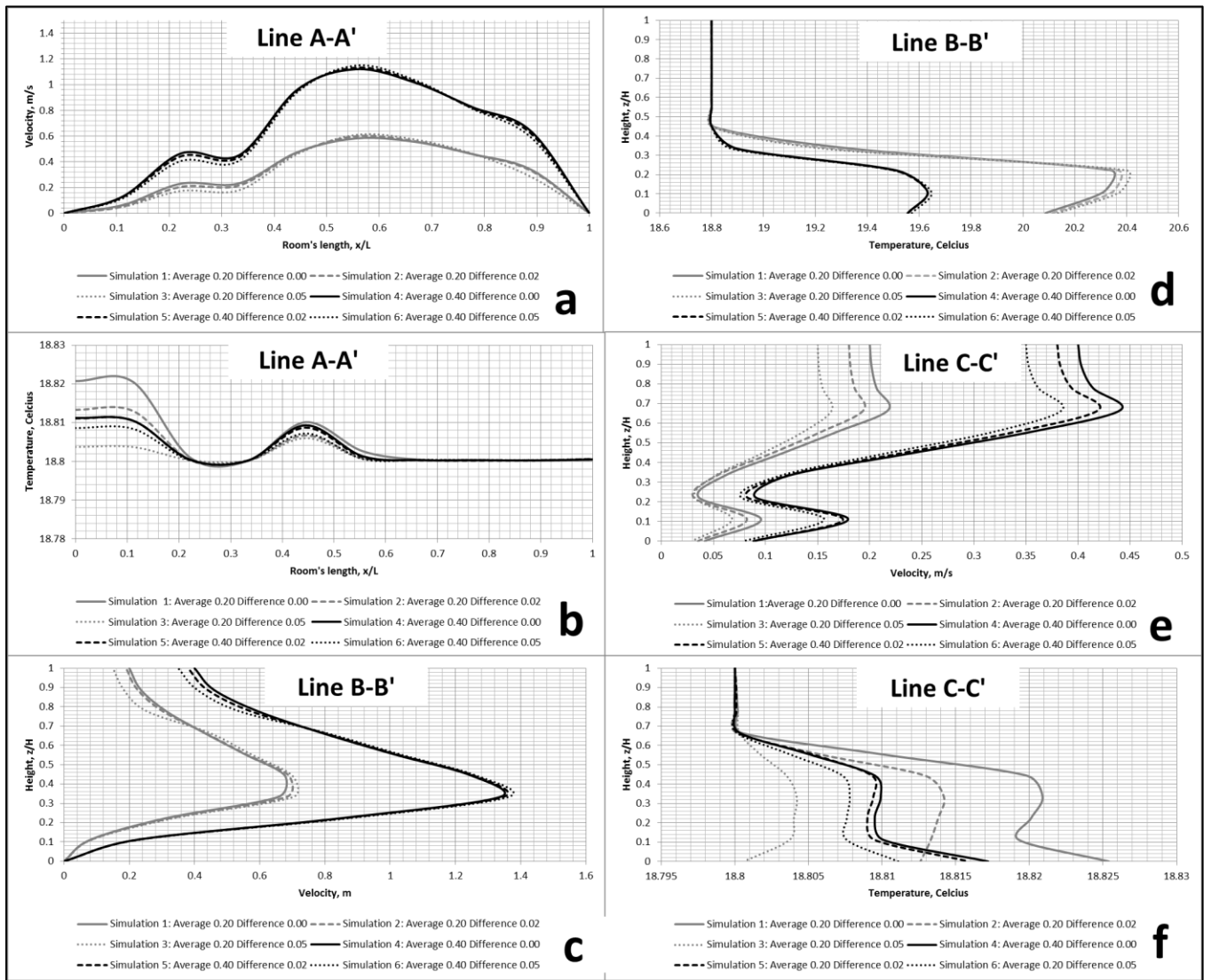


Figure 6.29: Comparison of inlet air velocity variations to the air distribution in the room.

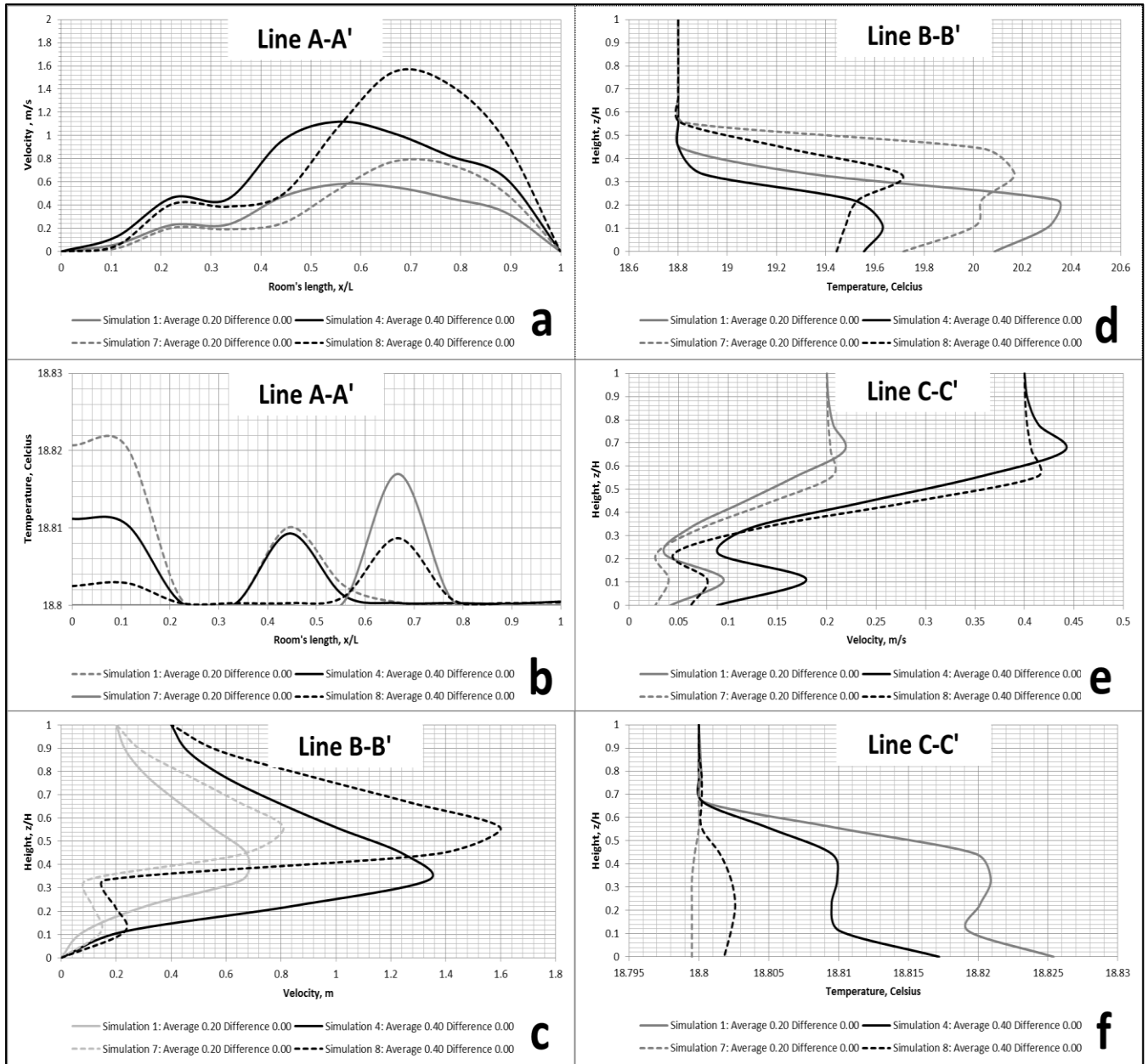


Figure 6.30: Comparison of heat source (obstacle) variations to the air distribution in the room.

6.2.5 Concluding summary

The maldistribution of inlet velocity does not significantly affect the average room velocity, and it only affects the magnitude of maximum or minimum air velocity. When equipment is located closer to the exhaust, it will accelerate the fluid downstream, causing higher air velocity at the activity area, and reducing the air velocity upstream the activity area.

7.0 Conclusion and Recommendations

7.1 Conclusion

In order to ensure an OR is functioning well, four main design considerations, namely temperature, humidity, ACH and pressure have to be in accordance with available stipulated standards. Nowadays, LAF type of OR design is widely adopted. However, from the on-site survey in numbers of ORs located at Malaysia, most of the ORs designs are not fully comply with the recommended design criteria. Two common problems found are high RH in the OR as well as inappropriate architectural design. During the OR's design stage, the designer should evaluate different design schemes which the design of air inlet, air outlet, air flow rate and OR's layout may vary. After a long time in operation, the layout inside OR will change and hence the conformity on the performance of air distribution, checking of ACH and pressure differential as well as microbiology sampling should be carried out, to ensure the sustainability of OR. There is a lack of in-depth investigation on ventilation and distribution of air in a non-standard OR, especially in developing countries (that often operate with a non-standard OR). Therefore, a case study to provide a sufficient overview on the non-standard OR is favorable. As CFD has served as an important tool for researchers to conduct the prediction on the airflow in an OR, hence this work had discussed the governing equations, boundary conditions, on-site measurement and a proper CFD modeling approaches for OR in Chapter 3.

The first case study in this work was started by the investigation of air distribution in SGHHC OT-5 which located at Sarawak, Malaysia. Through the study, it confirmed that the obstruction and heat dissipation effect from surgical light could not be neglected, since the combination of both effects will result in a heat trap at the region

below the surgical light. Under same total flow volume for OT-5, OT-5 with uneven inlet velocities performs better than OT05 with even velocities distribution at the inlets. In terms of reducing the supply air, it was found that a reduction of air flow rate by 15% (to average inlet air velocity of 0.3 m/s) is possible in OT-5.

Then, for UMMC OT-11, its current design with 14 inlets seems excessive, since the air discharge from inlets 4 and 8 bypass the operating region. The case study on UMMC OT-11 had shown that due to the improper design of the OR the advantage of high ACH is badly curtailed in UMMC OT-11. The outcome for the case study suggests, the room air inlet should locate above the surgical site, rather than periphery of the surgical site, since current design will result in inefficiency in ventilation.

In the study of inlet design on the airflow in a Class 7 clean room (which an OR also fall into this class), two different inlet arrays (1 x 4 and 2 x 2 arrays) with inlet velocity 0.2 m/s and 0.4 m/s were discussed. From the study, inlet velocity of 0.2 m/s does not possess the ability to oppose the buoyant force from the heat source, even at a height of 1.7 m above the floor. At inlet velocity of 0.2 m/s, the array of air inlets does not carry significant influence on the airflow distribution since buoyant force dominating the airflow inside the room. With a velocity inlet of 0.4 m/s, the effect of thermal plume is diminished. For both inlet velocity of 0.2 m/s and 0.4 m/s, inlets with 1 x 4 array performs better than 2 x 2 array in terms of diluting the contaminant and better evenness of temperature distribution. Also, from this study, in determining the design of inlet array in a clean room, the behaviour of air jet impingement on the surface of the obstacle should be considered.

From the 2-D simulation to study the effect of maldistribution of air velocity in a clean room, the maldistribution of inlet velocity does not significantly affect the average room velocity, and it only affects the magnitude of maximum or minimum air velocity. Equipment located closer to the exhaust will accelerate the fluid downstream, causing higher air velocity at the activity area, and reducing the air velocity upstream the activity area.

7.2 Recommendations

In order to achieve high level of cleanliness in an OR, it requires a high demand of supply air into the OR. Hence, it will directly increase the energy demand for treating the fresh air. In future, study should concentrate on optimizing the energy consumption in an OR, without compromising the cleanliness in the OR. Consequently, this study requires an investigation in a full scale laboratory with a mock-up OR in a controlled environment in order to minimize any assumption and study the air distribution in an OR effectively.

References

- AIA. (2006). Guidelines for design and construction of hospital and health care facilities. Washington (DC): The American Institute of Architects Press.
- AIAA. (1998). Guide for the verification and validation of computational fluid dynamics simulations. AIAA Standard G-077-1998. American Institute of Aeronautics and Astronautics, Reston, VA.
- Akabayashi, S., Murakami, S., Kato, S. & Chifuru, S. (1986). Visualization of air flow around obstacles in laminar flow type clean room with laser light sheet. 8th International Symposium on Contamination Control held on 9-12 September 1986 at Milan (pp. 691-697). Milan.
- Al-Waked, R. (2010). Effect of ventilation strategies on infection control inside operating theatres. *Engineering Applications of Computational Fluid Mechanics*, **4**(1), 1-16.
- Al-Waked, R. (2010). Reply to comments on 'effect of ventilation strategies on infection control inside operating theatres'. *Engineering Applications of Computational Fluid Mechanics*. **4**(2), 328-330.
- ANSI/ASHRAE. (2003). Standard 62.1 Ventilation for acceptable indoor air quality. Atlanta, GA: ASHRAE.
- ANSI/ASHRAE. (2006a). Standard 70 Method of testing the performance of air outlets and air inlets. Atlanta, GA: ASHRAE.
- ANSI/ASHRAE. (2006b). Standard 113 Method of testing for room air diffusion. Atlanta, GA: ASHRAE.
- ANSI/ASHRAE. (2010). Standard 55 Thermal environmental conditions for human occupancy. Atlanta, GA: ASHRAE.
- ANSYS. (2009a). ANSYS FLUENT 12.0 User's guide. Canonsburg, Pennsylvania: ANSYS Inc.
- ANSYS. (2009b) ANSYS Workbench User's Guide
URL:
http://www1.ansys.com/customer/content/documentation/121/wb2_help.pdf
- ASHRAE. (2003a). HVAC Applications Handbook, Chapter 7: Health care facilities. Atlanta, GA: ASHRAE.
- ASHRAE. (2003b). HVAC Applications Handbook, Chapter 16: Clean spaces. Atlanta, GA: ASHRAE.
- ASHRAE. (2008). ANSI/ASHRAE/ASHE Standard 170, Ventilation of health care facilities. Atlanta, GA: ASHRAE.

- ASHRAE. (2009). Fundamentals, Chapter 13: Indoor environmental modeling. Atlanta, GA: ASHRAE.
- Assar, S.K., & Block, S.S. (2001). Survival of microorganisms in the environment. In Block, S.S. (ed). Disinfection, sterilization, and preservation. 5th ed, Philadelphia: Lippinkott-Williams & Wilkins. (p 1221-1224).
- Awbi, H. (2003). *Ventilation requirement in ventilation of buildings*, 2nd ed. London: Spon Press.
- Ayliffe, G.A.J. (1991). Role of the environment of the operating suite in surgical wound infection. *Reviews of Infectious Diseases*. **13** (suppl 10), S800-S804.
- Babb, J.R., Lynam, P., & Ayliffe, A.J. (1995). Risk of airborne transmission in an operating theatre containing four ultraclean air units. *Journal of Hospital Infection*. **31** (3), 159-168.
- Balaras, C.A., Dascalaki, E., & Gaglia, A. (2007). HVAC and indoor thermal conditions in hospital operating rooms. *Energy and Building*. **39** (4), 454 - 470.
- Batchelor, G.K. (1970). An introduction to Fluid Dynamics, Cambridge University Press, London.
- Beltaos, S., & Rajaratnam N. (1973). Plane turbulent impinging jets. *Journal of Hydraulic Research*. **11**, 29-59.
- Berglund, L.G. & Fobelets, A.P.R. (1987). Subjective human response to low-level currents and asymmetric radiation. *ASHRAE Transactions*. **93**(1), 493-523.
- Blowers, R., & Crew, B. (1960). Ventilation of operating-theatres. *The Journal of Hygiene*. **58**, 427-448.
- Bolashikov, Z.D. & Melikov, A.K. (2009). Methods for air cleaning and protection of building occupants from airborne pathogens. *Building and Environment*. **44** (7), 1378-1385.
- Brohus, H., Balling, K.D., & Jeppesen, D. (2006). Influence of movements on contaminant transport in an operating room. *Indoor Air*. **16**(5), 356-372.
- Brundrett, G.W. (1990). Criteria for moisture control. London: Butterworth.
- Carter, C.D. & Barr, B.A. (1997). Infection control issues in construction and renovation. *Infection Control and Hospital Epidemiology*. **18**(8), 587-596.
- Chang, Z., Chen, Q. (2007). Comparison of the Eulerian and Lagrangian methods for predicting particle transport in enclosed spaces. *Atmospheric Environment*. **41**, 5236-5248.
- Chen, Q. (1997). Computational fluid dynamics for HVAC: successes and failures. *ASHRAE Transactions*. **103**(1), 178-187.
- Chen, Q., Jiang, Z., & Moser, A. (1992). Control of airborne particle concentration and draught risk in an operating room. *Indoor Air*. **2**(3), 154-67.

- Chen, Q., & Srebric, J. (2002). A Procedure for verification, validation, and reporting of indoor environment CFD analyses. *HVAC&R Research*, **8**(2), 201-216.
- Chow, T.T., Kwan, A., Lin, Z., & Bai, W. (2006). Conversion of operating theatre from positive to negative pressure environment. *Journal of Hospital Infection*. **64**:371-378.
- Chow, T.T., & Yang, X.Y. (2003). Performance of ventilation system in a non-standard operating room. *Building and Environment* . **38**, 1401-1411.
- Chow, T.T., & Yang, X.Y. (2004). Ventilation performance in operating theatres against airborne infection: review of research activities and practical guidance. *Journal of Hospital Infection* .**56**, 85-92.
- Chow, T.T., & Yang, X.Y. (2005). Ventilation performance in the operating theatre against airborne infection: numerical study on an ultra-clean system. *Journal of Hospital Infection*. **59**, 138–147.
- Craven, B.A., & Settles, G.S. (2006). A computational and experimental investigation of the human thermal plume. *Journal of Fluids Engineering*.**128** (6), 1251-1258.
- Dharan, S. & Pittet, D. (2002). Environmental controls in operating theaters. *Journal of Hospital Infection*. **51**(2), 79-84.
- Dong, S., Tu, G., Cao, R., & Yu, Z. (2009). Numerical study on effect of door opening on air flow patterns and dynamic cross-contamination in an ISO class 5 operating room. *Transactions of Tianjin University*.**15** (3), 210-215.
- Edge, B.A., & Paterson, E.G. (2005). Computational study of the wake and contaminant transport of a walking human. *Journal of Fluids Engineering*. **127** (5), 967-977.
- El-Gamal, N., El-Kassabany, N., Frank, S.M., Amar, R., Khabar ,H.A., El-Rahmany, H.K., et al. (2000). Age-related thermoregulatory differences in a warm operating room environment (approximately 26°C). *Anesthesia & Analgesia*. **90**(3),694-698.
- Essex-Lopresti, M. (1999). Operating theatre design. *The Lancet*. **353**(9157), 1007-1010.
- Essex-Lopresti, M & Hubert, D.(1962). Planning operating-theatre suites. *British Medical Journal* . **1** (5290), 1470–1473.
- Fanger, P.O. (1970). Thermal comfort. Copenhagen: Danish Technical Press.
- Fanger, P.O. & Christensen, N.K. (1986). Perception of draught in ventilated spaces. *Ergonomics*. **29**(2), 215-235.
- Fong K.F., Chow T.T., Li C., Lin Z., & Chan L.S. (2009). Effect of neutral temperature on energy saving of centralized air-conditioning systems in subtropical Hong Kong. *Applied Thermal Engineering*. **30** (13), 1659-1665.
- Friberg, B., Lindgren, M., Karlsson, C., Bergstrom ,A., & Friberg, S. (2002). Mobile zoned/exponential LAF screen: a new concept in ultra-clean air technology for

- additional operating room ventilation. *Journal of Hospital Infection*. **50**(4), 286-292.
- Friberg, B.E.E., Friberg, S., & Burman, L.G. (1996). Zoned vertical ultraclean operating room ventilation. A novel concept making long side walls unnecessary. *Acta Orthop Scand* .**67**(6), 578-582.
- Friberg, B., Friberg, S., Burman, L.G., Lundholm, R., & Östensson, R. (1996). Inefficiency of upward displacement operating theatre ventilation. *Journal of Hospital Infection*. **33**(4), 263-272.
- Fu, J.W., Yau, Y.H., Ng, W.B., & Lai, C.M. (2011). Improvement of the Indoor Environment and Airborne Contamination Control in an Operating Room. *Advanced Materials Research*, **255-260**, 1532-1536.
- Gutmark E., Wolfshtein, M., & Wygnanski, I. (1978). The plane turbulent impinging jet. *Journal of Fluid Mechanics*. **88** (4), 737-756.
- Hambraeus, A., & Laurell, G. (1980). Protection of the patient in the operating suite. *Journal of Hospital Infection*. **1**, 15-30.
- Harriman, L. (2001). Hospitals. In Harriman, L.G., Brundrett, G.W., Kittler, R. (ed). Humidity control design guide, Atlanta, GA: ASHRAE. (p 360-371).
- Hatch, M.T., & Wolochow, H. (1969). Bacterial survival: consequences of airborne state. In: Dimmick, R.L., Akers, A.B. (ed). An introduction to experimental aerobiology, New York: John Wiley and Sons. (p 267–295).
- Huang, C.J., Chen, C.L., Tseng, C.C., Luk, H.N., De Villa, V., Wang, C.S., et al. (2005). Maintenance of normothermia at operation room of 24°C in adult and pediatric patients undergoing liver transplantation. *Transplant International*. **18**(4), 396-400.
- Ho, S.H., Rosario, L., & Rahman, M.M. (2009). Three-dimensional analysis for hospital operating room thermal comfort and contaminant removal. *Applied Thermal Engineering*. **29** (10).2080-2092.
- Hoffman, P.N., Williams, J., Stacey, J., Bennett, A.M., Ridgway, G.L., Dobson, C., et al. (2002). Microbiological commissioning and monitoring of operating suites. *Journal of Hospital Infection*. **52** (1), 1-28.
- Horworth, F.H. (1985). Prevention of airborne infection during surgery. *ASHRAE Transactions*. **91**,291-304.
- Howard, J.L., & Hanssen, A.D. (2007). Principles of a clean operating room environment. *The Journal of Arthroplasty*. **22**(7 supplement), 6-11.
- Hu, S.C., Wu, Y.Y., & Liu, C.J. (1996). Measurements of air flow characteristics in a full scale clean room. *Building and Environment*. **31**(2), 119-128.
- ISO. (1999). Cleanrooms and associated controlled environments, Part 1: Classification air cleanliness. Standard 14644-1. International Organization for Standardization Technical Committee (ISO TC 209).

- Jensen, P.A., Lambert, L.A., Iademarco, M.F., & Ridzon, R. (2005). Guidelines for preventing the transmission of mycobacterium tuberculosis in health-care settings. 2005. *MMWR Recommendations and Reports*. **54** (RR-17), 1-141.
- Jowitt ,D., & Morris, A.J. (2005). The questionable value of microbiological sampling when commissioning new operating theatres [letter]. *Journal of Hospital Infection*.**59** (3), 267-268.
- Kasatpibal, N., Jamulitrat, S., Chongsuvivatwong, V., Nørgaard, M., Sørensen, H.T., & on behalf of the Surgical Site Infection Study Group. (2006). Impact of surgeon-specific feedback on surgical site infection rates in Thailand. *Journal of Hospital Infection*. **63**(2), 148-155.
- Kameel R, & Khalil E (2003). The prediction of airflow regimes in surgical operating theatres: A comparison of different turbulence models. AIAA-2003-859, American Institute of Aeronautics and Astronautics, Reston, VA.
- Kelkar, U., Bal, A.M., Kulkarni, S. (2005). Fungal contamination of air conditioning units in operating theatres in India. *Journal of Hospital Infection*. **60** (1). 81-84.
- Krasinski, K., Holman, R.S., Hanna, B., Greco, M.A., Graff, M., & Bhogal, M. (1985). Nosocomial fungal infection during hospital renovation. *Journal of Infection Control*. **6** (7), 278-282.
- Kowalski, W.J. (2006). Aerobiological engineering handbook. A guide to airborne disease control. New York: McGraw Hill.
- Kurazami, Y., Tsuchikawa, T., Ishii, J., Fukagawa, K., Yamato, Y., & Matsubara, N. (2008). Radiative and convective heat transfer coefficients of the human body in natural convection. *Building and Environment*. 43(12), 2142-2153.
- Landrin, A., Bissery, A., & Kac, G. (2005). Monitoring air sampling in operating theatre: can particle counting replace microbiological sampling? *Journal of Hospital Infection*. **61**, 27-29.
- Lee, E., Feigley, C.E., & Khan, J. (2002). An investigation of air inlet velocity in simulating the dispersion of indoor contaminants via computational fluid dynamics. *The Annals of Occupational Hygiene*. **46**(7), 701-712.
- Leung, M., & Chan, A.H.S. (2006). Control and management of hospital indoor air quality. *Medical Science Monitor*. **12**(3), SR17-23.
- Lewis, J.R. (1993). Operating room air distribution effectiveness. *ASHRAE Transactions*. **99**, 1191-1199.
- Li, Z., Liu, X., Jiang, Y., & Chen, X. (2005). New type of fresh air processor with liquid desiccant total heat recovery. *Energy and Buildings* .**37**, 587-593.
- Lidwell, O.M., & Blowers, R. (1962). Design and ventilation of operating-room suites for control of infection and for comfort. *The Lancet*. **280**(7263), 945-951.

- Lidwell, O.M., & Towers, A.G. (1969). Protection from microbial contamination in a room ventilated by a uni-directional air flow. *Journal of Hygiene*.**67** (1), 95-106.
- Lipsett, P.A. (2008). Do we really need laminar air flow ventilation in the operating room to prevent surgical site infections? *Annals of Surgery*.**248** (5), 701-703.
- Liu, J., Wang, H., & Wen, W. (2009). Numerical simulation on a horizontal airflow for airborne particles control in hospital operating rooms. *Building and Environment* . **44**,2284–2289.
- Loosli, C.G., Lemon, H.M., Robertson, O.H., & Appel, E. (1943). Experimental airborne influenza infection. I. influence of humidity on survival of virus in air. *Proceedings of the Society for Experimental Biology and Medicine* . **53**,205–206.
- Lowen, A.C., Mubareka, S., Steel, J., & Palese, P (2007). Influenza virus transmission is dependent on relative humidity and temperature. *PLoS Pathogens* . **3** (10 e151),1470–1476.
- McLaws, M.L. (2007). Malaysian national nosocomial infection surveillance system. Report of WHO Mission.
- Melikov, A.K., Popiolek, Z., Silva, M.C.G., Care, I., & Sefker, T. (2007). Accuracy limitations for low-velocity measurements and draft assessment in rooms. *HVAC&R Research*, **13**(6), 971-986.
- Memarzadeh, F. (2010). Comments on 'effect of ventilation strategies on infection control inside operating theatres'. *Engineering Applications of Computational Fluid Mechanics*,**4**(2),326-327.
- Memarzadeh, F., & Jiang, Z. (2004). Effect of operating room geometry and ventilation system parameter variations on the protection of the surgical site. *IAQ*, 1-6.
- Memarzadeh F., & Manning A.P. (2002). Comparison of operating room ventilation systems in the protection of the surgical site, *ASHRAE Transactions*. **108**(2), 3-15.
- Memarzadeh F., & Manning A.P. (2003). Reducing risk of surgery. *ASHRAE Journal* .**45**(2), 28-33.
- MOH (2010). Policies and procedures on infection control. 2nd ed. Malaysia: Ministry of Health.
- Mora, R., English, & M.J.M., Athienitis. (2001). Assessment of thermal comfort during surgical operations, *ASHRAE Transactions*.**107** (1), 52–62.
- Möritz, M., Peter, H., Nipko, B., & Rüden, R. (2001). Capability of air filters to retain airborne bacteria and molds in heating, ventilating and air-conditioning (HVAC) systems. *International Journal of Hygiene and Environmental Health*.**203**, 401-409.
- Morley-Forster, P.K. (1986). Unintentional hypothermia in the operating room. *Canadian Journal of Anesthesia* .**33**(4), 515-527.

- Morris, R.H. (1971a). Influence of ambient temperature on patient temperature during intraabdominal surgery. *Annals of Surgery*. **173**(2),230-233.
- Morris, R.H. (1971b). Operating room temperature and the anesthetized, paralyzed patient. *Achieves of Surgery*. **102**(2), 95-97.
- Morsi, S.A., & Alexander, A.J. (1972). An investigation of particle trajectories in two-phase flow systems. *Journal of Fluid Mechanics*. **55**(2). 193-208.
- Murakami, S., Kato, S., & Zeng, J. (1997). Flow and temperature fields with various room air distribution, part 1-CFD study on computational manikin. *ASHRAE Transactions*. **103**,3-15.
- Murakami, S., Kato, S., & Zeng, J. (2000). Combined simulation of airflow, radiation and moisture transport for heat release from a human body. *Building and Environment*.**35** (6), 489-500.
- National Health Services Estates. (1994). Health Technical Memorandum 2005: Ventilation in healthcare premises, London: HMSO.
- National Research Council. (1976) .Committee on Prosthetics Research and Developmental. Informal papers of a workshop on control of operating room airborne bacteria, November 8-10, 1974, Washington. Washington (DC): National Academy of Science.
- Nilsson, K.G., Lundholm. R., & Friberg, S. (2010). Assessment of horizontal laminar air flow instrument table for additional ultraclean space during surgery. *Journal of Hospital Infection*. **16**,243-246.
- Ninomura, P., Rousseau, C., & Bartley, J. (2006). Design and construction of hospital and health care facilities. *ASHRAE Journal*. **48** (6), H33–37.
- Panni, M.K., & Corn, S.B.(2002). The use of a uniquely designed anesthetic scavenging hood to reduce operating room anesthetic gas contamination during general anesthesia. *Anesthesia and Analgesia* . **95** (3),656–660.
- Peccia, J., & Hernandez, M. (2001). Photoreactivation in airborne *Mycobacterium parafortuitum*. *Applied and Environmental Microbiology*.**67**(9),4225-4232.
- Peccia, J., Werth, H.M., Miller, S., & Hernandez, M. (2001). Effects of relative humidity on the ultraviolet induced inactivation of airborne bacteria. *Aerosol Science and Technology*. **35** , 728-740.
- Piziali, R.L., Witcher, C., & Sher, R. (1976). Distribution of waste anesthetic gases in the operating room air. *The Journal of the American Society of Anesthesiologist* . **45**(5), 487-494.
- Pfost, J.F. (1981). A re-evaluation of laminar air flow in hospital operating rooms. *ASHRAE Transactions*. **87**,729–739.
- Posner, J.D., Buchanan, C.R., & Dunn-Rankin, D. (2003). Measurement and prediction of indoor air flow in a model room. *Energy and Building*. **35**, 515-526.

- Prek, M. (2005). Thermodynamic analysis of human heat and mass transfer and their impact on thermal comfort. *International Journal Of Heat And Mass Transfer*. **48**, 731-739.
- Putzu, M., Casati, A., Berti, M., Pagliarini, G., & Fanelli, G. (2007) Clinical complication, monitoring and management of perioperative mild hyperthermia: anesthesiological features. *Acta Bio Medica* .**78**(3), 163-169.
- Rajaratnam, N. (1976). Turbulent jet. Amsterdam: Elsevier.
- Rao, S.K.M. (2004). Designing hospital for better infection control: an experience. *Medical Journal Armed Forces India* . **60** (1), 63-66.
- Rentschler, H.C., & Nagy, R. (1942). Bactericidal action of ultraviolet radiation on airborne microorganisms. *Journal of Bacteriology*.**44** (1), 85-94.
- Riley, R.L., & Kaufman, J.E. (1972).Effect of relative humidity on the inactivation of airborne *serratia marcescens* by ultraviolet radiation. *Applied and Environmental Microbiology*. **23**(6), 1113-1120.
- Ritter, M.A., Olberding, E.M., & Malinzak, R.A. (2007). Ultraviolet lighting during orthopaedic surgery and the rate of infection. *The Journal of Bone and Joint Surgery* .**89**, 1935-1940.
- Roache,P.J. (1994). Perspective: a method for uniform reporting of grid refinement studies. *Journal of Fluids Engineering*, **116**, 405-413.
- Roache,P.J. (1998). *Verification and Validation in Computational Science and Engineering*. Albuquerque, NM: Harmosa Publishers.
- Salvati, E.A., Robinson, R.P., Zeno, S.M., Koslin, B.L., Brause, B.D., & Wilson, P.D. (1982). Infection rates after 3175 total hip and total knee replacements performed with and without a horizontal unidirectional filtered air-flow system. *Journal of Bone Joint Surgery*. **64** (4), 525–535.
- Scherrer, M. (2003). Hygiene and room climate in the operating room. *Journal of Minimally Invasive Therapy and Allied Technologies* .**12**(6), 293-299.
- Scott, C.C. (1970).Laminar/linear flow system of ventilation: its application to medicine and surgery. *The Lancet* .**295** (7654),989–993.
- Sehulster, L., & Chinn, R.Y.W.(2003).Guidelines for environmental infection control in health-care facilities: recommendations of CDC and the healthcare infection control practices advisory committee (HICPAC). *MMWR Recommendations and Reports*. **52** (RR-10), 1-41.
- Smylie, H.G. & Dudley, H.A.F.(1961). Some principles in operating theatre design. *Scottish Medical Journal*, **6**, 588–596.
- Songer, J.R. (1967). Influence of relative humidity on the survival of some airborne viruses. *Applied Microbiology*. **15**(1), 35-42.

- Sun, Y., & Zhang, Y. (2007). An overview of room air motion measurement: technology and application. *HVAC&R Research*, **13**(6), 929-950.
- Streifel, A.J. (2000). Health-care IAQ: guidance for infection control. *HPAC Engineering*. **72**(10), 28-35.
- Tumia, N., & Ashcroft, G.P. (2002). Convection warmers- a possible source of contamination in laminar airflow operating theatre? *Journal of Hospital Infection*.**52**, 171-174.
- Wells, W.F.(1934). On airborne infection. Study II: Droplets and droplets nuclei. *American Journal of Epidemiology*. **20**(3), 611-618.
- Whyte, W. (2010). Cleanroom technology: fundamental of design, testing and operation, 2nd ed. UK: John Wiley & Sons.
- Whyte, W., Lidwell, O.M., Lowbury, E.J.L., & Blowers, R. (1983). Suggested bacteriological standards for air in ultraclean operating rooms. *Journal of Hospital Infection*. **4** (2),133–139.
- Whyte, W., Shaw, B.H., & Barnes R. (1973). A bacteriological evaluation of laminar-flow systems for orthopaedic surgery. *Journal of Hygiene* .**71**, 559–64.
- Wilcox, D.C. (1993). Turbulence modeling for CFD. La Canada, California: DCW Industries.
- Woods, J.E., Reynolds, G.L., Montag, G.M., Braymen, D.T., & Rasmussen, R.W. (1986). Ventilation requirements in hospital operating rooms- part I. control of airborne particles. *ASHRAE Transactions*. **92**, 396–426.
- Wolfshtein, M. (1969).The velocity and temperature distribution in one-dimensional flow with turbulence augmentation and pressure gradient. *International Journal of Heat and Mass Transfer*. **12**(3), 301-318.
- Woloszyn, M., Virgone, J., & Mélen, S. (2004). Diagonal air-distribution system for operating rooms: experiment and modelling. *Building and Environment* .**34**, 1171-1178.
- Xu, P., Peccia, J., Fabian, P., Martyny, J.W., Fennelly, K.P., Hernandez, M., et al. (2003). Efficacy of ultraviolet germicidal irradiation of upper-room air in inactivating airborne bacterial spores and mycobacteria in full-scale studies. *Atmospheric Environment*. **37** (3), 405–419.
- Yuan, X., Chen, Q., & Glicksman, L.R. (1998). A critical review of displacement ventilation. *ASHRAE Transactions*.**104**, 78-90.
- Yau, Y.H. (2008).The use of double heat pipe heat exchanger system for reducing energy consumption of treating ventilation air in an operating theatre-A full year energy consumption simulation. *Energy and Buildings* .**43**, 917-925.
- Yevdjovich, V.M. (1966). *Diffusion of slot jets with finite orifice length-width ratios*. Hydraulic Paper 2. Ford Collins: Colorado State University.

Zamuner, A (1986). Operating room environment with turbulent airflow. *ASHRAE Transactions*. **92**, 343-349.

Zhang, Y., Novieto, D., & Ji, Y. (2009) Human environmental heat transfer simulation with CFD – the advances and challenges. Eleventh International IBPSA Conference held on 27-30 July at the Glasgow, Scotland. Retrieved 22 Feb 2012 from http://www.ibpsa.org/proceedings/BS2009/BS09_2162_2168.pdf

Zhang, Z., Zhang, W., Zhai, Z., & Chen, Q. (2007). Evaluation of various turbulence models in predicting airflow and turbulence in enclosed environments by CFD: Part 1-summary of prevalent turbulence models. *HVAC&R Research*, **13**(6), 853-870.

Appendices

Appendix A: Permission letter for UMMC visit

**UNIVERSITI
MALAYA**
PUSAT PERUBATAN UM

No Rujukan : PPUM/1000/01/003/001(874)

24 Jun 2011

Encik Ding Lai Chet
Tutor and Master of Engineering Science Candidate
Jabatan Kejuruteraan Mekanik
Fakulti Kejuruteraan
Universiti Malaya
50603 Kuala Lumpur

Melalui: Ketua
Jabatan Kejuruteraan Mekanik, Fakulti Kejuruteraan

Tuan

*PERMISSION TO VISIT AND CONDUCT RESEARCH ON AIR-CONDITIONING
SYSTEMS IN OPERATING THEATRE IN UNIVERSITY OF MALAYA MEDICAL
CENTRE (UMMC)*

Dengan hormatnya merujuk kepada surat tuan bertarikh 1 Jun 2011 mengenai perkara di atas.

2. Adalah dimaklumkan bahawa pihak pengurusan Pusat Perubatan Universiti Malaya (PPUM) bersetuju memberi kebenaran kepada pihak tuan untuk membuat lawatan dan menjalankan penyelidikan mengenai sistem pendingin udara di dewan bedah. Pihak tuan boleh berhubung terus dengan Encik Zabaha b. Samari, Ketua, Jurutera PPUM, Jabatan Kejuruteraan dan Puan Sharipah Asiah Syed Junid AlJunid, Ketua Pegawai Kejururawatan PPUM, Jabatan Kejururawatan bagi urusan selanjutnya.

Sekian, terima kasih.

"BERKHIDMAT UNTUK NEGARA"

Yang benar



PROFESOR DATO' DR. IKRAM SHAH B. ISMAIL
Pengarah
Pusat Perubatan Universiti Malaya

s.k. Ketua Jurutera PPUM, Jabatan Kejuruteraan
Ketua Pegawai Kejururawatan PPUM, Jabatan Kejururawatan

No Dokumen: 201409

Pejabat Pengarah
PUSAT PERUBATAN UNIVERSITI MALAYA
(University Malaya Medical Centre)
LEMBAH PANTAI, 59100 KUALA LUMPUR, MALAYSIA
☎+603-79494422 (Hunting Line) : ☎ +603-79542253


Leading Healthcare


SIRIM
1200 WAKIL JAJAR
CERT.NO. AK2597


IQNet
INTERNATIONAL CERTIFICATION CENTRE


STANDARDS
MALAYSIA
MS ISO 15189:2013

Figure A.1: Permission letter for UMMC visit.

Appendix B: The Star News on Sarawak General Hospital Heart Centre (Formerly known as Sarawak International Medical Centre, SIMC)

Published: Wednesday December 29, 2010 MYT 6:41:00 PM
Updated: Wednesday December 29, 2010 MYT 8:32:29 PM

SGH Heart Center to be new heart referral hospital

Heart Valve Surgery Book
For Patients And Caregivers. Avoid Stress. Know What To Expect.
www.Heart-Valve-Surgery.com

Ads by Google

KUCHING: The new Sarawak General Hospital Heart Centre (SGH Heart Centre) in Kota Samarahan will become a heart referral hospital in the state, Deputy Chief Minister Tan Sri Dr George Chan said Wednesday.

He said the RM400mil centre, formerly known as Sarawak International Medical Centre, would start operating the heart care centre on Saturday while cancer and kidney care would start in stages.

"Previously, Chief Minister Tan Sri Abdul Taib Mahmud and I had suggested that the state needed a world class referral hospital in Sarawak as the state's vastness and challenging geography caused difficulties in getting specialists and doctors at divisional hospitals.

"With the new SGH Heart Centre, we plan to make this centre a heart referral hospital for cardiac care.

"The divisional hospitals can refer their heart patients to the SGH for better cardiac treatment, which is equipped with highly skilled cardiac specialist, modern and latest technology with a minimum charge of RM5," he told reporters after visiting the centre Wednesday.

Earlier, Dr Chan, spent about an hour visiting the centre, accompanied by Sarawak Health Director Dr Zulkifli Jantan and SGH Cardiology and Clinical Research Centre Head, Professor Dr Sim Kui Hian.

Dr Chan said Prime Minister Datuk Seri Najib Tun Razak was expected to officiate the opening of the new SGH Heart Centre in mid-January.

He also suggested that the SGH Heart Centre get medical helicopters to fly in patients from other divisions in the state since the centre was near the Kuching International Airport.

In the long term, Dr Chan said the state aims to transform Kota Samarahan into a health care hub.

"Maybe in future, we can have cancer, renal or other disease centres here. Then it will be a health care hub equipped with a cluster of medical facilities, as there is ample land for expansion.

"This will certainly benefit the people in the state since we will not have to send our patients overseas," he said. - Bemama

Figure B.1: News on Sarawak General Hospital Heart Centre.

Appendix C: AHU design for OT-5

Table C.1: Schedule of air conditioning for level 3.

REF.NO	COOLING CAPACITY (KW)		REHEAT	AIR FLOW	OUTDOOR	E.S.P	EDB/WB	DESCRIPTION	ELECTRICAL	CIRCUIT NO.
	THL	SHL		L/S	AIR L/S	(Pa)	(°C)			
3AHU-OPT-1	57.4	42.7	-	3306	348	582	24.1/18	AHU - HORIZONTAL TYPE	15KW, 3Ø	CP/3AHU-OPT-1
3AHU-OPT-2	69	53	-	4168	333	608	24.2/18.1	AHU - HORIZONTAL TYPE	15KW, 3Ø	CP/3AHU-OPT-2
3AHU-OPT-3	62.9	47.2	-	3441	311	577	24.2/18.3	AHU - HORIZONTAL TYPE	11.2KW, 3Ø	CP/3AHU-OPT-3
3AHU-OPT-4	91.6	53.5	-	3431	1067	712	26.3/20.6	AHU - HORIZONTAL TYPE	11.2KW, 3Ø	CP/3AHU-OPT-4
3AHU-STL	139.7	59.8	29.52	2423	2447	1030	31.5/26.2	AHU - HORIZONTAL TYPE	7.5KW, 3Ø	CP/3AHU-STL
3AHU-OT-1	87.6	37.4	17.5	1544	1390	1010	31.5/26.2	AHU - HORIZONTAL TYPE	5.6KW, 3Ø	CP/3AHU-OT-1
3AHU-OT-2	86.9	37.1	17.23	1526	1373	1012	31.5/26.2	AHU - HORIZONTAL TYPE	5.6KW, 3Ø	CP/3AHU-OT-2
3AHU-OT-3	107.6	47.4	21.35	1890	1701	1009	32.3/26.3	AHU - HORIZONTAL TYPE	5.6KW, 3Ø	CP/3AHU-OT-3
3AHU-OT-4	88.1	38.8	17.3	1543	1389	998	32.2/26.3	AHU - HORIZONTAL TYPE	5.6KW, 3Ø	CP/3AHU-OT-4
3AHU-OT-5	129.1	55.6	27	2258	2032	1015	31.7/26.3	AHU - HORIZONTAL TYPE	7.5KW, 3Ø	CP/3AHU-OT-5
3AHU-OT-6	140.9	60.2	30.1	2486	2238	1000	31.4/26.2	AHU - HORIZONTAL TYPE	7.5KW, 3Ø	CP/3AHU-OT-6
3AHU-CCL	110.5	85	-	6030	577	614	24.5/17.8	AHU - HORIZONTAL TYPE	22KW, 3Ø	CP/3AHU-CCL
3AHU-INV	66.4	28.3	5.7	1198	1198	1020	31.5/26.3	AHU - HORIZONTAL TYPE C/W PRIMARY, SECONDARY & HEPA FILTER	5.6KW, 3Ø	CP/3AHU-INV
3AHU-CSD-L	71.7	48.5	-	3006	613	642	26.2/19.3	AHU - HORIZONTAL TYPE	7.5KW, 3Ø	CP/3AHU-CSD-L
3AHU-CSD-R	87.3	65.5	-	4779	522	810	24.5/18.1	AHU - HORIZONTAL TYPE	15KW, 3Ø	CP/3AHU-CSD-R
3AHU-CSD-STERILE	121	93	-	6800	635	1235	24.3/17.8	AHU - HORIZONTAL TYPE C/W PRIMARY, SECONDARY & HEPA FILTER	25KW, 3Ø	CP/3AHU-CSD-STERILE
4FCU-UPS-2	9.8	8.6	-	711	90	70	23.3/16.6	CEILING CONCEALED FAN COIL UNIT	0.3KW, 1Ø	CP/3AHU-CCL
4FCU-BATTERY-014-1	4.2	4.2	-	523	Ø	-	20.0/15.7	CEILING EXPOSED FAN COIL UNIT	0.3KW, 1Ø	CP/4FCU-PLT
4FCU-BATTERY-014-2	4.2	4.2	-	523	Ø	-	20.0/15.7	CEILING EXPOSED FAN COIL UNIT	0.3KW, 1Ø	CP/4FCU-PLT
4FCU-UPS/TRX-013-1	7.8	7.8	-	652	Ø	-	23.4/16.5	CEILING EXPOSED FAN COIL UNIT	0.3KW, 1Ø	CP/4FCU-PLT
4FCU-UPS/TRX-013-2	7.8	7.8	-	652	Ø	-	23.4/16.5	CEILING EXPOSED FAN COIL UNIT	0.3KW, 1Ø	CP/4FCU-PLT

Table C.2: Schedule of exhaust fan units for level 3.

REF.	AIR FLOW (L/S)	E.S.P (Pa)	DESCRIPTION	ELECTRICAL	CIRCUIT NO.
3EF-STL-1	434	1200	CENTRIFUGAL IN-LINE FAN C/W PRIMARY, SECONDARY & HEPA FILTER	2.0KW, 3Ø	CP/3AHU-STL
3EF-STL-2	1168	1300	CENTRIFUGAL IN-LINE FAN C/W PRIMARY, SECONDARY & HEPA FILTER	3.0KW, 3Ø	CP/3AHU-STL
3EF-OT-1	1149	355	CENTRIFUGAL IN-LINE FAN C/W PRIMARY, SECONDARY & HEPA FILTER	0.75KW, 3Ø	CP/3AHU-OT-1
3EF-OT-2	1140	377	CENTRIFUGAL IN-LINE FAN C/W PRIMARY, SECONDARY & HEPA FILTER	0.7KW, 3Ø	CP/3AHU-OT-2
3EF-OT-3	1435	329	CENTRIFUGAL IN-LINE FAN C/W PRIMARY, SECONDARY & HEPA FILTER	1.2KW, 3Ø	CP/3AHU-OT-3
3EF-OT-4	1154	337	CENTRIFUGAL IN-LINE FAN C/W PRIMARY, SECONDARY & HEPA FILTER	0.75KW, Ø	CP/3AHU-OT-4
3EF-OT-5	1694	311	CENTRIFUGAL IN-LINE FAN C/W PRIMARY, SECONDARY & HEPA FILTER	1.2KW, 3Ø	CP/3AHU-OT-5
3EF-OT-6	1860	328	CENTRIFUGAL IN-LINE FAN C/W PRIMARY, SECONDARY & HEPA FILTER	2.3KW, 3Ø	CP/3AHU-OT-6
3EF-INV	1298	325	CENTRIFUGAL IN-LINE FAN C/W PRIMARY, SECONDARY & HEPA FILTER	0.75KW, 3Ø	CP/3AHU-INV
3EF-CCL	526	237	CENTRIFUGAL IN-LINE FAN	0.7KW, 3Ø	CP/3AHU-CCL
3EF-BAT	160	114	CENTRIFUGAL IN-LINE FAN	0.3KW, 1Ø	CP/3AHU-BAT
1EF-LAB-2	5181	1069	CENTRIFUGAL IN-LINE FAN (CHEMICAL RESISTANCE TYPE) C/W PRIMARY, SECONDARY & HEPA FILTER	10KW 3Ø	CP/1AHU-LAB-2
1EF-LAB-3	438	1800	CENTRIFUGAL IN-LINE FAN (CHEMICAL RESISTANCE TYPE) C/W PRIMARY, SECONDARY & HEPA FILTER	2.5KW 3Ø	CP/1EF-LAB-FUME-1,2&3
1EF-LAB-4	438	1800	CENTRIFUGAL IN-LINE FAN (CHEMICAL RESISTANCE TYPE) C/W PRIMARY, SECONDARY & HEPA FILTER	2.5KW 3Ø	CP/1EF-LAB-FUME-1,2&3
1EF-LAB-5	438	1900	CENTRIFUGAL IN-LINE FAN (CHEMICAL RESISTANCE TYPE) C/W PRIMARY, SECONDARY & HEPA FILTER	2.5KW 3Ø	CP/1EF-LAB-FUME-1,2&3
1EF-LAB-6	438	1800	CENTRIFUGAL IN-LINE FAN (CHEMICAL RESISTANCE TYPE) C/W PRIMARY, SECONDARY & HEPA FILTER	2.5KW 3Ø	CP/1EF-LAB-FUME-1,2&3
4EF-COMP	380	280	CENTRIFUGAL IN-LINE FAN	0.35KW, 1Ø	CP/3EF-COMP

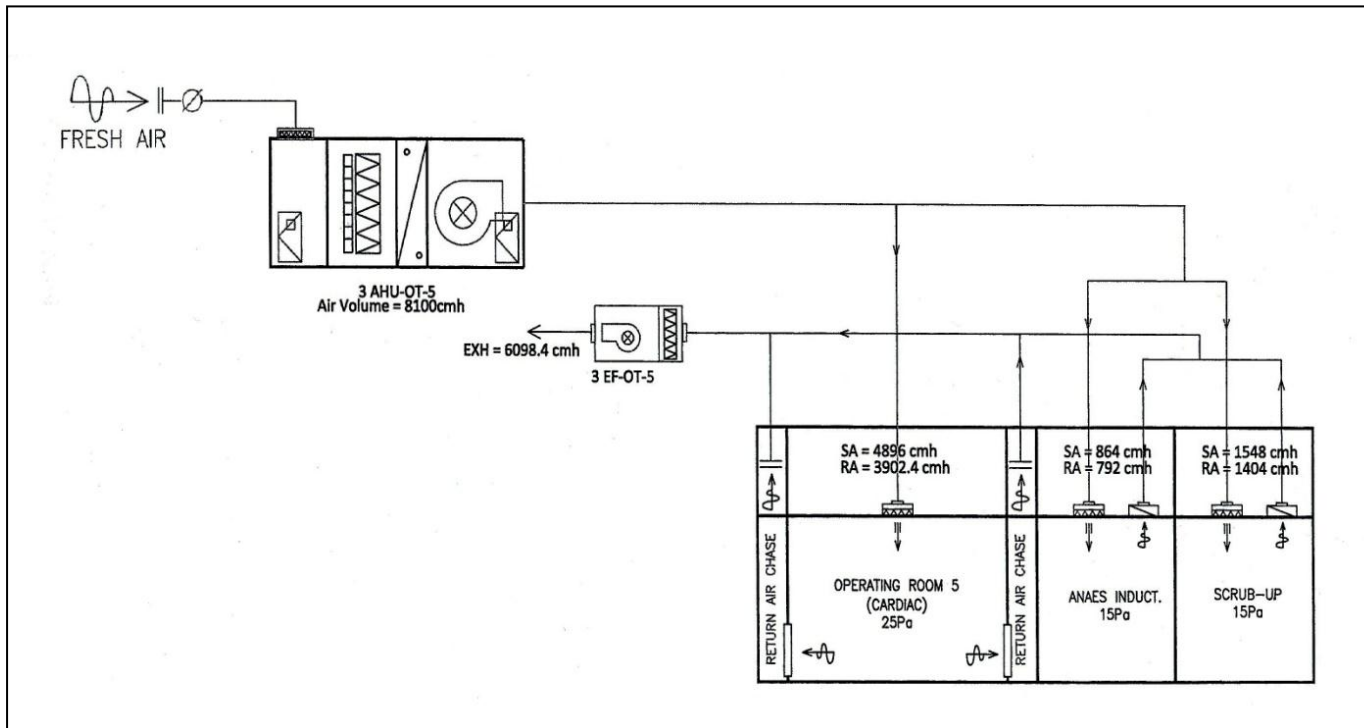


Figure C.1: Ducting system for OT-5.

Appendix D: Room dimension (on-site measurement)

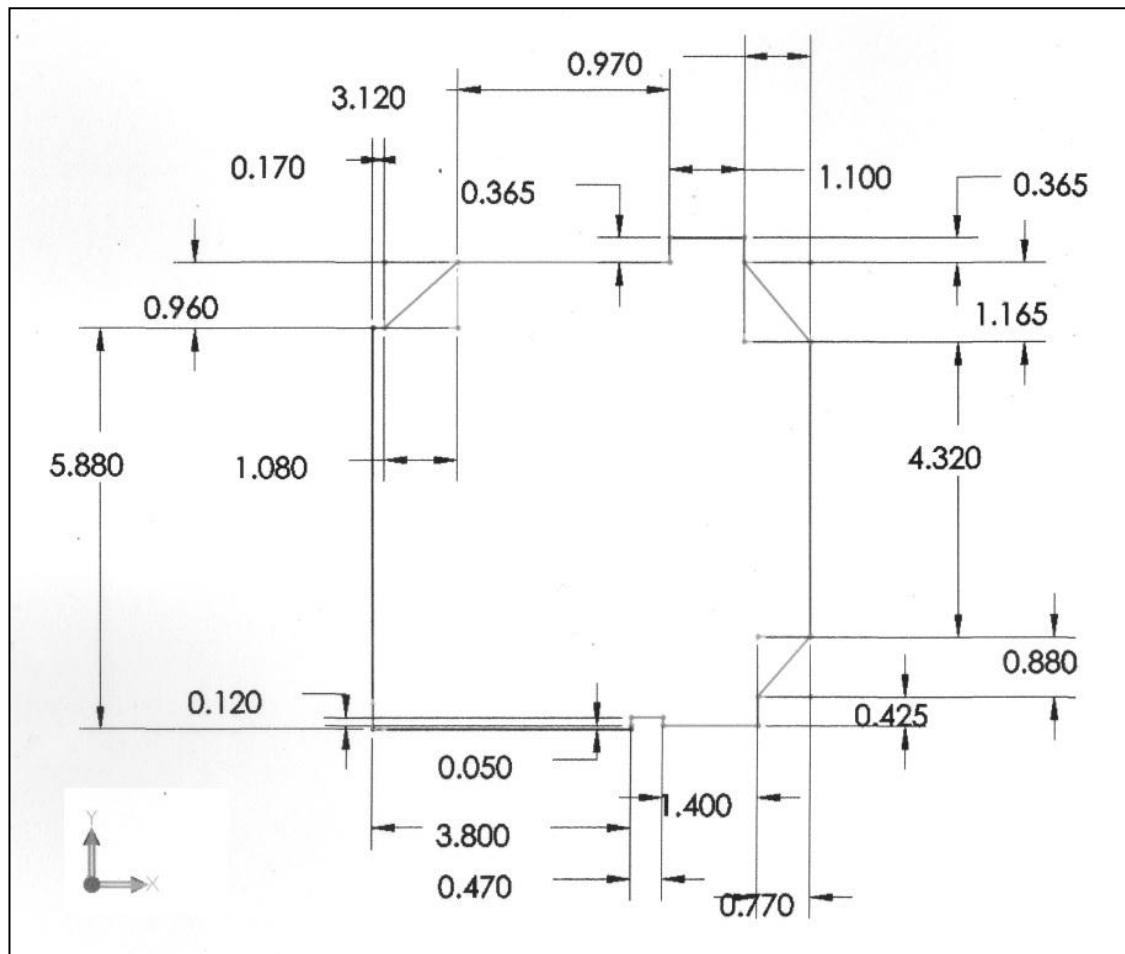
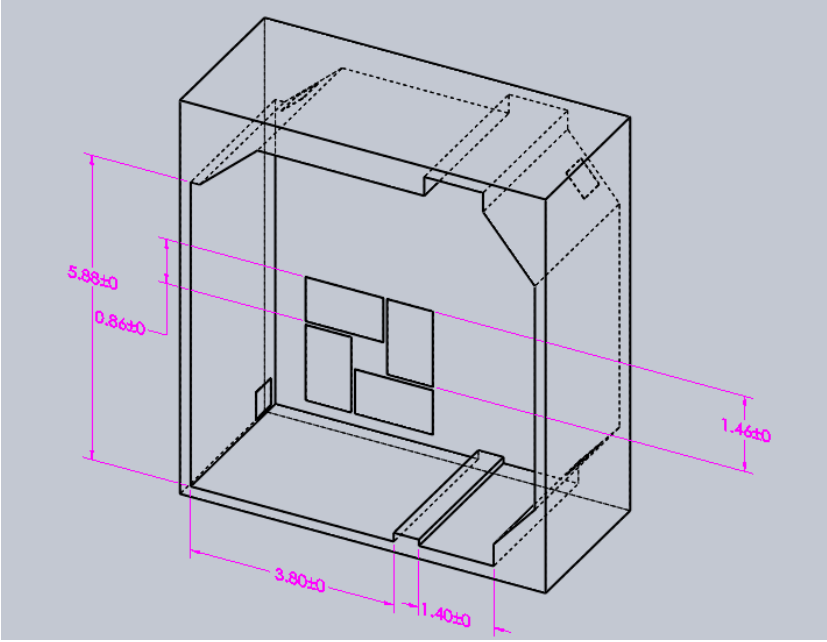
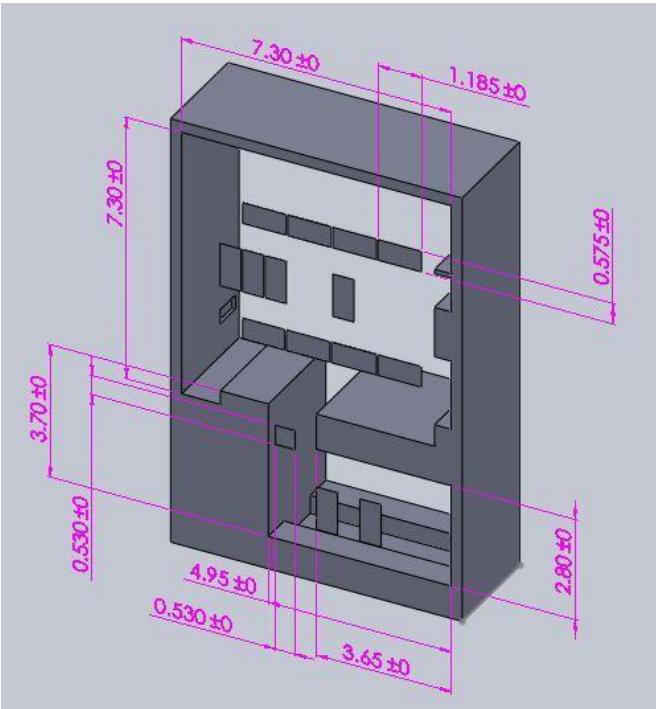


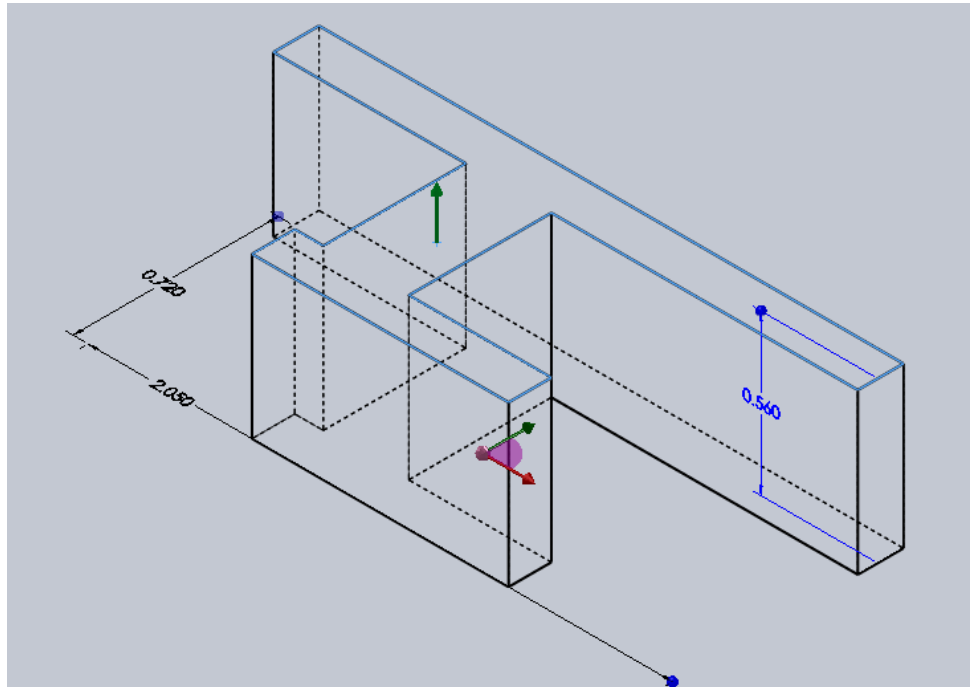
Figure D.1: SIMC OT-5 cross sectional dimension (unit in meter).

Appendix E: Equipment dimensions in OR modeling

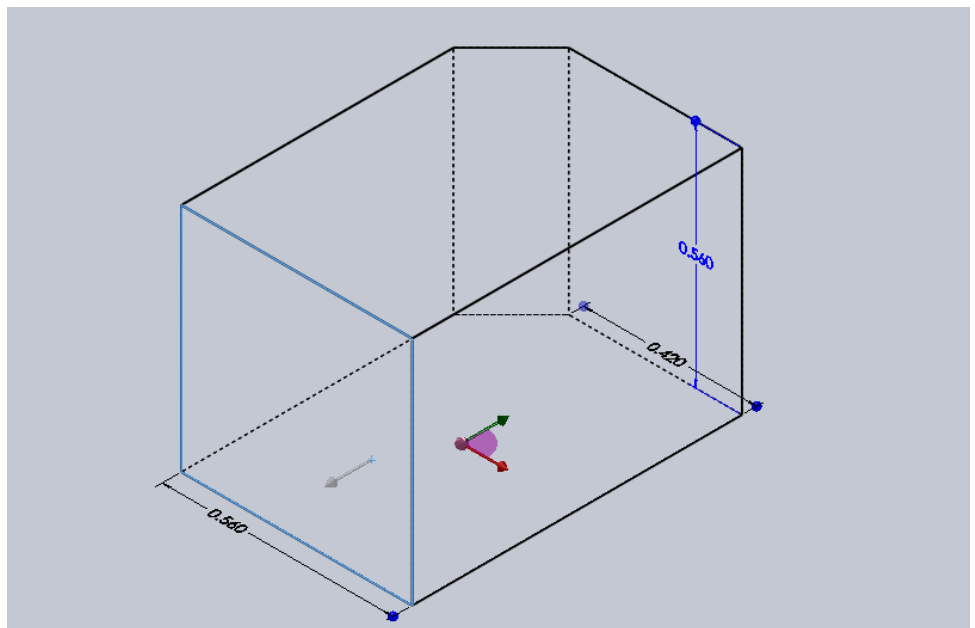
Table E.1: Equipment dimensions in OR modeling.

Item & Dimension ^{1,2}
<p data-bbox="443 472 719 506">a. Operating room</p> <p data-bbox="491 506 810 539">i. (SGHHC OT-5)</p>  <p data-bbox="491 1211 831 1245">ii. (UUMMC-OT11)</p> 

b. Operating table

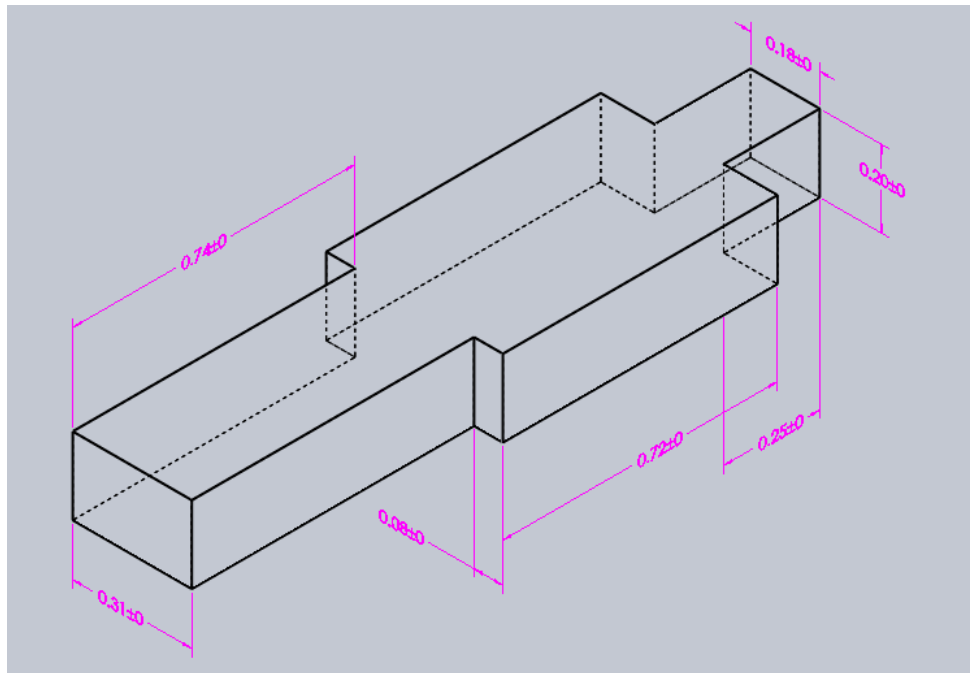


c. Machine



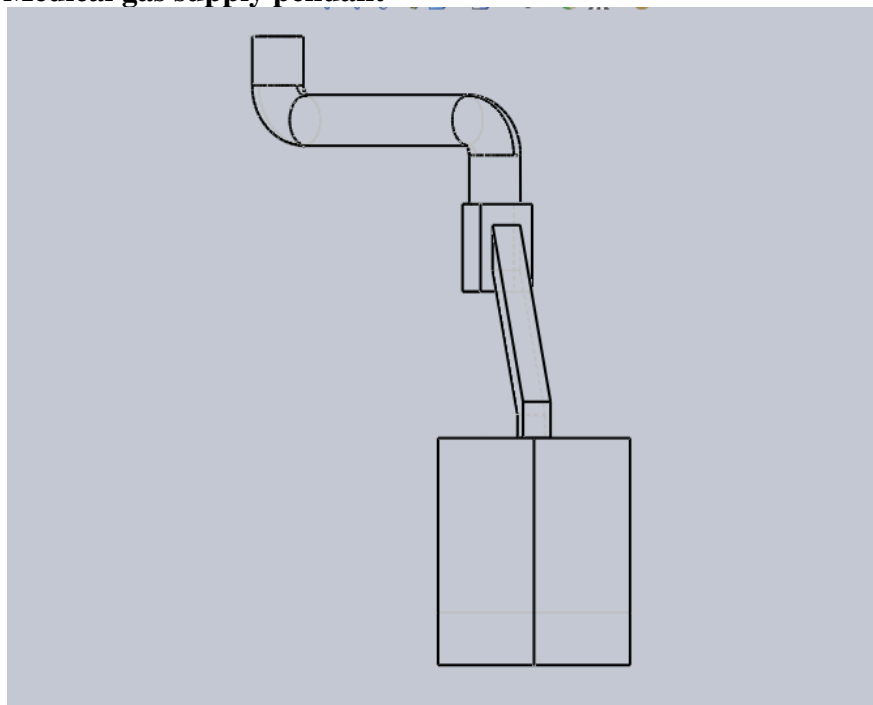
Regarded as one of the heat source. Net surface area exposed to air is 2.0364 m^2 .

d. Personnel and patient



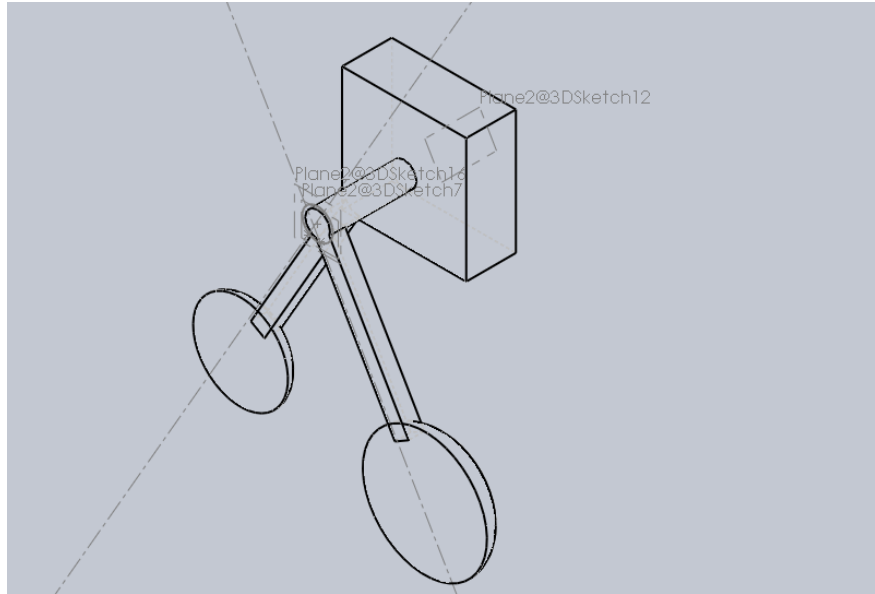
Regarded as one of the heat source. Net surface area exposed to air is 2.008 m² for personnel, while 1.47 m² for patient.

e. Medical gas supply pendant



f. Surgical lamp

i. SGHHC-OT5

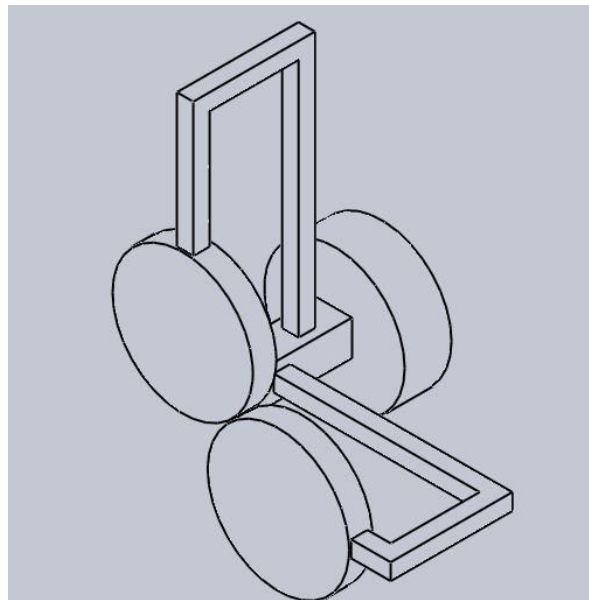


Regarded as one of the heat source.

For small lamp ($\varnothing = 0.42m$). Front surface area= 0.2376 m^2 , back surface area= 0.3424 m^2 .

For big lamp ($\varnothing = 0.55m$). Front surface area= 0.1385 m^2 , back surface area= 0.1915 m^2 .

ii. UMMC OT-11

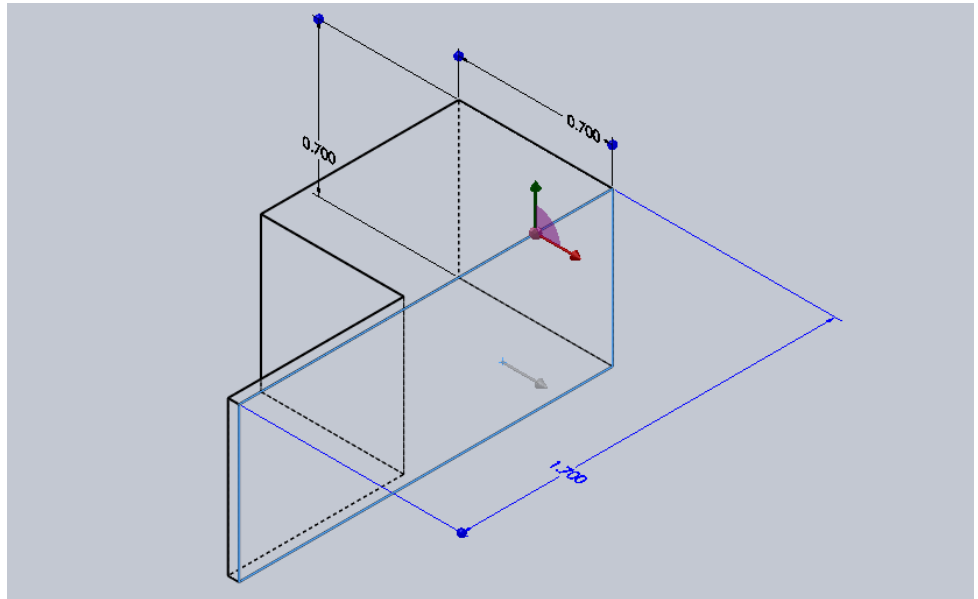


Regarded as one of the heat source.

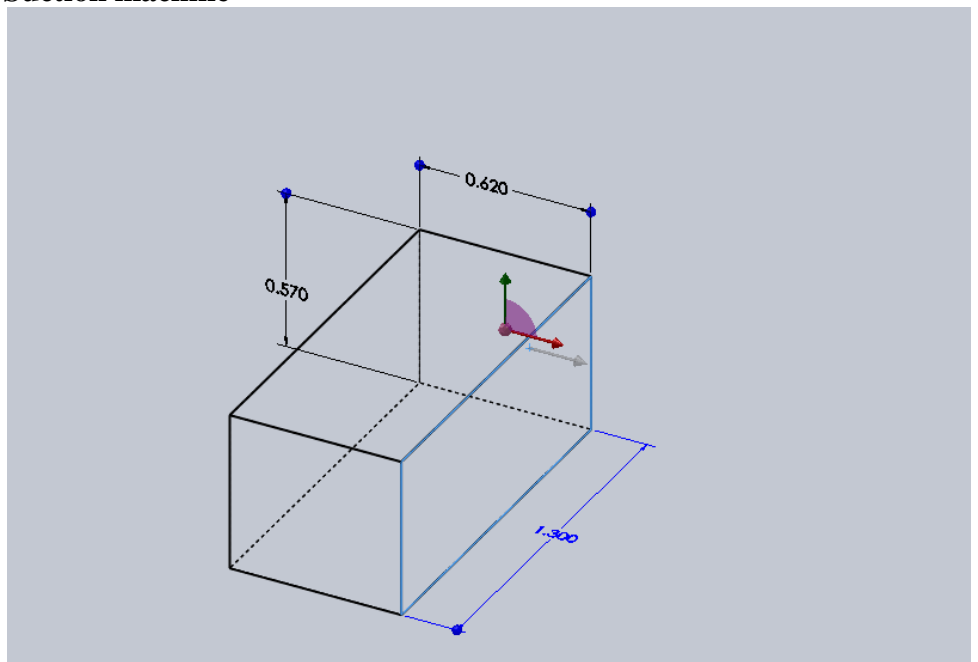
Each lamp has identical dimension.

For small lamp ($\varnothing = 0.6m$). Front surface area= 0.28 m^2 , back surface area= 0.47 m^2 .

g. Drawer

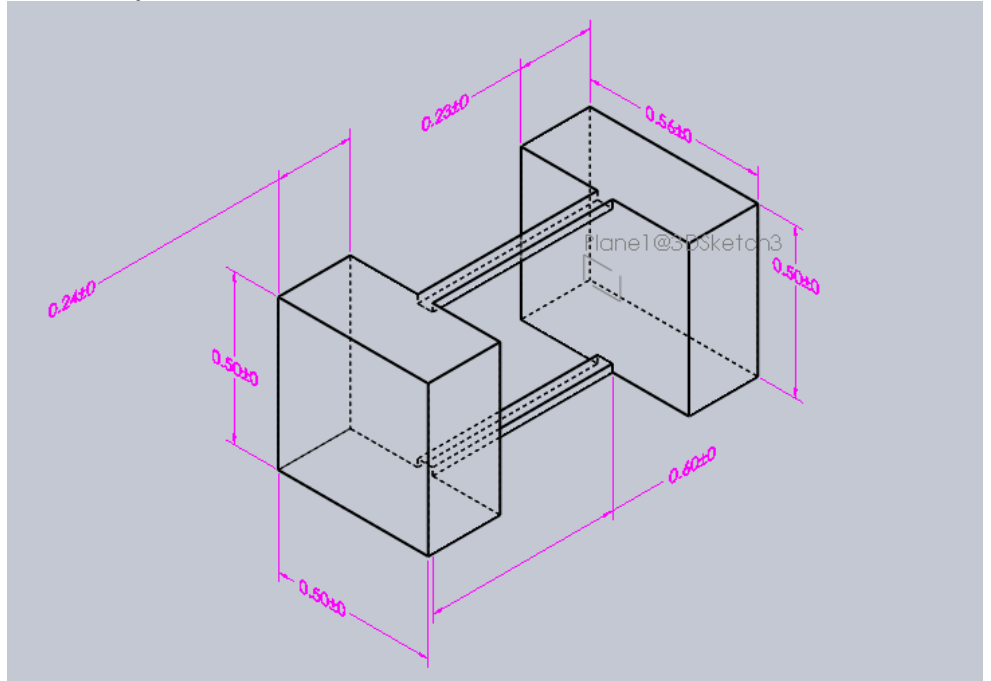


h. Suction machine

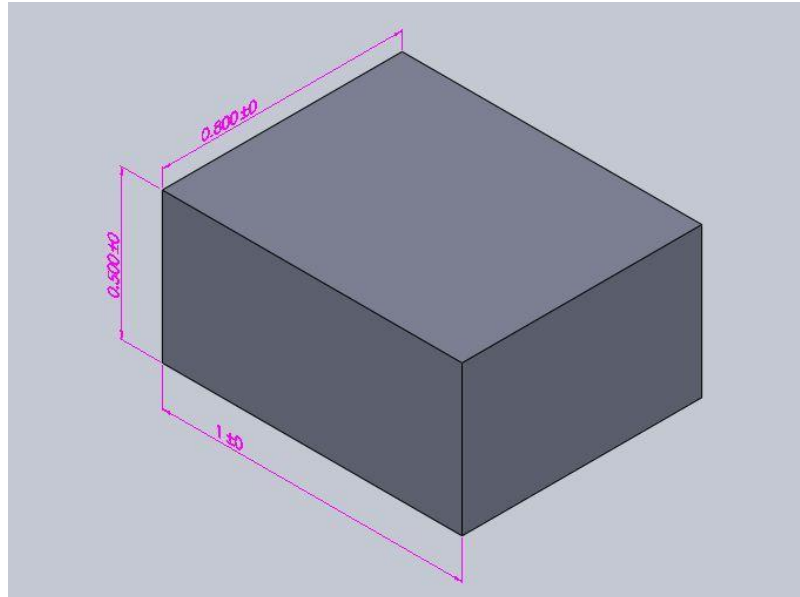


Regarded as one of the heat source. Net surface area exposed to air is 3.4466 m^2 .

i. Diathermy



j. Table



Length x Width x Height = 1 x 0.5 x 0.8 m

¹The sketching of the items listed above is performed using SolidWorks 2010.

²The dimension indicated is in meters.

Appendix F: Private communication

Subject: Fwd: Re: Seeking opinion for indoor airflow simulation.
From: "Dr. Yat Yau" <yhyau@um.edu.my>
Date: 21/11/2011 5:03 PM
To: lcding@um.edu.my

----- Original Message -----
Subject: Seeking opinion for indoor airflow simulation.
Date: Sat, 19 Nov 2011 16:18:15 +0800
From: Gao Naiping <gaonaiping@gmail.com>
To: lcding <lcding@um.edu.my>
CC: yhyau <yhyau@um.edu.my>

Dear Ding Lai Chet,

very pleased to hear from you. In the simulation of airflow in operating rooms, whether leakage should be considered or not depends on the leakage rate. If the leakage rate is high, as be comparable with the air change rate, it must be taken into account. However, in fact, the leakage is small and it could be ignored.

So far I have not taken any measurement in operating rooms. In the future, if I have the experimental data on airflow in operating rooms, I will share with you and Prof Yau Yat Huang.

Good Luck!

Regards
Naiping Gao

Associate professor
Department of Refrigeration and Thermal Engineering
College of Mechanical Engineering, Tongji University
Shanghai, China
Tel: 86-21-65983867
Fax: 86-21-65983867
Email: gaonaiping@tongji.edu.cn

附件人: lcding
发送时间: 2011-11-15 16:10:40
收件人: gaonaiping
抄送: yhyau
主题: Seeking opinion for indoor airflow simulation.
Dear Prof N.P Gao,
Good Day!

I am Ding Lai Chat, a master degree student from University of Malaya, Malaysia.

supervised by A,Prof Ir,Dr. Yau Yat Huang. My master degree topic is regarding the study of air distribution in operating room (OR).

After a discussion with Dr. Yau, we decide to seek for Prof's opinion regarding: In the modeling of OR in CFD, did we need to consider or neglect the exfiltration or leakage (since OR is positively pressurized) in the OR? From the literatures, i could hardly find the consideration of exfiltration in the CFD study.

Meanwhile, for Prof's information,fieldwork study was conducted at an OR in a hospital, and the geometry and layout for the OR was recorded, air velocity had been measured at certain point inside the OR in order to compare with the simulation's result.

Thank you for Prof's concern,
Have a nice day!

Best Regards,
Ding Lai Chet
Department of Mechanical Engineering,
University of Malaya

Appendix G: Requirement for the characteristic of velocity and temperature measurement

Table G.1: Minimum requirement for the characteristic of velocity and temperature measurement¹

Parameter	Measuring range	Accuracy	Response Time
Air speed	0.1-1.5 m/s	± 0.05 m/s or $\pm 5\%$ of reading, whichever is greater	0.2 sec. (If the turbulent intensity is not required to be determined, then the response time is allowed to be larger than 1 second)
Air temperature	10-40°C	$\pm 0.1^\circ\text{C}$	The shortest possible of response time

¹ANSI/ASHRAE (2005). Standard 113 Method of testing for room air diffusion. Atlanta, GA: ASHRAE.

Appendix H: Temperature and velocity contour for UMMC OT-11 simulation

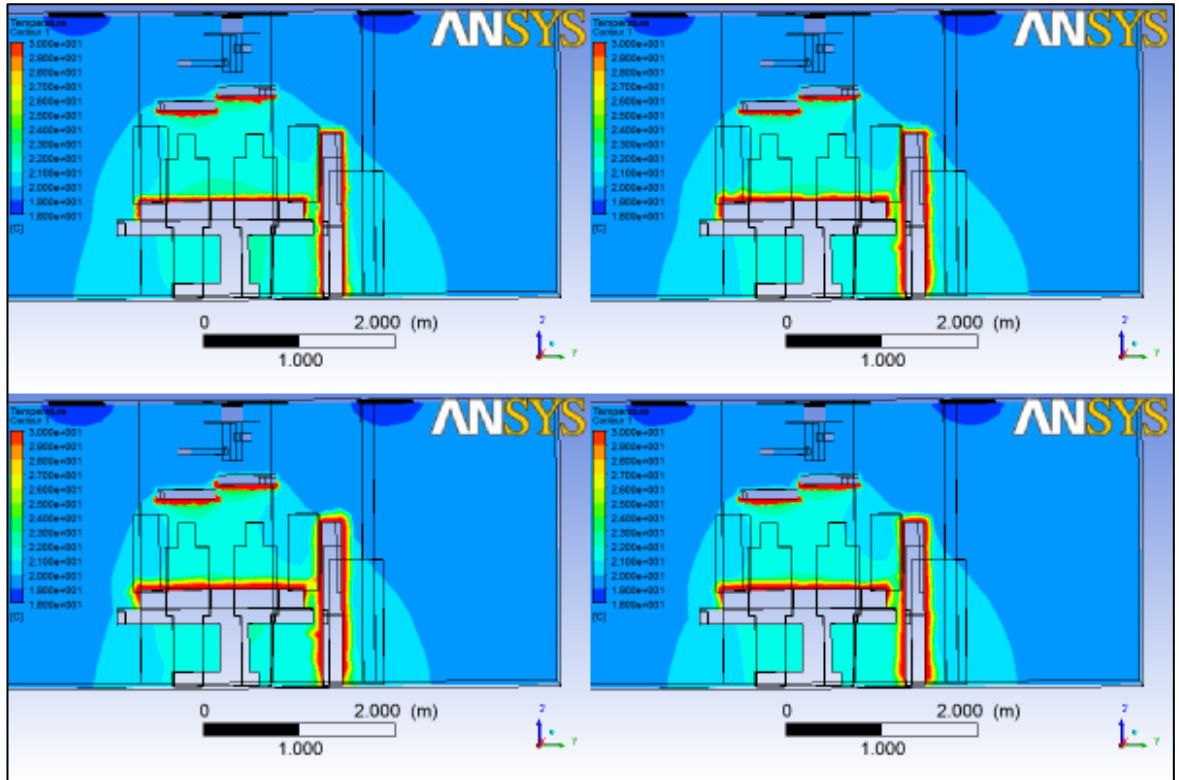


Figure H.1: Temperature contour for different mesh elements at surgical plane (Plane 1) of OT-11. Starting from upper left, moving clockwise for simulation I, II, III, and IV.

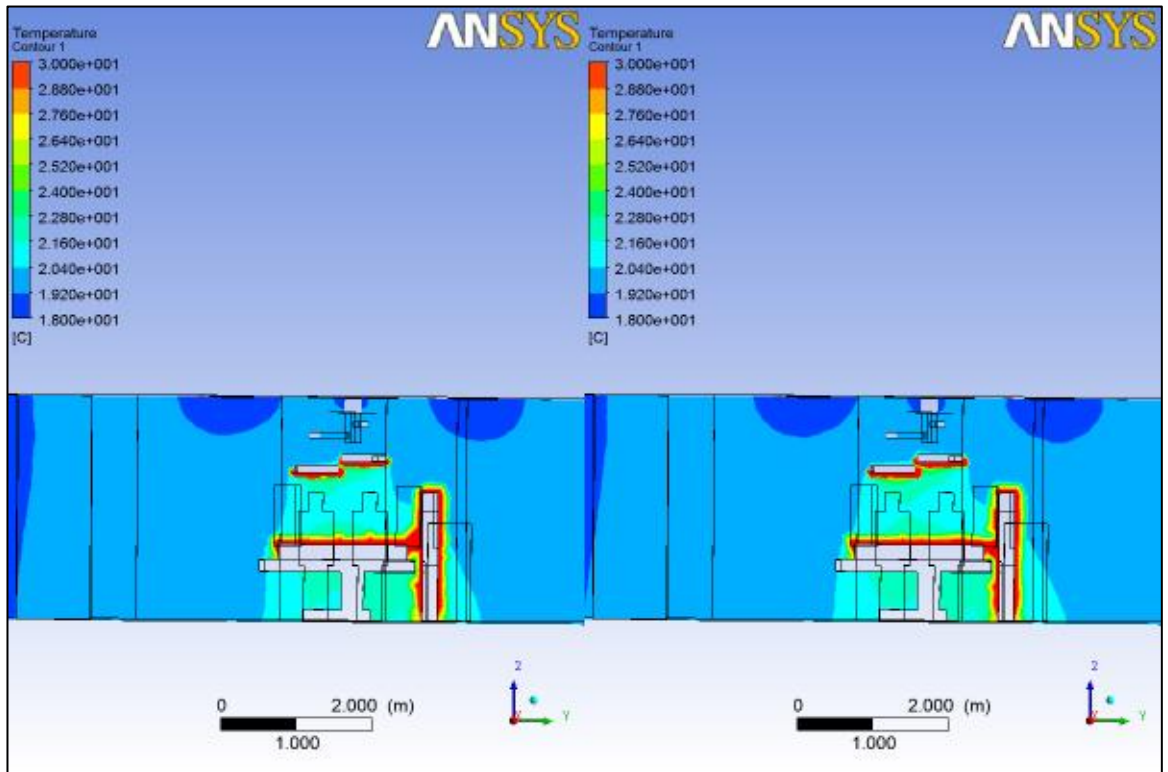


Figure H.2: Temperature contour for different mesh elements at surgical plane (Plane 1) of OT-11. Left : Simulation V and right: Simulation VI.

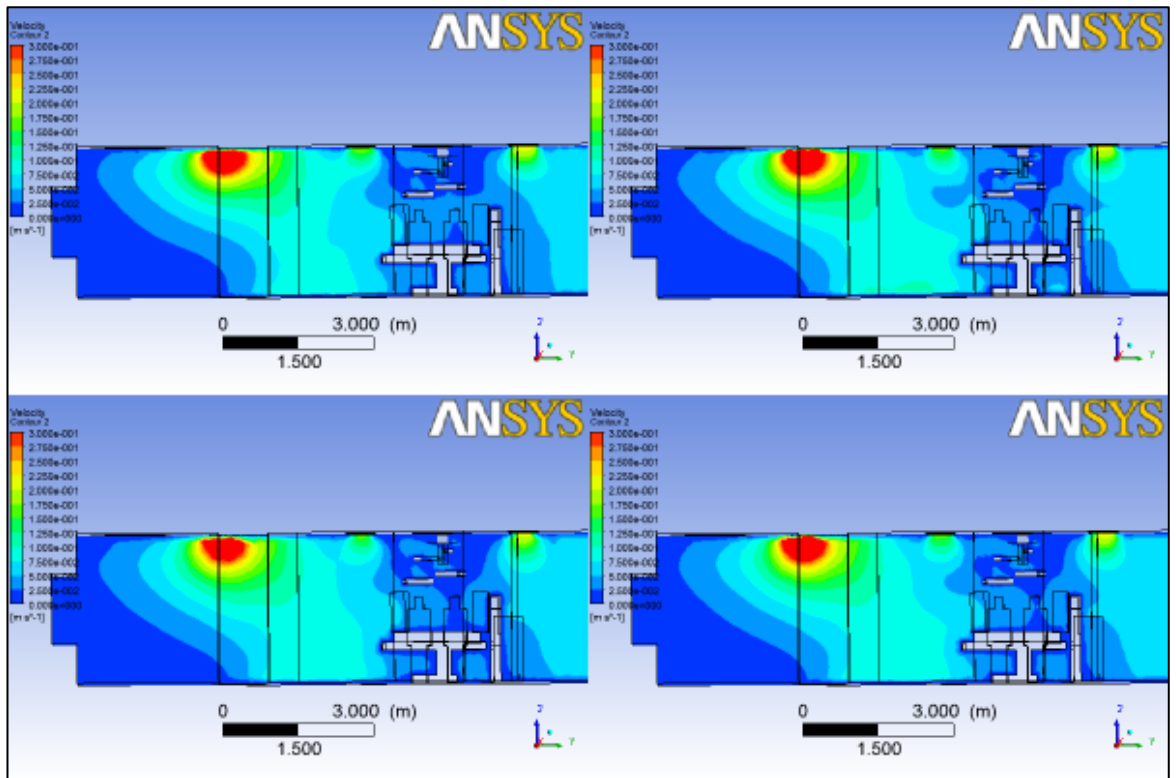


Figure H.3: Velocity contour for different mesh elements at surgical plane (Plane 1) of OT-11. Starting from upper left, moving clockwise for simulation I, II, III, and IV.

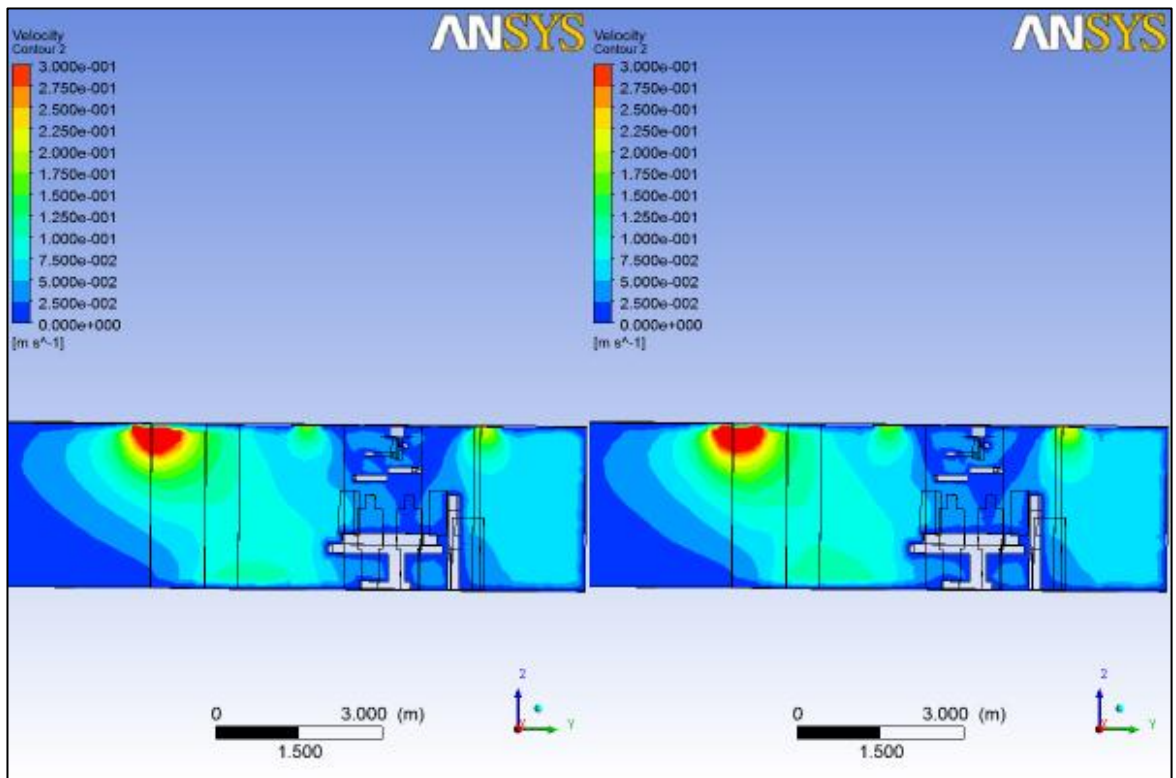


Figure H.4: Velocity contour for different mesh elements at surgical plane (Plane 1) of OT-11.

Left : Simulation V and right: Simulation VI.

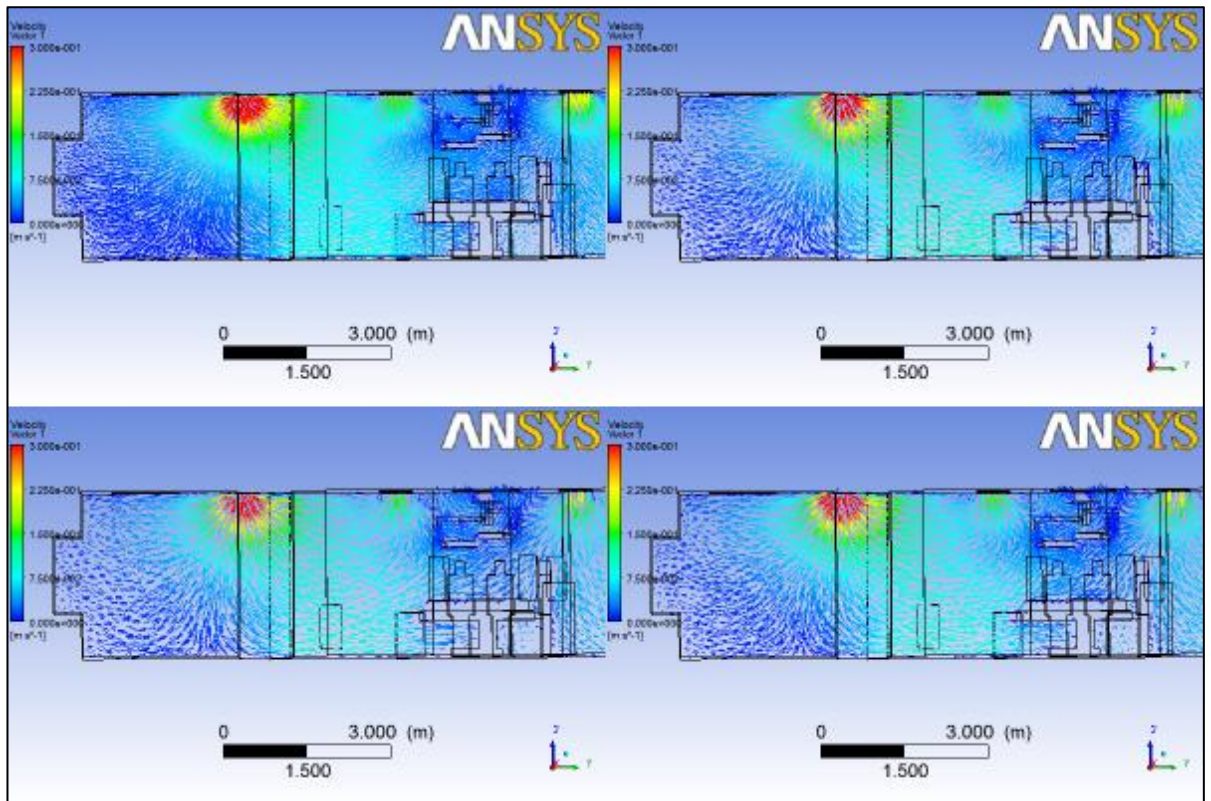


Figure H.5: Velocity vector for different mesh elements at surgical plane (Plane 1) of OT-11. Starting from upper left, moving clockwise for simulation I, II, III, and IV.

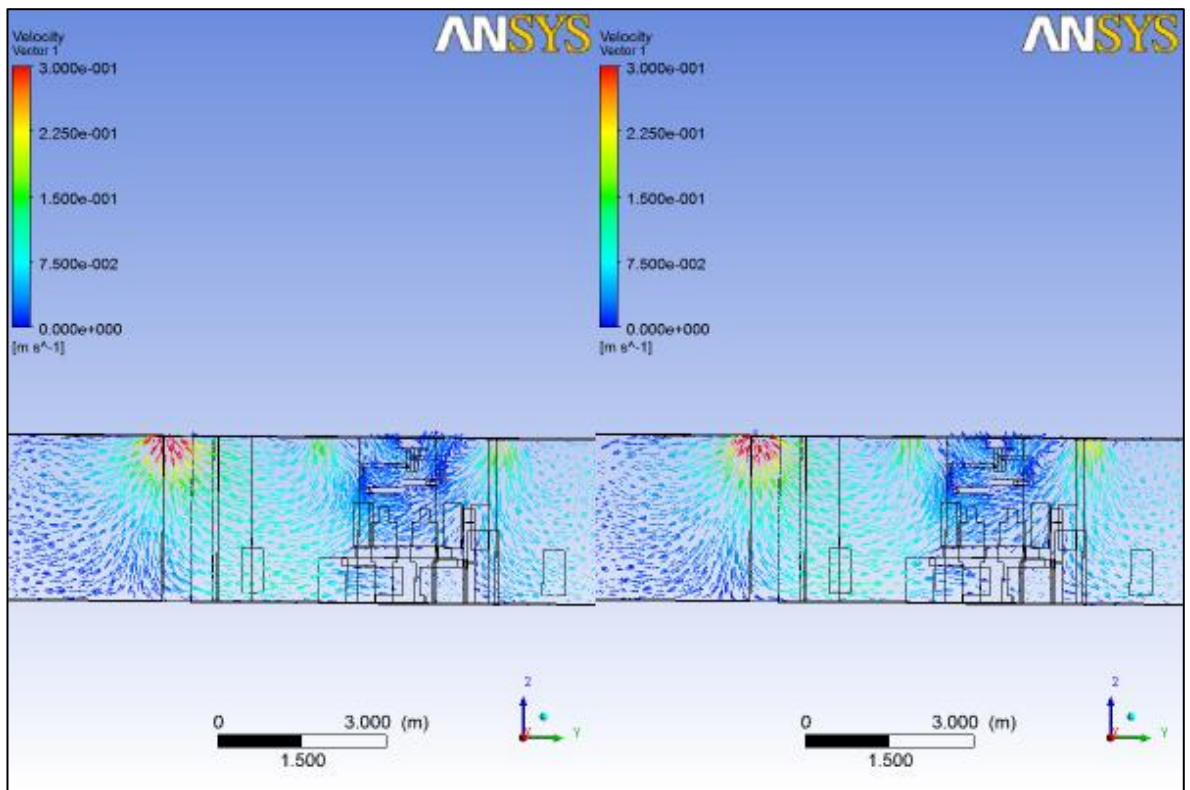


Figure H.6: Velocity vector for different mesh elements at surgical plane (Plane 1) of OT-11. Left : Simulation V and right: Simulation VI.

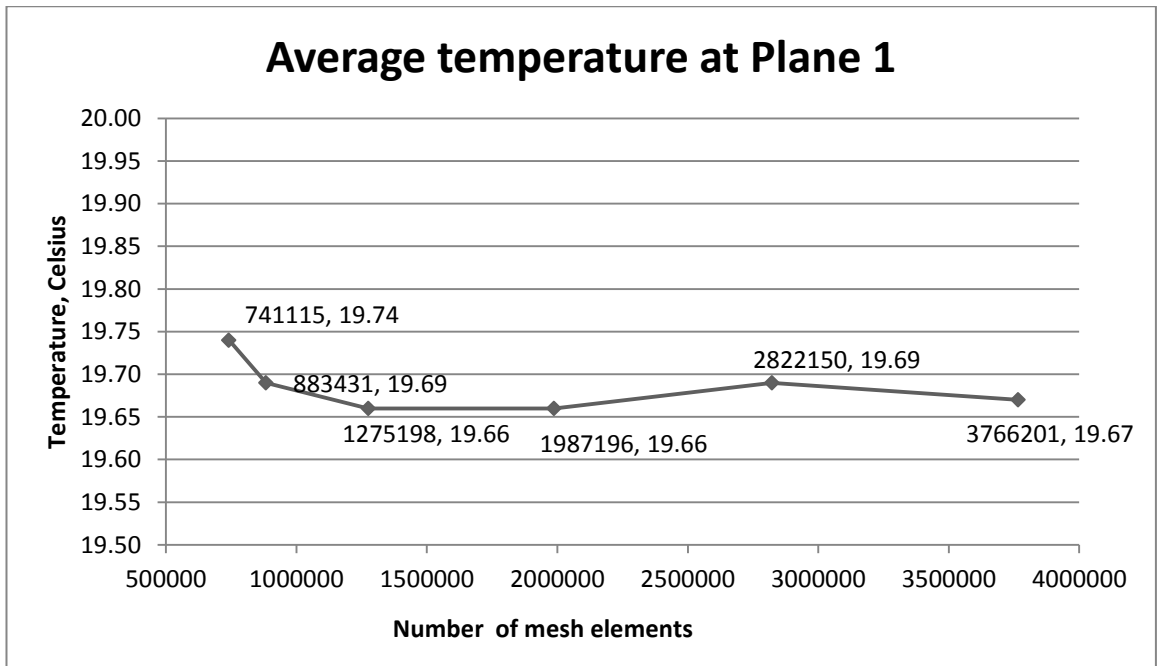


Figure H.7: Average temperature at Plane 1 for Simulation I, II, III, IV, V and VI UMMC OT-11.

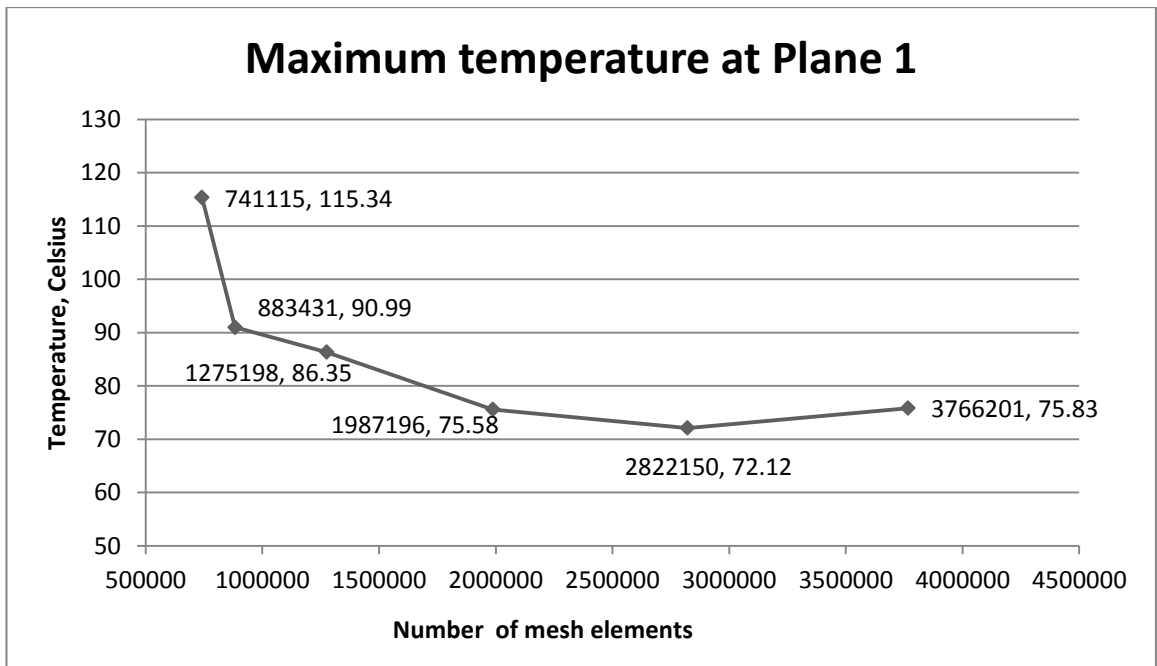


Figure H.8: Maximum temperature at Plane 1 for Simulation I, II, III, IV, V and VI UMMC OT-11.

Table H.1: Grid convergence index for Simulation I, II and III UMMC OT-11.

Simulation	I	II	III
Domain volume,(m^3)	191.78	191.78	191.78
Number of cells	3766201	2822150	1987196
Solution function, f	19.67	19.69	19.66
Representative mesh size, h (m)	0.0371	0.0408	0.0459
Refinement ratio,r	1.101		1.124
Error, ϵ	0.02		-0.03
Approximate relative error, e_a	0.001017		-0.001526
s	-1		
Apparent factor, p	3.7338		
Grid convergence index, GCI_{fine} (%)	0.294%		-0.348 %

Appendix I: Grid independence study

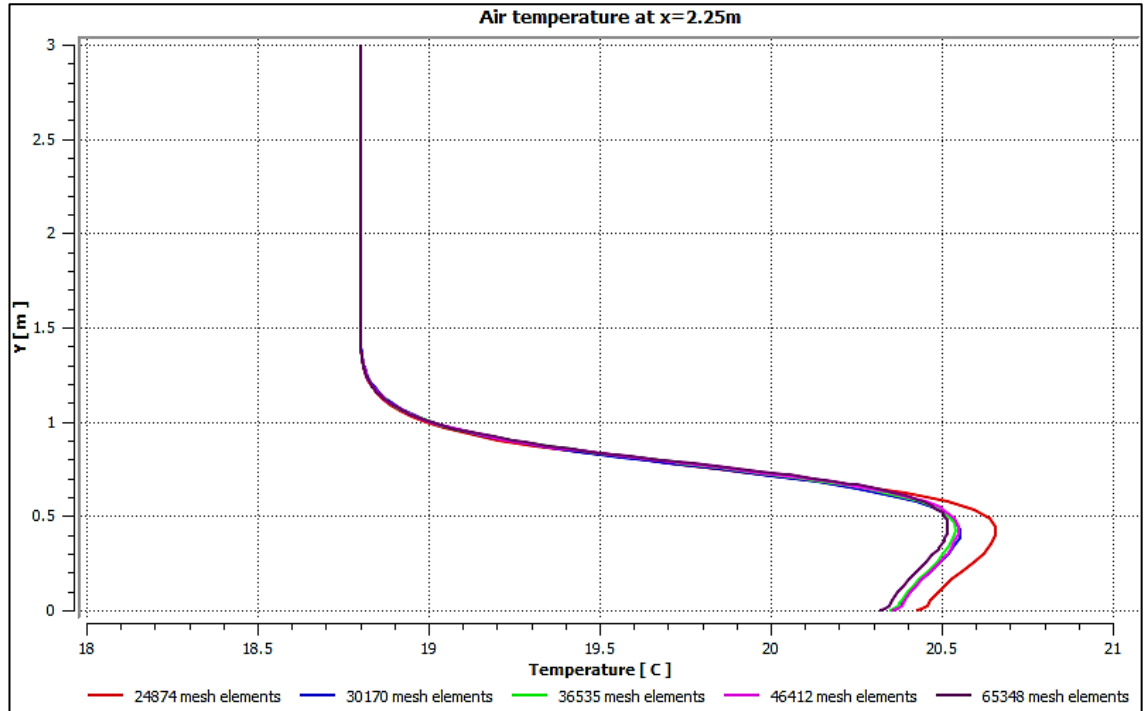


Figure I.1: Air temperature at line x=2.25 m from origin.

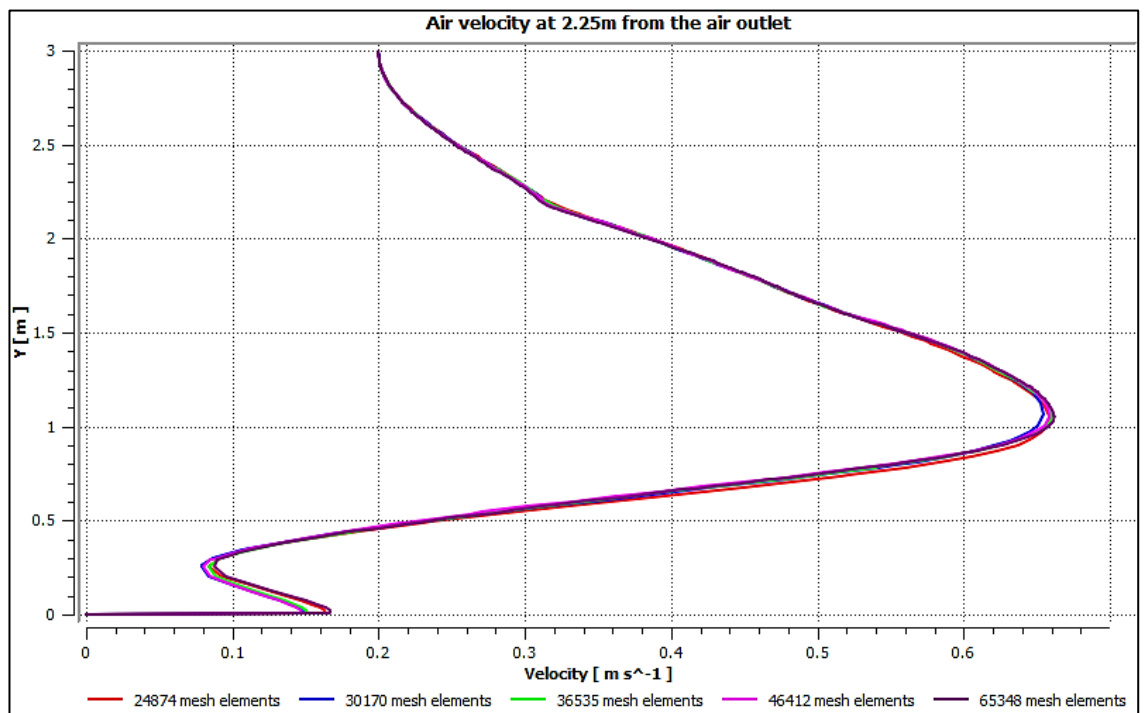


Figure I.2: Air velocity at line x=2.25 m from origin.

Table I.1: Grid convergence index for 46412, 36535, 30170 mesh elements.

Simulation	Fine	Medium	Coarse
Domain area, (m^2)	20.938	20.938	20.938
Number of cells	46412	36535	30170
Solution function, f	19.30	19.31	19.4
Representative mesh size, h (m)	0.0212	0.0239	0.0263
Refinement ratio, r	1.127		1.100
Error, ϵ	0.01		0.09
Approximate relative error, e_a	0.000518135		0.004660798
s	1		
Apparent factor, p	22.494		
Grid convergence index, GCI_{fine} (%)	0.005 %		0.077 %

